Institute of Paper Science and Technology

PERFORMANCE ATTRIBUTE VALIDATION STUDY ON CORRUGATING MEDIUM

Project 3471

Report ~~One~~ 2

to

MEMBER COMPANIES OF THE INSTITUTE OF PAPER SCIENCE AND TECHNOLOGY

April 1991

IPST

Atlanta, Georgia

PERFORMANCE ATTRIBUTE VALIDATION STUDY

ON CORRUGATING MEDIUM

Project 3471

Report One

to

MEMBER COMPANIES OF THE

INSTITUTE OF PAPER SCIENCE AND TECHNOLOGY

April 1991

THE INSTITUTE OF PAPER SCIENCE AND TECHNOLOGY

PERFORMANCE ATTRIBUTE VALIDATION STUDY ON CORRUGATING MEDIUM

Project 3471

Gary L. Jones

April, 1991

TABLE OF CONTENTS

TABLE OF CONTENTS

TABLE OF CONTENTS

TABLE OF CONTENTS

ABSTRACT

The MAPPS process simulation and end-use performance models accurately predict the effects of process conditions on handsheet and machine paper properties for corrugating medium. The models were validated through detailed analysis of mill trial data from a MacMillan Bloedel corrugating medium paper machine and through extensive modelling of the papermaking process using MAPPS.

The major objective was to validate the capability of the system to predict a variety of end-use performance characteristics for a major paper grade such as corrugating medium. The study reveals the sensitivity of compressive and other properties to key process variables such as OCC content, refining power, press loads and calendering. The analysis shows that the PAT's model system is a much more useful tool to determine the interactions of process and product variables than standard statistical techniques alone. The simulation model is useful for both process and product development and can provide valuable insights into the effects of process and furnish conditions on product properties.

The models correlated the property data within a very high R-squared value indicating not only that the models are significant but that the data are not random. Property data were obtained on 24 reel samples and 120 sets of composite pulp samples collected at five locations over a three-day period. Good statistical agreement was obtained on both machine paper and handsheets from composite pulps. This report describes the test conditions, data analysis, modelling techniques and conclusions about the effects of processing conditions on properties. Other reports are planned which describe the models in more detail.

The sensitivity case study using the validated model determined the sensitivity (slope) of machine paper properties to each of the test variables over the maximum range of the test. These results are summarized in the following report.

The study also revealed several weaknesses in the models in the area of pressing and property development. These will require review and modification before additional validation work is undertaken. Future model validation work planned for 1991-1992 includes completion of a mill trial for multi-ply linerboard grade and initiation of a free sheet trial.

EXECUTIVE SUMMARY

This report summarizes the results of a machine trial to validate the MAPPS Performance Attribute System for corrugating medium grades. The objective was to determine the ability of the MAPPS models to track the response of handsheet and machine paper properties, primarily compressive strength, to changes in several important process variables. The variables selected for the test were OCC content, primary and tickler refiner conditions, calender loading, third press loading and machine speed.

Statistical analysis of the data showed that the models performed well and are generally valid for this grade. Model adequacy was based on two tests, one based on measurement error and one based on model regression. Over the twenty-four reel sampling intervals, the MAPPS model tracked machine paper properties within measurement variance. This indicates that the models may be useful in predicting short term variations in properties and in determining whether variability is real or due to measurement error.

A second measure of model adequacy was based on a regression of the data against model predictions for each property. These regressions showed excellent agreement. The R-squared values for each property ranged from 0.99 to 0.998 with a confidence interval of 95%. Each regression generated a single correction or multiplier for each property. Many of these correction factors were close to one, indicating the models accurately predict the mean data for many properties. The correction factors for several of the compressive properties and Gurley porosity were significantly different from 1. It is not clear at this stage whether these correction factors are universal or specific to this particular paper machine.

CD variability was a significant factor for a number of variables, such as basis weight, caliper, and density, and for several tensile variables, such as breaking length and burst factor, but was not significant for compressive or elastic properties. CD variability was not modelled in the current study but is within the capability of the MAPPS system.

Because several variables were changing simultaneously during the trial, it was not possible to determine exact measures of the sensitivity of individual properties to individual variables from the raw data. In part two of the study, a sensitivity study using the validated model determined the slope dependence of each property on the key independent variables.

Statistical tests showed that third press and lump breaker loading had no effect at the testing levels. Similarly, OCC content and machine speed had little influence on compressive properties and only a statistically weak effect on tensile properties. The absence of an OCC content effect could have been predicted

beforehand by a comparison of the performance attributes of the OCC and semi-chem pulps. With the exception of fiber length and freeness, the semi-chem PAT's are very similar to the OCC PAT's indicating that a change in OCC content will have little effect on paper properties.

Of all the test conditions, calender load produced the most surprises. Calender load had a strong effect on caliper, density and elastic properties. However, the calender load effect was reduced or nonexistent on measured compressive and tensile properties. Predicted compressive properties were similarly insensitive to calender load while predicted caliper, density and elastic properties showed a similar strong influence of calender loading.

The calender influence can be explained through an examination of the models. Densification during calendering increases specific modulus but reduces caliper. Compressive properties are functions of the product of specific modulus and sheet thickness. When the calender stack is lifted, the increased caliper tends to cancel the effect of the decreased modulus and there is little effect on compressive properties as a result.

Only two minor problem areas were found in the property predictions. One area was in the predicted effect of calender loading on tensile properties. The second was in the prediction of densification in the presses on the sidedness of the sheet. These problem areas, corrective actions and future work are discussed in more detail.

INTRODUCTION

A novel system of Performance Attribute (PAT) models has been integrated with existing and/or new mass and energy balance models to give MAPPS the ability to predict the development of both handsheet and machine-paper properties. The resulting system is capable of predicting properties of paper and paperboard grades made from a variety of wood species. The machine trial outlined in this document is designed to validate the PAT system for corrugating medium.

The concept of end-use performance modelling was developed to include the generally non-conservative properties of fibers and the fiber network as an extension to the standard mass and energy balance process models. The resulting PAT Modeling system in MAPPS has the following capabilities:

1) to predict the end-use performance characteristics of paper and paperboard,
2) to quantify the interactions between fibers and the fiber network, processing conditions, and end-use performance characteristics,
3) to provide the framework for a new approach to the solution of product quality problems,
4) to provide a platform for process optimization and control which includes both process and product quality parameters,
5) to provide the technical "first principles" basis for understanding the fundamentals of product quality relationships.

Specifically, performance attributes are composed of a set of 29 variables which describe the state of the fiber furnish or the fiber network at any given point in the papermaking process. A species data base was constructed to initialize performance attributes, and PAT models were developed to predict the effects of the various pulp and paper unit operations and operating conditions on these PAT's. Finally, product quality models were developed to use the performance attributes and the mass and energy characteristics of the process system to predict the quality characteristics of the fiber furnish and the fiber network. With this system MAPPS now can simulate quality development from the wood yard to the reel.

PAT's can be classified as component (i.e., fiber or filler) attributes or network attributes as shown in Figure 1. As fiber or filler attributes, PAT's can be categorized as composition, shape, surface area, physical properties and optical properties. Network PAT's are related to contact area, bond area, and anisotropy. Anisotropy, in turn, includes such factors as sidedness, formation, fiber orientation and stress distribution variables. Each of these variables may be affected differently, or perhaps not at all, by each pulp and paper unit operation.

For example, chemical pulping leads to a reduction in yield, kappa number, hemicellulose content, absorption coefficient and a change in other fiber tensile or physical properties. High yield or stock refining results in changes in fiber length, surface area (both internal and external), and shive content. At the paper machine, the forming operations influence fiber contacts, mass distribution, fiber orientation, etc. The wet pressing operation further increases fiber contacts and, finally, the dryer section creates the hydrogen bonded fiber network.

Using a modular approach, changes in performance attributes can be modelled separately for each of the processing unit operations. At the reel, the cumulative effects of these operations culminate with the final machine-made paper properties, calculated from the PAT's by a property module. Property calculations, however, are not limited to the end of the paper machine because the property module can also predict handsheet properties based on user-specified TAPPI testing conditions.

The models discussed above were developed from a host of literature sources and are based on a mixture of theory and experimental data. The novel nature of the modelling system, and the new concepts involved in combining many different sources of theory and experimental data into a unified system, has resulted in the creation of a completely new and expanded version of MAPPS. Thus, a validation procedure must be established so that the predictions of the new MAPPS can be systematically confirmed for each of the major paper and paperboard grades.

Previous studies, some conducted as early as 1987, showed that the new model calculations were reasonable and consistent. However, these studies did not deal with issues such as variability, trends and process sensitivity. The two-part machine trial procedure which follows has been designed to consider these issues.

OBJECTIVES

1) Model Validation

In order to develop significant credibility and widespread use of the MAPPS Performance Attribute (PAT) system within the industry, it is important to demonstrate agreement of the system predictions with mill process data. This project was directed specifically to validate the system for corrugating medium. Validation is defined as "reasonable" agreement between measurements and predictions, taking into account measurement variance and other sources of error such as CD variability.

2) Process Variable Sensitivity

If the PAT models are found to be valid, the MAPPS flowsheet model will then be used to quantify the sensitivity of medium properties to several important independent variables such as OCC content, refining load, press load and calender application.

SCOPE

The validation study is limited to two main characteristics: 1) reasonable prediction of short-term and long-term property variability and 2) correct prediction of sensitivity of important sheet properties to key process variables.

For purposes of this study, the validation was limited to the paper machine area beginning at the high density tanks and including the major paper machine operations such as stock preparation, sheet forming, white water recovery, wet pressing, drying and converting.

Although CD variations are expected for some properties, the model is restricted to predictions of an MD profile. A detailed CD variability study may be justified in future validation work.

Comparisons between measurements and predictions are based on both handsheet and machine paper properties. Handsheets were made from composite pulps collected at several (five) key locations in the paper machine area. Only the heavier 26 lb. handsheet data were used in the analysis because compressive properties were not determined on the lighter weight (13 lb.) sheets.

Validation criteria are based primarily on statistical measures of "goodness of fit" and estimates of various factors contributing to variability such as measurement error, errors in estimating process conditions and transient effects. Predictions which fall within a well-defined band around the mean measurements indicate a valid model. The band includes the average measurement error plus CD variability and errors associated with uncertainty in input data.

PROCESS VARIABLES

The test was conducted during three eight-hour periods from 0600 hours to 1400 hours on April 3 through 5, 1990. Test conditions are shown in Table I. Variables can be broken down into three categories: (1) primary - controlled, (2) secondary - uncontrolled but monitored and (3) uncontrolled or controlled but not monitored. Only variables in the first two categories will be discussed.

The original intent of the test was to change each variable about its mean value and to achieve a "steady state" between each change. In actuality, a number of variables (both controlled and uncontrolled) were changing simultaneously, and the results show the superposition of a number of variables.

Table I: Test Variables and Data Ranges

	Primary Variables	Range	Mean
1	Percent OCC, %........................	18 - 38	27
2	OCC Consistency, %...................	5.1 - 6.0	5.57
3	Primary (Hole) Refiner Power, hpd/t..	1.47 - 5.16	2.87
4	Primary Refiner Feed Consistency, %..	4.0 - 5.9	5.17
5	Calender Stack Loading (Assumed), PHI	15	
6	Tickler Refiner Loading, hpd/t.......	0.047 - 0.283	0.14
7	Tickler Refiner Feed Consistency, %..	4.1 - 5.3	4.78
8	Wire speed, ft/min..................	1372 - 1862	1698
9	Machine Speed, ft/min................	1400 - 1900	1733
10	Third Press Loading, PLI.............	480 - 650	576
	Secondary Variables	**Range**	**Mean**
1	Semi-chem flow rate $x10^{-4}$, lb/hr.....	1.62 - 3.78	2.97
2	Semi-chem CSF, ml....................	656 - 768	716
3	OCC fiber flow $x10^{-3}$, lb/hr..........	7.7 - 18.1	11.6
4	Headbox consistency, %...............	0.80 - 0.92	0.86
5	Headbox liquid head, ft of H_2O.......	88.0 - 167	140.25

A complete set of process data are shown in the section titled RUN CONDITIONS and in Appendix I.

PROCESS SAMPLING

Reel Samples

Machine paper samples were obtained according to the schedule in Table II.

Table II: Machine Paper Sampling

Time period..	3 Days..............................
Reels........	8 Reels Per Day (Day Shift).........
Rolls........	3 Rolls Per Reel....................
Sets.........	1 Set Per Reel For Reels 1-3 & 5-7..
	2 Sets Per Reel For Reels 4 & 8.....

Testing

The following tests were performed on the machine paper:

Table III: Machine Paper Testing

Property	Tests/Sample
Basis Weight........	1
Caliper.............	1
Density.............	1
MD Breaking Length..	10
CD Breaking Length..	10
Gurley Porosity.....	10
MD Stretch..........	10
* CD Stretch..........	10
Burst Factor........	10
* TEA.................	10
MD STFI.............	20
CD STFI.............	20
* MD Ring Crush.......	10
CD Ring Crush.......	10
Concora.............	10
* Moisture............	5
MD Modulus..........	10
CD Modulus..........	10

* Indicates no model comparisons were made with these data.

Pulp Samples

Pulp composite samples were collected at 15-minute intervals within a reel period at the following locations:

Table IV: Pulp Composite Sampling

Number 4 High Density Tank..	* Blend Chest Discharge.......
OCC Raw Stock Tank..........	* Tickler Discharge...........
* Broke Tower..................	* Machine Headbox..............
* Hole Refiner Discharge......	Silo White Water............

* Indicates locations from which handsheets were made.

Handsheets

Five of the above locations -- headbox, hole refiner discharge, blend chest, tickler refiner and broke tank -- were selected for handsheet tests. Handsheets at two basis weights -- 26/1000 ft^2 and 40/3000 ft^2 -- were formed and tested for the following properties:

Table V: Handsheet Testing

26/1000	40/3000
* Tensile - 10 Tests......	Tensile - 10 Tests..........
* Burst - 4 Tests.........	Burst - 10 Tests............
* Basis weight - 4 Tests..	Basis Weight - 5 Tests......
Moisture - 2 Tests......	Moisture - 2 Tests..........
* Porosity - 8 Tests......	Porosity - 10 Tests.........
* Caliper - 10 Tests......	Caliper - 10 Tests..........
* Density - Calculated....	Density - Calculated........
* STFI - 20 Tests.........	* Zero span Tensile - 10 tests
* Ring Crush - 10 Tests...	
* Concora - 10 Tests......	
* CSF.....................	

* Indicates properties which were compared to model predictions.

METHODOLOGY

The validation procedure was broken down into several phases: a preliminary phase, data collection, simulation, data analysis and report generation.

Preliminary Phase

In the preliminary phase a MAPPS flowsheet model was developed at the appropriate level of detail and run under "typical" corrugating medium conditions to determine if the results were reasonable. The preliminary model was evaluated with best estimates for initial furnish conditions, refining, forming, pressing and calendering conditions. Preliminary evaluation focused mainly on property development, caliper changes and dewatering in the press section, freeness changes in refining, retentions and moistures in forming, and final calendered machine paper properties.

Having obtained reasonable agreement with the preliminary model and data, the most significant variables were identified and a preliminary experimental plan developed. The flowsheet model was reviewed and corrected.

Data Collection Phase

A final plan was developed by MacMillan and the test was run. Handsheet forming procedures were developed and the appropriate tests performed. Machine paper testing procedures were developed and the data generated. Data were stored initially in Lotus spreadsheet data files and later translated into SAS (Statistical Analysis System) data files for detailed analysis and plotting.

Data Analysis

A series of 24 MAPPS simulations were run with each simulation corresponding to a reel sample. The process simulation model and data are described in the following sections. Handsheet and machine paper properties predicted by the model were entered into individual data bases for later analysis. The data were analyzed through graphical as well as statistical techniques to break down overall variance into its components such as measurement variance, CD variability and contributions from individual processing conditions. The model validity is established through the combined analysis.

The analysis also exposed weaknesses and deficiencies in the models as well as insights into the effects of processing conditions on properties.

Sensitivity Study

The validated simulation model was then used to determine the sensitivity of the properties to four process variables: OCC content, freeness from tickler refiner, third nip pressing pressure and calender stack loading. A sensitivity coefficient is defined as the ratio of the change of each property to a change in one of these variables. Reel 1 conditions were used as the base case. The maximum variation of each variable is based on the maximum variations used in the test.

Ideally the predicted sensitivity or slope values should be compared with estimates from the experimental data. However, in this situation where several variables were changing simultaneously, it was not possible through statistical means to determine the experimental values of the sensitivities. This points out one of the advantages of using a valid model.

RUN CONDITIONS

Run conditions, summarized in Table VI, are broken down by day. The reel numbers 1 through 24 apply only to this study and are not production numbers. More detailed information including broke and saveall flows can be found in Appendix I.

Table VI: Summary of Run Conditions (Day 1)

Reel Number	1	2	3	4	5	6	7	8
Fiber, lb/hr x 10^{-3}								
Semi-Chemical	37.8	36.8	30.9	36.2	32.1	32.1	36.0	33.3
OCC	8.5	8.5	8.7	8.7	12.2	12.2	10.9	10.9
Refiner Conditions								
Primary Consistency	5.9	5.6	4.7	5.3	4.7	4.7	5.1	4.7
Specific Power	1.47	1.95	2.36	1.97	2.23	2.20	2.09	2.27
OCC Consistency	5.6	5.6	5.7	5.7	6.0	6.0	5.4	5.4
Tickler Consistency	4.7	4.1	4.4	5.1	4.9	4.9	4.9	4.9
Specific Power x 10^2	5.2	6.2	5.8	4.9	4.9	4.9	4.8	4.8
Stuff Box Consistency, %	4.0	4.0	3.5	3.5	4.0	4.0	3.7	3.7
Headbox Consistency, %	0.84	0.86	0.82	0.80	0.92	0.86	0.86	0.84
Paper Machine								
Speed, ft/m	1900	1900	1900	1900	1900	1900	1900	1900
Jet-To-Wire Ratio	0.96	0.96	0.96	0.96	0.96	0.96	0.96	0.96
Lump Breaker Roll Load, pli	145	145	145	145	145	145	145	145
1st Press Loads, pli	380	380	380	380	380	380	380	380
2nd Press Loads, pli	550	550	550	550	550	550	550	550
3rd Press Loads, pli	600	600	600	600	600	600	600	600
Calender Load, (on/off)	on	on	on	on	on	on	off	off

Table VI: Summary of Run Conditions (Day 2)

Reel Number	9	10	11	12	13	14	15	16
Fiber, lb/hr x 10^{-3}								
Semi-Chemical	34.0	29.5	30.9	32.1	35.1	32.1	32.1	34.7
OCC	18.1	18.1	18.1	17.8	16.4	13.7	13.7	13.7
Refiner Conditions								
Primary Consistency	5.6	5.3	5.2	5.4	5.9	5.4	5.4	4.9
Specific Power	2.42	2.90	2.76	2.67	2.38	2.67	2.56	2.16
OCC Consistency	5.5	5.5	5.5	5.4	5.4	5.4	5.4	6.0
Tickler Consistency	4.5	4.9	4.5	4.8	4.8	4.7	5.2	4.4
Specific Power x 10^2	4.9	4.7	14.4	28.3	14.9	13.0	11.5	26.4
Stuff Box Consistency, %	3.9	3.9	3.9	3.3	3.3	3.3	3.3	3.3
Headbox Consistency, %	0.84	0.84	0.82	0.84	0.82	0.84	0.84	0.84
Paper Machine								
Speed, ft/m	1900	1900	1900	1900	1900	1900	1900	1900
Jet-To-Wire Ratio	0.96	0.96	0.96	0.96	0.96	0.96	0.96	0.96
Lump Breaker Roll Load, pli	140	140	140	140	140	140	140	140
1st Press Loads, pli	380	380	380	380	380	380	380	380
2nd Press Loads, pli	550	550	550	550	550	550	550	550
3rd Press Loads, pli	650	650	650	650	650	650	650	650
Calender Load, (on/off)	on	on	on	on	on	on	on	on

Table VI: Summary of Run Conditions (Day 3)

Reel Number	17	18	19	20	21	22	23	24
Fiber, lb/hr x 10^{-3}								
Semi-Chemical	16.2	18.2	25.0	24.5	26.0	22.8	22.7	22.7
OCC	8.5	8.5	8.8	8.8	8.5	8.5	8.8	7.7
Refiner Conditions								
Primary Consistency	4.0	4.0	5.2	5.1	5.4	5.3	5.6	5.6
Specific Power	5.16	4.57	3.18	3.58	3.61	4.11	3.78	3.54
OCC Consistency	5.3	5.3	5.8	5.8	5.6	5.6	5.8	5.1
Tickler Consistency	5.3	4.1	5.2	4.7	4.7	5.2	5.1	4.8
Specific Power x 10^2	0.056	0.069	0.054	0.059	0.059	0.056	0.060	0.066
Stuff Box Consistency, %	3.7	3.7	3.7	3.7	4.1	4.1	4.0	3.5
Headbox Consistency, %	0.88	0.88	0.90	0.90	0.92	0.90	0.88	0.88
Paper Machine								
Speed, ft/m	1400	1400	1400	1400	1400	1400	1400	1400
Jet-To-Wire Ratio	0.95	0.95	0.95	0.95	0.95	0.95	0.95	0.95
Lump Breaker Roll Load, pli	145	145	145	145	145	145	145	145
1st Press Loads, pli	380	380	380	380	380	380	380	380
2nd Press Loads, pli	540	540	540	540	540	540	540	540
3rd Press Loads, pli	480	480	480	480	480	480	480	480
Calender Load, (on/off)	on	on	on	on	on	on	on	on

The data in Table VI were used as input for each MAPPS simulation run. A separate run was made for each reel. These conditions are only a portion of the data requirements for the MAPPS simulation. Additional data requirements are discussed in the following sections.

SUMMARY OF PROCESS CHANGES

OCC flow ratio gradually increased from about 18% to a maximum of 38% on reel 10 and then dropped to 25% by the end of the test. Refiner power remained in the range of 1.5 to 2.5 hsp-day/ton except for reels 17 through 24 where power increased to 3 to 5 hp-day/ton. Tickler refiner power was approximately 0.05 except for reels 11 through 16 where it was increased from 0.11 to 0.28 hp-day/ton. Headbox CSF, one of the most important single variables, reflecting the sum total of refining changes and OCC swings, varied over a relatively narrow range from 260 on reel 4 to 335 on reel 16. Headbox freeness is also strongly dependent on fines recycle and wire retention.

The calender stack was applied on all reels except reels 7 and 8 where it was lifted. Press loading was only changed on the third press nip. The press load was 600 for reels 1 - 8, 650 for reels 9 - 16 and dropped to 480 for reels 17 through 24. Machine speed was 1900 ft./min. for the first two days (reels 1 through 16) and then dropped to 1400 ft./min. for the third day (reels 17 through 24).

On the first day of testing, the main process changes were increasing OCC and varying calender loading (reels 7 and 8). Each reel interval was approximately 45 minutes. The total testing period for each day was thus about 6 hours. Each test was begun about 7 AM and concluded at around 2 PM. The time between the last reel sample on one day and the first reel sample of the next day was about 17 hours. This delay should have been sufficient to eliminate any transients in the system caused by deliberate process changes.

PERFORMANCE ATTRIBUTES

This section provides a brief overview of performance attribute concepts. For a more detailed discussion of PAT's please review References 1 through 6. Reference 1 describes the development of the system as of 1988. References 2 through 6 describe applications of the system and previous validation work. Those already familiar with performance attribute concepts may proceed to the PROCESS MODEL section.

PAT's are process variables which represent characteristics of individual fibers and the developing fiber network during the papermaking process. PAT variables apply to all areas of pulping and papermaking where fibers are found from the wood yard to the reel. The current set of PAT variables, shown in Figure 1, is grouped into seven categories: composition, shape, physical properties, surface area, fillers, network bonds, and network anisotropy.

Figure 1: Overview of Performance Attributes PAT's

Attribute	Category	Group	
Yield	Composition	Fibers	Paper
Kappa	Composition	Fibers	Paper
Xhemi	Composition	Fibers	Paper
C_k	Composition	Fibers	Paper
L, σ_l	Shape	Fibers	Paper
W. σ_w	Shape	Fibers	Paper
JDIST	Shape	Fibers	Paper
CWT	Shape	Fibers	Paper
Tensile	Physical	Fibers	Paper
Modulus	Physical	Fibers	Paper
Smod	Physical	Fibers	Paper
CSF	Surface Area	Fibers	Paper
SUSL	length	Fillers	Paper
SUSD	absorption	Fillers	Paper
SCC	scattering	Fillers	Paper
SHP	shape	Fillers	Paper
S_{b1}	Contacts and Sidedness	Network	Paper
S_{b2}	Contacts and Sidedness	Network	Paper
S_a	Bonds	Network	Paper
STSTR	Bonds	Network	Paper
Formation Factor	Anisotropy	Network	Paper
Wet Strain	Anisotropy	Network	Paper
Orientation	Anisotropy	Network	Paper

Figure 1 illustrates the concept that paper of any type consists of fibers and other materials (non-fibrous suspended solids) formed into a network. The components of the furnish, i.e., fibers or non-fibers (fillers), have a variety of characteristics, each with a unique contribution to end-use performance and each influenced differently during the papermaking process.

Composition Attributes and Specific Light Absorption

The first three attributes, Yield (pulping yield), Kappa (Kappa Number) and Xhemi (hemicellulose to total cellulose ratio), represent the current state of the chemical composition of the fibers. These attributes can be used to account for fiber species, pulping and bleaching operations and other process steps which influence fiber composition. In this application they account for the semi-chemical pulping of the virgin hardwood as well as the chemical pulping treatments of the OCC during its manufacture, without actually simulating these operations in detail. However, when these operations are of interest, detailed models can be added to simulate both the mass and energy flows as well as the changes in PAT's over these process steps.

C_k, the specific absorption coefficient, is placed with the composition attributes because of its relationship to color bodies and lignin.

Many of the PAT variables are initialized through the fiber property data base. This data base consists of composition, shape and tensile properties for nineteen fiber species including northern and southern US hardwoods and softwoods and eucalyptus. The data base also contains typical values for cellulose, hemicellulose, lignin, extractives and ash content for each species. There data have two major uses, 1) to initialize the flows of pulping and bleaching stream components and (2) to initialize the composition PAT's.

Initialization of component flows for a pulping type stream is straightforward because there is a direct correspondence between the data base and the components in the stream. For a wood fiber stream such as a paper stream, of interest in this application, the stream components are initialized through the fiber shape attributes discussed later.

The link between the database composition values and the composition attributes is more subtle. For any stream type, the initial yield is assumed to be that of an unpulped wood, i.e., 100% unless overridden by the user. If the yield is less than 100%, a hierarchy of pulping reactions is assumed. The order of the hierarchy is removal of extractives, hemicellulose, lignin and finally alpha-cellulose. In all cases, the extractives are assumed to be removed in the form of turpentine and tall oil. For the paper-type stream these removed components are placed in the generic dissolved components category. If the hemicellulose ratio is not overridden in the WOOD02 block, the lignin content is based on the yield and the unpulped lignin. The kappa number is then based on a direct correspondence between lignin and kappa number. If hemicellulose ratio is not overridden, the hemi-cellulose components are assumed to be reduced before lignin and the kappa number is then based on the remaining lignin.

Specific light absorption coefficient, C_k, is based on Kubelka-Monk theory and an assumed relationship between the fiber composition and the specific absorption of cellulose and lignin. C_k is actually the average absorption of the entire furnish mixture valid at a specific wavelength of light, 457 nm. If other materials are added to the fiber stream, such as dyes or suspended solids, C_k is updated based on standard mixing rules. In this application, C_k and other optical properties are not considered further.

Fiber Morphology

Fiber morphology or shape attributes are L, weight-average fiber length, σ_l, standard deviation of the length distribution, W, number-average fiber width, σ_w, standard deviation of the width distribution, JDIST, type of distribution (normal, log-normal or Weibull) and CWT, cell wall thickness. One of the most important characteristics of pulp is the wide range in these attributes, particularly fiber length. Fiber width is primarily useful in accounting for shives. CWT is required to account for the wide variations in cell wall thickness between species. The shape attributes help to account for the differences between species, refining histories, as well as cleaning and screening, and recycling effects. They are essential in tracking the fiber morphology when using pulping and bleaching streams and also provide a link to flows of individual fiber components.

As with composition attributes, the shape attributes may be initialized from the species data base or overridden with user input. The final values are used to initialize the shape PAT's and the flows of fiber components.

JDIST is a flag which defines the type of fiber length distribution applicable. Options include normal, log-normal, modified log-normal and Weibull. Only one type of distribution is assumed to apply locally. Thus, if a log-normal distribution is specified, both length and width must follow a log-normal distribution. However, JDIST may be assigned different values at different points in the flowsheet to simulate different types of furnish or process operations.

Physical Properties

Fiber physical properties which affect end-use performance are Z_f, fiber tensile, E_f, fiber modulus; and Smod, fiber flexibility factor. Z_f has units of breaking length in kilometers and represents the zero-span tensile strength of the sheet. The fiber tensile has a direct effect on sheet tensile strength and indirectly affects burst factor through the Page tensile and modified van den Akker burst relationships. The fiber modulus has a direct influence on sheet elastic properties and indirectly on compressive properties such as STFI, Concora and Ring Crush.

Specific Bond Strength, (SBS) is a measure of the potential bond strength when bonds are developed. In the absence of species dependent data, the same value is used for all species. Along with bond area and formation factor described later, SBS contributes to sheet strength through the Page tensile model.

The fiber flexibility factor accounts for subtle changes in fiber bonding flexibility and conformability resulting from changes in cell wall composition and thickness during drying, pulping and refining. This factor is meant to account for effects not handled directly by CWT. Smod is initialized to one and changes only slightly in refining and drying. In the current application, Smod increases during drying to reflect the stiffening of the fibers as the cell wall material collapses during drying. Smod decreases during refining reflecting the swelling of cell wall components.

Surface Area Attributes

Another important characteristic of fibers which influences bonding potential is hydrodynamic specific surface, S_h. It is well known that Canadian Standard Freeness (CSF) is directly related to hydrodynamic specific surface. While bonding and end-use performance are directly related to the more fundamental variable, S_h, the variable of choice followed in this system is CSF since it is measured directly and is readily known by mill process engineers.

CSF, S_h and fiber length distribution are linked together within the PAT modelling system. The combination of CSF and fiber length distribution determines the specific surface area for each fiber length. Fiber length distribution is determined from the mean and standard deviation, L and σ_l. Once the specific surface areas are known at each fiber length, the specific surface area for the entire distribution can be readily determined.

Suspended Solids Attributes

Fibers are not the only significant components of the paper. For filled grades, suspended material such as fillers and extenders, which may represent 50% of the basis weight, can have a major influence on end-use performance. Attributes in this category are the average particle size, SUSL, SUSD, average light absorption coefficient at 457 nm, SCC, average light scattering coefficient; and SHP, average shape factor. These attributes play an important role in modelling filled sheet grades but are not used in this application.

Network Attributes

As the fiber network forms in the forming section and is consolidated throughout the press section, the fundamental variables of interest are the fiber contacts for the top side and wire side represented by S_{b1} and S_{b2}. These variables also take into account some of the aspects of the sidedness characteristics of the sheet but do not include effects such as wire mark. The values of S_{b1} and S_{b2} are generated automatically during the forming and pressing processes and are used automatically by the property modules. It is not really necessary to pay much attention to these variables except to note that the higher the value of these variables the higher the sheet density, other things being equal. Also, when the sheet is dried, the fiber contact variables determine the degree of fiber bonding and the bond density. As S_{b1} and S_{b2} increase, the bond density also increases. This in turn leads to an increase in sheet strength and stiffness (modulus).

Fiber contact area is influenced by the degree of fiber conformability which in turn is influenced by pulping yield, cell wall thickness, surface area (CSF), and fiber stiffness factor, Smod. Contact area is also increased by pressing pressure and can be increased or decreased by calendering load. S_{b1} and S_{b2} are the only attributes which change during wet pressing.

Fiber-fiber Bonds

S_a represents the bonded area developed during forming, pressing and drying. This variable has a direct influence on bond density and sheet strength. S_a is generally proportional to the fiber contact areas discussed previously as well as to the drying temperature and moisture. As sheet moisture increases above 6%, cellulose hydrogen bonds are replaced by water hydrogen bonds and S_a decreases. This applies whether the sheet is being dried or is re-wetting. As S_a decreases, bond density decreases, which leads to a loss in sheet strength and modulus.

Calendering conditions can influence S_a either positively or negatively depending on the moisture and temperature conditions, the calendering load, and the thermal softening temperature of the fibers. The thermal softening temperature or glass transition temperature is a function of composition, moisture and temperature of the fibers. In summary, S_a is a direct result of the cumulative effects of species type, pulping, refining and forming conditions throughout the process and is a direct link between these conditions and end-use performance characteristics.

Sheet Anisotropy

Three types of non-uniformity in the plane of the sheet are accounted for. These are formation, variation of residual stresses and sidedness.

Residual Stresses

MD, CD and ZD variability can result from a built-in stress distribution within the sheet resulting from forming and drying conditions. Two factors which contribute to this built-in stress distribution are fiber orientation and stretch due to speed differentials along the machine. Significant deviations from random orientation and significant MD stretch will dramatically increase MD/CD tensile ratio. MD stretch at failure will also decrease with increasing MD wet strain. These factors are accounted for by the two attributes, OR and WS, which represent the average fiber orientation and cumulative set strain in the sheet. Fiber orientation is determined during sheet forming while wet strain is introduced as a result of the speed differentials at each pickup point in the forming section. These attributes will also affect elastic properties and compressive strength properties such as STFI, Ring Crush and combined board properties such as Concora.

Formation

A second type of variability of great importance is formation. This type of anisotropy results from nonuniform mass distribution in the plane of the sheet. This attribute is determined completely during forming and is influenced by factors such as fiber length, forming consistency, jet-to-wire ratio and CSF. The formation attribute is not assumed to change during pressing and drying. This attribute works with S_a to determine bond density and sheet strength. The relationships are based on the concept that the weakest link determines the strength of the sheet. Formation does not influence bulk density or porosity.

Sidedness

The third type of variability, sidedness, is handled through S_{b1} and S_{b2} above. This type of variability is affected by forming, pressing and calendering conditions. Sidedness is one aspect of the more fundamental Z-D variability resulting from one-directional drainage and retention conditions during forming. Sidedness can be corrected through calendering by densifying one side more than the other to achieve a similar degree of smoothness on each side of the sheet. S_{b1} and S_{b2} form the basis for modelling surface density, which may differ from bulk density. Surface density forms the basis for modelling such end-use performance characteristics as gloss, smoothness/roughness and printability. These characteristics are not important in the current application and will not be discussed further.

Property Flag

The property flag is really not an attribute. Its purpose is to point to the appropriate group of property models. By passing this flag throughout the flowsheet as a stream variable, it is possible to point to the desired set of end-use performance models at many points in the flowsheet simultaneously without having to list it at many individual locations.

PROCESS MODEL

The process model, shown schematically in Figures 2 through 4, is divided into three parts:

I Fiber blending and refining,
II Stock preparation and cleaning and
III Forming.

Each section is discussed in detail below. For a detailed understanding of the individual models, please refer to the MAPPS technical documentation (Reference 7).

I Fiber Blending and Refining

The high density storage tanks are represented by stream initialization blocks called WOOD02. These blocks serve the dual purposes of initializing both the material/energy and the performance attribute streams for the virgin semi-chem and OCC furnishes. By means of module parameters, each WOOD02 block initializes the total mass flow, composition, temperature, pressure and fiber characteristics of an entering fiber stream. Because the OCC is a true mixture of hardwood and softwood components, it is necessary to use two WOOD02 blocks, one for the softwood and one for the hardwood components of the OCC. The characteristics of the hardwood component of the OCC are assumed to be close to the semi-chem hardwood. The softwood component is assumed to be similar to a southern pine.

The OCC blend is obtained by mixing the two streams in Module 4. The STOMIX module determines the mixture attributes as well as the mixture composition and thermodynamic properties of the OCC.

The virgin semi-chemical pulp is initialized by Module 1, representing the high density chest, thickened to refining consistency by Module 5 and refined by the primary (hole) refiner (Module 7) then mixed with refined OCC in the blend chest (Module 9). OCC furnish consists of a recycled hardwood initialized by Module 2 which is then mixed with a softwood component initialized in Module 3. The OCC consists of equal portions of hardwood and softwood fibers.

Entering fiber streams 1 through 3 are initialized by specifying the total stream mass flow rate, moisture content, temperature and pressure in Blocks 1 through 3, respectively. The individual fiber flows are not specified. Instead, the individual fiber component flows are determined from the fiber length and width distributions based on either the species data base default values or user-specified values of the mean and standard deviation of length and width distribution parameters.

The default values for all PAT's are determined for each stream by specifying a wood species. WOOD02 initializes all the PAT's using the species data base which assumes that each pulp consists of fibers which have not been pulped or refined. To represent the pulping steps the fibers have been exposed to, selected PAT values are manually overridden in each WOOD02 block. For example, for the semi-chemical HW pulp, the yield, fiber length statistics, fiber width statistics, freeness and several other parameters have been overridden in Module 1. Initialization values chosen for each furnish are shown in Table IV. The OCC column contains information on the hardwood and softwood components of the OCC specified in Modules 2 and 3 and the mixture values determined in the mixer block (Module 4).

Table VII: PAT Initialization Data Parameters Used in WOOD02

Species	Semi-chem Pulp Hardwood	OCC Furnish Comp.		OCC Mix
		Hardwood	Softwood	
Fiber Length Distribution				
Weight Average, mm.......	1.4	1.4	3.0	2.2
Standard Deviation, mm t.	2.5	2.5	2.5	2.5
Fiber Width Distribution				
Number Average, mm.......	0.02	0.02	0.04	0.03
Standard Deviation, mm t.	2.0	2.0	1.15	1.65
Cell Wall Thick, microns...	1.2	1.2	1.2	1.2
Yield, %..................	74	74	60	67
Kappa Number...............	46.2	23.9	185.5	104.7
* CSF, ml....................	656	150	667	316
Specific Bond Str $x10^{-8}$....	0.2	0.2	0.2	0.2
Fiber Tensile, km..........	10	10	10	10
Fiber Elastic Modulus, GPa.	4.5	4.5	4.5	4.5
* Total Wood Flow, $lb/hrx10^{-6}$	3.88	4.254	4.254	8.5
Wood Moisture (fraction)...	0.99	0.90	0.90	0.90

Notes: (1) Dry fiber flow is one minus wood moisture multiplied by total wood flow. (2) The OCC freeness was not known and the CSF values in Modules 2 and 3 were based on experience. (3) The * indicates that the semi-chem HW CSF and the total mass flows of semi-chem and OCC were varied.

The ratio of OCC to total pulp flow was varied by changing the dry wood flow rate in the OCC initialization blocks, Modules 2 and 3. Refining consistency into the refiner was adjusted by varying the discharge consistency in Modules 5 and 6 and refining load was adjusted by varying the specific power in Module 7. The specific power was set to zero in the OCC stock refiner to reflect the fact that this refiner was not used.

The apparently large standard deviation values for length and width may be explained by the fact that the terms involving the standard deviations in the distribution functions are based on the natural logarithm of the standard deviations.

The blended stock was brought to tickler refiner consistency in Module 10 and refined in Module 11. Stock was then passed to the machine chest, Module 12, which was modelled as a mixer with only one inlet stream. The pulp then passes to the stuff box which is treated as a simple splitter, Module 23. The overflow, stream 34, is returned to the blend chest, module 9.

Each of the fiber streams contains a range of fibers with names FINES, FIBER1, FIBER2 to FIBER10 and shive components called SHIVE1 through SHIVE3. Each fiber fraction represents a specific range of Bauer-McNett fiber lengths and a narrow range of Sommerville shive slotted screen fiber widths, all 0.15 mm or greater. Each shive component covers the entire range of fiber length but has a specific range of fiber widths greater than 0.15 mm. These dimensions are somewhat arbitrary and may be varied by changing the model coding.

For a given set of fiber statistics, mean and standard deviation, the discrete distribution is determined and represents the weight fraction of each fiber component. Each component flow is then determined directly from the total fiber flow and the fiber fractions.

Refiner feed consistency was controlled by specifying the discharge consistency in each of the thickener blocks (Modules 5, 6 and 10).

Refining

The virgin stock and OCC are refined in Modules 7 and 8, respectively. The stock is then combined in the blend chest (Module 9) with broke (Stream 31) and Stuff Box overflow (Stream 34). The combined stock is refined in the tickler refiner (Module 11). In the current process the OCC was not refined initially, so the specific power in Module 8 was set to zero. Other refining conditions are summarized in Table VIII.

The HYRFN1 module simulates a wide range of refiner conditions from groundwood to chemical pulps. Two major categories of refiners can be modelled, chip refiners and all other types of refiners, classified in MAPPS as secondary refiners. The key difference is that chip refiners expect the inlet stream to contain chips while "secondary" refiners work with stock streams containing no chips. The freeness development and fiber length kinetic models are different for these two major types of refiners. For this application refiner type switch is set to 2 to indicate a stock refiner.

Both refiners are specified as atmospheric with minimal idle power loss. Conditions for the OCC refiner (Module 8) are not listed since this refiner was not used during the test. The user may specify refiner specific power directly or indirectly. For this study, the specific power was input directly for each case. For indirect specification, specific power is determined by means of a model based on plate gap, rotational speed, rpm, and inlet consistency.

Table VIII: Refiner Parameters (typical values)

Parameters	Hardwood Primary	Blended Stock Tickler
Refiner Type...............	2	2
Outlet Pressure............	14.7	14.7
Power Model (Not Used).....	--	--
* Specific Power............	1.95	0.05
Idle Power (Fraction)......	0.05	0
Plate Geometry (Not Used)..	--	--
Species....................	3	Not Specified
Process Model Flag.........	5	5
Distribution Type flag.....	1	1
Kinetic Parameters:		
AL1 (Mean Length)........	30	3
AL2 (Standard Deviation).	-1	0
AW1 (Mean Width).........	0.98	-0.5
AW2 (Standard Deviation).	0	0
Fiber swelling parameter...	0.001	0.001

The refiner "kinetic" parameters were tuned to agree with the generally observed discharge CSF and fiber length for the base case. These parameters determine the change in fiber length and width distributions for a given specific power load, consistency and pulping yield. The tuned parameters were then fixed and the only parameter which was changed for the remaining cases in the refiner modules was the gross specific power. The fiber swelling parameter is used to tune the fiber swelling model which uses the specific power, rpm, plate and fiber geometry, and energy per impact to determine the degree of fiber swelling. Generally, the fiber stiffness parameter, Smod, calculated by MAPPS is reduced as fiber swelling increases. However, fiber swelling conditions do not appear to be significant at the yield level used in this study.

Other Streams

When chemical pretreatment is used, as in CTMP, the pretreatment unit generates an information stream containing data on the degree of penetration of the pulping liquor. These data are passed to the refiner by an information stream which influences refining performance. The "information streams," all represented by Stream 87 entering the refiners, are not used in this application.

In addition to the fiber discharge streams, such as streams 9, 11 and 14, refiners units generate steam and heat loss streams. These streams are generally only significant for mechanical pulping systems but are shown here for completeness.

Adjustments

The GENPRS block, Module 40, is placed after the blend chest to adjust selected PAT's at this stage of the simulation. GENPRS, which stands for "general process module," can function as a generic module which influences PAT's but has no effect on mass and energy flows, or it can, as it is used here, adjust PAT's up or down. No adjustments were required for the current study.

Handsheet Properties

Handsheet properties at the discharges of the hole refiner, blend chest and tickler refiner were determined through PROPS blocks Modules 46, 47 and 48, respectively. The setup of a PROPS module is described in detail in a later section. Generally, the only parameters which are required are the stream number of interest (i.e., streams 9, 11 and 14) and the handsheet basis weight. Additional parameters which were needed for this study were the handsheet press pressure and the formation index. This was necessary because there was evidence that the handsheet forming conditions varied significantly from sample to sample. After specifying the handsheet pressing pressure and fiber formation index, the models predicted the handsheet properties more accurately. Handsheet conditions are discussed in detail in a later section.

II Screening and Cleaning System

Refined pulp from the tickler refiner enters the Machine Chest, Module 12, and is pumped directly to the Stuff Box, represented by a total flow splitter, Module 23. In the white water silo, mixer Module 24, the refined pulp, saveall fibers (Module 50) and accepts from the secondary screen and secondary cleaner (Modules 34 and 27, respectively) are diluted with white water. Pulp consistency is controlled by means of a thickener block, Module 37, before entering the primary cleaner, Module 25. The cleaning and screening system consists of four cleaners, Modules, 25, 27, 29 and 30, and three screens, Modules 32, 34, and 35, respectively. The flow is counter-current with accepts passing back into silos and reject chests as shown. Saveall cloudy filtrate is used for dilution in tertiary cleaner chest, Module 31, and clear filtrate is used for dilution in this tertiary screen chest, Module 38. Streams 45 and 53 represent cleaner and screen sewer rejects, respectively.

All screens, cleaners and thickeners are modelled through the same HYFRAC module by specifying a switch (1 = screen, 2 = cleaner, 3 = thickener). In addition to the unit switch, only one parameter is required for this module. For screens and cleaners, the only required parameter is the reject total flow split, while for thickeners, the parameter is the discharge consistency. Cleaners and screens fractionate the pulp removing shives and separating the fibers on the basis of aspect ratio or fiber length.

When used to model a screen or cleaner, HYFRAC determines the separation of all components and, from the specified total flow split, determines the consistency of the accept and reject streams. In addition, HYFRAC determines the freeness and selected handsheet properties of the feed, accept and reject streams. Generally, rejects tend to be enriched in shives while accepts tend to be enriched in shorter fibers.

Module parameters for the screening and cleaning system are summarized in Table IX. All parameters in this section were adjusted initially to predict the generally observed level of fiber reject losses for the base case and were then fixed for the duration of the study.

Table IX

	Module Parameters	Fiber Losses lb/hr
Consistency Controller........	1	
Cleaners - Reject Flow Split %		
Primary.....................	15	---
Secondary...................	10	---
Tertiary....................	10	---
Fourth......................	10	651
Screens - Reject Flow Split %		
Primary.....................	5	---
Secondary...................	10	---
Tertiary....................	10	775

Typical fiber losses predicted from the system are shown in Table IX for the fourth cleaner and tertiary screen. The total losses of 1400 lb/hr were in the range of values reported by MacMillan Bloedel.

Paper machine headbox consistency is controlled in the model by module 36 which passes excess dilution water into reject chest 33.

III Forming Section

The paper machine is modelled in four parts with four different Fourdrinier blocks, Modules 13, 41 42 and 45, to represent the CD variations possible across the machine. However, no attempt was made to model CD variations, and the conditions specified for each module are currently the same. The headbox stock stream is split into four equal parts by Module 43 and each Fourdrinier block represents the headbox, slice, gravity drainage forming board, foils, vacuum boxes and couch roll over one-fourth of the width of the machine. The Fourdrinier block computes the mass and energy flow and attributes of the mat, trim and white water drained and, to confirm that the property level of dewatering has occurred, an "undewatered slurry" stream is also calculated if excess slurry remains.

Since the slurry and mat streams are recombined in Module 14 to represent a single sheet of machine paper, all differences between the four CD sheets are lost in this particular model. However, by passing each CD mat stream through a parallel series of press modules, CD variations could have been tracked using the Property block (Module 22). After re-combining the CD sheets into a single sheet in Module 14, the machine-width sheet is passed through three successive press nips (Modules 15, 16, and 17). No attempt was made to model the lump breaker roll, and its effects have been assumed to be accounted for in the sheet leaving the first press (Module 15).

Parameters used in modelling the Fourdrinier are summarized in Table X and typical profiles predicted by the Fourdrinier blocks are shown in Table XI.

It should be noted that no mill data were available to verify the profiles presented in Table XI and no adjustments were made to the Fourdrinier modules during the validation study. The drainage profiles are simply presented as information.

The forming section performs a variety of tasks too numerous to mention in detail. For instance, the fiber contact area, formation factor, fiber orientation and wet strain attributes are initialized and the sidedness and Z-D variability information are generated. Calculated parameters include the sheet moisture, freeness and the fiber length distribution of the mat, white water and "undewatered slurry", and the retention of suspended solids.

<u>White Water Recycle and Saveall</u>

To model the saveall system, all trim and white water streams were combined into white water tank, Module 44, and then passed directly to Module 19 representing the saveall. Losses from the saveall, assumed to be negligible, were set by adjusting the split ratio of splitter module 50 to 0.001, a loss of only 0.01%. The disk saveall model generates three fiber streams, the recovered fiber (Stream 30), cloudy filtrate (Stream 29) and clear filtrate (Stream 16). The filtrate streams were sent back to the screening and cleaning to be used for dilution and consistency control and the recovered fiber was returned to the stock blending system.

<u>Press Section</u>

The press section of the machine consists of a lump breaker followed by three press nips. In the model, the lump breaker is combined with the first press nip, Module 15. Each press nip is represented by a wet press model, the WPRESS block, which computes the degree of water removal and web consolidation as a function of lineal press load, the number of felts and basis weight, machine speed, press speed and fiber characteristics such as CSF, yield and CWT. The attributes changed by the presses are the fiber contact areas, S_{b1} and S_{b2}. The module also determines the power requirements of the press and nip residence time but neither of these variables is discussed in this study.

Table X: Forming Conditions (applied to all four FOUR01 modules)

* Machine Speed............................	31/67 ft/sec
Headbox..................................	
* Slice height (typical)................	40 mils
JWR (typical)..........................	0.934
Pressure...............................	14.4 psi
Pond Height............................	12.5 ft
Lip Extent.............................	5 mils
Lip Angle..............................	10 degrees
Machine Dimensions	
Width..................................	24 ft
Gravity Drainage Section	
Length.................................	50 ft
Foil Section	
Section Length.........................	20 ft
Number.................................	10
Angle..................................	5 degrees
Length.................................	0.6 ft
Table Roll Section	
Section Length.........................	20 ft
Number.................................	3
Diameter...............................	0.1 ft
Wet Vacuum Box Section	
Length.................................	1 ft
Number.................................	7
Vacuum.................................	1 psig
Dry Vacuum Box Section	
Length.................................	1 ft
Number.................................	4
Vacuum.................................	1 psig
Dandy Roll.............................	None
Diameter............................	-
Speed Difference....................	-
Wire Geometry..........................	defaults
Trim Fraction..........................	0.0075
Fiber Orientation......................	1.5
Wet Stretch (Speed Differnce)..........	0.0
Suspended Solids Diameter..............	100 microns
Drainage & Retention Parameters........	
CRESIS (Mat Resistance Parameter)....	350
VCOEF (Foil Coefficient).............	1.0
AFP (1st Fiber Retention Parameter)..	8.0
BFP (2nd Fiber Retention Parameter)..	10.0
ABW (Drainage & Retention Parameter).	-0.02

* indicates parameters which were varied during the study.

Table XI: Typical Forming Conditions

Cumulative Drainage Rate, cu ft/hr	
Forming Board....................	1460.5
Foils..............................	50970
Table Rolls.......................	53501
WVB's.............................	61190
DVB's.............................	64289
White water consistency, %	
Inlet..............................	0.65
Forming Board....................	0.513
Foils..............................	0.3178
Table Rolls.......................	0.3035
WVB's.............................	0.2665
DVB's.............................	0.2540
Mat Consistency Profile, %	
Forming Board....................	0.86
Foils..............................	1.97
Table Rolls.......................	2.36
WVB's.............................	6.90
DVB's.............................	25.0
Basis Weight Profile, g/m_2	
Forming Board....................	0.9
Foils..............................	78.46
Table Rolls.......................	85.91
WVB's.............................	108.7
DVB's.............................	118.0

Table XII: Press Parameters

	1st Nip	2nd Nip	3rd Nip
* Machine Speed, fpm.................	1900	1900	1900
Width, ft...........................	21.33	21.33	21.33
Number of Felts....................	1	1	1
Top Roll Radius, ft................	1.5	1.5	1.5
Bottom Roll Radius, ft.............	1.5	1.5	1.5
Felt Basis Weight, oz/100 ft^2......	1313	1313	1313
* Press Speed, fpm..................	1890	1890	1890
* Press Loading (PLI), lb/lineal in..	380	550	600
Mat Compressive Modulus............	1	1	1
Optimum Basis Wt, lb/1000 sq ft....	26	26	26
Typical moisture profile, %			
Entering.........................	25	30.5	37.2
Exiting..........................	30.5	37.2	42.0

* indicates parameters which were varied during the study

Other attributes calculated by the WPRESS module are the caliper of the sheet entering and leaving the nip, determined by the estimated degree of densification during pressing, and the degree of sheet consolidation relative to water removal, determined by the compressive modulus, C_{mod}. C_{mod} can be determined internally but it may be necessary to override the default value of C_{mod} to obtain reasonable values of the dewatering for a given caliper change. After tuning the modules to match the base case, only the third nip press loading was changed. Press conditions are summarized in Table XII.

Drying

The pressed sheet is passed through a single dryer block, Module 18, which simulates a conventional air-hood multi-can dryer system. For more detailed simulation of the dryer system, multiple dryer blocks could be used. In each case, the steam flow was varied by hand to achieve the desired dry sheet solids of approximately 93% while holding steam pressure and air flow constant. The dryer input parameters are summarized in Table XIII.

Table XIII: Dryer Conditions

Steam Economy........................	0.5
Blowthrough Ratio....................	0.10
Steam Pressure Drop..................	3.00
Web temperature Rise.................	4.00
Leakage Air Ratio....................	-0.02
Room Temperature.....................	28.0
Room Humidity........................	0.85
Electrical Power Coefficient.........	1.00
Web Stretch (Speed Differential), %..	1.3

The total, cumulative MD stretch of 1.3% was assumed to occur in the section. This stretch was one of the key factors contributing to the predicted MD/CD tensile and modulus ratios.

Performance Attribute Parameter Adjustments

Module 49 is a GENPRS or general purpose simulation block which can be used to modify PAT's on a relative basis. In this particular application, two variables, contact areas Sb_1 and Sb_2, were decreased by 10 and 30%, respectively. This adjustment was required to reflect the over-prediction in the densification of the sheet which occurred during pressing, particularly on the top side of the sheet where Sb_2 increased from 4 to 18 while the contact area on the wire side, Sb_1, entering with a value of 4.26, did not increase at all.

Because of the loss of fines during the initial phases of drainage, the hydrodynamic specific surface of the wire side of the sheet was significantly lower than that of the top side and the effective freeness and fiber length were significantly higher. The top side of the sheet approached the average fiber length and freeness of the entering slurry, 0.50 mm and 415 ml, respectively, while the wire side fiber length and freeness were 1.55 mm and 611 ml, respectively. Since the caliper change predicted in the press and property modules (WPRESS and PROPS) depends on the change in fiber contacts averaged over the top and bottom of the sheet, the excessive increase in Sb_2 increased the average contact area and the average bond area, S_a. This resulted in a prediction of excessive sheet density and properties such as tensile strength and modulus which depend on either sheet density or bond density. By correcting S_{b1} and S_{b2}, the entire system of properties was adjusted to more accurately reflect the mill data.

In retrospect, the sidedness differences predicted by the model can be seen to be a function of the large quantity of fines recycled within the white water system. These fines significantly reduce the freeness and fiber length at the headbox from the average of the fiber furnishes, and the characteristics of the final sheet reflect the selective retention of fibers, particularly fines, during forming. The forming model predicts that the retention of fibers increases from the bottom to the top of the sheet, resulting in higher fines retention as the basis weight develops. Thus, the top of the sheet retains most of the fines present in the headbox slurry while the bottom is nearly devoid of fines and the model makes no provision for migration of fines between the layers. However, the average contact area is assumed to be an average of the typical level of fiber contact throughout the thickness of the mat and is in good agreement with the average fiber length and freeness values carried in the PAT stream for the mats which are 0.76 mm and 544 ml.

In the future, this modelling problem can be reduced by reducing the sensitivity of the compressibility model to CSF. Alternatively, a new adjustable parameter could be added to the press model to allow the user to adjust the sensitivity of the compression to CSF. A similar approach would also be necessary for any other module which densifies the sheet, such as the calender block. These options are discussed in more detail in the section on FUTURE WORK (Module Modifications).

Calendering

To represent calendering, the medium (Stream 28), at 93% dryness is sent through a single nip calender, Module 51, to the reel.

The calender changes sheet caliper, and bulk and also influences sheet bonding levels. The calendering effect is strongly dependent on nip loading and the response of the fibers to loading and, in turn, bonding or debonding behavior depends on the relationship between the sheet moisture and temperature and the thermal softening temperature of the fibers. Because the nip loading was not known, the load used in the simulation was tuned to 15 lb/in where the observed caliper under load and without load was in reasonable agreement with the mill data. The calender model considers heat transfer in the nip and on the roll surface as well as the effects of wrap geometry, machine speed, roll temperature, roll radii, sheet basis weight and speed differentials and also allows for additional moisture addition by adding a steam or water stream.

The input parameters for the calender block are summarized in Table XIV. Calender speed and loading were varied during the study. The calender loading was set at 15 lb/in for reels 1 through 6 and zero for reels 7 and 8. For reels 9 through 14, loading was gradually increased to 15 to reflect the apparent transitional change in caliper, density and modulus after the load was reapplied. Although thermal transients are not considered in the model, these effects could be simulated in the future by assuming roll temperature increases gradually after reapplying the load.

Although sheet basis weight measured at the reel is known to fluctuate, an assumed average value of 0.117 kg/m^2 was used for the calender calculations. CD basis weight variability could also play a roll in the application of pressure to the sheet and, in the future this variation could be taken into account by the addition of multiple sets of presses and calenders to track the CD basis weight and PAT's through the machine.

The wrap configuration flag was set to 0 to indicate that the sheet passes directly through the nip without a roll wrap. No MD sheet strain or change in orientation was assumed for the calender nip as all MD strain was lumped into the dryer section. The compressibility parameter was adjusted to increase the nip intensity factor to fit the initial caliper levels of the calendered sheet at the assumed low nip loading. Since both the compressibility and the loading affect caliper and density, no unique combination of these parameters can be determined unless the actual lineal loading is measured.

Table XIV: Calendering Data

* Calender Speed	579
* Calender Load	15
Roll Temperature	
Top	180
Bottom	180
Roll Radius	
Top	37.5
Bottom	37.5
Basis Weight	0.117
Wrap	0
Strain	0
Orientation	0
Compressibility Parameter	-0.220

* Indicates parameters which were varied during the study.

Broke System

The recycle of broke was modelled by splitting off a portion of the calendered medium using splitter Module 20. The percentage of broke was varied to match mill conditions and the broke was mixed with other furnish in the blend chest, module 9.

Property Calculations

All property calculations were performed by a PROPS block. The PROPS block computes a set of handsheet and machine paper properties for a specific stream using the PAT and mass flow information in the stream. Valid handsheet properties can be determined on any fiber-containing stream in the flowsheet, but paper property predictions apply only to the formed, pressed, and dried sheet.

To calculate machine-made paper properties, the sheet basis weight must be specified as a parameter in the PROPS block or, alternately, the machine speed and width must be specified elsewhere. For handsheet properties, the handsheet basis weight must be specified in the PROPS block. Properties calculated by PROPS are shown in Table XV.

Table XV: Properties Determined by PROPS

* Basis Weight...............	* Directional Moduli............
* MD/CD Tensile Ratio........	MD, CD and ZD.................
* Density....................	Directional Tensiles..........
	(ultrasonic models)...........
Wet Web Strength...........	MD, CD, ZD....................
Tear Factor................	Shear Modulus (MD/CD plane)...
* Burst Factor...............	Directional Compressive Moduli
* MD & CD Breaking Length....	MD and CD.....................
Drainage Time..............	Taber Stiffness...............
Scattering Coefficient.....	Surface Roughness.............
* Gurley Porosity............	* Caliper.......................
Opacity....................	* STFI (MD CD) Rupture Energy...
* Flat Crush.................	
* Elongation At Break........	* Concora.......................
Young's Modulus............	* CD Ring Crush.................
Brightness.................	

* Indicates properties considered in this study

Machine Paper Properties

Machine paper properties were predicted for the dry calendered medium, Stream 103, by using PROPS Module 22. Although Module 22 was used to predict both handsheet and machine paper properties, the machine paper properties are of primary interest at this location and are discussed in later sections. All measured and predicted machine paper properties are listed in Appendix II.

Machine paper properties are based on the PAT values in the stream of interest and the basis weight. The basis weight may either be specified or determined from the stream flow rate and the specified machine width and speed supplied as module parameters.

Handsheet Properties

Five PROPS blocks, Modules 46, 47, 48, 52 and 53, were used to predict handsheet properties for the hole refiner discharge (Stream 9), blend chest discharge (Stream 11), tickler refiner discharge (Stream 14), the headbox (Stream 55), and the broke tank discharge (Stream 31), respectively. Handsheet properties are dependent upon the component PAT values (i.e., fibers and fillers) and on handsheet formation factors such as pressing pressure, formation index and fiber orientation. This information can be provided by the PROPS module parameters or as a backup; default values will be assumed. PROPS Module parameters specified for each case in the study are shown in Table XVI. The complete set of handsheet properties, both measured and predicted, is listed in Appendix III.

Table XVI: Input information to PROPS

Handsheet Fiber Orientation..	1.0 (random)
Wet Strain....................	1.0 %
Pressing Pressure............	Variable (20-50 psi)
Formation Factor.............	Variable (0.5 to 1.0)
Basis Weight.................	Measured input

DATA ANALYSIS

Assumptions which apply to the analysis of the data can be summarized as follows:

1) Transient process data can be analyzed using the steady-state MAPPS simulation program.

2) Data which were not known can be estimated.

3) Input data conditions obtained from the mill were assumed to be accurate.

4) Only variations attributed to the primary variables were analyzed.

Testing Variability

Testing replicates, varying from 10 to 20 on each sample resulted in a distribution of measured values. The number of replicates was higher for tests such as concora which have greater variability or lower reproducibility. For each reel, the standard deviation of each distribution was determined about the mean value for each test property. The average of these values over all 24 reels was then used as the overall measure of testing variance for each property. The standard deviation of the measurements is summarized in Table XVI. Measurement variances could not be determined on variables such as density, basis weight and caliper, which had only a single measurement.

Table XVIII summarizes statistical data relating to CD variability (Rolls) on each paper property. Data include the maximum value (Max), minimum value (Min), and Mean for each CD position, indicated by roll positions 1 through 3. The table measures the overall variations which occurred during the tests and these variations are based on the average test values, rather than the individual test total variation for each sample. The mean values indicate the average CD variability in the data and indicate that, on the average, the CD variability is within individual test measurement variances and, therefore, is not statistically significant. However, visual inspection of the data over portions of the test groups indicates that certain variables may exhibit some meaningful CD variability. These are discussed in a later section.

Table XVII: Measurement Variance

	Std Dev	Number of Tests	T-Test	90% Confid Interval 2 Std Dev
MD Tensile, km.........	0.39	10	1.812	0.78
CD Tensile, km.........	0.188	10	1.812	0.38
MD Stretch, %..........	0.19	10	1.812	0.38
CD Stretch, %..........	0.425	10	1.812	0.85
Burst Factor...........	2.33	10	1.812	4.66
MD Modulus, GPa........	0.155	10	1.812	0.31
CD Modulus, GPa........	0.112	10	1.812	0.22
Caliper, mils..........	0.39	1	6.314	0.78
Gurley Porosity, %.....	3.07	10	1.812	6.14
Concora, lb............	3.6	10	1.812	7.2
MD Ring Crush, lb/6 in	6.2	10	1.812	12.4
CD Ring Crush, lb/6 in	3.2	10	1.812	6.4
MD STFI, lb............	1.9	20	1.725	3.8
CD STFI, lb............	1.6	20	1.725	3.2
Moisture, %............	0.38	5	2.015	0.78

A complete list of machine paper properties (measured and predicted) may be found in Appendix II.

Although statistically the means do not vary significantly across the machine, plots of the data against reel number show that some of the variables such as basis weight, caliper, density and tensile strength, may exhibit a persistent CD bias. In some cases, the CD bias lasts only one shift and then shifts to a different but also consistent bias on another day. In cases where CD bias is not visually obvious, the overall statistics are based on the pooled data for all rolls.

A comparison of the overall variation with the average measurement error (standard deviation) indicates that the overall variation is not significantly greater than the measurement variation. For example, the MD tensile standard deviations for rolls 1 through 3 are .285, .317 and .394, respectively, while the average measurement standard deviation is 0.39. The results are similar for the CD tensile.

Table XVIII: Machine Property Data Summary CD Variability

Roll Position 1	Min	Max	Mean
Basis weight, lb/1000 ft^2..	24.92	26.48	25.59
Caliper, mils...............		8.16	
Density, g/cc...............	0.508	0.657	0.585
MD Tensile, km..............	5.52	6.48	5.90
CD Tensile, km..............	2.25	2.77	2.52
Burst Factor................	25.6	33.3	28.8
MD Stretch, %...............	1.45	1.77	1.61
CD Stretch, %...............	2.53	3.03	2.81
MD Modulus, GPa.............	3.41	4.78	4.27
CD Modulus, GPa.............	1.37	2.05	1.80
MD STFI, lb/in..............	21.0	24.1	22.78
CD STFI, lb/in..............	13.2	15.7	14.6
CD Ring Crush, lb...........	48.86	59.12	53.70
Concora, lb.................	48.17	67.59	54.10
Gurley Porosity, sec/cc....	14.25	28.80	20.84
Moisture, %.................	6.5	7.26	6.80

Roll Position 2	Min	Max	Mean
Basis weight, lb/1000 ft^2..	24.7	26.0	25.2
Caliper, mils...............		7.9	
Density, g/cc...............	0.515	0.67	0.59
MD Tensile, km..............	5.55	6.68	6.00
CD Tensile, km..............	2.47	2.86	2.65
Burst Factor................	27.0	31.12	29.4
MD Stretch, %...............	1.46	1.81	1.66
CD Stretch, %...............	2.11	2.57	2.39
MD Modulus, GPa.............	3.44	4.82	4.40
CD Modulus, GPa.............	1.53	2.38	2.00
MD STFI, lb/in..............	21.0	24.5	22.72
CD STFI, lb/in..............	13.7	*30.56	15.1
CD Ring Crush, lb...........	48.3	59.15	54.11
Concora, lb.................	47.8	59.6	52.8
Gurley Porosity, sec/cc....	11.75	29.0	19.5
Moisture, %.................	6.44	8.10	6.91

Table XVIII: Machine Property Data Summary CD Variability

Roll Position 3	Min	Max	Mean
Basis weight, lb/1000 ft^2..	24.9	26.2	25.44
Caliper, mils..............		8.0	
Density, g/cc..............	0.515	0.660	0.590
MD Tensile, km.............	5.07	6.74	5.93
CD Tensile, km.............	2.18	2.71	2.43
Burst Factor...............	25.6	33.3	28.9
MD Stretch, %..............	1.44	1.80	1.63
CD Stretch, %..............	2.39	3.21	2.72
MD Modulus, GPa............	3.51	4.86	4.32
CD Modulus, GPa............	3.51	4.86	4.32
MD STFI, lb/in.............	19.55	25.22	22.67
CD STFI, lb/in.............	12.0	16.77	14.28
CD Ring Crush, lb..........	46.3	59.0	53.0
Concora, lb................	47.7	60.1	54.2
Gurley Porosity, sec/cc....	11.0	28.61	20.6
Moisture, %................	6.43	7.11	6.82

Qualitative Data Comparisons

Property comparisons are divided into two parts: Machine Paper Properties and Handsheet Properties.

Machine Paper Properties

Machine paper property data are listed in Appendix II. For analytical purposes, the properties are plotted against a "reel number" in Figures 5 through 19. Each figure shows the predicted values and one or more sets of measured values. Where more than one set of measured value is available for a reel, the values shown correspond to tests at roll positions 1 through 3, indicating CD variability may be significant. Those properties with only a single set of measured values show all rolls and sets for each reel using the same symbols. CD variability was not significant for these properties.

Basis Weight

Figure 5 indicates the model tracked machine paper basis weight reasonably well with the exception of reels 3, 8, and 11 through 13. The basis weight was controlled in the simulations by adjusting the amount of broke recycle, i.e., by varying the total split fraction in Module 20. By adjusting the broke flow after the calender, it was possible to change the basis weight while maintaining constant overall production. However, the broke adjustment was accomplished by trial-and-error, and the predicted results indicate that a couple of reels were not tuned to the observed basis weight.

Basis weight varied across the machine in a consistent fashion throughout the trial as shown by Figure 5. Basis weight for roll 2 was generally lower than that for rolls 1 or 3. However, the model was not tuned to predict a variation in basis weight in the cross machine direction due to limitations in the size of the MAPPS data file and lack of detailed information on the machine design. The model did contain four separate paper machine modules (Fourdrinier modules 13, 41, 42 and 45). If to complete the CD model each of these could have been adjusted to predict higher retentions on the outside of the reel compared to the center of the reel it would have been necessary to add corresponding presses, calenders and PROPS blocks for each CD section of the sheet. This added computational burden was not considered necessary for the purpose of the study, i.e., to validate the MAPPS module database.

Basis weight showed a downward trend during the later half of the test but did not appear to coincide with changes in any of the major variables changed during this period, i.e., OCC content and machine speed. A reduction in broke flows is one likely cause of the gradual drop in basis weight. The predicted retention profiles did not show much sensitivity to machine speed.

Since most properties are independent of basis weight, any error in prediction of basis weight will have little direct effect on the prediction of other machine paper properties. Exceptions are the compressive properties which are strongly dependent on caliper. Since caliper is directly related to basis weight at a fixed density, the basis weight variations will affect compressive properties.

Sheet Density

The machine paper density profiles, Figure 6, show good agreement between the measured and predicted values with the possible exception of reels 11 through 16 where the model predicts densities that are too high. The most obvious feature of the profile is the change caused by unloading the calender for reels 7 and 8 which the model tracks very well. Both the measured and predicted density are higher before the calender stack is lifted than after it is lifted. Although the model seems to predict the same average density level before and after reels 7 and 8, the measured density seems significantly different. The measured data show a fairly consistent, although weak, CD profile with roll 1 density consistently lower than that of rolls 2 and 3. Measured density also fluctuates significantly during the first 6 reels while the model tracks through the center of the data, and there is no obvious explanation for this fluctuation. It is interesting to note that reel-to-reel variations after the calender is reapplied are considerably lower.

Plots of density against several of the major independent variables showed no obvious direct correspondence between density and these variables (other than calender stack loading). Statistical analysis of the data described in detail in later sections confirmed these observations.

Caliper

Figure 7 shows predicted dry sheet caliper was in good agreement with the measured values from IPST. The most salient feature of the caliper plot is the sharp increase for reels 7 and 8 when the calender stack was lifted. The caliper obviously reflects changes in basis weight and density described previously, and good agreement in these variables implies good agreement in predicted caliper. Other features observable from the figure are the weak CD profile and the different levels of caliper before the stack is lifted (reels 1-6) and after the stack is reapplied (reels 9 through 24). A general downward trend in caliper can also be detected from reels 13 onward. The model tracks these trends quite well throughout the test.

The caliper predicted by the PROPS module is based on a bone dry basis weight and so does not include the small effects of moisture fluctuations in the sheet. However, the tests (measured values) were conducted at conditioned moisture levels at 50% humidity and should have had only a minor effect on caliper.

MD Tensile Strength

The MD tensile profiles shown in Figure 8 indicate that the model followed the data very well except when calender loading was removed where the model predicted a drop in strength which was not observed. During the study MD tensile appeared to have two basic levels, approximately 5.8 to 5.9 km for reels 1 through 11 and approximately 6.3 for reels 12 through 16. A similar trend can be seen in the CD tensile profiles discussed next. The model did not predict the plateau at the same time as the measured results and tended to be lagging in phase. This behavior may be somewhat fortuitous due to the fact that the model assumes steady state conditions and there was no conscious attempt to correct the data for time delays or process lags.

The differences between the average MD tensile and model values was 0.2 to 0.4 km during this plateau period, which is within experimental error. It does not appear that the change is due to a shift in MD/CD tensile ratio, as discussed in a later section.

Possible reasons for the differences in measured and predicted calender loading effects are discussed in the section on individual variable effects (Calender Loading).

CD Tensile Strength

Figure 9 shows that the model tracks the CD tensile within the experimental error of 0.38 km. As with MD tensile, however, the discrepancy is relatively high for reels 7 and 8 where the model predicts a strength loss when the calender stack is lifted. Examination of the data shows a very significant CD profile which tends to drop for roll 3, particularly when machine speed dropped over reels 17 through 24. CD tensile tended to increase during reels 12 through 16. The causes of the discrepancies shown for reels 7 and 8 are discussed in the section on Calender Loading Effects.

MD/CD Tensile Ratio

Table XIX and Figure 18 summarize the general trends for the measured and predicted tensile ratio.

Table XIX: Comparison of Measured and Predicted MD/CD Tensile Ratio

	Minimum	Maximum	Mean	Std Dev
Measured	2.08	2.69	2.35	0.115
Predicted	2.30	2.42	2.39	0.023

These data show that the model predicted the average tensile ratio very accurately and indicates that the MAPPS module assumptions about the degree of wet stretch and fiber orientation were reasonable. The fact that the predicted variations in tensile ratio are lower than the measurements can be explained by the wet strain and orientation. The major contributors to the ratio were assumed constant throughout the test while the measured data reflect the effects of large changes in machine and press speeds. Other contributions to variability, such as shrinkage and loading in the dryer section, are not accounted for in the model.

MD/CD Modulus Ratio

The MD/CD modulus ratio, a measure of the fiber stiffness anisotropy, is also influenced by fiber orientation and speed differentials, and shrinkage. Again, the agreement between measured and predicted values is very good on the average (Table XX). For reasons stated above, the model predicts less variability than is observed. The mean measured modulus ratio is nearly identical to the mean tensile ratio while the predicted modulus ratio is somewhat lower than the value for the tensile ratio.

Table XX: Comparison of Measured and Predicted MD/CD Modulus Ratio

	Minimum	Maximum	Mean	Std Dev
Measured	1.87	2.77	2.36	0.160
Predicted	2.05	2.19	2.15	0.021

MD Stretch

Figure 10 shows that predicted MD Stretch is consistently higher than measured values by a nearly constant factor. For measured values, there is considerable variation across the machine as well as within reels as indicated by the wide bands connecting points at the same reel number.

The effect of lifting the calender on the measured MD stretch is not seen on reels 7 and 8. Again the calender appears to have little or no effect on straining the sheet or on the normal bonding characteristics which influence stretch at break. However, the average value starts out lower on day 2 (reel 9) and then increases significantly by reel 12. The highest values are seen for reel 18 just after the beginning of day 3. There is a gradual downward trend in stretch throughout day 3 at the lower machine speed.

The model predicts that stretch should not really change much over reels 1 through 6 but drop significantly for reels 7 and 8 as a result of less bond development in the absence of calender load. The stretch does not return to the previous levels for reels 9 and 10 because the simulated stack loading was not immediately reset to 15 PLI, as with reels 1 through 6, but was increased in steps. The 15 PLI stack loading was set, the predicted stretch was at or above that of reel 1 through 6.

Burst Factor

Burst factor profiles, shown in Figure 11, show trends similar to breaking length as expected. The burst factor model, a modified version of the van den Akker model, assumes that burst is a function of the geometric mean of the MD and CD tensile strength and the MD stretch, as follows:

$$BF = Constant * STR\ (Z_{md}\ Z_{cd})^{1/2}$$

where

BF = burst factor
STR = MD stretch
Z = Breaking Length

The model suggests that BF will vary directly with MD stretch. Comparing the figures for tensile and stretch with burst, it appears that burst values on day one do vary directly with tensile and stretch values. BF starts out low on day 2 (reels 9 and 10) and then increases to a general maximum around reels 12 or 13 and, on day 3, a general downward trend in BF, again coinciding directly with tensile and stretch.

Although not statistically significant, there is visual evidence of CD variability in BF, as shown in Figure 11. As with tensile and stretch, there is no apparent effect of calender stack loading shown by the model. There is little visual evidence of a consistent CD burst profile.

The general coincidence of the four tensile properties indicates that the measured trends are real and not random, and the general agreement of the model with the measured data suggests that the trends are predictable. However, there are no data to suggest what may have happened over the 16-hour period between the end of day 1 and the beginning of day 2 to cause all four tensile properties to be lower than the previous day. Particularly puzzling is the fact that the paper density decreased at the same time that tensile strength increased toward a maximum at reel 13.

Except for the effect of calender loading where the models predict a drop in burst, the models tend to predict burst somewhat high. However, the model predictions still lie within a band defined by the combined variability in burst due to measurement error and CD variability. The measurement variability is discussed in a later section.

MD Elastic Modulus

The MD Modulus profiles shown in Figure 12 clearly indicate the close correspondence between measured and predicted values with a small but consistent offset of about 0.3 GPa which is comparable in magnitude to the measurement variance. The most important feature of the data is the effect of calender loading, which is consistently predicted by the model. Unlike the tensile properties, the modulus values start out day 2 at about the same levels as the end of the day 1 before the calender stack was lifted. The modulus tends to increase to a maximum at about reel 15 toward the end of day 2. There is a generally lower level of modulus for day 3 whose dominant variable is the lower machine speed. These lower levels coincide with the lower density levels as predicted by the models.

The property development models are based on a theory that there is a general correspondence between sheet densification and bond formation during the papermaking process up until the sheet is dry. Increased density leads to increased bond density, relative bonded area and, other things being equal, increased strength and elastic properties. The calender model is based on a theory that additional densification during calendering can either increase or decrease strength by creating additional bonds or by breaking existing bonds. The bond formation/bond breakage process is proportional to the degree of densification and is controlled by the moisture and temperature of the sheet in the calender. It is generally observed that increased densification leads to strength loss and a decrease in modulus. Only rarely, as with glassine to which moisture is added, is a strength increase observed. Also there is substantial evidence that modulus and strength are both governed by bonding levels and should therefore behave in the same way with densification.

CD Modulus

CD modulus profiles shown in Figure 13 also indicate a good level of tracking between the model and the measured values with a nearly constant offset. This offset is discussed in more detail in a later section. The calender effect is the dominant effect predicted. The modulus levels at the beginning of day 2 (reels 9 through 11) are lower than at the end of day 1 as seen with the tensile properties and in slight contrast to the MD modulus. The general levels of CD modulus also tend to peak toward the end of day 2. There is a slightly lower modulus level throughout day 3 at the lower machine speed, which is consistent with the generally lower density levels on day 3.

Gurley Porosity

Gurley porosity (Figure 19), which is inversely proportional to sheet porosity, follows several swings throughout the three-day period. The lowest Gurley, or highest sheet porosity, corresponds to the low calender stack loading as predicted by the model. Here the predicted Gurley tends to track density while the measured Gurley tends to track density and other variables as well. Porosity is generally lower on day three while density is lower, which is contrary to the effect predicted.

The effect of calendering on Gurley appears to be stronger than predicted. Since the model assumes porosity is proportional to bulk density, the effect of calendering, which may be mainly a surface effect, could lead to an under-prediction of the effect of calendering. In other words, if the calender tends to increase the surface density more than the bulk density, the porosity measurement, which should be more sensitive to surface porosity, should be more strongly affected. This suggests that the Gurley model should be based on surface density rather than bulk density and would be consistent with the gloss and smoothness models which are also based on surface density.

Compressive Properties

MD and CD STFI

The MD and CD STFI data do not show a significant trend throughout the three-day period as shown in Figures 14 and 15. The model's predictions tend to show a similar insensitivity to most variables except for a downward blip for one reel with the calender backed off. The variations in the data are less than the measurement variance indicating that there are no significant variable effects, and the offset between the model and measurements is consistently about 1.5 lb/in, which is within experimental error. The statistical analysis, which is discussed in the validation analysis, shows that with the correction multiplier for MD and CD STFI taken into account, the model fits the data extremely well.

It is interesting to note that STFI was not strongly affected while modulus was. Here the theory provides some insight. The model for STFI stiffness is related to the product of MD and ZD modulus and the sheet thickness. The moduli, as already demonstrated, are directly related to the density and inversely related to the thickness. Also, the moduli contain a strong linear density component but are basically nonlinear over a large range. Therefore, one would expect qualitatively that a variable which increased caliper would have the opposite effect on modulus and no effect on STFI, consistent with the behavior seen throughout the test.

CD Ring Crush

Data for both MD and CD Ring Crush were obtained, but only CD Ring Crush was modelled and analyzed. Although CD Ring Crush behaves very similarly to STFI, the measurement errors indicate that Ring Crush, and CD Ring Crush in particular, is highly variable, as shown by Figure 16. With a 6.4 lb/6 in. variance due to measurement error, the model predictions fall close to the lower end of the confidence range. However, if a constant correction factor is used as discussed in a later section, the predictions fall well within the 90% confidence band.

Ring Crush levels were about the same at the end of the trial as at the beginning even though the OCC content had increased by 7%. This and other evidence indicates that OCC has little effect on compressive properties. Machine speed appears to have little effect also. Lower ring crush for the period when the stack was lowered indicated there is some sensitivity to calender load and the model predicts a drop for reel 8 but little effect for reel 7. The effect of calender loading on compressive properties is discussed in more detail in the following sections.

Concora

It is apparent from the concora profiles of Figure 17 that this property is also highly variable. However, the model predictions, while offset by about 25% (high), track the changes in level consistently. The model for concora is based on a relationship to flat crush which is in turn related to STFI. Thus the predictions for concora should be similar to STFI. The measurement variance for concora is 7.2 lb and the predicted values are generally slightly outside the upper limit of the confidence range without correction. Given a constant correction factor (multiplier), discussed in later sections, the predictions fall well within this confidence region.

The general agreement between the measured data and the model predictions for concora shows that the basic elements of the model system form a consistent framework. Calender loading appears to have some effect on concora, although primarily on reel 8. This is likely due to the fact that concora and, by implication, STFI and Ring Crush, are influenced by basis weight variations more than other variables, and the basis weight is strongly correlated with caliper or sheet thickness. However, since density is generally independent of basis weight, modulus is (or should be) relatively independent of basis weight. Thus basis weight and caliper increases should also increase concora provided density remains the same. However, if density decreases, i.e., when the calender stack load is removed, the density and modulus effects may overwhelm the caliper increase, perhaps causing a decrease in concora.

SUMMARY OF VARIABLE EFFECTS ON MACHINE PAPER PROPERTIES

OCC Content

OCC concentration varied from 18% to 36% during the test but had a relatively minor affect on compressive properties. The reel-to-reel variability observed during the first 16 reels, over which OCC varied, may have been influenced by changes in semi-chem freeness and refining conditions which were occurring at the same time.

The MAPPS models show that two factors, fiber characteristics and caliper/modulus, contribute to the relative insensitivity of compressive properties to OCC content. Fiber characteristics do not change significantly as OCC content changes. Average fiber length does change gradually but this effect is masked by other variables, particularly CSF.

The second factors, caliper and modulus, tend to have opposite effects. Conditions which influence density tend to have opposite affects on modulus and caliper. Because the modulus and thickness occur together in the basic compressive strength models for STFI and Flat Crush, variables which tend to increase density and modulus tend to decrease caliper, provided basis weight is under good control. Deviations between predictions and measurements were most pronounced when basis weight varied, resulting in larger changes in caliper that were not reflected in modulus.

Calender Load

Although the calender stack loading was known on only two reels (7 and 8) where it was zero, the calender appears to have influenced many of the properties, both before and after these reels.

As might be expected, the calender stack loading had a significant affect on density, caliper and elastic moduli. However, the affect on sheet stiffness was generally the opposite of what is normally seen for grades such as newsprint where stiffness and strength tend to decrease with increased load. In agreement with measured data, the compressive property models predicted that when the stack was pulled the increased caliper would cancel the decreased modulus resulting in little observable effect of calender stack loading on compressive properties such as STFI, Ring Crush and concora.

From the models, one might predict that the MD/CD ratio of the sheet could have been affected by the calender stack loading, possibly as a function of stretch or stress relief. However, the measured properties did not support this conclusion.

After reel 8, the modulus did not return to its previous levels, indicating that the stack may not have been returned to the original loading and/or the temperature/load levels were not densifying to the earlier levels. To predict the observed effect, the load levels in the model were increased in two stages over reels 9 through 12 up to 15 pli. However, since the loading was not known at any time during the test, the model adjustments could not be verified.

Another observed anomaly was that the desired breaking length and burst factor were relatively insensitive to the release of calender loading, while the models predicted significant decreases in these properties.

Using the unverified calendering conditions, the models predicted that the calender densified and increased internal bonding in the sheet. When the calender stack was lifted, both sheet density and the bond density decreased, resulting in a drop in elastic moduli, breaking length, and burst factor. Because the measured strength did not decrease, the data did not support a change in breaking length and, therefore, burst factor, indicating that the actual levels of bonding were not significantly affected by loading under the relatively mild conditions used. This result may imply that the modulus is not a function of bond density but only of actual bulk density.

Table XXI below shows the statistical effect of calender stack loading on machine paper properties. N indicates the number of data points for each condition and the minimum, maximum, mean and standard deviation values are shown for each variable, with the calender stack on or off. It may be concluded that the mean values average the effects of other variables while the standard deviations indicated the variability about the mean due to other effects such as refining, pressing, OCC and machine speed.

The caliper, density, MD and CD moduli, and ring crush change significantly with calender stack position (on or off). Density increases by 0.08 g/cc or 16% with calendering, as a result of the caliper change. Surprisingly, modulus increases significantly, indicating that bonding increases in the calender nip. This effect was unexpected since the load was low and the sheet was relatively dry. In fact much of the literature shows the opposite trend, i.e., a decrease in modulus and strength due to dry calendering.

As a result of stack loading, MD modulus increased by about 0.9 GPa, approximately 30%, while CD modulus increased by 0.42 GPa, approximately 25%. The CD ring crush increased by 6.7 lb/in (25%) and is comparable to the measurement standard deviation discussed below, an insignificant change. Concora changed less than the measurement standard deviation and was not significant at 90% confidence.

Mean tensile properties such as breaking length and burst factor were independent of calender loading, differing by less than the average measurement standard deviation. This result indicates that there was little, if any, net bonding or debonding occurring due to the calendering operation.

Table XXI: Effect of Calender Stack on Average Medium Properties

Property	N	Minimum	Maximum	Mean	Std Dev
Modulus					
on........	105	3.91	4.86	4.40	0.21
off.......	9	3.41	3.62	3.52	0.07
CD Modulus					
off.......	9	1.30	1.63	1.46	0.11
on........	105	1.49	2.38	1.88	0.16
MD Tensile					
off.......	9	5.60	6.05	5.81	0.16
on........	105	5.07	6.75	5.97	0.35
Burst Factor					
off.......	9	26.51	30.37	28.77	1.20
on........	105	25.61	33.45	29.02	1.59
Caliper					
off.......	9	9.45	10.02	9.65	0.18
on........	105	7.41	8.82	8.21	0.29
Concora					
on........	105	47.70	54.70	50.62	2.88
off.......	9	47.80	63.93	53.89	2.65
MD STFI					
on........	105	19.75	25.23	22.80	0.85
off.......	9	19.55	23.76	21.87	1.53
CD STFI					
on........	105	12.00	16.77	14.48	0.61
off.......	9	14.22	15.09	14.63	0.29
Ring Crush					
on........	105	22.79	43.23	33.06	5.12
off.......	9	19.48	30.35	26.35	3.35
Density					
on........	105	0.56	0.67	0.60	0.02
off.......	9	0.51	0.52	0.52	0.01
Basis Weight					
on........	105	24.72	26.36	25.38	0.37
off.......	9	25.32	26.48	26.00	0.32

Machine Speed

Comparisons of machine paper properties at the two test machine speeds of 1400 and 1900 ft/min are shown in Table XXII, with 75 data points at 900 ft/min and 39 data points at 1400 ft/min for each property. Again, it may be concluded that the mean values average variations such as calender stack loading, refining and press loading while the standard deviations include variability due to these and other effects.

Table XXII: Effect of Machine Speed

Property	N	Minimum	Maximum	Mean	Std Dev
MD Modulus, GPa					
1900......................	75	3.41	4.86	4.30	0.38
1400......................	39	4.14	4.54	4.39	0.10
CD Modulus, GPa					
1900......................	75	1.30	2.38	1.82	0.21
1400......................	39	1.67	2.17	1.90	0.15
MD Tensile, km					
1900......................	75	5.52	6.75	6.08	0.33
1400......................	39	5.07	6.03	5.72	0.21
Burst Factor					
1900......................	75	26.51	33.45	29.60	1.41
1400......................	39	25.61	30.35	27.85	1.14
Caliper, mils					
1900......................	75	7.42	10.02	8.43	0.56
1400......................	39	7.95	8.34	8.11	0.12
Concora, lb					
1900......................	74	47.70	63.93	53.13	2.97
1400......................	39	50.20	59.60	54.57	2.19
MD STFI, lb/in					
1900......................	39	21.22	23.67	22.68	0.61
1400......................	75	19.55	25.23	22.75	1.08
CD STFI, lb/in					
1900......................	39	12.61	15.30	14.30	0.53
1400......................	74	12.00	16.77	14.60	0.59
Ring Crush, lb					
1900......................	39	23.53	42.40	34.81	4.39
1400......................	75	19.48	43.23	31.35	5.39
Density, g/cc					
1900......................	75	0.51	0.67	0.59	0.04
1400......................	39	0.57	0.61	0.595	0.01
Basis weight lb/1000 ft^2					
1900......................	75	24.84	26.48	25.60	0.37
1400......................	39	24.72	25.80	25.10	0.21

As shown by Table XXII, there is no statistically significant effect due to machine speed for any of the properties considered, with the possible exception of MD Ring Crush. Also, the standard deviations at both machine speeds were significantly higher than the average difference, again indicating that there is no significant difference between the properties for the two speeds.

HANDSHEET PROPERTIES - 26 lb/1000 ft^2

This section summarizes the data and predictions for 26 lb handsheets made from composite samples taken from five locations during the test: hole refiner discharge, blend chest, tickler refiner discharge, headbox and broke chest. Composites were collected at several other locations such as the high density tanks and the white water chest but these were not formed into sheets. Only the heavier handsheet data were studied in detail. The 13 lb data can be found in Appendix IV. These data are discussed in a later section.

The discussion is broken down by property with contrast between positions and time trends forming the basis of the discussion.

CANADIAN STANDARD FREENESS

CSF should depend on such factors as the freeness of the semi-chemical and OCC furnish from high density storage, refiner power and consistency, fines retention on the wire, broke and saveall recycle and fines losses in stock prep. Freeness profiles, shown in Figures 20 through 24, indicate that with the exception of the headbox predicted values are lower than measured values.

For the simulation model, the predicted freenesses were initialized at the high density storage tanks using a WOOD02 block. The semi-chem freeness was varied for each reel using data from the mill, and freeness changes through the refining system were predicted. Variability in the measured CSF from IPST was greater than the predicted freeness variability, possibly due to measurement error.

Headbox CSF was predicted to be higher than measured CSF and the difference is thought to be due to variations in fines freeness. The model predicted the fines freeness to be in the 200-300 ml range and although no white water freeness data were obtained, the headbox freenesses suggest that the white water freeness was in the 100 ml range. The predicted difference may not be extremely important since most of the fines are not retained in the sheet and the final sheet freeness is more a function of the broke tank or tickler refiner freeness. Thus, the effect of headbox freeness on dry sheet properties may not be as important as stock freeness. However, the headbox CSF does control drainage rates and moisture profiles and should not be glossed over.

Statistical modeling indicates that the three major factors affecting freeness values measured are semi-chem freeness, refiner loading and OCC ratio. On the first day the semi-chem freeness dropped from 722 to 686, but the measured CSF from the primary and tickler refiners decreased by only about 20 ml. This effect is likely due to the "dilution" of the blend stock by the OCC (assuming the OCC CSF is constant). On the first day, the OCC content increased from 18% to 25% and primary refiner power increased by 50% for a brief period.

Hole Refiner Discharge CSF

The hole refiner CSF is the simplest CSF data to analyze because it is influenced only by the semi-chem furnish and the primary refiner load and consistency. Referring to Figures 20 through 23, the predicted CSF from the hole refiner remained essentially constant for the first two days with the exception of the period when the hole refiner power was increased on reel 2. The predicted variation tracks the measured variation over the first three reels but does not follow the oscillations over the following reels. In particular the large drop in CSF over reels 9 through 12 was not predicted. The measured drop cannot be related to high density CSF since that remains in the 720 ml range. The same relative change was not observed in the mill data.

The measured CSF values shown in Figures 20 through 23 are all IPST measurements. The mill CSF data can be found in Appendix I along with the processing conditions while the IPST CSF data and predictions are shown in Appendix III with the other handsheet data. Comparison of the two sets of measurements shows that the model predictions track the mill data more closely than the IPST data and that there is a much smaller offset between the predicted CSF's and the mill data. The major shift in the predicted CSF and the measured mill and IPST data began on reel 17. But, the magnitude of the CSF drop was not as great as the measured drop. The predicted CSF does track the direction of the change but does not always track the magnitude. The drop is the result of a relatively large increase in primary refiner power over the last 8 reels.

In summary, the model predicts the effect of refining on the semi-chem furnish reasonably well, but the effect of the entering CSF on the discharge CSF is not strong enough. Also, the predicted change in CSF with refiner power was not as strong as observed, indicating that the K-factor model for the refiners may need to be tuned to show greater sensitivity to specific power. The prediction models were validated against the IPST data, and the calculated offset is specific to IPST measurements. The offset against MB data is much smaller (the regression coefficient is closer to 1) since the overall CSF levels were set by the level in the high density chest as specified by mill data. Thus, the model predictions also track the mill data more closely than the IPST data.

Blend Chest CSF

Freeness from the blend chest, as shown in Figure 21, was influenced by the hole refiner freeness, the OCC freeness and the OCC ratio. However, the predicted OCC freeness was assumed to be constant at 316 ml, the "average" of 150 and 650 ml for the hardwood and softwood components of the OCC. Since the OCC freeness was significantly less than the semi-chem freeness the blend chest freeness decreased with increasing OCC content. Generally, the blend chest freeness was approximately 30 ml lower than the hole refiner CSF, as expected for an OCC content of 18%. As OCC content increased to 38% during day 2, the CSF decreased to a minimum of about 450. However, the IPST measured freeness from the blend chest was approximately 50 ml lower than the hole refiner, indicating that the OCC CSF may have been lower than the value used in the simulations. Unfortunately, no mill measurements were available from either of the high density chests.

The model predicted a drop in CSF on reel 2, followed by a return to the initial level and a relatively large drop beginning at reel 9, followed by a gradual return to earlier levels. With the exception of reel 9, the measurements did not show these trends and fluctuated significantly, especially during the second day.

The blend chest discharge CSF for the third day was influenced primarily by the higher power to the primary refiner, which lowered the hole refiner CSF, and by the higher final OCC content, which also lowered CSF. The predicted and measured data showed very similar responses but the values were offset.

Tickler Refiner CSF

The tickler refiner discharge CSF was a function of the blend chest discharge CSF, the tickler power, and the tickler feed consistency. Thus, the tickler CSF was expected to drop for reel 2, as predicted by the model and observed by the IPST measurements and the mill measurements. However, a comparison of the "Measured Tickler Refiner CSF" in Appendix I with the IPST measured values in Figure 22 show that the mill measurements corresponded more closely with the predicted values than the IPST values. Since the trends established in the blend chest should be reflected by the tickler discharge for a constant tickler power, the lowest CSF values should have occurred when the blend chest CSF was low and the tickler power was high. The predicted blend chest CSF reached a minimum during reels 9 through 14 and at reel 23, while the IPST data showed a minimum at reel 23 but did not show the predicted trend. The mill data showed a local shallow minimum for reels 9 through 14 and a sharp drop for reels 18, 20 and 23-24, which did not agree qualitatively with the IPST trends. In addition, the sharp minimum for reel 18 was not predicted by the models.

Headbox

The headbox CSF, shown in Figure 23, was likely influenced by many process streams but particularly by the fines retention and recycle. The predicted CSF was approximately 60 ml higher than both the IPST and the mill data, indicating that the CSF of the fines in the white water, saveall and broke system was lower than predicted. However, no direct measurement of white water CSF was available.

At times the mill CSF values were as much as 100 ml lower than the predicted values. The predicted low trough for reels 9 through 14 was reflected in the mill data (see Appendix I) but not in the IPST data. Although it was difficult to compare the successive CSF profiles of the IPST measurements, the large "hump" in the IPST data for reels 9 through 14 appeared to persist through the headbox. All data and predictions showed the sharp drop-off in CSF over the last few reels.

Broke Tank CSF (Figure 24)

The CSF of the broke fibers as shown in Figure 24 should be similar to those of the paper sheet, i.e., a lower fines level and a higher CSF. One would also expect the broke CSF to resemble the tickler discharge CSF, as indicated by a comparison of Figures 22 and 24. The minimum value of broke CSF and tickler discharge CSF was also shown by the predicted profile for broke. Variations in CSF due to refining, while still discernable, were more muted, but could be seen in the data. However, the drop in CSF seen throughout the data at other locations for reels 9 though 14 was not as pronounced for the broke. Mostly, the high value for broke CSF at reel 20 is an outlier since it did not appear in the headbox data.

Transient effects

The transient behavior of the paper machine system was dominated by the first-order lags of the various storage tanks: high density tanks, blend chest, broke chest and machine chest, and screening and cleaning system. The largest capacity tanks were the high density and broke chests, but these chests were not a problem because the system boundaries began at the chest discharges. With the exception of the broke tank the remaining tanks had very small time constants and did not contribute significantly to transient effects. The estimated time constant for the broke tank was 1 to 2 hours, corresponding to 2 to 3 reels. However, the impact of the broke flow on the transient because of the system depends on the relative contribution of broke to the total flow to the headbox, as shown in Table XXIII. The calculated fiber flows shown in the model are simulated flowrates from the base case (reel 1) conditions, and, except for OCC which increased by a factor of 2, the flows remained at these magnitudes throughout the trial.

Table XXIII Contribution of Broke to Total Fiber Flow Rates

	Fiber Flows lb/hr	Relative Contribution
Semi-chem..	37700 }	50
OCC........	4250 }	
Broke......	21400	25
Saveall....	22500	25

Table XXIII indicates that the broke and saveall flows were significant contributors to the total headbox flow and that about half the total flow was raw stock and OCC while the other half was internal recycle from the broke and saveall systems. This represented about 25% of the total flow; since the broke was returned to the blend chest, both the handsheet data and the machine paper properties could have been influenced by transients due to broke flow. The affect of a single first-order lag on the machine paper properties would be to extend the affect of a process variable such as refining power, freeness change or OCC change beyond the time period the change. This suggests that handsheet properties from the broke chest onward could have been affected by the characteristics of the broke chest furnish.

However, other evidence suggests that the transient effect may not have been very significant. Comparing Figures 20 and 24, the initial high level of broad maxima in hole refiner discharge CSF followed by a minimum at reel 17 may have resulted in a somewhat broader maximum and a minimum broke CSF value at reel 16 to 17. Similarly, a second maximum CSF value from the hole refiner over reels 19 and 20 shows up as a very large maximum over reels 19 and 20. This somewhat qualitative correspondence between hole refiner and broke CSF indicates that the transients may be negligible.

Summary

The predicted CSF values track many of the observed freeness trends, and the reasonably close agreement between the predictions and the mill measurements may indicate that significant inter-laboratory differences exist. Additional modeling error could have been introduced by not accounting for the transient effects of the broke fibers.

DENSITY

Predicted and measured density profiles are shown in Figures 25 through 29. Density should be influenced by fiber compressibility, which is primarily a function of freeness since other factors (PAT's) remain relatively constant throughout the test. However, the data profiles indicate that density varied erratically for all handsheet data and it was not possible to relate the handsheet density statistically to process conditions. The handsheet density also did not relate to the machine paper density.

However, fundamental principles indicate that density, which is strongly influenced by pressing pressure, should have a strong affect on virtually all other handsheet properties. Thus, the pressure used by the PROPS blocks was varied to approximate the measured density in each case. An hypothesis was set up that, once reasonable agreement with measured densities was obtained, other properties should "fall into line."

Based on CSF data alone, one would expect the density of the hole refiner handsheets to remain relatively constant throughout much of the test, with a gradual increase toward the end of the test as CSF decreased with increased refiner power. However, this response could only be observed in the data by averaging the wide and sudden swings in the densities to see the overall trend. Based on these difficulties, no attempt is made to link the CSF measurements with the density measurements.

An additional factor, sheet forming, may also influence the general trends of the data. When the sheet formation index was varied in the model, the caliper and basis weight variations would result in a variable "effective" handsheet pressing pressure, leading to variable (e.g., lower) density than expected for a 50 psi.

load. Based on these considerations, the press load in the PROPS block was varied for each reel sample and location to approximate the measured density with the hope that the change in density would cause the remaining predicted properties to fall into line with the measurements. Using this approach, the overall fit to the density data was good.

CALIPER

Caliper profiles are shown in Figures 30 through 34. Since caliper is related directly to density and basis weight and the basis weight data were used to specify each set of handsheet predictions, the caliper predictions agreed quite well with the measurements.

TENSILE

The handsheet tensile profiles, shown in Figures 35 through 39, show excellent agreement between predicted and measured data, indicating that the measured data were internally consistent and that the models were able to predict the variable tensiles after fitting the pressing and formation parameter to fit the measured density and burst factor data. The largest disagreement in the results was, as expected, in the broke data where the measured tensiles were generally below the predictions and well below most of the predicted values at other locations. It should be noted that a number of data were missing for the broke tank, possibly influencing the comparisons.

STRETCH

Profiles of stretch at break are shown in Figures 40 through 44. There was a persistent offset of at least 50% to 70% between the predictions and data at all locations except the broke tank but the stretch profiles did follow the tensile and density profiles, as expected. Generally, the measured values of stretch over the trial were much greater than predicted, possibly due to experimental error. Stretch levels were highest for the headbox and lowest for the hole refiner and broke tank.

BURST FACTOR

The Burst Factor profiles are shown in Figures 45 through 49. Initially, the predicted and the measured burst values did not agree very well as the predicted values varied frequently with no obvious relationship to freeness changes. However, as discussed above, the density variations were assumed to result from variable formation, and it was reasoned that formation differences would also result in variable strength. Thus, in each case, the burst factor was fit by choosing the appropriate formation level in the PROPS block to obtain reasonably good agreement with the measured values.

It is interesting to note that the predicted average burst level tended to increase from the hole refiner to the blend chest, tickler refiner and headbox, consistent with the notion of improved fiber quality as the fiber approaches the forming section. However, the measured burst for the hole refiner was significantly higher than that of the blend chest which, in turn, was somewhat higher than the tickler refiner, contrary to intuition. Also the broke levels were even lower than the tickler discharge, contrary to the expected effect of freeness differences between the two tanks. These unexpected measured values could possibly be the result of unexpected changes in the fines contact of the furnish.

COMPRESSIVE PROPERTIES

Ring Crush

Profiles of Ring Crush, shown in Figures 50 through 54, indicate a high variability over the trial with no significant trends. There was a large offset between the predicted and measured levels which was relatively constant at each location. The model's predicted values of ring crush showed little change from the hole refiner to the tickler refiner discharge although the measured data did decrease, contrary to expectations. As expected, the headbox values are higher and the broke chest values lower.

The predictive model used in MAPPS indicated that ring crush will depend on directional moduli as well as caliper. However, the modulus was not measured for the handsheets so there was no independent measurement to decouple caliper and moduli.

Concora

Profiles of the measured Concora values, Figures 55 through 59, indicate that there was an oscillatory variation, particularly at the hole refiner, and it is unlikely that this variation could be real. Therefore, interpretation of the concora data was based on the average trending of the data. Using this approach, it can be concluded that there was very little change over the 24 test reels, in agreement with the average predicted trend. However, there was a constant offset of about 10 to 12 lb between measured and predicted values, with the predictions consistently higher than the IPST measurements. The mill concora data were consistently higher than the IPST data, but these data were not included in the statistical analysis so no direct comparisons could be made.

The models predict that concora values were about the same for the first three locations and then increased at the headbox and decreased at the broke chest. However, the predicted broke values were generally higher than the concora from the tickler refiner while the measured values were consistently lower.

In summary, the absence of a trend in compressive properties was predicted by the models. In theory, the major effect of furnish composition on compressive properties was expected to be a function of CSF. However, this effect was masked by significant variations in handsheet density and formation levels which affect bonding. Generally, for the range of density levels used, the predicted compressive property levels were in good agreement with literature and other IPST data of Whitsitt on which the models were based. Thus, it may be concluded that the offset between predictions and IPST data can be applied to the mill lab data and historical data from Whitsitt to adjust the model parameters.

The handsheet data do confirm one result of the machine paper property analysis, namely, that OCC content has no significant affect on compressive properties. Refining was also predicted to have only a very slight affect for similar reasons. The primary effect of refining, a decrease of CSF and an increase in surface area, increases density and, for constant basis weight, decreases caliper and increases modulus.

As discussed above, the decreased caliper tended to cancel the increase in modulus and no net affect on compressive properties was expected. However, the models did show that fiber modulus could be affected by refining and that changes in fiber modulus could bring about changes in sheet modulus without corresponding changes in sheet caliper. This could result in some affect on compressive properties. For similar reasons, the models indicate that different species would show considerably different compressive strength even at the same freeness and density.

Porosity

Gurley porosity profiles are shown in Figures 60 through 64. The models indicate that porosity profiles should vary directly with density profiles since Gurley porosity is inversely related to porosity and porosity should be inversely related to density. However, the measured porosity data were highly variable and no conclusions could be drawn from the individual values. It is interesting that many of the local variations in porosity, particularly at the blend chest, are predicted but with lower amplitude. The high variability of the measured porosity is also indicative of the assumption that the handsheet formation index varied significantly from sample to sample.

Porosity predictions at the hole refiner tended to pass through the average of the data values. The blend chest and other locations showed an offset between the porosity predictions and measured data with the greatest offset occurring at the headbox. The porosity model depends primarily on freeness and density. The headbox furnish was dominated by fines, resulting in higher predictions of the headbox freeness, which, because porosity is a function of freeness and density, led to the higher predicted porosity values.

MODEL DISCREPANCIES - PROBLEM AREAS

Large deviations in predicted versus measured property behavior occurred when the calendering effects were modeled. In particular, the predicted effect of calender loading on tensile strength and burst was higher than measured values. This is due to the fact that the models predicted that, under the mild calendering conditions used at the mill, calendering increased both bulk density and bond density, resulting in increased modulus and tensile strength. However, there is a large body of evidence linking modulus to strength and it was expected that the strength properties would parallel the stiffnesses. Thus, the apparent decoupling between densification and tensile strength observed in the measured data will require some review of the models.

A second problem area was related to densification in the press section where the models predicted much higher levels of fiber-fiber contact on one side of the sheet than on the other. These differences were a result of the gradient in fiber length through the thickness of the mat which caused the freeness and fiber surface area to vary. The sensitivity of the fiber contact area developed during pressing to CSF was too great, and these models must be reviewed and modified to correct this problem.

VALIDATION

Model validity is based on the "goodness of fit" between the predicted and measured values for each property shown in Tables XXIV and XXV (See Appendix V). The model used for the goodness of fit analysis has the following form:

measured property = C * predicted property

To perform the intercept, the model was forced to zero so that "perfect fit" would be one for which correction coefficient, C, is 1 and the R-squared error value is 1.0. The correction coefficient is a measure of the error in the model in predicting the mean value of the data. Based on the R-squared criteria, the goodness of fit for most of the properties was excellent since the correction coefficient and R-Squared statistic were close to 1. Corrections for machine paper properties are generally closer to one than for handsheets. The general variability of the handsheet data was the likely cause of the higher correction factors. For example, the correction for handsheet concora was 0.766 while that for machine paper concora is 0.92 indicating that handsheet concora on the average predicted higher values 24% of the time while machine paper concora predicted higher values only 8% of the time.

It should be noted that the R-squared values only apply to the corrected models and that those for the uncorrected models would be expected to be somewhat lower.

Table XXIV: GOODNESS OF FIT

Handsheet Data 103 Observations							
Variable	R^2	Coeff-icient	F	Mean	CV	T for H0	Root MSE
CSF, ml..............	0.984	1.0711	6745	503	12.8	82.13	64.5
Breaking Length, km..	0.959	0.936	2392	3.64	20.9	48.91	0.76
Concora, lb..........	0.964	0.766	2973	54.53	19.4	54.53	8.35
Ring Crush, lb.......	0.939	1.62	1685	53.5	25.14	41.05	13.5
Burst Factor.........	0.968	1.01	3377	23.0	18.06	58.12	4.15
Porosity.............	0.647	1.033	200	16.0	75.2	14.15	12.0
Density, g/cc........	0.992	0.982	13608	0.411	9.08	116.65	0.037

Table XXV Goodness of Fit

Machine Paper 24 Data Values							
Property	R^2	Coeff-icient	F	Mean	CV	T for H0	Root MSE
MD Tensile, km........	0.996	0.994	31831	5.955	5.98	178	0.35
CD Tensile, km........	0.995	1.01	20601	2.54	7.43	49	0.188
Burst Factor..........	0.995	0.957	21818	29.0	7.22	147	2.09
Density, g/cc.........	0.998	0.96	57067	0.589	4.47	239	0.026
Concora, lb...........	0.997	0.92	44207	53.63	5.06	210	2.71
CD Ring Crush.........	0.967	1.45	3316	32.53	18.4	58	6.0
MD STFI...............	0.998	1.233	62279	22.72	4.278	250	0.97
CD STFI...............	0.998	1.173	53574	14.5	4.59	231	0.67
MD Modulus, GPa.......	0.998	0.948	54201	4.33	4.59	232	0.199
CD Modulus, GPa.......	0.993	0.871	15481	1.85	8.60	124	0.159
MD Stretch, %.........	0.997	0.915	32404	1.637	5.93	180	0.097
Density...............	0.998	0.961	57067	0.589	4.47	239	0.026
MD/CD Ratio..........							
Modulus.............	0.995	1.094	22127	2.36	7.18	149	0.169
Tensile.............	0.998	0.984	49882	2.35	4.78	223	0.112
Porosity............	0.960	0.974	2690	20.48	20.6	52	4.22
Basis Weight........	0.999	0.993	9999	25.4	3.26	328	0.828
Caliper, mils.......	0.998	1.031	5678	8.319	5.0	214	0.416

Statistically, the R-Squared criteria overestimates the goodness of fit but the over estimate is not significant when the correction factors approach 1. Since the correction factors represent the average error in the predictions, a second criteria for model validity is that the average error of the model should fall within the confidence limits of measurement error for each property (See Tables XXVI & XXVII).

Table XXVI: Goodness of Fit Based on Measurement Error

Goodness of Fit - Handsheet Data						
Based on all Handsheet Data 103 out of 120 Observations						
Property	Correl Coeff-icient	Avg Error %	Mean	Measure Std Dev	Confid Band 90% Absol	%
CSF, ml..............	1.0711	7.0	503	-	-	-
Tensile, km..........	0.936	6.4	3.64	0.39	0.78	21
Concora, lb..........	0.766	23.4	54.5	3.6	7.2	13
Ring Crush...........	1.62	62.0	53.5	3.2	6.4	12
Burst Factor.........	1.01	1.0	23.0	2.3	4.6	20
Porosity.............	1.033	3.3	16.0	3.07	6.1	38

Table XXVII Goodness of Fit Based on Measurement Error

Machine Paper					
Goodness of Fit Based on Measurement Error					
Property	Correl Coeff-icient	Avg Error %	Mean	Measure Std Dev	Confid Band 90% Absol %
MD Tensile, km.......	0.994	1	5.98	0.39	13
CD Tensile, km.......	1.01	1	2.54	0.19	15
Burst Factor.........	0.96	4	29.0	2.3	16
Density, g/cc........	0.96	4	0.589	-	-
Concora, lb..........	0.92	8	54.53	3.6	13.2
CD Ring Crush........	1.45	45	32.5	6.4	39.4
MD STFI..............	1.233	23	22.7	3.8	33
CD STFI..............	1.173	17	14.5	3.2	44
MD Modulus, GPa......	0.948	5	4.33	0.31	14.3
MD Stretch, %........	0.915	8.5	1.637	0.22	27

The confidence bands for each variable are based on twice the standard deviation divided by the mean and expressed as a percent. When the confidence bands are compared with the percent error of the model based on the correction factors, all the models except CD Ring Crush are within measurement error. When the high level of correlation for the corrected model is taken into account, it could be stated that the model is not biased and is therefore also valid as corrected. Thus, a second validation criteria is that the model predictions are valid within measurement error.

Correction factors outside of the measurement error do not necessarily indicate an invalid model. In some cases, the corrections may also include the effects of variability of the laboratory testing procedures. In particular, differences between mill and IPST compressive strength measurements such as STFI and concora indicate that an interlaboratory study may be desirable.

Statistically, it may be concluded that, if the correction is a single factor and the resulting corrected values agree very well with the measurements as measured by R-squared, the model is a useful tool and therefore valid for this grade.

Handsheet Properties - 13 lb/1000 ft^2

The data on the lighter weight handsheets were used primarily to study the zero span tensile strength variations during the trial; for individual data see Appendix IV. The model did not predict a significant variation in zero span tensile. Both the OCC and semi-chem fiber zero-span tensile were initialized with a breaking length of 10 km and the final predicted zero-span values were about 9.5 km as compared to an average of 9.05 km for all 13 lb handsheets measured. The statistics on the 13 lb sheets are summarized in Table XXVIII.

Table XXVIII: Light Weight Handsheet Properties

Property	Minimum	Maximum	Mean	Std Dev
Basis Weight...........	50.7	81.5	65.0	3.27
Caliper, mils..........	6.05	13.7	8.45	1.42
Density, g/cc..........	0.185	0.397	0.313	0.05
Tensile, km............	1.51	4.99	3.55	0.71
Burst Factor...........	12.5	26.4	19.7	3.15
Stretch, %.............	0.61	2.30	1.47	0.34
Gurley Porosity........	1.45	18.0	4.75	3.43
Zero Span Tensile, km..	6.74	12.00	9.05	0.90
Moisture, %............	4.92	7.33	6.12	0.51

The examination of the measured zero span data for each location indicates that the zero span tensile did not change significantly throughout the process or with time during the trial. Some handsheet data from the mill were available to compare with the data from IPST and the model predictions. These data, which represent a single set of beating curves from 280 to 606 ml CSF, are summarized in Table XXIX.

The 13 lb handsheet had lower densities than the 26 lb sheets. The mean density of the light weight sheets was 0.313 as compared to a mean value of 0.411 for the 26 lb handsheets. Over most of the range in basis weight, density does not depend on basis weight. However, for low basis weight, density apparently increases with basis weight. One possible explanation for the higher density of the 13 lb is that the formation was more variable and could have resulted in a variation in caliper causing a nonuniform application of pressing pressure and nonuniform densification. Both the nonuniformity in density and formation itself would have contributed to lower tensile properties for the lower basis weight sheets.

Gurley porosity of the light weight handsheets (4.75) was also considerably lower than the 26 lb handsheet values of 16, indicating that the light weight handsheets had considerably higher porosity. The porosity differences were in agreement with the observed density differences.

It is interesting to note that the mean tensile strength (breaking length) of the light weight sheets, 3.55 km, was not significantly lower than the mean of the 26 lb sheets, 3.64 km, while the burst factor of 19.7 for the 13 lb handsheets was significantly lower than the value of 23.0 for the 26 lb handsheets. The similar tensile strength values indicate that formation of the 13 lb handsheet was equal or superior to that of the 26 lb handsheets. Theoretically, the more uniform formation (higher formation index) compensates for the lower density resulting in about the same tensile strength (other things being equal).

The models would have been able to predict the light weight handsheet data although this work was not done. It would have been necessary to assume a lower effective pressing pressure for the light weight sheets to fit the density and a corresponding higher formation index to fit the tensile or burst data.

Interlaboratory Differences

A limited set of property data were provided by the mill. The properties of interest were concora, STFI and freeness at the primary discharge, tickler discharge and headbox discharge. The Concora and Headbox CSF are summarized in Table XXX along with the IPST data and model predictions. These comparisons indicate that the model predictions tend to follow the mill concora and CSF data rather than the IPST data. Said another way, the mean values of the model prediction for each of these variables was closer to the mean of the mill data than to the mean of the IPST data. However, it was shown above that the models "tracked" the IPST data quite well with an offset. The concora model is based on data of Whitsitt obtained from numerous laboratory and mill sources and the differences shown in Table XXX indicate that the concora testing procedure at IPST may have been different.

The CSF data are indicative of the large variations that can occur with CSF measurements. The differences between the model predictions of headbox CSF were the largest of any location as a result of the high fines content of the predicted headbox stock fines as with Concora the predicted values were closer to the mill CSF values than to the IPST values.

Analysis of the mill beater data (See Table XXIX) also indicates laboratory differences; for instance, the zero span values of the beaten pulps were 7.3 km, as compared to 9.05 km measured by IPST and 9.5 km predicted by the model. The mean CSF of the handsheets tested at IPST was about 500 ml, corresponding to the column at a beating time of 8 minutes where the freeness was 493. At this level of CSF the mill handsheet density was 0.527 g/cc compared to 0.411 g/cc for the IPST handsheets. The breaking lengths were similar, however, with the mill breaking length of 3.9 km being only slightly higher than the IPST mean breaking length of 3.64 km. The mill handsheet data at 500 ml CSF and mean IPST handsheet data at 493 ml CSF.

Table XXIX: Mill Handsheet Data

	Beating Time, minutes			
	0	8	13	18
CSF, ml.........	606	493	407	280
Basis Weight....	28.24	28.31	28.29	28.49
Density, g/cc...	0.475	0.527	0.549	0.582
Tensile, km.....	2.1	3.9	4.7	5.1
Burst Factor....	14.0	23.1	28.6	32.7
Stretch ,%......	1.3	2.8	3.3	3.6
Gurley Porosity.	1.1	4.1	11.7	44.6
Concora, lb.....	27.8	49.0	66.2	73.9
Ring Crush, lb..	33.9	49.2	61.1	65.1
Zero Span, km...	5.0	7.3	7.3	7.3
STFI, lb./in....	12.2	16.7	19.0	20.9

It may be concluded from these data that the comparable breaking length for the two sets of handsheets is a result of the higher density for the mill data, which offsets the lower zero span tensile. The burst factors of the two handsheet were also very close, indicating that the tensile strengths and compressive properties were comparable. The slightly lower mill compressive properties were likely a result of the lower caliper of the mill sheets at the same basis weight due to the higher sheet. Thus, the compressive properties would be expected to be comparable because, as mentioned above, the compressive property models show that there is a trade-off between caliper and modulus.

Table XXX: Comparison of Selected Data Values Machine Paper Data and CSF

Reel	Concora			Headbox CSF		
	MB	Model	IPST	MB	IPST	Model
1	59.6	59.1	51.7	367	305	447
2	67.4	59.6	56.4	371	286	413
3	63.2	62.3	55.8	331	280	449
4	61.8	58.7	53.3	350	260	444
5	61.0	58.0	52.7	355	264	428
6	59.2	57.5	50.5	405	324	422
7	60.6	56.4	51.7	398	321	432
8	58.0	53.1	51.5	346	305	431
9	58.6	57.9	48.3	383	277	412
10	61.4	59.2	50.1	400	277	386
11	62.2	60.1	51.6	375	310	380
12	66.2	60.0	55.8	397	272	376
13	62.8	60.5	52.9	407	309	383
14	60.6	57.1	52.3	409	286	386
15	64.4	57.1	53.1	386	293	386
16	64.8	59.4	55.0	374	335	398
17	66.4	57.5	54.8	354	295	407
18	67.6	57.9	51.9	374	275	407
19	63.6	57.4	53.1	361	290	426
20	63.4	56.7	53.6	363	286	416
21	67.0	57.7	57.2	355	296	416
22	66.2	57.2	56.7	338	280	398
23	60.8	57.5	55.7	339	255	367
24	59.4	57.8	54.8	372	295	401

Table XXXI: Comparison of MB and IPST Handsheet Data at Comparable Values of CSF

	IPST	MB
Density, g/cc....	0.411	0.527
Tensile, km......	3.64	3.9
Concora, lb......	54.5	49.0
Ring Crush, lb...	53.5	49.2
Burst Factor.....	23.0	23.1
Gurley Porosity..	16.0	4.1
Zero Span, km....	9.05	7.3

Correlative Analysis of Machine Property Data

A correlative analysis of the machine property data indicates that, with minor exceptions, machine paper properties data were not significantly affected by any single independent variable. Correlative models of all properties were used to test the importance of both independent and dependent variables on properties such as density, breaking length, burst, stiffnesses and compressive properties. For example, concora was tested for dependence on stiffness and caliper, reported by the literature to be significant, as well as density, stack loading, machine speed, press loading, OCC, etc. Dependent property variables such as burst were tested for correlation with breaking lengths and stretch as well as machine conditions and refining. All the models had a very poor overall fit to the data but the models did identify one or two variables which had some influence on the correlated property. The results of this analysis are summarized in Table XXXII.

Table XXXII: Correlative Analysis

Dependent Variables	Significant Independent Variables	Type I SS	F	Total SS
MD Tensile....	Density.............. Pullstack on/off..... Machine Speed........	0.47 1.55 3.72	4.4 24 58	12.9
MD Modulus.....	Density.............. $Density^2$.............	2.97 2.50	58 49	11.19
Burst Factor..	MD x CD Tensile......	146	-	275
Density.......	Pullstack on/off..... High Density CSF..... OCC ratio............	0.047 0.013 0.0087	131 19 25	0.108
CD Ring Crush.	Machine Speed........	231	-	3121
Concora.......	Pull stack on/off....	88.5	12	879

From the table, it can be seen that density was most strongly affected by calender loading which was confirmed by the models and the measured data. Density also showed a lower dependence on freeness and OCC ratio, but the contribution to the total sum of squares value of 0.108 was only 0.013 and 0.0087 for CSF and OCC ratio, respectively.

MD Modulus could be related only to sheet density or various powers of density. The density relationship is fundamentally sound and was confirmed by the correlative analysis. However, the contribution of density was only 50% of the total variation in the data indicating that other factors must contribute to the variability. The predictive model used by MAPPS assumes that the tensile and modulus ratio was relatively constant throughout the test and was confirmed by the measured data. Thus, it is unlikely that variable stretch and/or shrinkage resulted in MD/CD variations which would have influenced modulus.

Burst Factor was most strongly related to the product of the MD and CD tensile strength although the square root function used in the model would have given a stronger correlation. Stretch was not found to contribute, possibly due to the form of the model.

MD tensile strength was most strongly dependent on machine speed with a small but significant dependence on calender stack loading and density. All of these effects could be expected based on fundamental modelling considerations. Machine speed is a factor because it influences the MD/CD tensile ratio. Stack loading can affect tensile through bonding/debonding behavior or through stress relaxation which also affects MD/CD tensile ratio. Density affects tensile because it is a measure of the degree of bond formation or breaking occurring under load. However, the sum of these three terms was still not sufficient to provide a good predictive model for MD breaking length.

It is interesting to note that concora could not be related to ring crush, and STFI, or elastic moduli even though a fundamental relationship should exist. Ring Crush appeared to be dependent on machine speed, indicating that MD/CD tensile ratio may influence ring crush variations.

CONCLUSIONS - Validation Study

Based on the two validation criteria and estimates of measurement error, the model system appears to be valid for corrugating medium. Correction factors for some properties may need to be applied to some of the property predictions. Two areas in the models will require modification. A follow-up calendering test is recommended to reconcile and confirm the conclusions of the effects of calender load.

There is some evidence of transient effects when looking at the handsheet CSF and machine paper data but these effects could not be separated from the overall variations in the data. Property variation with time appeared to be a response to several causes:

1. property measurement error (no real cycling)
2. CD variability
3. semi-chem CSF and other inputs to the system (real effect)
4. unmeasured variables which changed
5. measured and controlled test variables
6. holdups in tanks (first-order lags) which propagated through the system diluting certain effects and propagating others

The high level of the correlations leads to the following conclusions:

1. The data were highly consistent internally.
2. The major factors affecting properties were accounted for in the models.
3. Many factors which were held constant or calculated to be constant, e.g., machine paper formation, were indeed approximately constant.
4. Those factors which did change during the trials were most probably the major factors affecting properties.
5. The fundamental basis for predicting property development appears to be reasonably well understood.
6. The properties depend on each other in a hierarchical structure, i.e., density, tensile, and elastic properties, derived properties such as burst factor (and tear), compressive properties such as STFI and flat crush and, finally, highly derived properties such as ring crush and concora.
7. The predictable response of the handsheet and machine paper properties to process changes indicates that the overall model structure and concepts are consistent.
8. Areas of weakness appear to be the exact sensitivity of the contact development with pressing and the relationship between density, bond density, modulus and strength.
9. It appears that modulus is a function of density rather than bonding per se. This conclusion seems reasonable because the elastic stiffnesses can be measured as the transmission of waves (ultrasonic) through the sheet which should depend on the contacts between fibers rather than the bonds.
10. Tensile properties which depend on bond failure should relate directly to bond density and strength, indicating that light calendering of this grade does not affect the bonding in the sheet but does affect the contacts and density of the sheet.

Overall, the models performed well from a statistical point of view -- the only objective means of determining model validity. A transient simulation model with CSTR's and first-order lags in the system would have been helpful. Such a system will be developed to use for future validation work.

Handsheet formation and pressing should be more consistently controlled in future work. The handsheet data were highly variable, apparently due to variable formation and pressing pressure. Thus, variability of the data limited their utility in the validation. There were also interlaboratory differences which should be studied further.

Future validation studies should include the modules necessary to predict CD variations through the paper machine, wet press, drier and calender sections for comparison with the measured CD property data.

The effects of OCC, refining, pressing and machine speed were surprisingly small for this grade. These effects were quantified in the following sensitivity study by using the simulation model to eliminate transient effects and interactions between variables.

Model Modifications

Based on the results of this analysis, the following model changes will be made:

1. Reduce the CSF dependence of the wet compressibility model.
2. Change the modulus models so they depend on bulk density rather than bond density.
3. Change the Gurley porosity to depend on surface density rather than bulk density.
4. Increase the sensitivity of CSF to specific power for lower yield furnishes in the refiner models.

SENSITIVITY ANALYSIS

The sensitivity analysis was performed using the model with Reel 1 conditions as the basis for determining the expected affect of four major test variables on end-user performance. By changing only one variable at a time using the model, it was possible to obtain unambiguous estimates of the decoupled sensitivity of each property to a specific variable. The four parameters were varied, as follows: (1) OCC content - 18% to 38%, (2) hole & tickler refiner loads - minimum to maximum values, (3) press load - minimum to maximum values, and (4) calender stack - loaded or unloaded. The variable conditions are summarized in Table XXXIII.

The sensitivity study was done without changing any of the models. In light of the findings of the validation study, the sensitivity coefficients for the effect of calendering on tensile properties were assumed to be zero even though the current models predicted a drop in tensile, burst and stretch. The sensitivity coefficients for the contact areas and bond area PAT's, S_{b1}, S_{b2} and S_a may also change after the wet press densification model is modified.

Table XXXIII: Sensitivity Case Study - Process Conditions

Case	Base	2	3	4	5	6
OCC Content, %....	18	38	18	18	18	18
Refining Primary..	1.47	1.47	5.16	1.47	1.47	1.47
Refining Tickler..	0.052	0.052	0.283	0.052	0.052	0.052
3 Press Load, pli.	600	600	600	800	450	600
3 Press Calender..	on	on	on	on	on	off

Sensitivity Factors

Machine paper properties and PAT values for each case are summarized in Table XXXIV.

Table XXXIV: Properties and Attributes of Calendered Medium Predicted by the Model

Case......................	Base	2	3	4	5	6
Properties		Hi OCC	Hi Refi-ning	Hi pli	Lo pli	Calend Load Off
BW (dry)....................	26.8	26.9	26.8	26.8	26.8	27.0
Caliper.....................	7.93	7.82	7.82	7.93	7.93	9.02
Density.....................	0.65	0.662	0.66	0.65	0.65	0.576
MD/CD tensile...............	2.39	2.39	2.39	2.39	2.38	2.38
Burst Factor................	29.7	32.2	27.77	29.7	29.7	26.0
MD Tensile, km..............	5.73	6.18	5.31	5.73	5.73	5.24
CD Tensile, km..............	2.40	2.59	2.23	2.40	2.40	2.19
Gurley Porosity, sec/cc.....	22.2	23.7	25.7	22.2	22.2	19.71
Stretch, %..................	1.87	1.90	1.90	1.88	1.88	1.72
MD Modulus, GPa.............	4.03	4.15	4.0	4.03	4.04	3.51
CD Modulus, GPa.............	1.87	1.91	1.85	1.88	1.88	1.63
MD STFI.....................	17.34	17.55	17.2	17.34	17.34	16.77
Flat Crush..................	30.6	30.9	30.3	30.6	30.58	29.62
Ring Crush..................	17.35	18.2	16.72	17.34	17.35	15.0
Concora, lb.................	54.2	54.88	53.7	54.2	54.2	52.2
Moisture, %.................	6.5	7.0	7.0	6.2	6.9	7.0
CSF Primary Refiner.........	528	528	388	528	528	528
CSF Blend Chest.............	496	470	401	496	496	496
CSF Tickler Refiner.........	491	464	387	491	491	491
CSF Headbox.................	457	429	365	457	457	457
CSF Broke Tank..............	536	507	470	536	536	536

Table XXXIV Continued: Properties and Attributes of Calendered Medium Predicted by the Model

Performance Attributes Case.	Base	2	3	4	5	6
Properties		Hi OCC	Hi Refi-ning	Hi pli	Lo pli	Calend Load Off
Yield	72.7	72.2	72.7	72.7	72.7	72.7
Kappa	56.9	61.0	56.9	56.9	56.9	56.9
Hemi	0.144	0.138	0.144	0.144	0.144	0.144
C_k, cm^2/g	31.9	31.9	31.9	31.9	31.9	31.9
L, mm	0.76	0.86	0.70	0.766	0.766	0.766
σ, mm	2.62	2.73	2.5	2.64	2.64	2.64
W	0.039	0.039	0.039	0.039	0.039	0.039
σ_W	1.88	1.88	1.88	1.88	1.88	1.88
Z_f	9.55	9.09	9.28	9.56	9.56	9.56
E_f	3.71	3.69	3.57	3.67	3.67	3.67
CWT	1.2	1.2	1.2	1.2	1.2	1.2
Smod	1.07	1.07	1.07	1.07	1.07	1.07
$S_{TR}x10^{-9}$	2	0.2	0.2	0.2	0.2	0.2
SB1	4.70	4.88	5.0	4.7	4.7	3.9
SB2	4.90	4.98	4.56	4.93	4.9	4.34
ASB	4.81	4.91	4.77	4.81	4.81	4.11
Form	0.98	0.98	0.984	0.98	0.98	0.98
WS	1.3	1.3	1.3	1.3	1.3	1.3
OR	1.5	1.5	1.5	1.5	1.5	1.5

Press moisture and caliper conditions for the first two press nips held constant in the study are shown in Table XXXV.

Table XXXV: First and Second Press Nip Profiles

Press	1	2
Load, pli	380	550
Inlet Consistency, %	25	30.5
Outlet Consistency, %	30.5	37.2
Caliper In, mils	32.4	16.6
Caliper Out, mils	16.5	13.6
Peak Pressure, GPa	0.915	1.32
Power Consumption, hsp	69000	86000

Interactions between Pressing, Drying and Calendering

One additional factor which influences the effect of press load on sheet properties is the final sheet moisture. In the cases above, the stream flows were adjusted to achieve a constant outlet dryness. If the steam flows had not been varied, sheet moisture levels would have been reduced to 90% for the low press load case and would have increased to 97% for the high press load case. The higher moisture would have resulted in a slight improvement in predicted tensile properties from calendering while the lower moisture predicted reduced tensile strength due to calendering.

Table XXXVI and XXXVII show the effect of dryer steam flow in combination with press load on final sheet moisture and machine paper properties from the calender, respectively. The modeling results indicate that the press loading level interacts with the calendering causing a bonding or debonding effect depending on the sheet moisture and roll temperature in the calender nip. This effect is independent of the basic consolidation effect of the press on the sheet in the wet state.

Table XXXVI: Press Load Sensitivity - Interaction with Calendering

	Base Case	High Press Load		Low Press Load	
3rd Press Load, pli	600	800		450	
Outlet Consistency, %	39.9	40.9		37.2	
Caliper out, mils	12.4	12.9		-	
Peak Pressure	1.45	1.93		1.08	
Power Consumption, x1-$_{-3}$	91.0	111.0		76.0	
Dryer Steam Flow, lb/hr	51500	51500	50000	51500	53500
Outlet Moisture, %	6.5	2.4	6.9	10.0	6.9

Table XXXVII: Machine Paper Properties - BW 26.8 lb/1000 ft ^{2}

	Base Case	High Press Load	Low Press Load
Caliper, mils...........	7.93	7.93	7.93
Density, g/cc...........	0.650	0.650	0.650
MD Tensile, km..........	5.73	4.70	5.73
CD Tensile, km..........	1.97	1.97	2.40
Burst Factor............	22.1	22.1	29.7
Stretch, %..............	1.88	1.54	1.88
Porosity, sec/cc........	22.2	22.2	22.2
MD Modulus, GPa.........	4.03	2.93	4.04
CD Modulus, Gpa.........	1.36	1.36	1.89
STFI, lb/in.............	14.2	14.2	17.35
Concora, lb.............	54.2	43.5	54.2
Ring Crush, lb..........	17.35	4.39	17.35

Table XXXVIII shows sensitivity coefficients rescaled by 100. Each coefficient is defined as change in property / change in independent variable. Calender stack sensitivity is defined as the absolute diffence between loaded and unloaded conditions. CSF sensitivity is defined as WOΔCSF/ΔIndependent variable.

Table XXXVIII: Sensitivity Coefficients - PAT's

Properties	OCC % inc	Refining Power hsp-day per ton	Third Nip load pli	Calender Stack on/off absolute
Caliper............	-0.55	0.0	0	1.09
Density............	0.06	0.27	0	-0.07
MD/CD tensile......	0	0.0	0	0.0
Burst Factor.......	12.5	-46.8	0	0.0
MD Break Length, km	2.25	-11.3	0	0.0
CD Break Length, km	1.0	-4.6	0	0.0
Gurley, sec/cc.....	7.5	94.8	0	-2.5
Stretch, %.........	0.15	0.8	0	0.0
MD Modulus, GPa....	0.6	0	0	-0.50
CD Modulus, GPa....	0.2	0	0	-0.24
STFI - MD..........	0.55	0	0	-0.6
Flat Crush.........	1.5	0	0	-2.35
Ring Crush.........	4.5	-17.2	0	-0.4
Concora, lb........	0.0	-13.6	0	-2.0
CSF Primary........	0	-3800	0	0.0
CSF Blend Chest....	-130	-2574	0	0.0
CSF Tickler Dis....	-130	-2818	0	0.0
CSF Headbox........	-130	-2493	0	0.0
CSF Broke..........	-130	-1787	0	0.0
PAT's at the Reel:				
Yield...........	-2.5	0	0	0.0
Kappa...........	20.5	0	0	0.0
Hemi............	-0.03	0	0	0.0
C_k..............	0	0	0	0.0
L...............	0.5	1.62	0	0.0
σ...............	0	0	0	0.0
W...............	0	0	0	0.0
σ_w..............	0	0	0	0.0
Z_f..............	-2.3	-7.3	0	0.0
E_f..............	0	0	0	0.0
CWT.............	0	0	0	0.0
Smod............	0	0	0	0.0
SBSTR $x10^{-9}$......	0	0	0	0.0
SB1.............	0.94	8.1	0	---
SB2.............	0.45	-9.2	0	---
ASB.............	0	0	0	---
Form............	0	0	0	0.0
WS..............	0	0	0	0.0
OR..............	0	0	0	0.0

CONCLUSIONS - Sensitivity Study

The sensitivity study showed that OCC had little effect on compressive properties but did increase some tensile properties slightly. Refining had a strong effect on CSF, improving the sheet density. However, the models predicted a reduction in fiber length (coincident with the CSF drop) and fiber tensile strength tending to reduce tensile properties such as breaking length and burst factor.

Third nip press load had little affect on properties, provided the sheet moisture entering the calender was constant. However, this effect is influenced by the debonding of the sheet predicted by the current model. Since this debonding did not occur, the interactions between the press load, moisture and calendering were probably not real for the low loading for this grade.

The calender stack, even at low loading, increased the sheet density and sheet stiffnesses but there was only a negligible affect on compressive properties. The affect on tensile properties was also negligible.

REFERENCES

PAT's Development

1. Jones, G. L., MAPPS Performance Attributes Simulation, Project 3471, Report 1, March 25, (1988).

Applications

2. Jones, G. L., "Simulating the Development of Pulp and Paper Properties in Mechanical Pulping Systems", Pulp and Paper Mag. Can., 91(2):T81(1989).
3. Jones, G. L., "Simulating End-use Performance", Tappi, 72(10):189-197 (1989).
4. Jones, G. L., Xuan N. Nguyen, "Analysis and Simulation of Property Development in Forming Newsprint", Tappi, 73(7): 160-168 (1990).
5. Jones, G. L., "Integration of Process Simulation with Mill-wide Information and Control", Tappi, 73(11):113-118 (1990).
6. Jones, G. L., Pulp Paper Can. 89(6):T213 (1988).

Technical Details

7. MAPPS 4.0 Technical Documentation, The Institute of Paper Science and Technology, Copyright 1991.

Theory - Refining

8. Yan, J., Tappi, 58(7): 156 (1975).
9. Strand, W. D., Edwards, L. L., Tappi J. 67(12):72 (1984).
10. Stationwala, M. I., D. Atack, J. R. Wood, D. J. Will, A. Karnis, Intern. Mech. Pulping Conf., Toronto, Can., (1979).
11. Atack, D., W. D. May, "Mechanical Reduction of Chips By Double-Disk Refining", Pulp Paper Mag. Can., Conv. Issue T-75 (1963).
12. Casey, J. P., Pulp and Paper Chemistry and Chemical Technology, Vol. 1, Wiley 3rd Ed., p 201-252.
13. Jackson, M., G. Akerlund, "Preheating and Refiner Housing Pressure Affect the Quality of TMP and CTMP", Tappi 76(1):54-58 (1984).
14. Jimenez, G., R. R. Gustafson, W. T. McKean, "Modelling Incomplete Penetration of Kraft Pulping Liquor", J. Pulp and Paper Sci., 15(3):J110-115 (1989).
15. Hoekstra, P. L., M. A. Veal, P. F. Lee, J. D. Sinkey, "The Effects of Chip Size on Mechanical Pulp Properties and Energy Consumption", Proc. Inter. Mech. Pulping Conf., p. 185-193 (1983).
16. Hoglund, H., U. Sohlin, G. Tistad, "The Effect of Physical Properties of Wood on Chip Refining", Inter. Mech. Pulping Conf. p. 77-85 (1975).
17. Kurdin, J., Univ. of Maine Summer Institute Lecture Notes, (1987).
18. MacDonald, R. G., J. N. Franklin, Pulp Paper Manufacture, Vol. 1 The Pulping of Wood, 2nd Ed., McGraw-Hill, p. 390-391.

19. Paranyi, N. I., W. Rabinovitch, "Determination of Penetration Rate of Liquid Media into Wood Using a Quartz Spiral Balance Part I-Water and Air-Dry Spruce Chip", Pulp Paper Mag. Can., Conv. Issue p. 163-170 (1955).
20. Siau, J. F., Transport Processes in Wood, Springer-Verlag, Berlin (1984).
21. Clark, J. D'A., "Freeness Fallacies and Facts", Svensk Papperstid. 3(15): 54 (1970).
22. Valade, "Chemithermomechanical Pulping of Mixtures of Different Species of Hardwoods", Tappi July issue, p. 80 (1986).
23. Leider, P. J., Nissan, A., Tappi 60(10):85 (1977).
24. Manfredi V., E. Claudio-Da-Silva Jr., "Refining - Operational Variables vs. Raw Materials", PIRA Inter. Conf. Advances in Refining Technol. Birmingham UK Vol II (1986).
25. Yan, J., "Kinetic Theory of Mechanical Pulping", Tappi J., 58(7):156-158, (1976).

Paper Property Models and Paper Physics

Fundamental Concepts

26. Nissan, A. H., Tappi, 60(10):98 (1977).

Elastic Properties

27. Fleischman, E. H., G. A. Baum, C. C. Habeger, Tappi 65(10):115 (1962).
28. Page, D. H., R. S. Seth, J. H. DeGrace, Tappi 62(9):99 (1979).
29. Baum, G. A., D. G. Brennan, C. C. Habeger, "Orthotropic Elastic Constants of Paper", Tappi 64(8):97 (1981).

Tensile Properties

30. Page, D. H., Tappi 52(4):674 (1969).
31. Van den Akker, Tappi 41(8):416 (1958).
32. Van den Akker J. A., A. L. Lathrop, M. H. Voelker, L. R. Dearth, "Importance of Fiber Strength to Sheet Strength", Tappi 41(8):416-425 (1958).

Compressive Properties

33. Habeger, C. C., W. J. Whitsitt, "A Mathematical Model of Compressive Strength in Paperboard", Fiber Science & Technology, 19:215-239 (1983).
34. Perkins, R. W. Jr., R. P. McEvoy, "The Mechanics of the Edgewise Compressive Strength of Paper", Tappi 64(2):99-102 (1981).
35. Wink, W. A., J. A. Watt, W. J. Whitsitt, G. A. Baum, "Role of Fiber Axial Modulus on Compressive Strength", Fiber Sci. Technol., 20:245 (1984).
36. Whitsitt, W. J., "Relationships Between Elastic Properties and End-Use Performance", Project 2695-23, Report One to FKBG of the API, (1985).

Calendering

37. Crotogino, R. H., Tappi 63(11):101 (1980).
38. Charles, L. A., J. F. Waterhouse, "The Effect of Supercalendering on Strength Properties of Paper", J. Pulp and Paper Sci., 14(3): J59 (1988).

Sheet Forming

39. Tellvik, A., O. Brauns, "Studies of Table Roll Drainage", Svensk Paperstid. 63(22):803 (1960).
40. Taylor, G. I., "Drainage at the Table Roll", Pulp Paper Mag. Can., 57:267 (Conv. Issue) (1956).
41. Kerekes, R.J., E. B. Koller, "Equations for Calculating Headbox Jet Contraction and Angle of Outflow", Tappi 64(1):95 (1981).
42. Meyer, H., "A Filtration Theory for Compressible Fibrous Beds Formed from Dilute Suspensions", Tappi 45(4):296 (1962).
43. Pires, E. C., A. M. Springer, V. Kumar, "Computational Model for Water Drainage in Fourdrinier Paper Machines", Tappi, April issue p. 183, (1988).
44. Smook, G. A., Handbook for Pulp & Paper Technologist, Joint Exec. Committee of the Vocational Ed. (1986).
45. Victory, E.L., "Computer Simulation of Drainage in the Forming Section of the Paper Machine", Tappi 52(7):1309 (1969).

Property Development

46. Alexander, S. D., R. Marton, S. D. McGovern, Tappi 51(6):283 (1968).
47. Bobelek, J. F., M. Chaturvedi, Tappi 72(6): 123 (1999989).
48. Kallmes, O. J., M. Perez, "Consolidation of the Paper Web", Cambridge Symposium, p. 507-8, Sept. (1965).
49. Ingmanson, W. L., E. F. Thode, "Factors Contributing to the Strength of a Sheet of Paper", II., Relative Bonded Area, Tappi 42(1):83 (1959).
50. Mayhood, C. H., O. Kalmes, M. M. Cauley, The Mechanical Properties of Paper. Part II: Measured Shear Strength of Individual Fiber to Fiber Contacts, Tappi 45(1):69(1962).
51. Robertson, A. A., S. G. Mason, "Specific Surface of Cellulosic Fibers by the Liquid Permeability Method", Pulp Paper Mag. Can. 50(B):1-7 (1949).
52. Wood, J. R., A. Karnis, "Distribution of Fiber Specific Surface of Papermaking Pulps", Pulp Paper Mag. Can., 80(4):T116-122 (1979).
53. Wardrop, A. B., "Fiber Morphology and Papermaking", Tappi 52(3): 396 (1969).

Anisotropy

54. Parsons, S. R., "Effect of Drying Restraint on Handsheet Properties", Tappi 55(10): 1516, (1972).
55. Setterholm, V. C., E. W. Kuenzi, "Fiber Orientation and Degree of Restraint During Drying - Effect on Tensile Anisotropy of Paper Properties", Tappi 53(10):1915 (1970).
56. Setterholm, V. C., W. A. Chilson, "Drying Restraint - Its Effect on the Tensile Properties of 15 Different Pulps", Tappi 48(11):634 (1965).
57. Sapp, J. E., W. F. Gillespie, "Influence of Tension During Drying Upon Paper Strength", Paper Trade J., 124:120 (1947).
58. Norman, B., D. Wahren, "Mass Distribution and Sheet Properties of Paper", Tech. Div., The British Paper and Board Industry Federation Symposium Trans., Cambridge, Vol. 1:7 (1973).

Formation

59. Hallgren, H., "The Influence of Stock Preparation on Paper Forming Efficiency on a Paper Machine", XXIII EUCEPA Conf., Harrogate, UK, Vol. 1, (1988).
60. Klaus-Bernhard Graber, "Operation of the Fourdrinier Paper Machine and Its Influence on the Uniformity of Basis Weight and Other Properties", EUCEPA Conf. on Web Formation/Consolidation (London), Paper No. 2, p. 23 (1979).

Unit Operations Models

Wet Pressing

61. Beck, D. A., "Re-examining Wet Pressing Fundamentals: A Look Inside the Nip Using Dynamic Measurement", Tappi 70(4): 129 (1987).
62. Caulfield, D. F., T. L. Young, T. H. Wegner, Tappi 65(2):(1982).
63. Han, S. T., "Compressibility and Permeability of Fiber Mats", Pulp Paper Mag. Can., 70:T134 (1969).
64. Wegner, T. H., T. L. Young, D. F. Caulfield, Tappi 66(4):85 (1983).
65. Caulfield, D. F., T. L. Young, T. H. Wegner, Tappi 69(6):90 (1986).
66. Wahlstrom, B., Tappi 64(1):75 (1981).
67. Young, T. L.,D. F. Caulfield, T. H. Wegner, "Role of Web Properties in Water Removal by Wet Pressing: Influence of Basis Weight and Forming Method", Tappi 66(10) (1983).
68. Wahlstrom P.B., "Our Present Understanding of the Fundamentals of Pressing", Pulp Paper Mag. Can., T349, p. 76 October (1969).
69. Wahlstrom, P. B., Web Formation & Consolidation, EUCEPA-79 International Conf. London, p. 91, (1979).

ACKNOWLEDGEMENTS

The author would like to thank the member companies of the Institute of Paper Science and Technology for their support of this project. Special thanks go to Joe Cook and all those at MacMillan-Bloedel, Inc. for their cooperation in all phases of the mill trial. Thanks also to J. D. Rushton and R. Ellis of IPST for their invaluable assistance in planning and design of the trial, design of the sampling plan and in sample collection and data interpretation.

The Institute of Paper Science & Technology

Gary L. Jones
Senior Research Engineer
Process Simulation & Control Group
Engineering Division

FIGURES

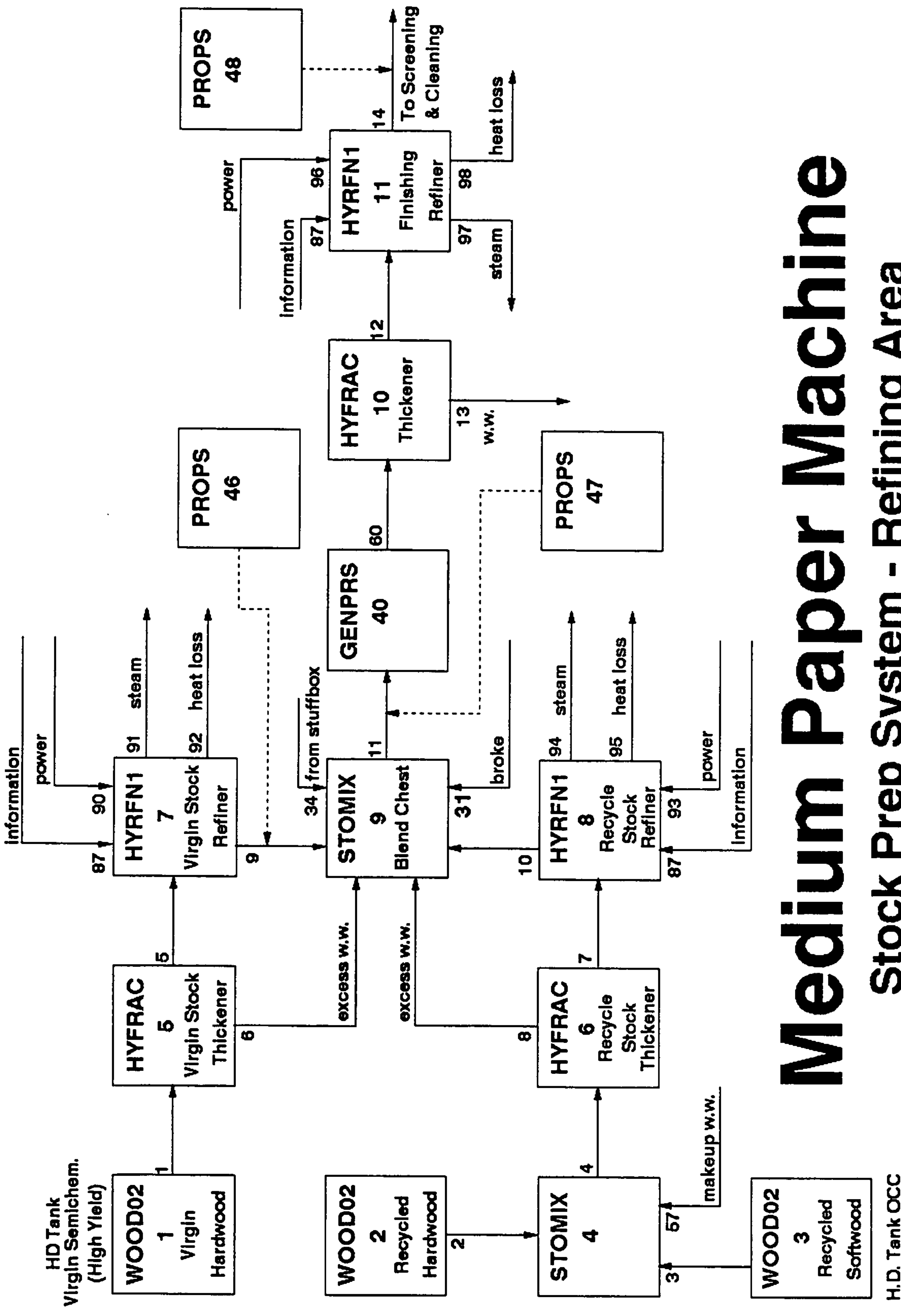

Medium Paper Machine

Stock Prep System - Refining Area

Figure 2

FIGURES

Medium Paper Machine Screening & Cleaning

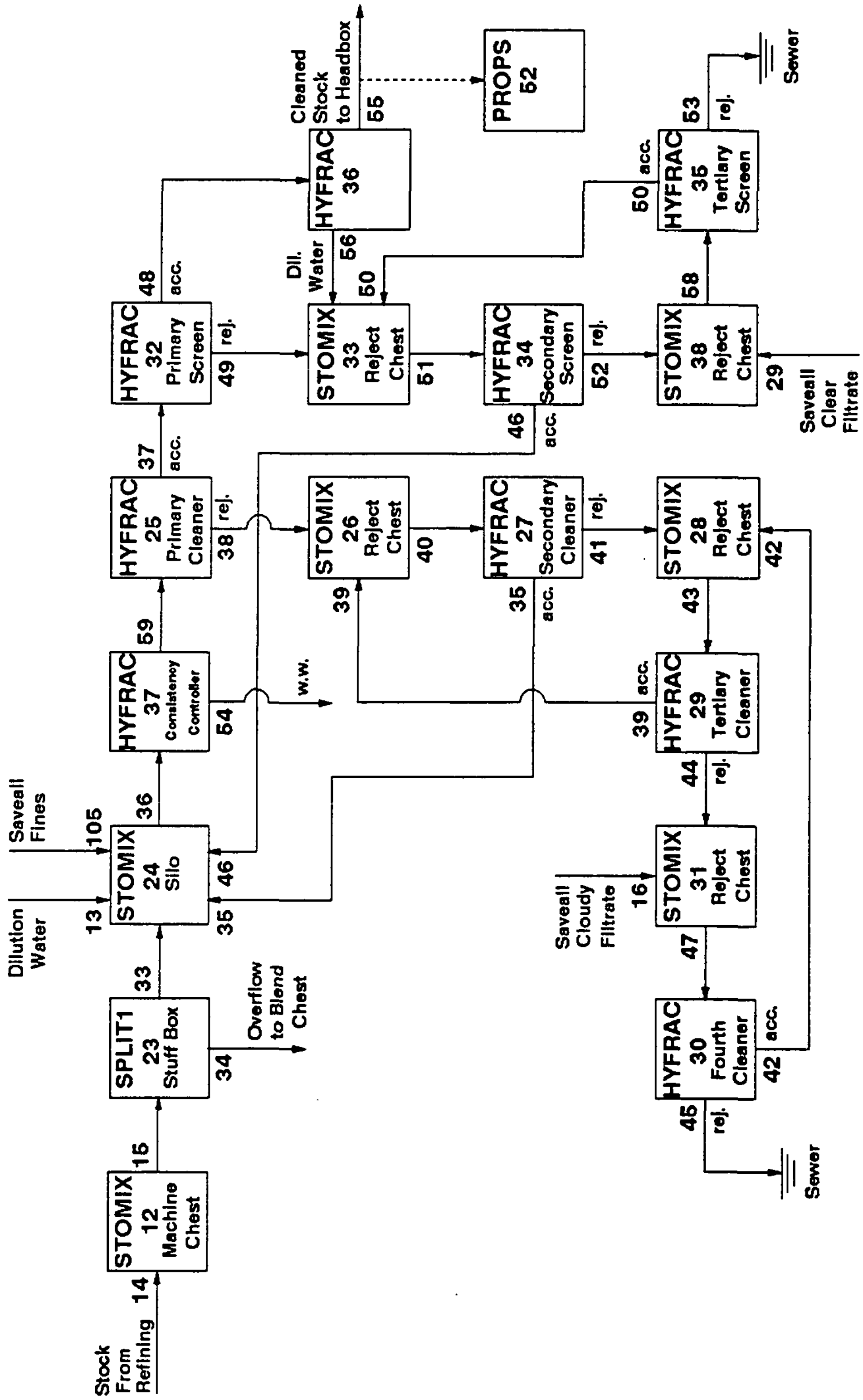

Figure 3

FIGURES

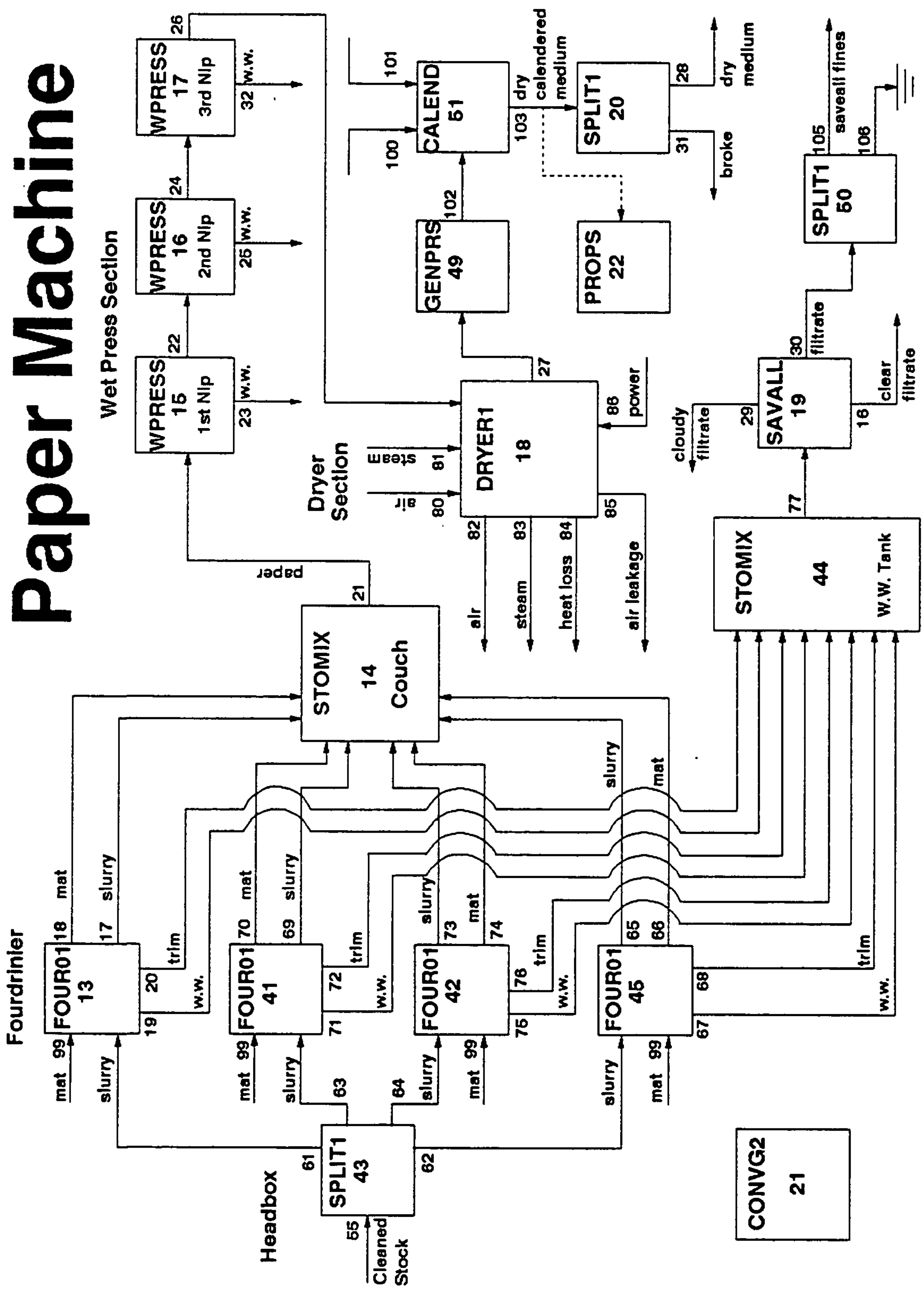

Figure 4

FIGURES

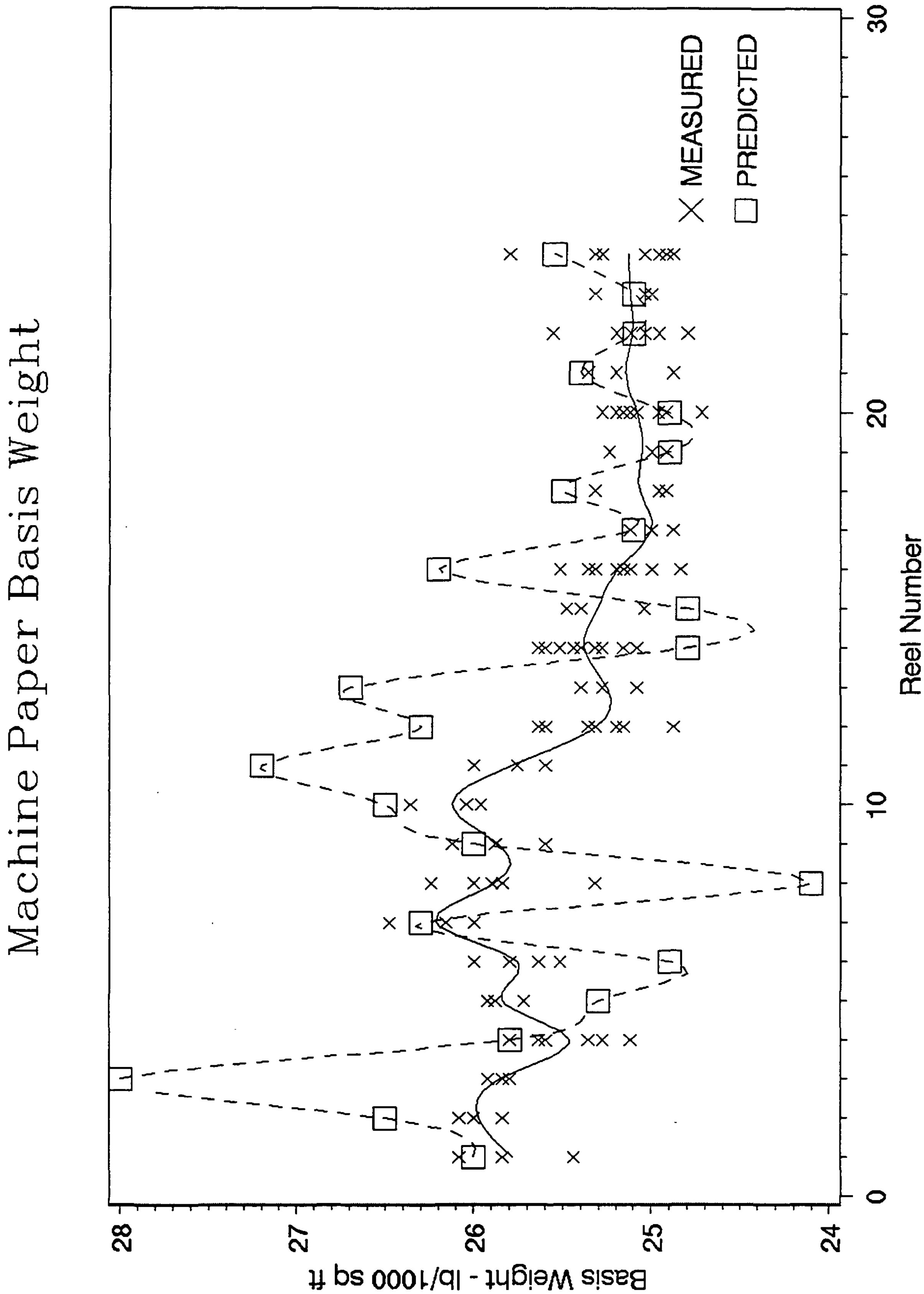

Figure 5

FIGURES

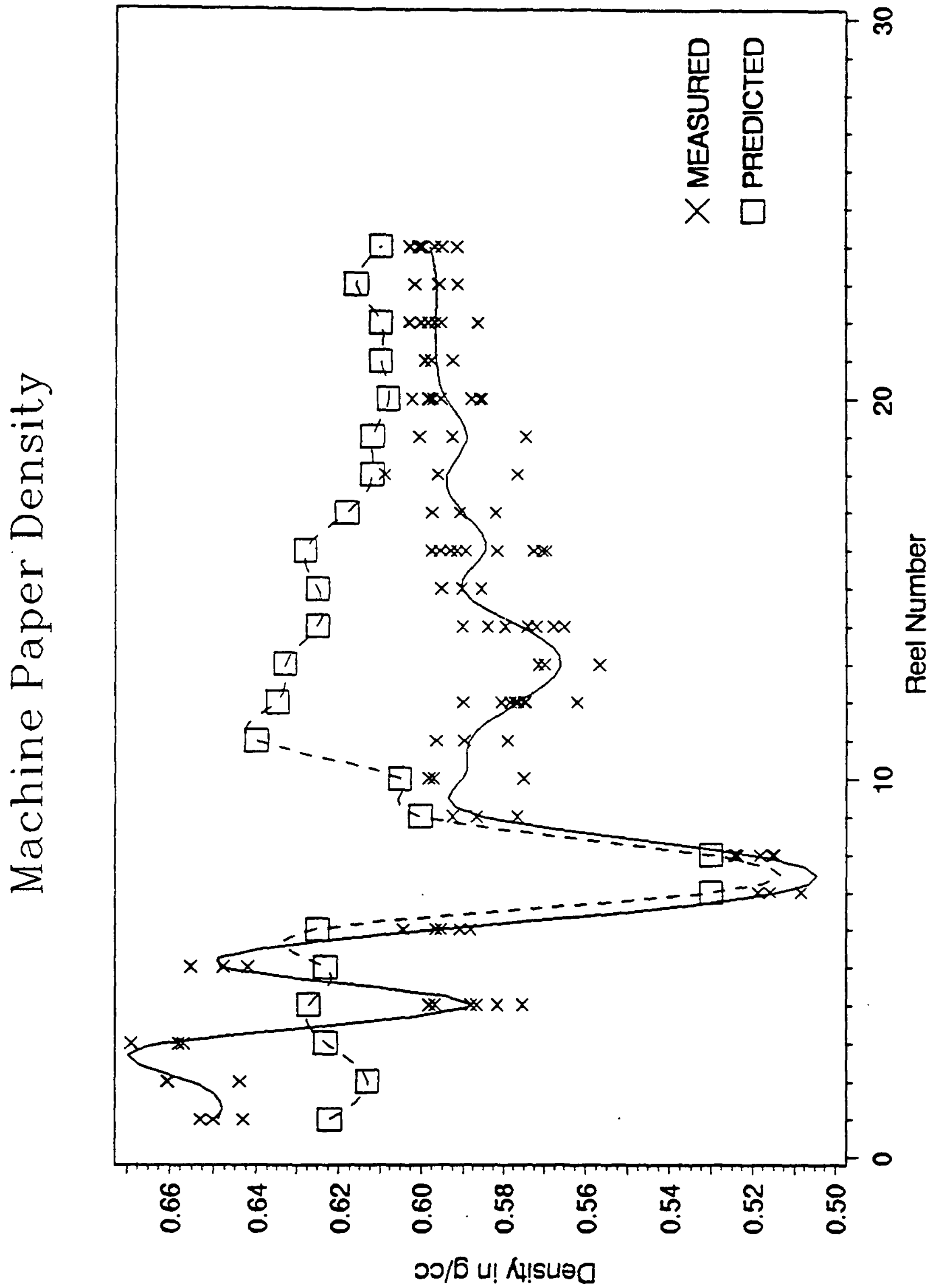

Figure 6

FIGURES

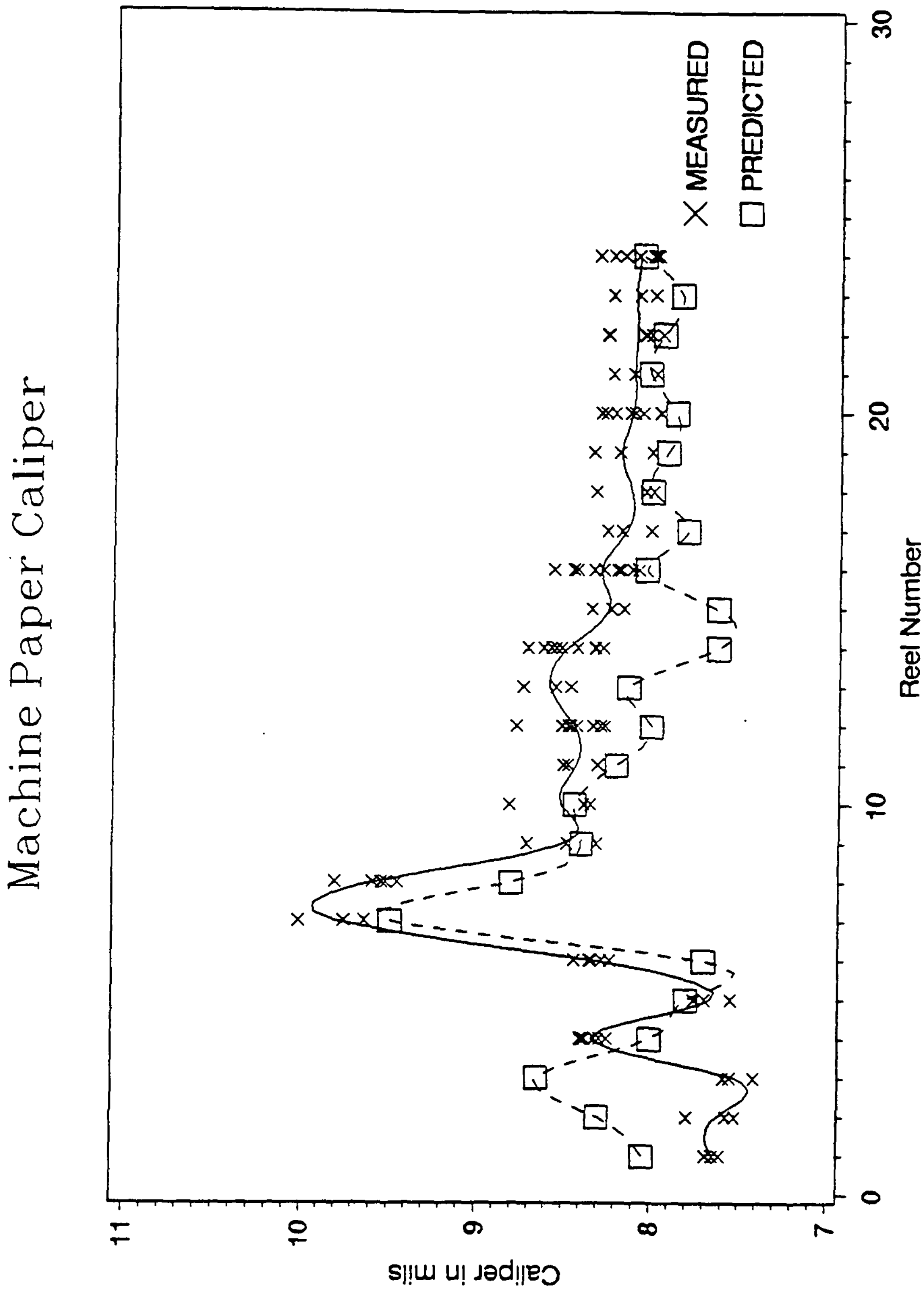

Figure 7

FIGURES

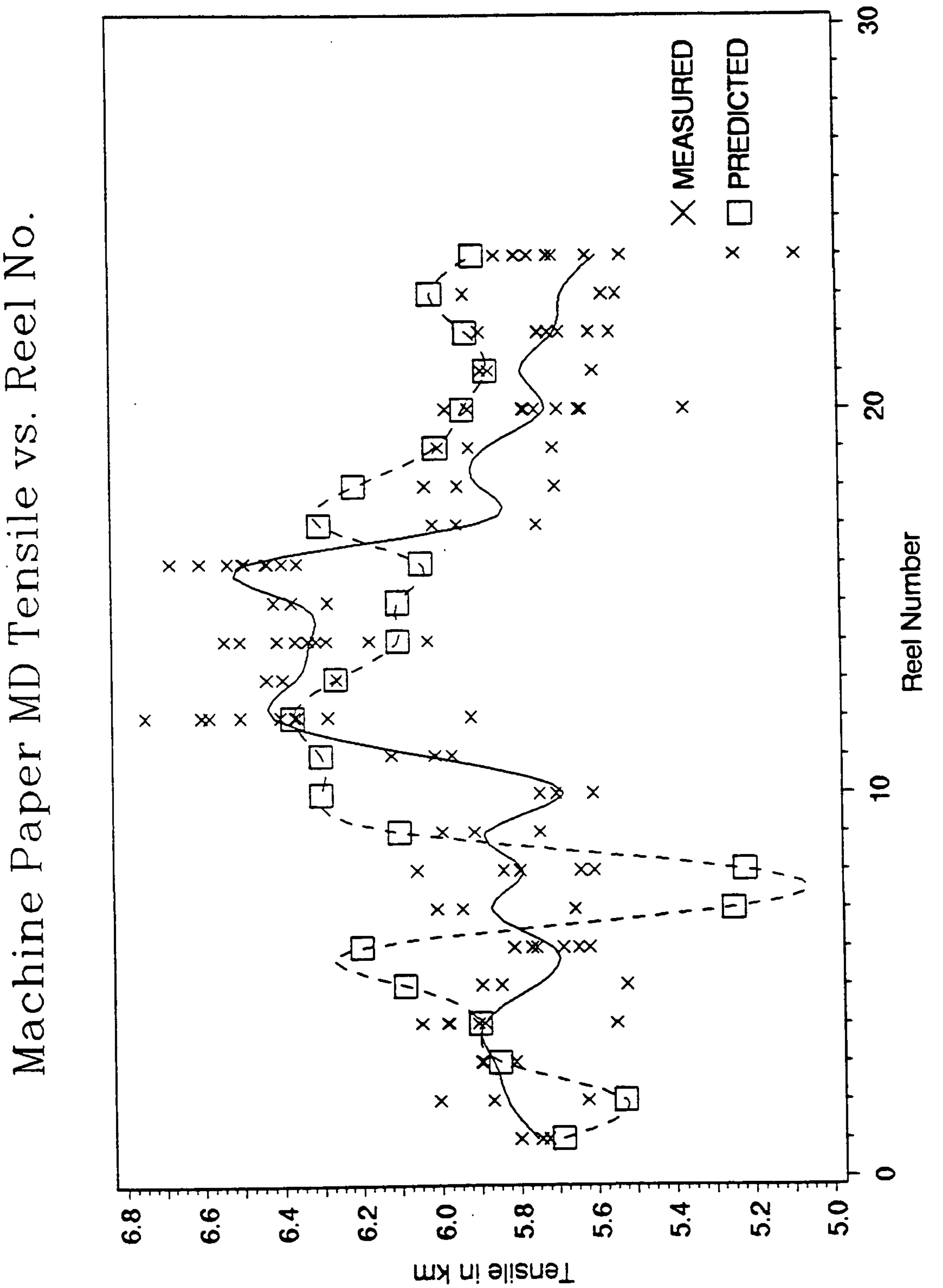

Figure 8

FIGURES

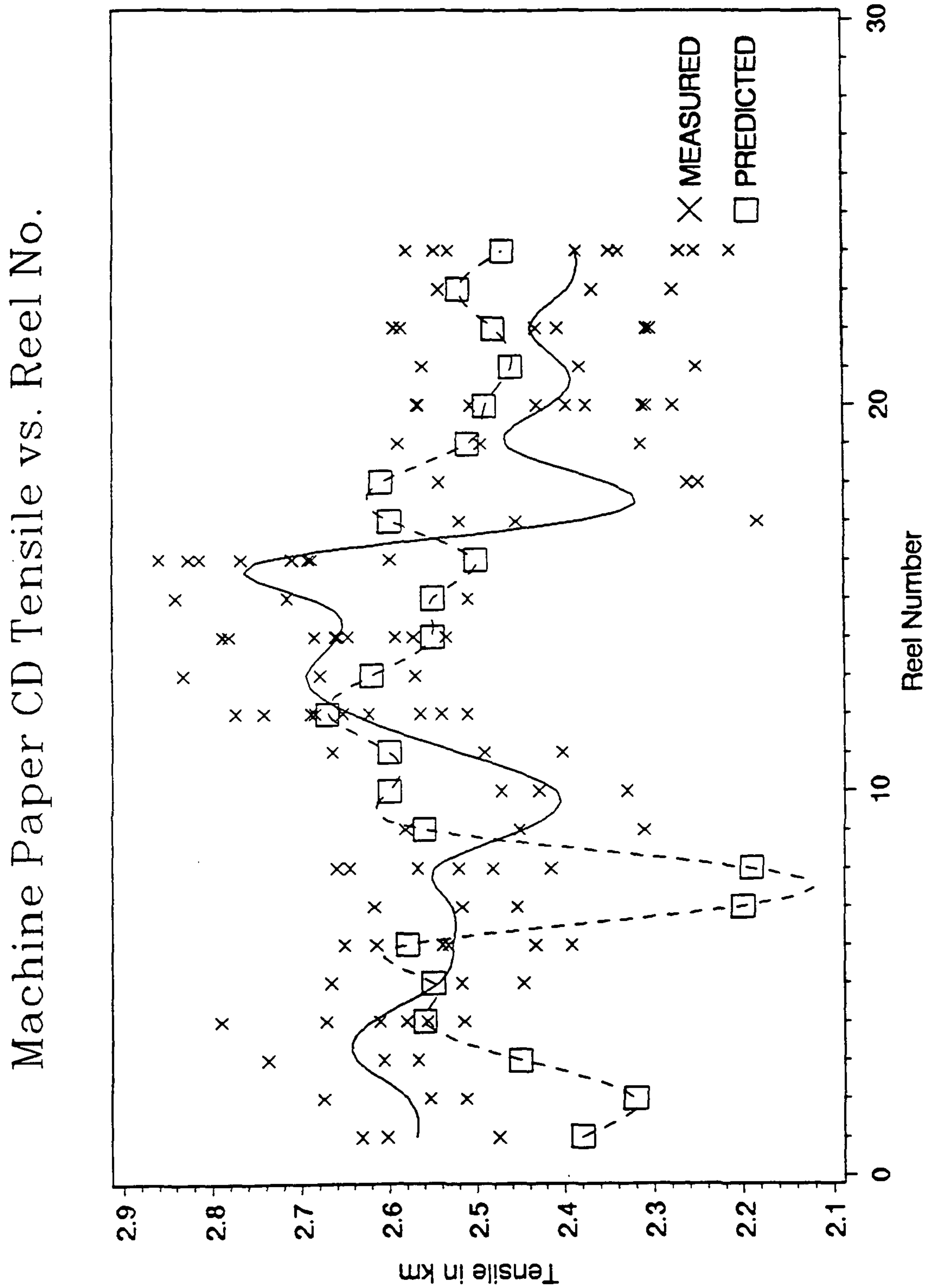

Figure 9

FIGURES

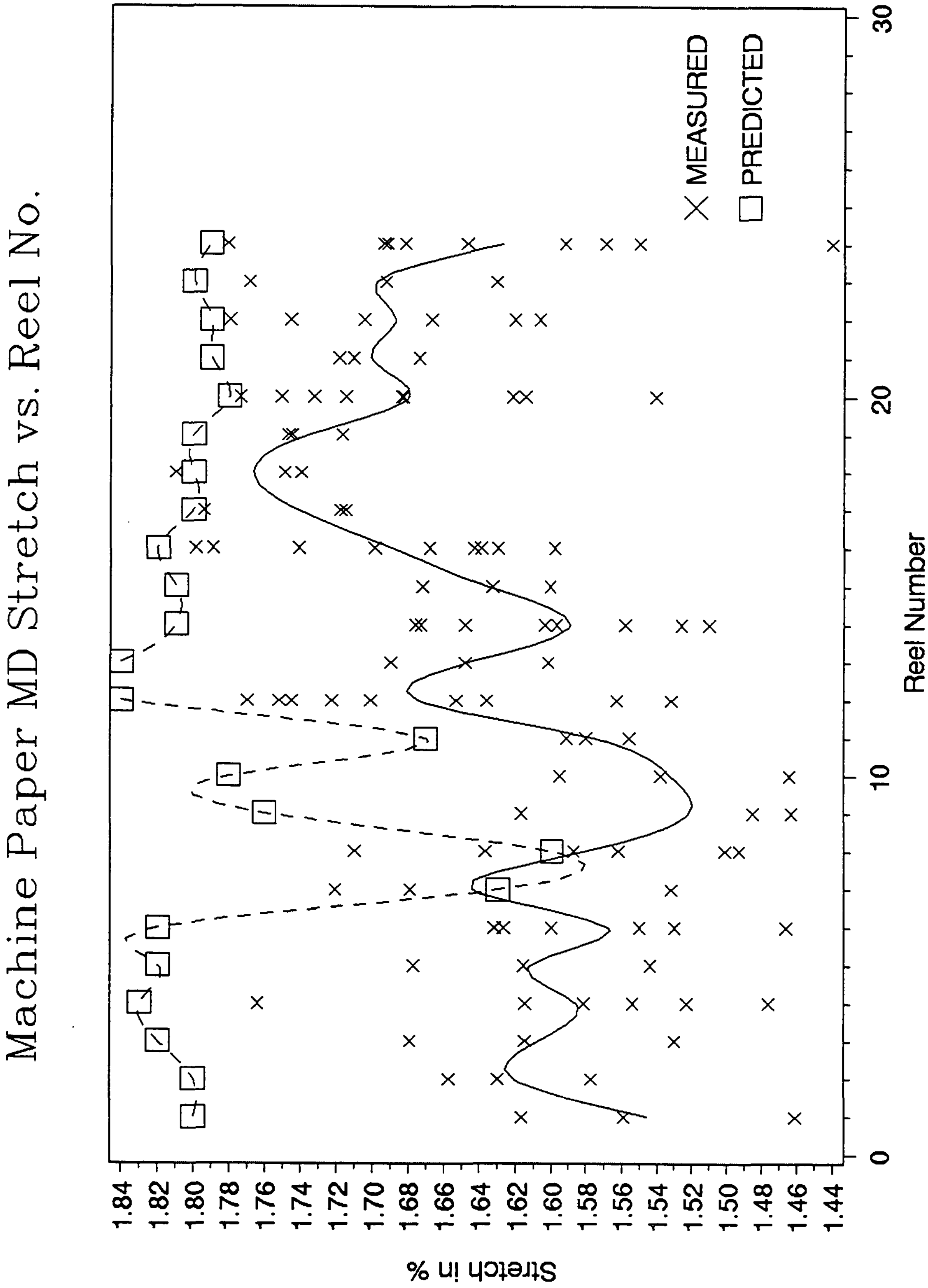

Figure 10

FIGURES

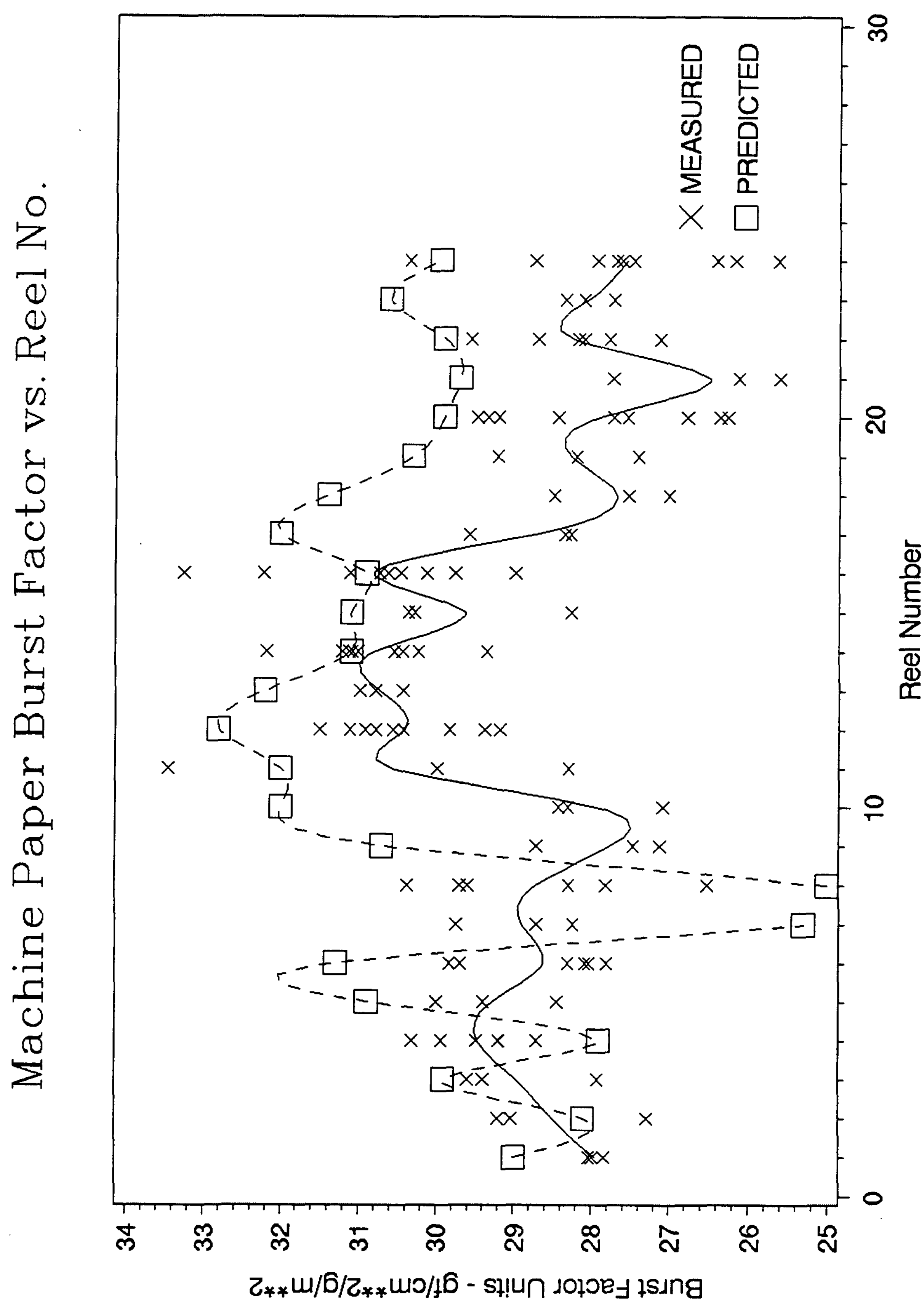

Figure 11

FIGURES

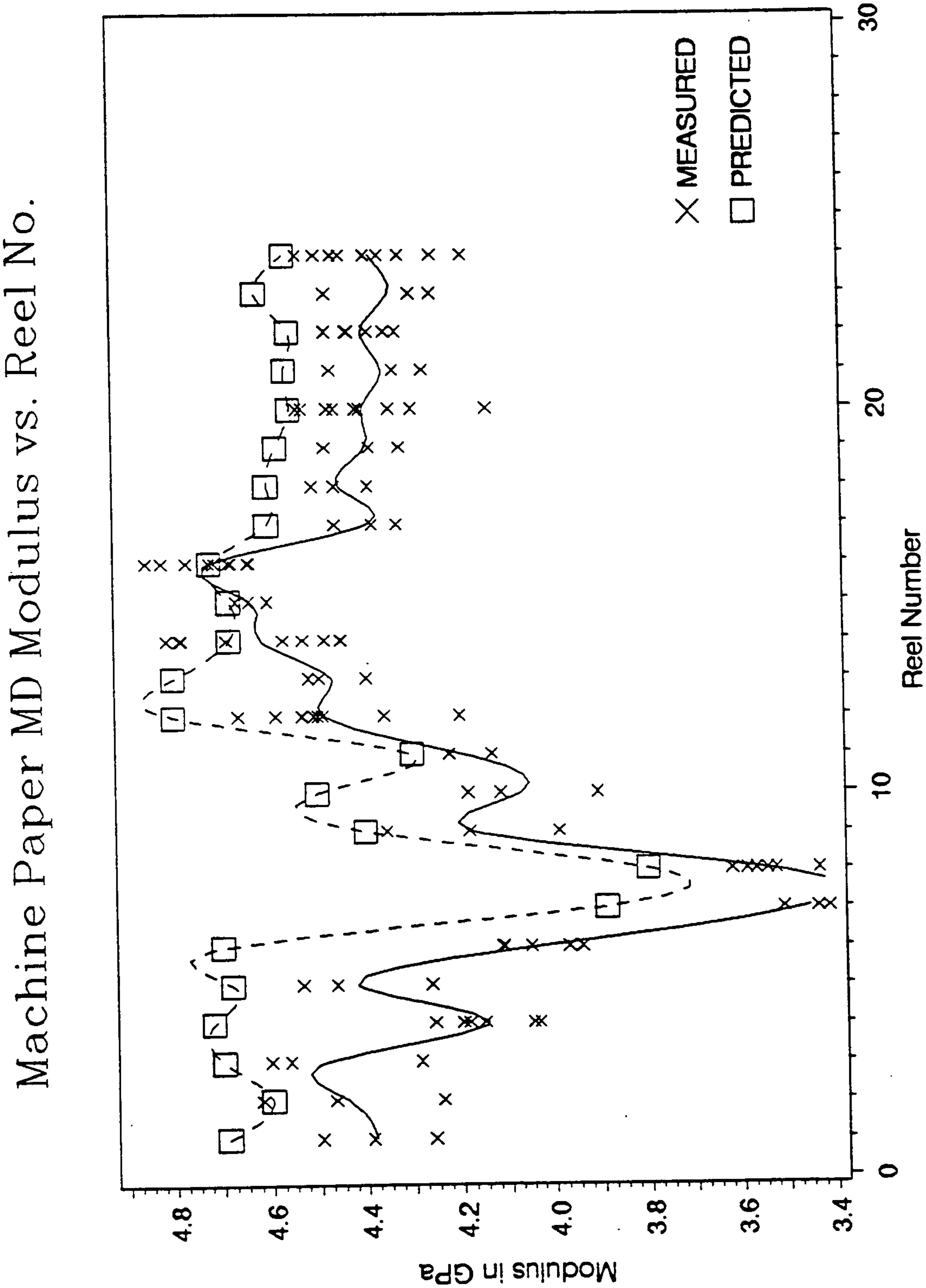

Figure 12

FIGURES

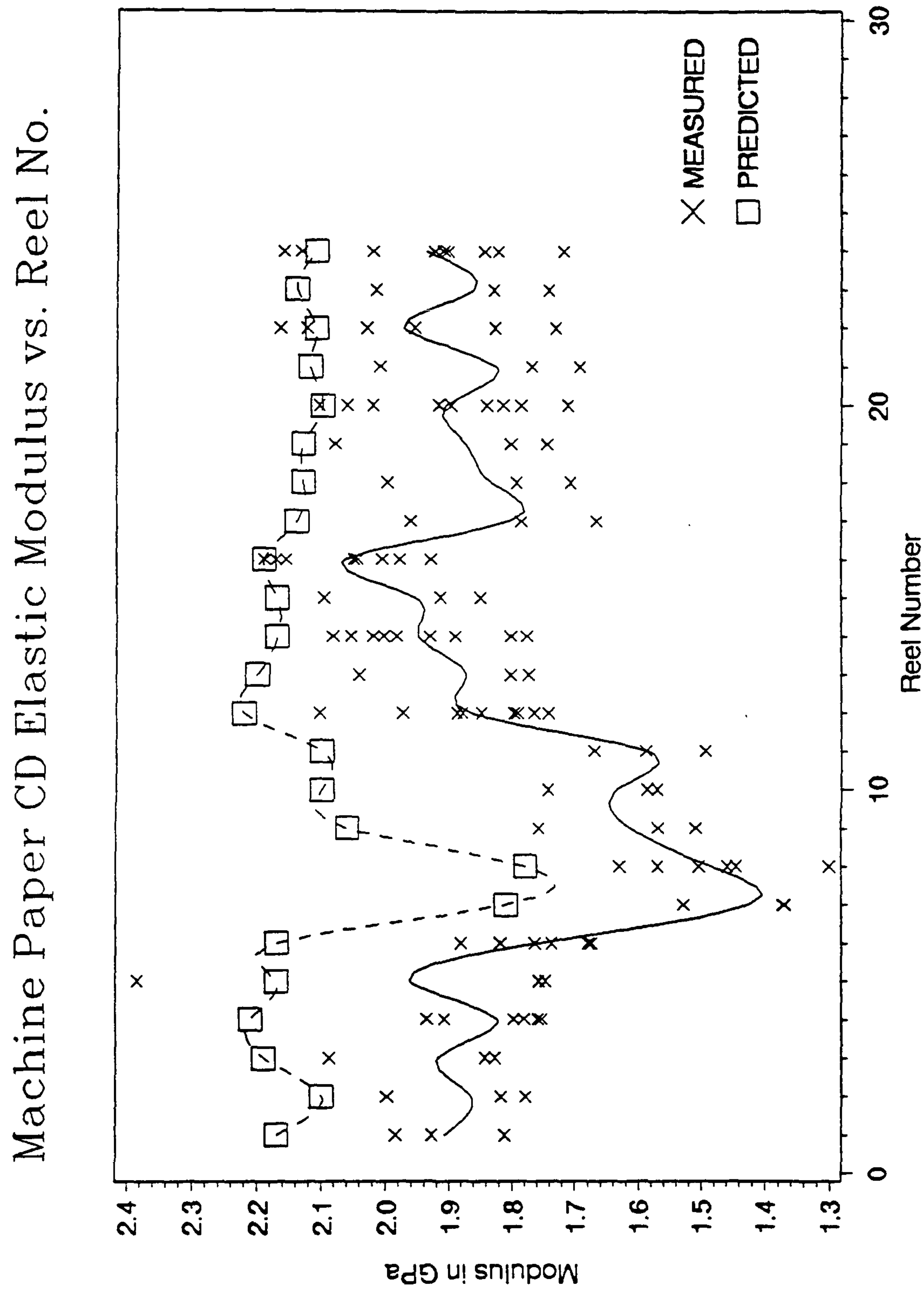

Figure 13

FIGURES

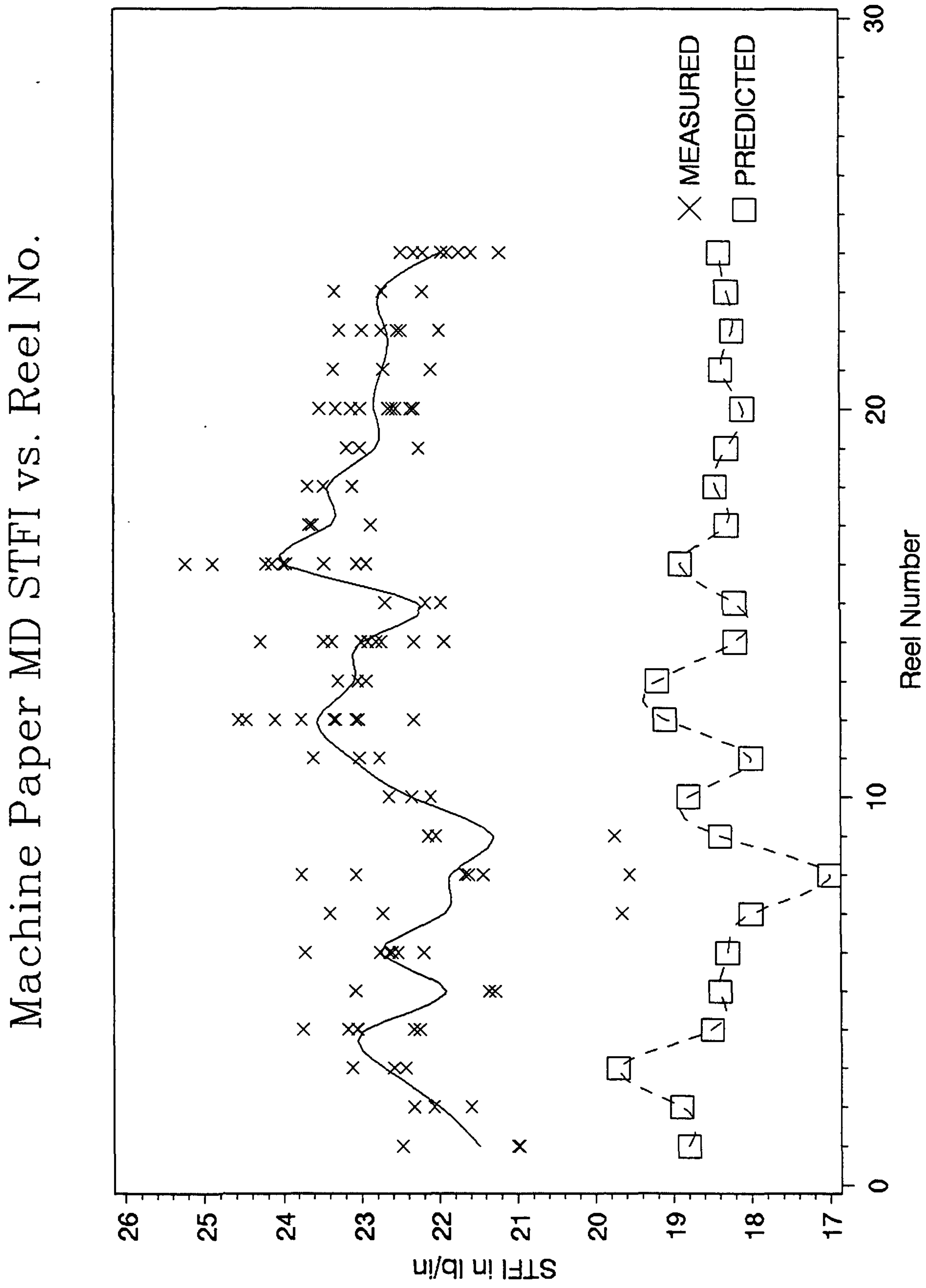

Figure 14

FIGURES

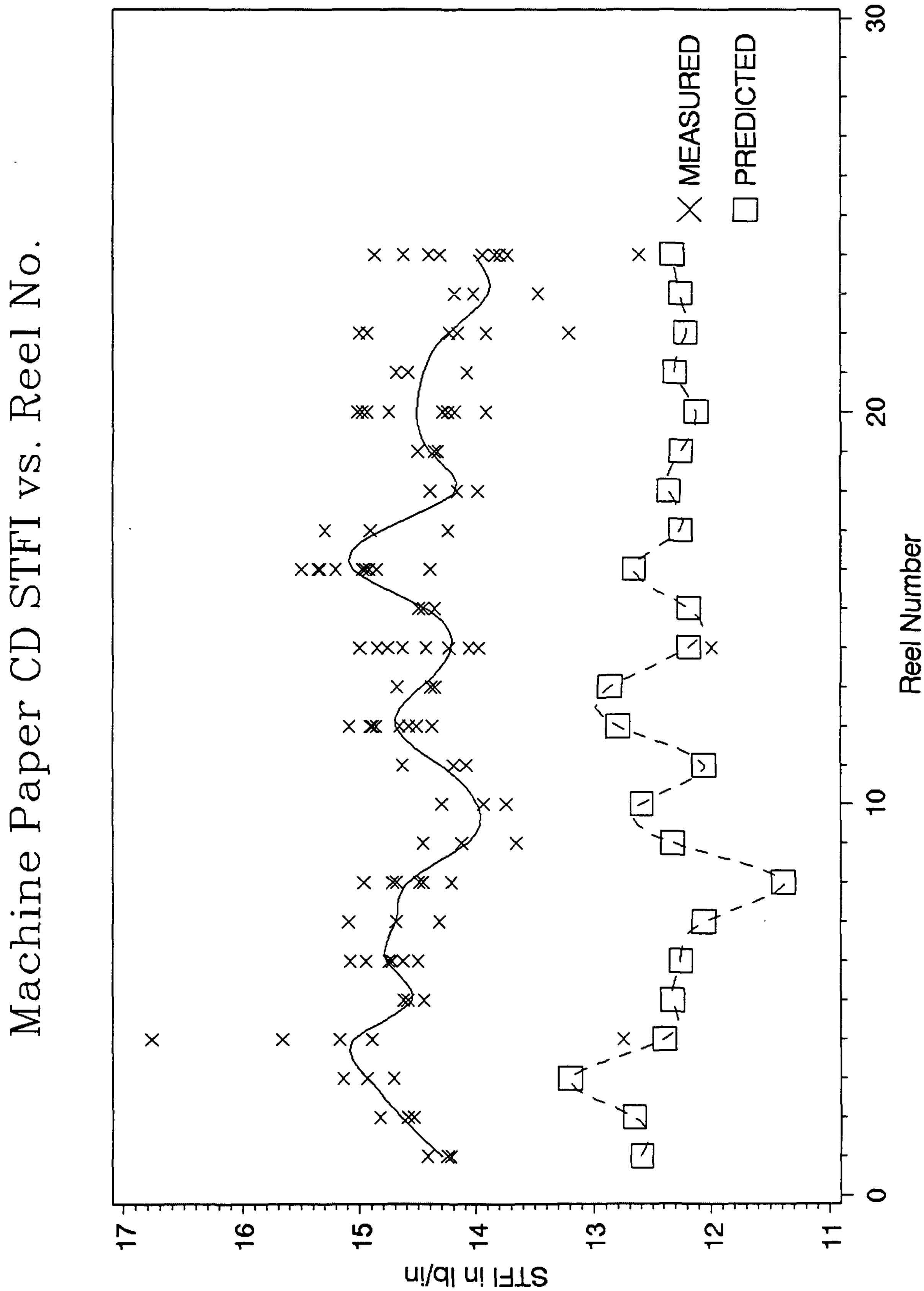

Figure 15

FIGURES

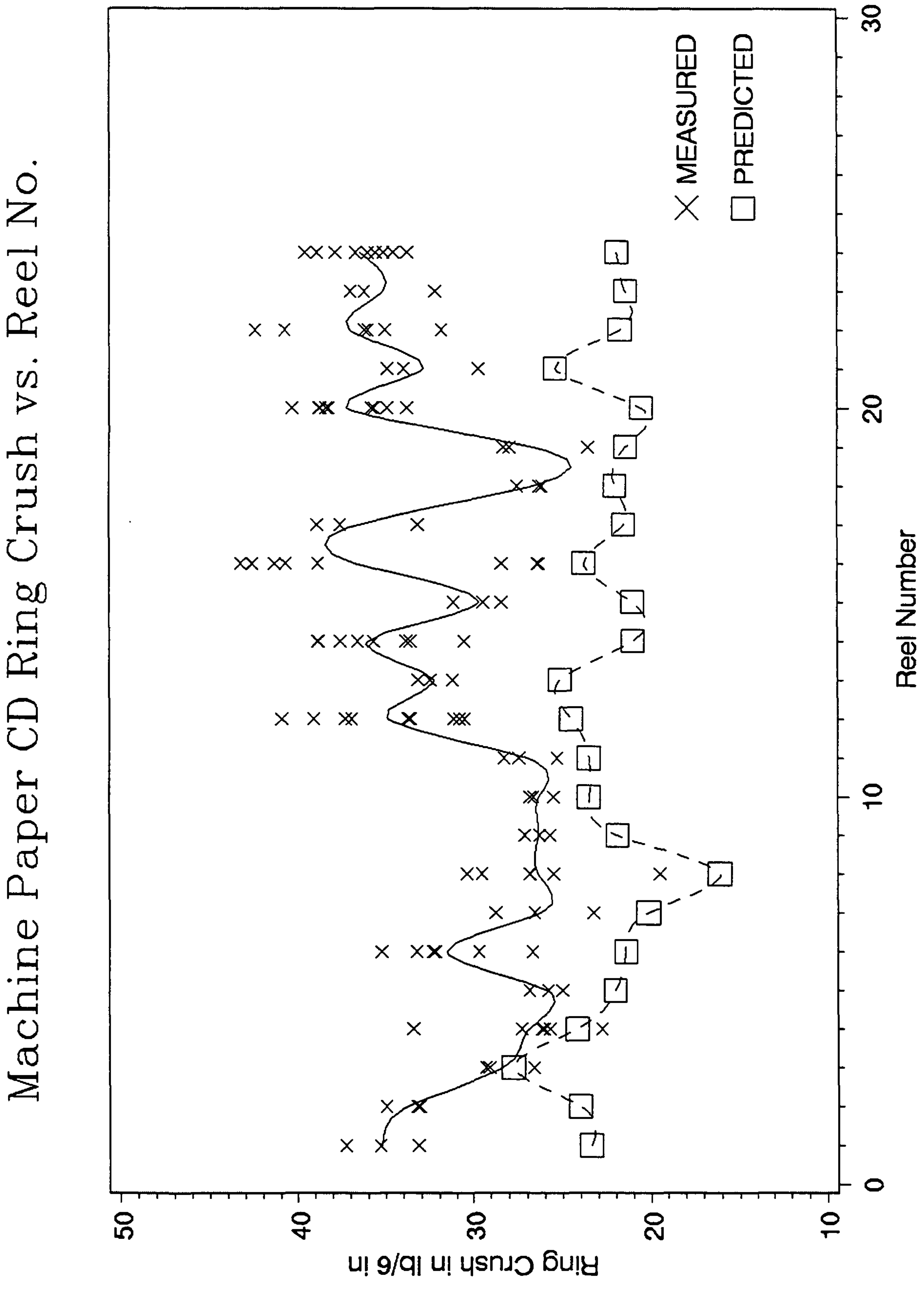

Figure 16

FIGURES

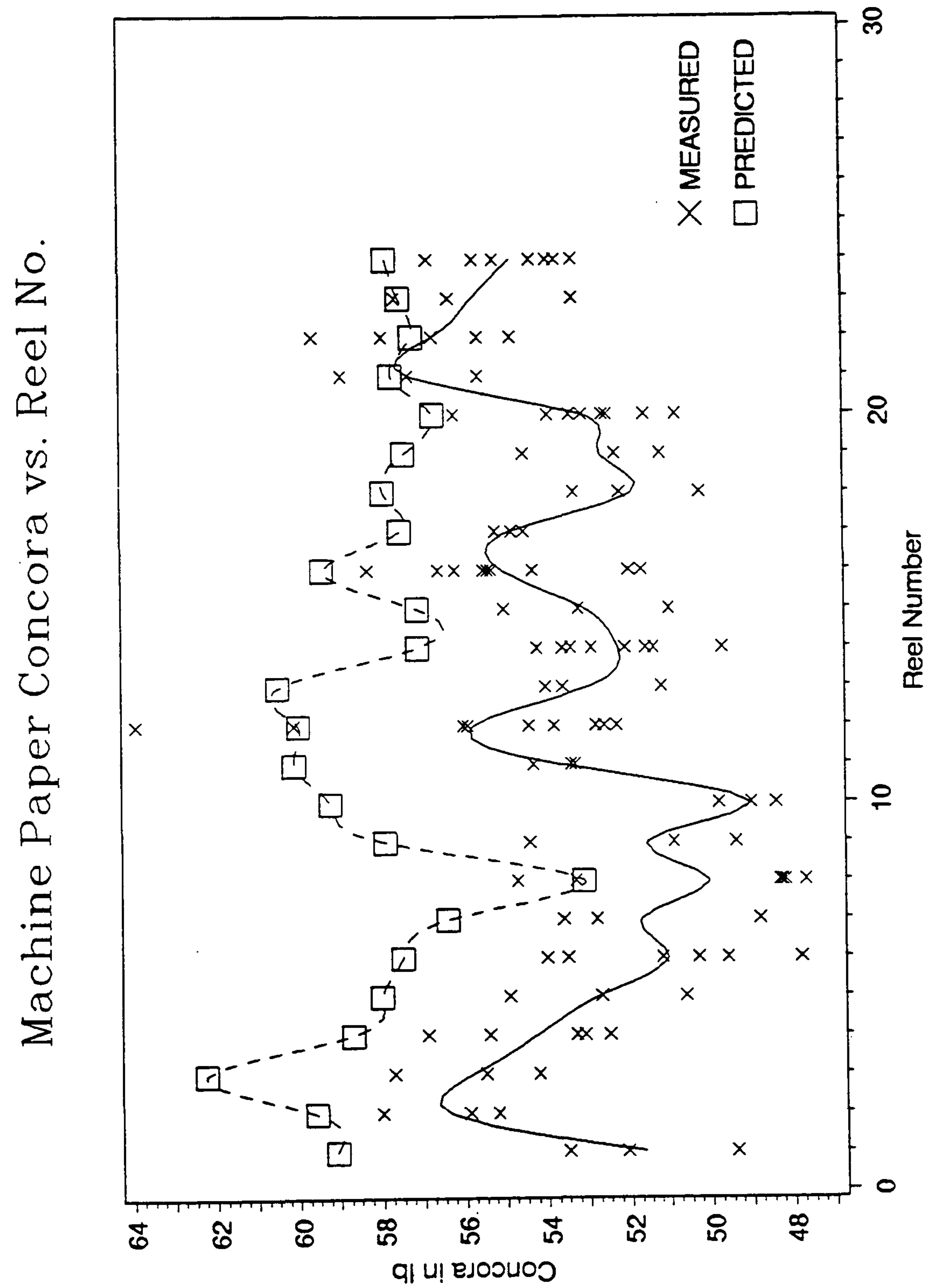

Figure 17

FIGURES

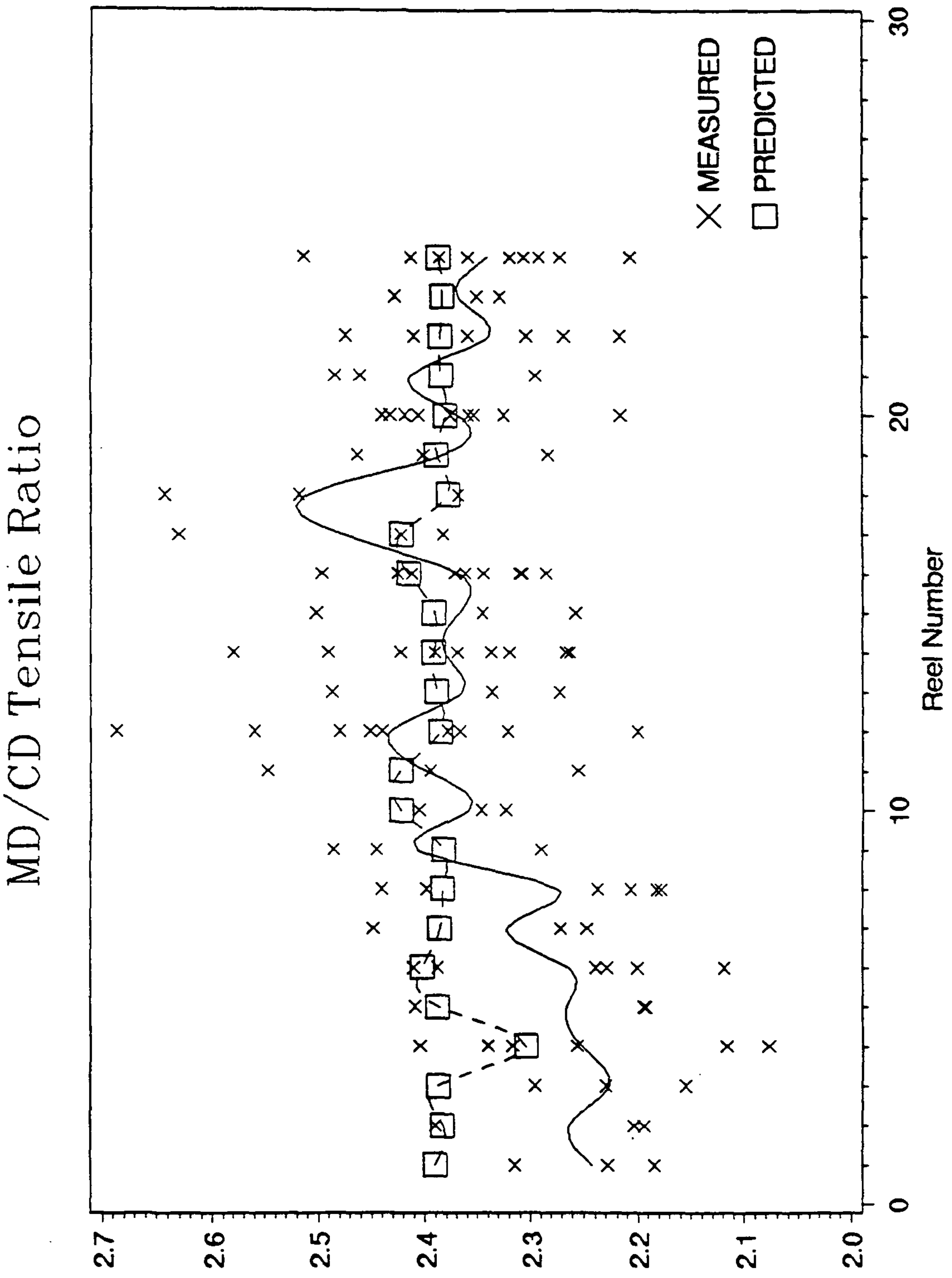

Figure 18

FIGURES

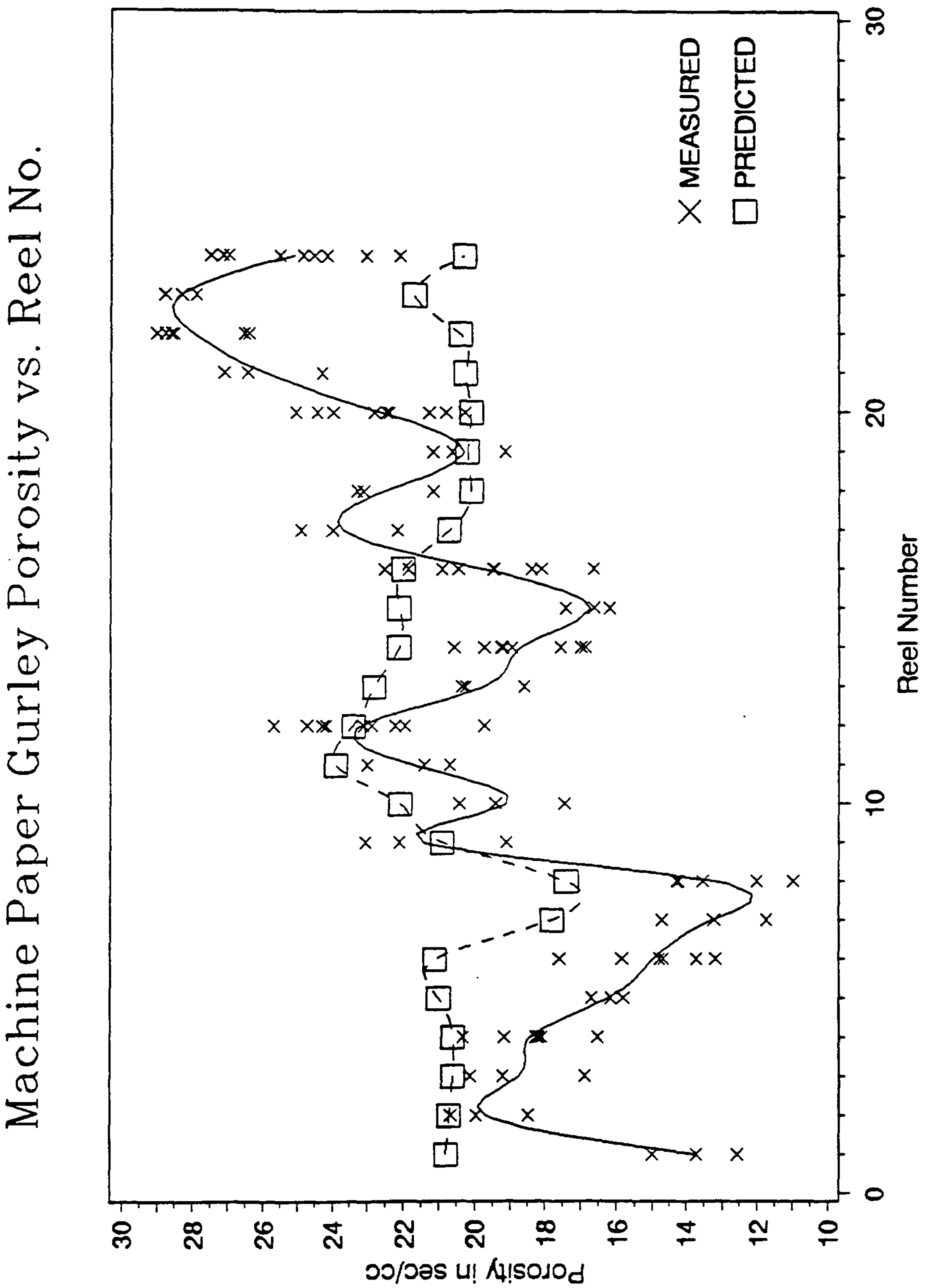

Figure 19

FIGURES

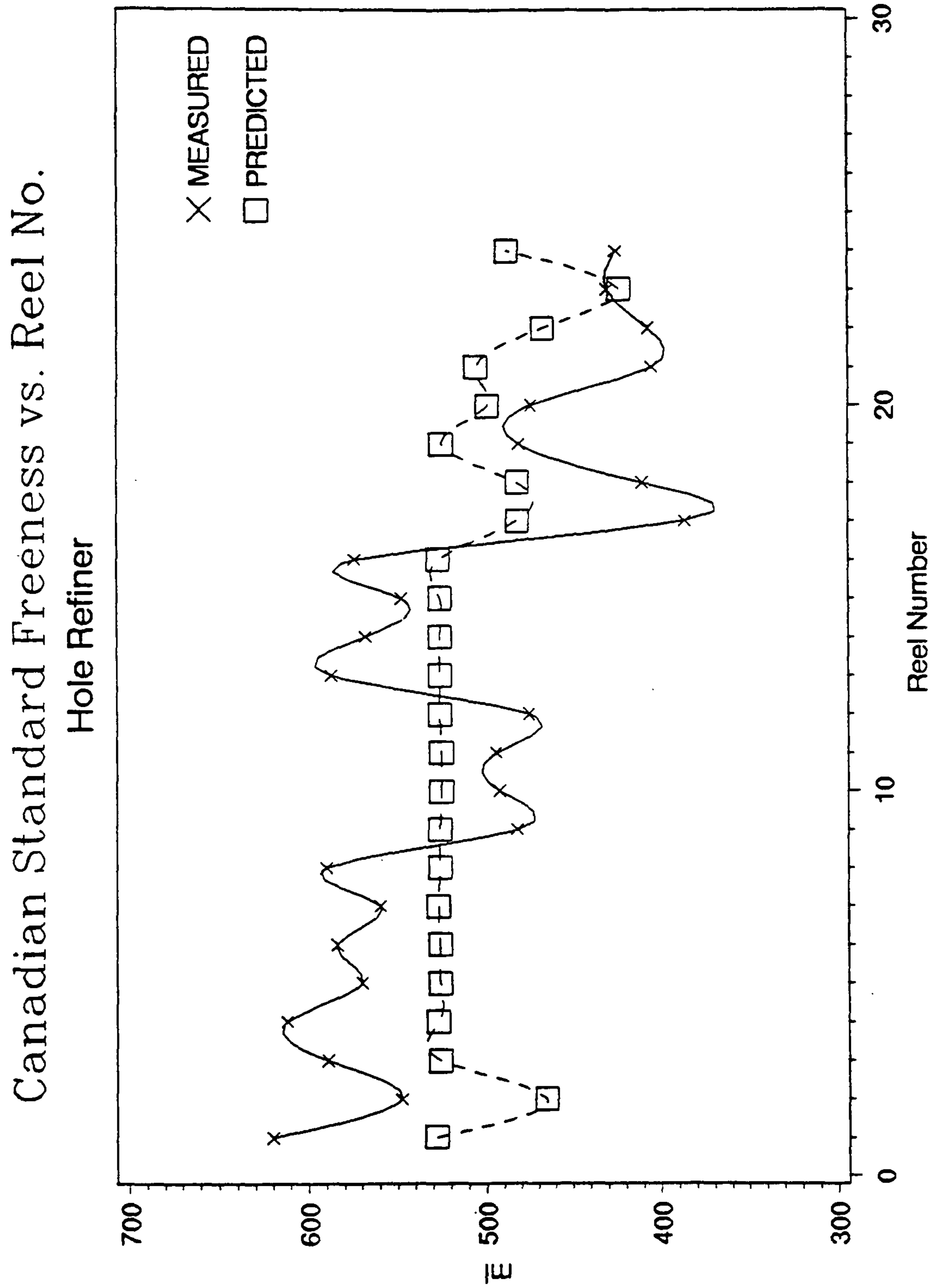

Figure 20

FIGURES

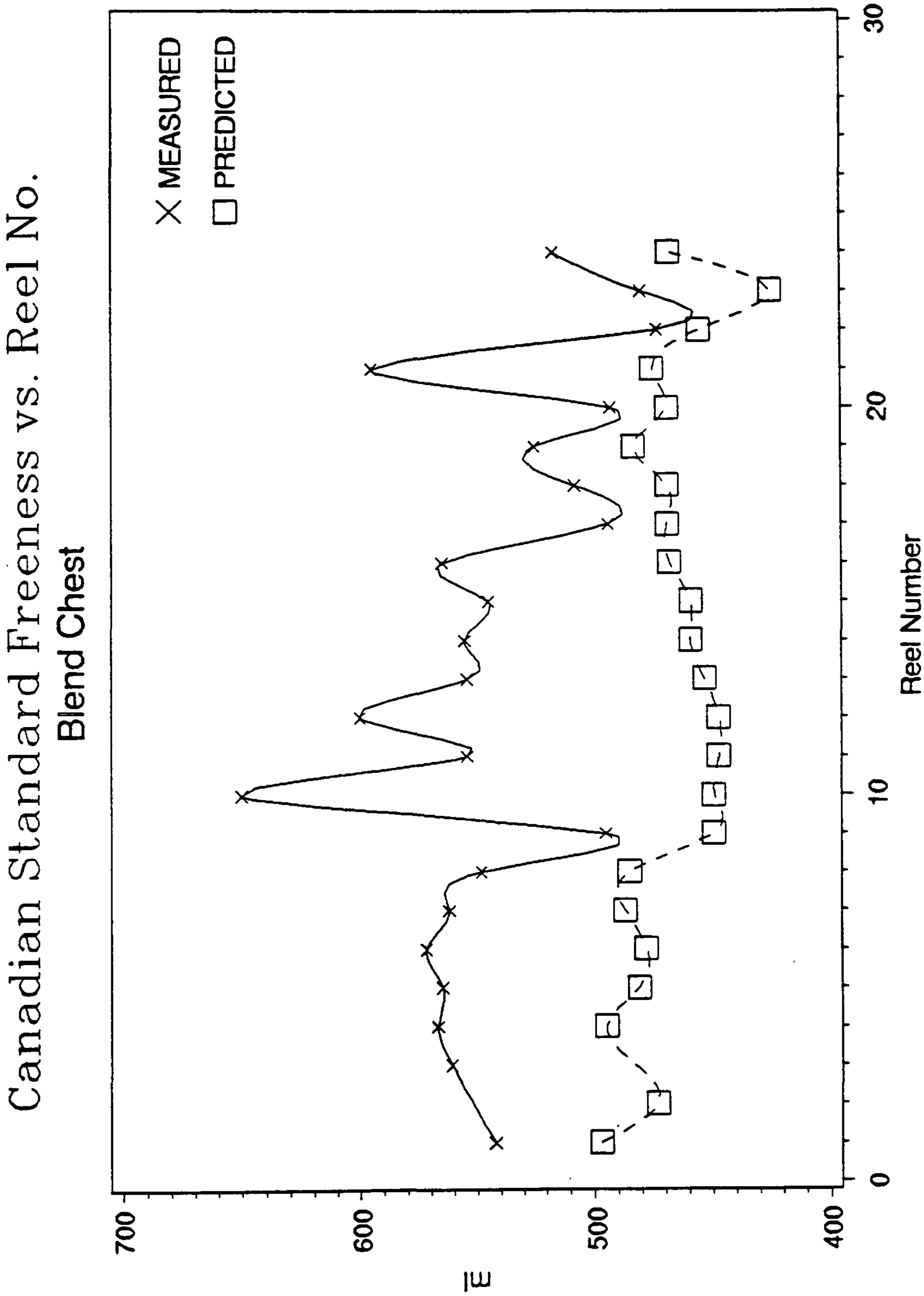

Figure 21

FIGURES

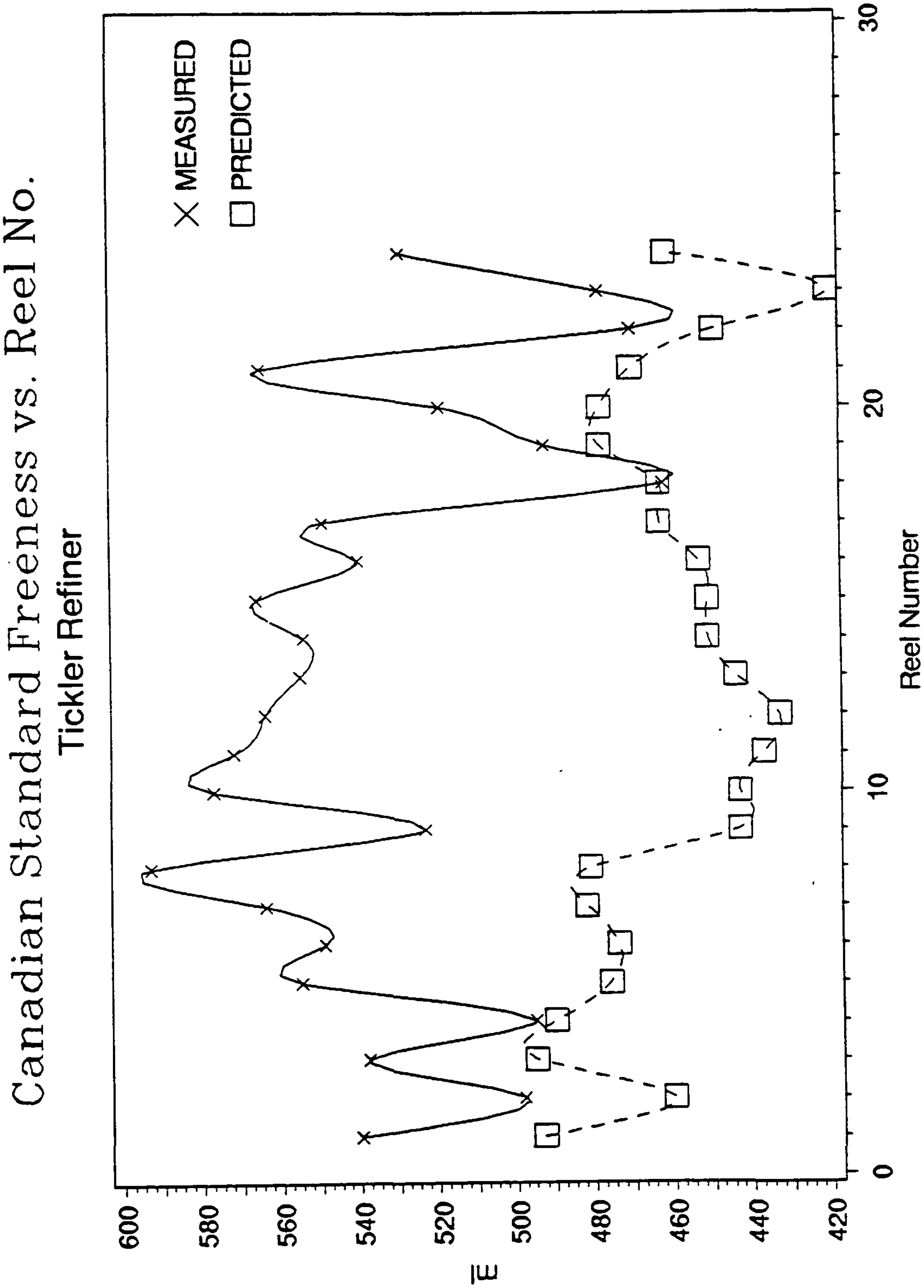

Figure 22

Table XXIV: GOODNESS OF FIT

Handsheet Data 103 Observations							
Variable	R^2	Coeff-icient	F	Mean	CV	T for HO	Root MSE
CSF, ml..............	0.984	1.0711	6745	503	12.8	82.13	64.5
Breaking Length, km..	0.959	0.936	2392	3.64	20.9	48.91	0.76
Concora, lb..........	0.964	0.766	2973	54.53	19.4	54.53	8.35
Ring Crush, lb.......	0.939	1.62	1685	53.5	25.14	41.05	13.5
Burst Factor.........	0.968	1.01	3377	23.0	18.06	58.12	4.15
Porosity.............	0.647	1.033	200	16.0	75.2	14.15	12.0
Density, g/cc........	0.992	0.982	13608	0.411	9.08	116.65	0.037

Table XXV Goodness of Fit

Machine Paper 24 Data Values							
Property	R^2	Coeff-icient	F	Mean	CV	T for HO	Root MSE
MD Tensile, km........	0.996	0.994	31831	5.955	5.98	178	0.35
CD Tensile, km........	0.995	1.01	20601	2.54	7.43	49	0.188
Burst Factor..........	0.995	0.957	21818	29.0	7.22	147	2.09
Density, g/cc.........	0.998	0.96	57067	0.589	4.47	239	0.026
Concora, lb...........	0.997	0.92	44207	53.63	5.06	210	2.71
CD Ring Crush.........	0.967	1.45	3316	32.53	18.4	58	6.0
MD STFI...............	0.998	1.233	62279	22.72	4.278	250	0.97
CD STFI...............	0.998	1.173	53574	14.5	4.59	231	0.67
MD Modulus, GPa.......	0.998	0.948	54201	4.33	4.59	232	0.199
CD Modulus, GPa.......	0.993	0.871	15481	1.85	8.60	124	0.159
MD Stretch, %.........	0.997	0.915	32404	1.637	5.93	180	0.097
Density...............	0.998	0.961	57067	0.589	4.47	239	0.026
MD/CD Ratio...........							
Modulus.............	0.995	1.094	22127	2.36	7.18	149	0.169
Tensile.............	0.998	0.984	49882	2.35	4.78	223	0.112
Porosity............	0.960	0.974	2690	20.48	20.6	52	4.22
Basis Weight........	0.999	0.993	9999	25.4	3.26	328	0.828
Caliper, mils.......	0.998	1.031	5678	8.319	5.0	214	0.416

Statistically, the R-Squared criteria overestimates the goodness of fit but the over estimate is not significant when the correction factors approach 1. Since the correction factors represent the average error in the predictions, a second criteria for model validity is that the average error of the model should fall within the confidence limits of measurement error for each property (See Tables XXVI & XXVII).

Table XXVI: Goodness of Fit Based on Measurement Error

Goodness of Fit - Handsheet Data

Based on all Handsheet Data 103 out of 120 Observations

Property	Correl Coeff-icient	Avg Error %	Mean	Measure Std Dev	Confid Band 90% Absol	Confid Band 90% %
CSF, ml..............	1.0711	7.0	503	-	-	-
Tensile, km..........	0.936	6.4	3.64	0.39	0.78	21
Concora, lb..........	0.766	23.4	54.5	3.6	7.2	13
Ring Crush...........	1.62	62.0	53.5	3.2	6.4	12
Burst Factor.........	1.01	1.0	23.0	2.3	4.6	20
Porosity.............	1.033	3.3	16.0	3.07	6.1	38

Table XXVII Goodness of Fit Based on Measurement Error

Machine Paper

Goodness of Fit Based on Measurement Error

Property	Correl Coeff-icient	Avg Error %	Mean	Measure Std Dev	Confid Band 90% Absol %
MD Tensile, km.......	0.994	1	5.98	0.39	13
CD Tensile, km.......	1.01	1	2.54	0.19	15
Burst Factor.........	0.96	4	29.0	2.3	16
Density, g/cc........	0.96	4	0.589	-	-
Concora, lb..........	0.92	8	54.53	3.6	13.2
CD Ring Crush........	1.45	45	32.5	6.4	39.4
MD STFI..............	1.233	23	22.7	3.8	33
CD STFI..............	1.173	17	14.5	3.2	44
MD Modulus, GPa......	0.948	5	4.33	0.31	14.3
MD Stretch, %........	0.915	8.5	1.637	0.22	27

The confidence bands for each variable are based on twice the standard deviation divided by the mean and expressed as a percent. When the confidence bands are compared with the percent error of the model based on the correction factors, all the models except CD Ring Crush are within measurement error. When the high level of correlation for the corrected model is taken into account, it could be stated that the model is not biased and is therefore also valid as corrected. Thus, a second validation criteria is that the model predictions are valid within measurement error.

Correction factors outside of the measurement error do not necessarily indicate an invalid model. In some cases, the corrections may also include the effects of variability of the laboratory testing procedures. In particular, differences between mill and IPST compressive strength measurements such as STFI and concora indicate that an interlaboratory study may be desirable.

Statistically, it may be concluded that, if the correction is a single factor and the resulting corrected values agree very well with the measurements as measured by R-squared, the model is a useful tool and therefore valid for this grade.

Handsheet Properties - 13 lb/1000 ft^2

The data on the lighter weight handsheets were used primarily to study the zero span tensile strength variations during the trial; for individual data see Appendix IV. The model did not predict a significant variation in zero span tensile. Both the OCC and semi-chem fiber zero-span tensile were initialized with a breaking length of 10 km and the final predicted zero-span values were about 9.5 km as compared to an average of 9.05 km for all 13 lb handsheets measured. The statistics on the 13 lb sheets are summarized in Table XXVIII.

Table XXVIII: Light Weight Handsheet Properties

Property	Minimum	Maximum	Mean	Std Dev
Basis Weight...........	50.7	81.5	65.0	3.27
Caliper, mils..........	6.05	13.7	8.45	1.42
Density, g/cc..........	0.185	0.397	0.313	0.05
Tensile, km............	1.51	4.99	3.55	0.71
Burst Factor...........	12.5	26.4	19.7	3.15
Stretch, %.............	0.61	2.30	1.47	0.34
Gurley Porosity........	1.45	18.0	4.75	3.43
Zero Span Tensile, km..	6.74	12.00	9.05	0.90
Moisture, %............	4.92	7.33	6.12	0.51

The examination of the measured zero span data for each location indicates that the zero span tensile did not change significantly throughout the process or with time during the trial. Some handsheet data from the mill were available to compare with the data from IPST and the model predictions. These data, which represent a single set of beating curves from 280 to 606 ml CSF, are summarized in Table XXIX.

The 13 lb handsheet had lower densities than the 26 lb sheets. The mean density of the light weight sheets was 0.313 as compared to a mean value of 0.411 for the 26 lb handsheets. Over most of the range in basis weight, density does not depend on basis weight. However, for low basis weight, density apparently increases with basis weight. One possible explanation for the higher density of the 13 lb is that the formation was more variable and could have resulted in a variation in caliper causing a nonuniform application of pressing pressure and nonuniform densification. Both the nonuniformity in density and formation itself would have contributed to lower tensile properties for the lower basis weight sheets.

Gurley porosity of the light weight handsheets (4.75) was also considerably lower than the 26 lb handsheet values of 16, indicating that the light weight handsheets had considerably higher porosity. The porosity differences were in agreement with the observed density differences.

It is interesting to note that the mean tensile strength (breaking length) of the light weight sheets, 3.55 km, was not significantly lower than the mean of the 26 lb sheets, 3.64 km, while the burst factor of 19.7 for the 13 lb handsheets was significantly lower than the value of 23.0 for the 26 lb handsheets. The similar tensile strength values indicate that formation of the 13 lb handsheet was equal or superior to that of the 26 lb handsheets. Theoretically, the more uniform formation (higher formation index) compensates for the lower density resulting in about the same tensile strength (other things being equal).

The models would have been able to predict the light weight handsheet data although this work was not done. It would have been necessary to assume a lower effective pressing pressure for the light weight sheets to fit the density and a corresponding higher formation index to fit the tensile or burst data.

Interlaboratory Differences

A limited set of property data were provided by the mill. The properties of interest were concora, STFI and freeness at the primary discharge, tickler discharge and headbox discharge. The Concora and Headbox CSF are summarized in Table XXX along with the IPST data and model predictions. These comparisons indicate that the model predictions tend to follow the mill concora and CSF data rather than the IPST data. Said another way, the mean values of the model prediction for each of these variables was closer to the mean of the mill data than to the mean of the IPST data. However, it was shown above that the models "tracked" the IPST data quite well with an offset. The concora model is based on data of Whitsitt obtained from numerous laboratory and mill sources and the differences shown in Table XXX indicate that the concora testing procedure at IPST may have been different.

The CSF data are indicative of the large variations that can occur with CSF measurements. The differences between the model predictions of headbox CSF were the largest of any location as a result of the high fines content of the predicted headbox stock fines as with Concora the predicted values were closer to the mill CSF values than to the IPST values.

Analysis of the mill beater data (See Table XXIX) also indicates laboratory differences; for instance, the zero span values of the beaten pulps were 7.3 km, as compared to 9.05 km measured by IPST and 9.5 km predicted by the model. The mean CSF of the handsheets tested at IPST was about 500 ml, corresponding to the column at a beating time of 8 minutes where the freeness was 493. At this level of CSF the mill handsheet density was 0.527 g/cc compared to 0.411 g/cc for the IPST handsheets. The breaking lengths were similar, however, with the mill breaking length of 3.9 km being only slightly higher than the IPST mean breaking length of 3.64 km. The mill handsheet data at 500 ml CSF and mean IPST handsheet data at 493 ml CSF.

Table XXIX: Mill Handsheet Data

	Beating Time, minutes			
	0	8	13	18
CSF, ml.........	606	493	407	280
Basis Weight....	28.24	28.31	28.29	28.49
Density, g/cc...	0.475	0.527	0.549	0.582
Tensile, km.....	2.1	3.9	4.7	5.1
Burst Factor....	14.0	23.1	28.6	32.7
Stretch ,%......	1.3	2.8	3.3	3.6
Gurley Porosity.	1.1	4.1	11.7	44.6
Concora, lb.....	27.8	49.0	66.2	73.9
Ring Crush, lb..	33.9	49.2	61.1	65.1
Zero Span, km...	5.0	7.3	7.3	7.3
STFI, lb./in....	12.2	16.7	19.0	20.9

It may be concluded from these data that the comparable breaking length for the two sets of handsheets is a result of the higher density for the mill data, which offsets the lower zero span tensile. The burst factors of the two handsheet were also very close, indicating that the tensile strengths and compressive properties were comparable. The slightly lower mill compressive properties were likely a result of the lower caliper of the mill sheets at the same basis weight due to the higher sheet. Thus, the compressive properties would be expected to be comparable because, as mentioned above, the compressive property models show that there is a trade-off between caliper and modulus.

Table XXX: Comparison of Selected Data Values Machine Paper Data and CSF

Reel	Concora			Headbox CSF		
	MB	Model	IPST	MB	IPST	Model
1	59.6	59.1	51.7	367	305	447
2	67.4	59.6	56.4	371	286	413
3	63.2	62.3	55.8	331	280	449
4	61.8	58.7	53.3	350	260	444
5	61.0	58.0	52.7	355	264	428
6	59.2	57.5	50.5	405	324	422
7	60.6	56.4	51.7	398	321	432
8	58.0	53.1	51.5	346	305	431
9	58.6	57.9	48.3	383	277	412
10	61.4	59.2	50.1	400	277	386
11	62.2	60.1	51.6	375	310	380
12	66.2	60.0	55.8	397	272	376
13	62.8	60.5	52.9	407	309	383
14	60.6	57.1	52.3	409	286	386
15	64.4	57.1	53.1	386	293	386
16	64.8	59.4	55.0	374	335	398
17	66.4	57.5	54.8	354	295	407
18	67.6	57.9	51.9	374	275	407
19	63.6	57.4	53.1	361	290	426
20	63.4	56.7	53.6	363	286	416
21	67.0	57.7	57.2	355	296	416
22	66.2	57.2	56.7	338	280	398
23	60.8	57.5	55.7	339	255	367
24	59.4	57.8	54.8	372	295	401

Table XXXI: Comparison of MB and IPST Handsheet Data at Comparable Values of CSF

	IPST	MB
Density, g/cc....	0.411	0.527
Tensile, km......	3.64	3.9
Concora, lb......	54.5	49.0
Ring Crush, lb...	53.5	49.2
Burst Factor.....	23.0	23.1
Gurley Porosity..	16.0	4.1
Zero Span, km....	9.05	7.3

MD Modulus could be related only to sheet density or various powers of density. The density relationship is fundamentally sound and was confirmed by the correlative analysis. However, the contribution of density was only 50% of the total variation in the data indicating that other factors must contribute to the variability. The predictive model used by MAPPS assumes that the tensile and modulus ratio was relatively constant throughout the test and was confirmed by the measured data. Thus, it is unlikely that variable stretch and/or shrinkage resulted in MD/CD variations which would have influenced modulus.

Burst Factor was most strongly related to the product of the MD and CD tensile strength although the square root function used in the model would have given a stronger correlation. Stretch was not found to contribute, possibly due to the form of the model.

MD tensile strength was most strongly dependent on machine speed with a small but significant dependence on calender stack loading and density. All of these effects could be expected based on fundamental modelling considerations. Machine speed is a factor because it influences the MD/CD tensile ratio. Stack loading can affect tensile through bonding/debonding behavior or through stress relaxation which also affects MD/CD tensile ratio. Density affects tensile because it is a measure of the degree of bond formation or breaking occurring under load. However, the sum of these three terms was still not sufficient to provide a good predictive model for MD breaking length.

It is interesting to note that concora could not be related to ring crush, and STFI, or elastic moduli even though a fundamental relationship should exist. Ring Crush appeared to be dependent on machine speed, indicating that MD/CD tensile ratio may influence ring crush variations.

CONCLUSIONS - Validation Study

Based on the two validation criteria and estimates of measurement error, the model system appears to be valid for corrugating medium. Correction factors for some properties may need to be applied to some of the property predictions. Two areas in the models will require modification. A follow-up calendering test is recommended to reconcile and confirm the conclusions of the effects of calender load.

There is some evidence of transient effects when looking at the handsheet CSF and machine paper data but these effects could not be separated from the overall variations in the data. Property variation with time appeared to be a response to several causes:

1. property measurement error (no real cycling)
2. CD variability
3. semi-chem CSF and other inputs to the system (real effect)
4. unmeasured variables which changed
5. measured and controlled test variables
6. holdups in tanks (first-order lags) which propagated through the system diluting certain effects and propagating others

The high level of the correlations leads to the following conclusions:

1. The data were highly consistent internally.
2. The major factors affecting properties were accounted for in the models.
3. Many factors which were held constant or calculated to be constant, e.g., machine paper formation, were indeed approximately constant.
4. Those factors which did change during the trials were most probably the major factors affecting properties.
5. The fundamental basis for predicting property development appears to be reasonably well understood.
6. The properties depend on each other in a hierarchical structure, i.e., density, tensile, and elastic properties, derived properties such as burst factor (and tear), compressive properties such as STFI and flat crush and, finally, highly derived properties such as ring crush and concora.
7. The predictable response of the handsheet and machine paper properties to process changes indicates that the overall model structure and concepts are consistent.
8. Areas of weakness appear to be the exact sensitivity of the contact development with pressing and the relationship between density, bond density, modulus and strength.
9. It appears that modulus is a function of density rather than bonding per se. This conclusion seems reasonable because the elastic stiffnesses can be measured as the transmission of waves (ultrasonic) through the sheet which should depend on the contacts between fibers rather than the bonds.
10. Tensile properties which depend on bond failure should relate directly to bond density and strength, indicating that light calendering of this grade does not affect the bonding in the sheet but does affect the contacts and density of the sheet.

Overall, the models performed well from a statistical point of view -- the only objective means of determining model validity. A transient simulation model with CSTR's and first-order lags in the system would have been helpful. Such a system will be developed to use for future validation work.

Handsheet formation and pressing should be more consistently controlled in future work. The handsheet data were highly variable, apparently due to variable formation and pressing pressure. Thus, variability of the data limited their utility in the validation. There were also interlaboratory differences which should be studied further.

Future validation studies should include the modules necessary to predict CD variations through the paper machine, wet press, drier and calender sections for comparison with the measured CD property data.

The effects of OCC, refining, pressing and machine speed were surprisingly small for this grade. These effects were quantified in the following sensitivity study by using the simulation model to eliminate transient effects and interactions between variables.

Model Modifications

Based on the results of this analysis, the following model changes will be made:

1. Reduce the CSF dependence of the wet compressibility model.
2. Change the modulus models so they depend on bulk density rather than bond density.
3. Change the Gurley porosity to depend on surface density rather than bulk density.
4. Increase the sensitivity of CSF to specific power for lower yield furnishes in the refiner models.

SENSITIVITY ANALYSIS

The sensitivity analysis was performed using the model with Reel 1 conditions as the basis for determining the expected affect of four major test variables on end-user performance. By changing only one variable at a time using the model, it was possible to obtain unambiguous estimates of the decoupled sensitivity of each property to a specific variable. The four parameters were varied, as follows: (1) OCC content - 18% to 38%, (2) hole & tickler refiner loads - minimum to maximum values, (3) press load - minimum to maximum values, and (4) calender stack - loaded or unloaded. The variable conditions are summarized in Table XXXIII.

The sensitivity study was done without changing any of the models. In light of the findings of the validation study, the sensitivity coefficients for the effect of calendering on tensile properties were assumed to be zero even though the current models predicted a drop in tensile, burst and stretch. The sensitivity coefficients for the contact areas and bond area PAT's, S_{b1}, S_{b2} and S_a may also change after the wet press densification model is modified.

Table XXXIII: Sensitivity Case Study - Process Conditions

Case	Base	2	3	4	5	6
OCC Content, %....	18	38	18	18	18	18
Refining Primary..	1.47	1.47	5.16	1.47	1.47	1.47
Refining Tickler..	0.052	0.052	0.283	0.052	0.052	0.052
3 Press Load, pli.	600	600	600	800	450	600
3 Press Calender..	on	on	on	on	on	off

Sensitivity Factors

Machine paper properties and PAT values for each case are summarized in Table XXXIV.

Table XXXIV: Properties and Attributes of Calendered Medium Predicted by the Model

Case........................	Base	2	3	4	5	6
Properties		Hi OCC	Hi Refi- ning	Hi pli	Lo pli	Calend Load Off
BW (dry)....................	26.8	26.9	26.8	26.8	26.8	27.0
Caliper.....................	7.93	7.82	7.82	7.93	7.93	9.02
Density.....................	0.65	0.662	0.66	0.65	0.65	0.576
MD/CD tensile...............	2.39	2.39	2.39	2.39	2.38	2.38
Burst Factor................	29.7	32.2	27.77	29.7	29.7	26.0
MD Tensile, km..............	5.73	6.18	5.31	5.73	5.73	5.24
CD Tensile, km..............	2.40	2.59	2.23	2.40	2.40	2.19
Gurley Porosity, sec/cc.....	22.2	23.7	25.7	22.2	22.2	19.71
Stretch, %..................	1.87	1.90	1.90	1.88	1.88	1.72
MD Modulus, GPa.............	4.03	4.15	4.0	4.03	4.04	3.51
CD Modulus, GPa.............	1.87	1.91	1.85	1.88	1.88	1.63
MD STFI.....................	17.34	17.55	17.2	17.34	17.34	16.77
Flat Crush..................	30.6	30.9	30.3	30.6	30.58	29.62
Ring Crush..................	17.35	18.2	16.72	17.34	17.35	15.0
Concora, lb.................	54.2	54.88	53.7	54.2	54.2	52.2
Moisture, %.................	6.5	7.0	7.0	6.2	6.9	7.0
CSF Primary Refiner.........	528	528	388	528	528	528
CSF Blend Chest.............	496	470	401	496	496	496
CSF Tickler Refiner.........	491	464	387	491	491	491
CSF Headbox.................	457	429	365	457	457	457
CSF Broke Tank..............	536	507	470	536	536	536

FIGURES

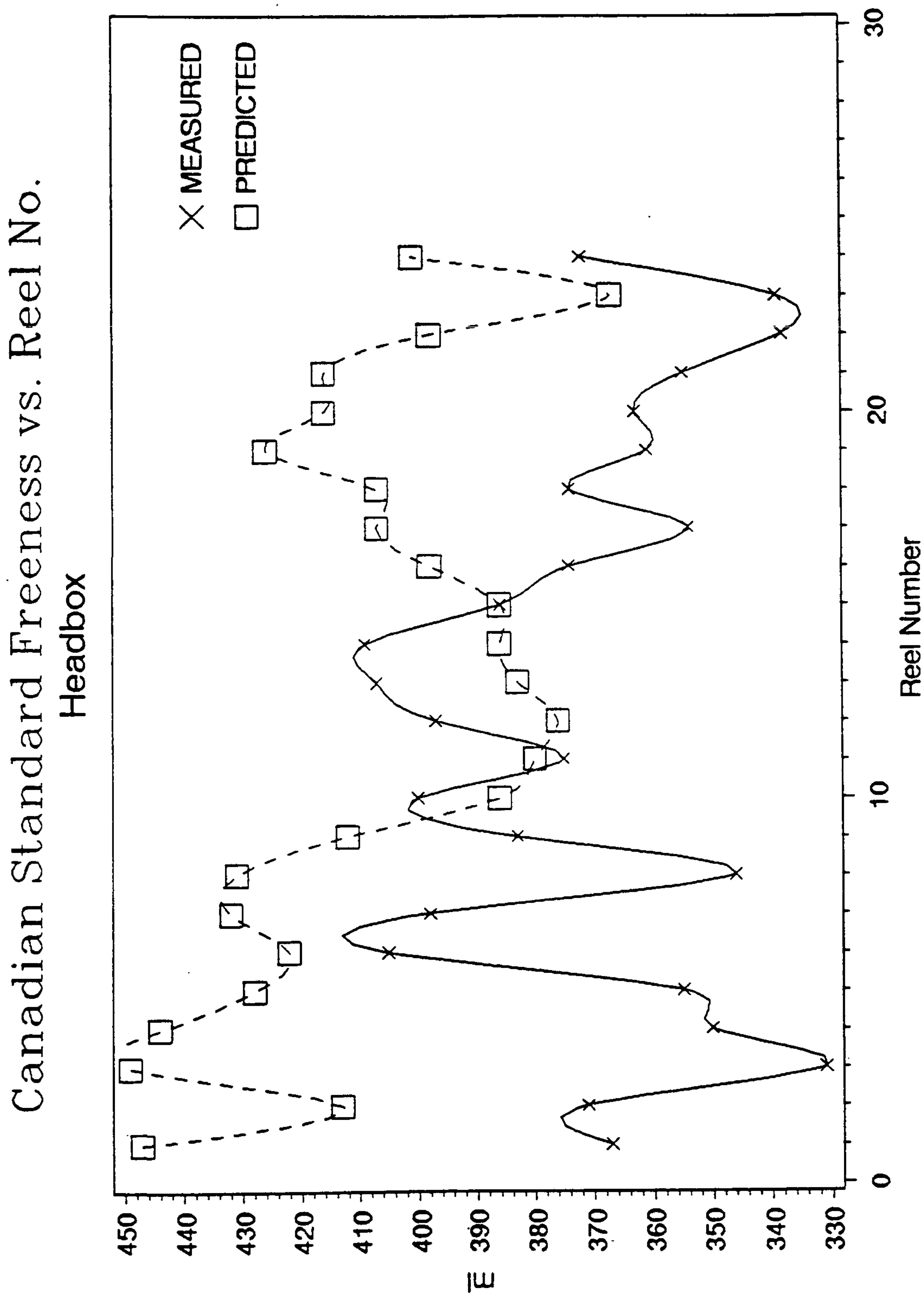

Figure 23

FIGURES

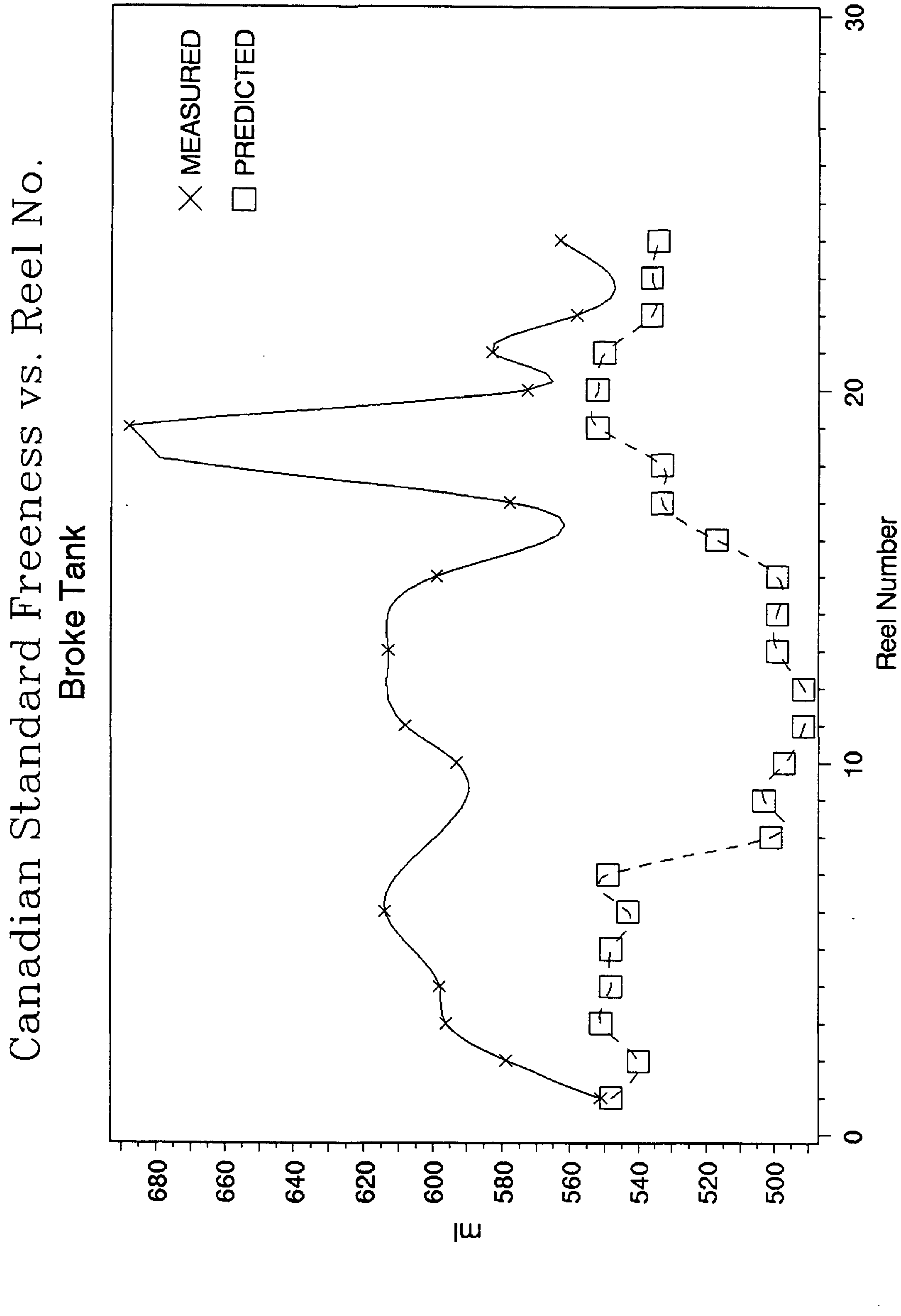

Figure 24

FIGURES

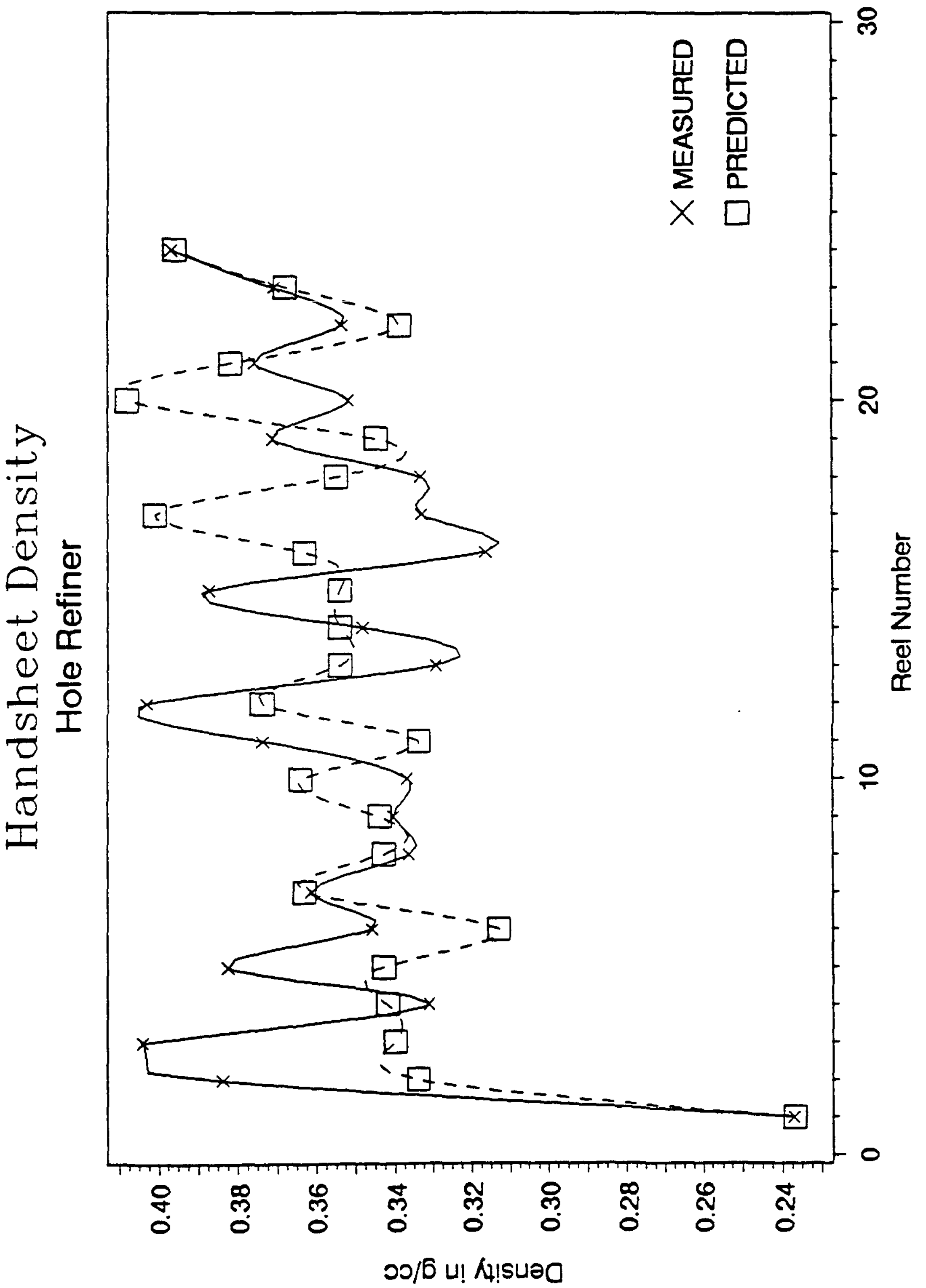

Figure 25

FIGURES

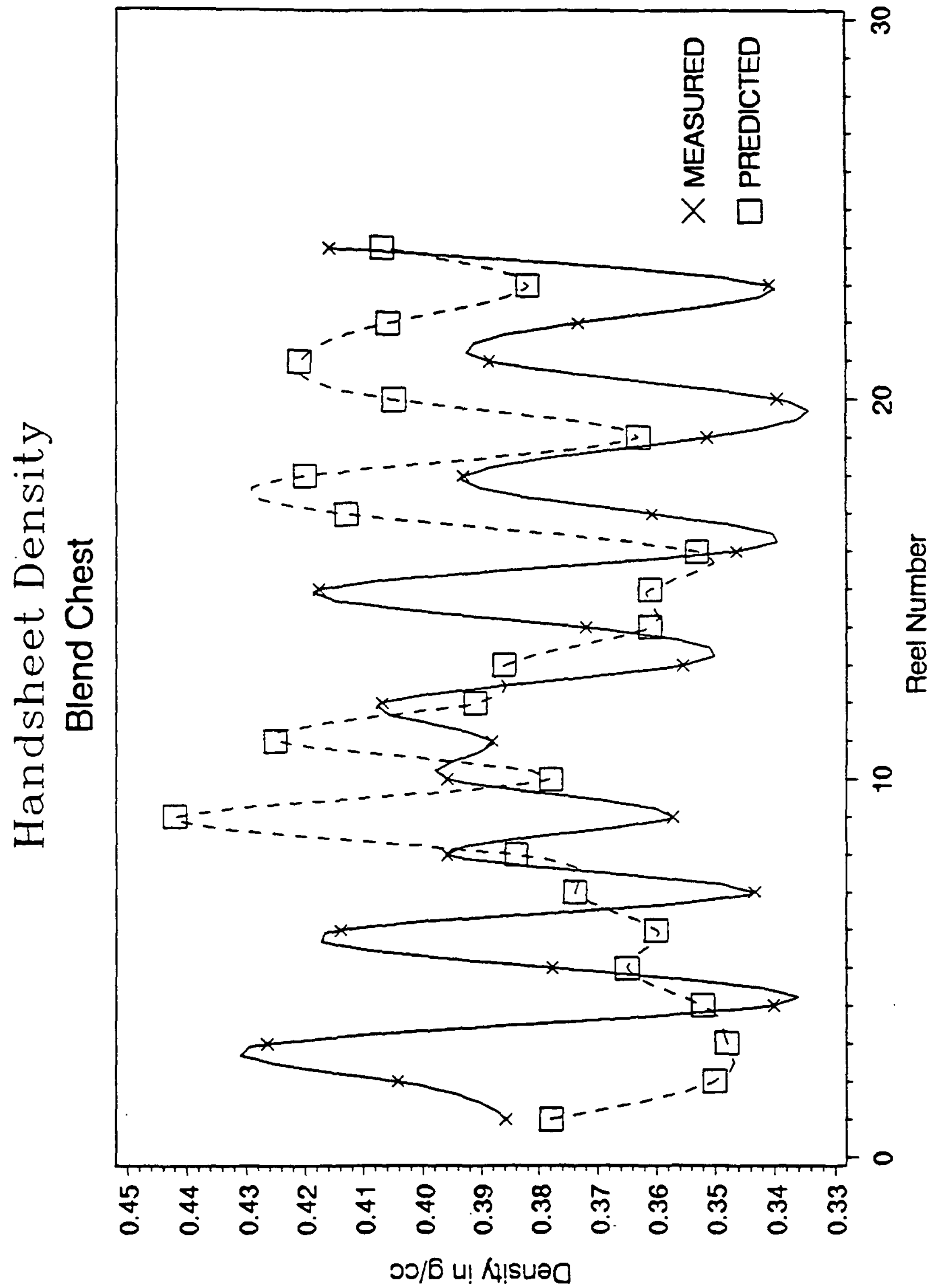

Figure 26

FIGURES

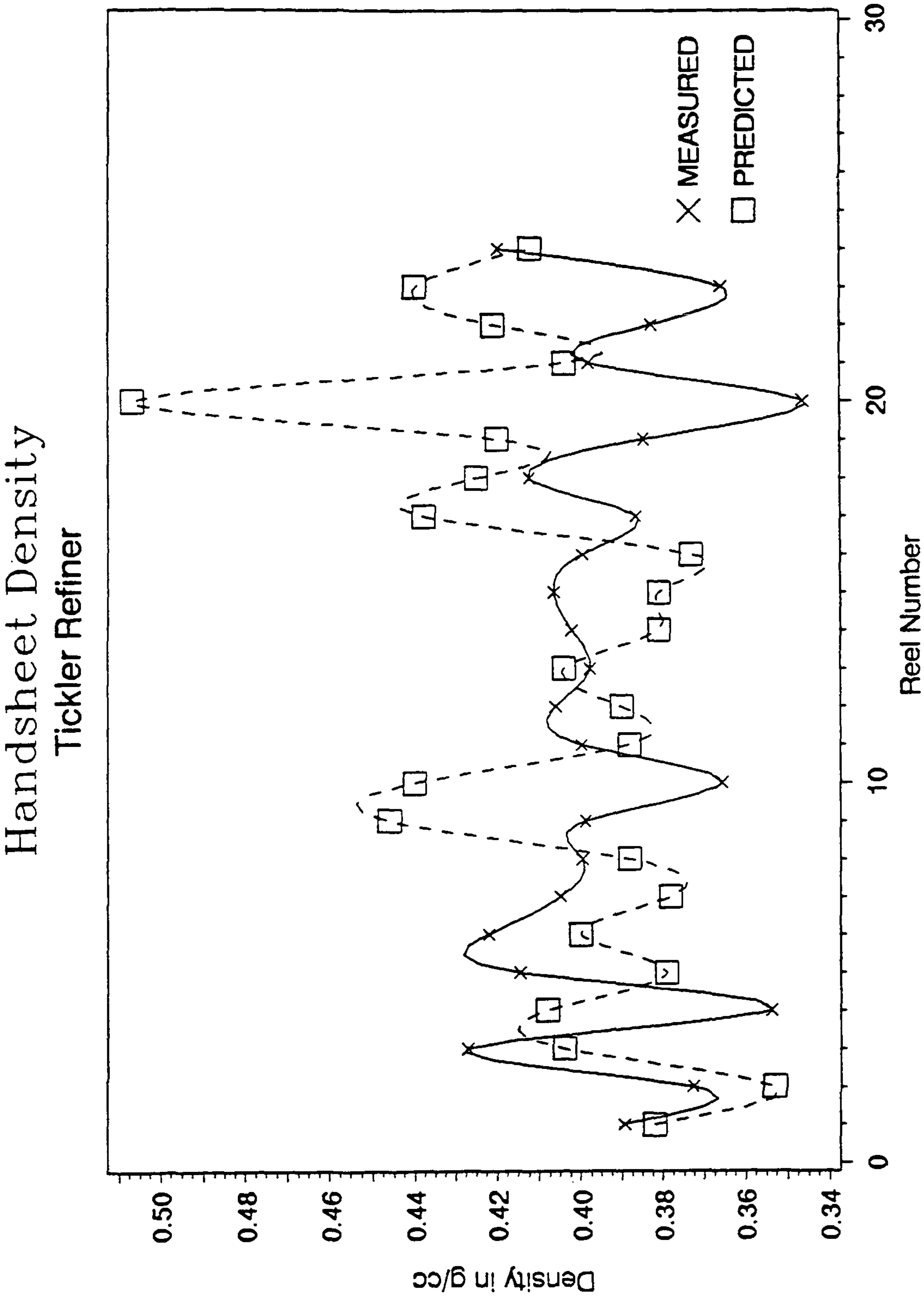

Figure 27

FIGURES

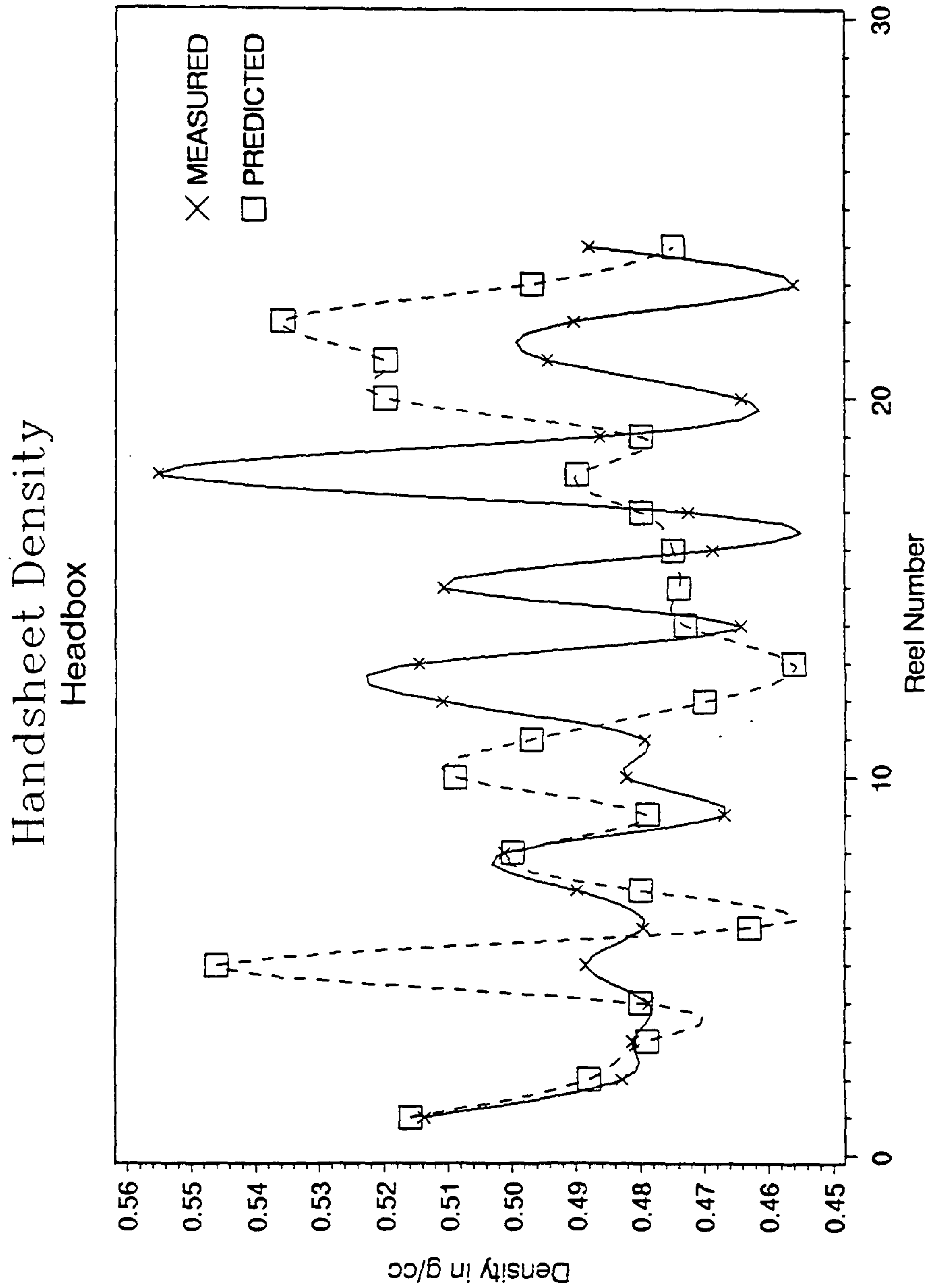

Figure 28

FIGURES

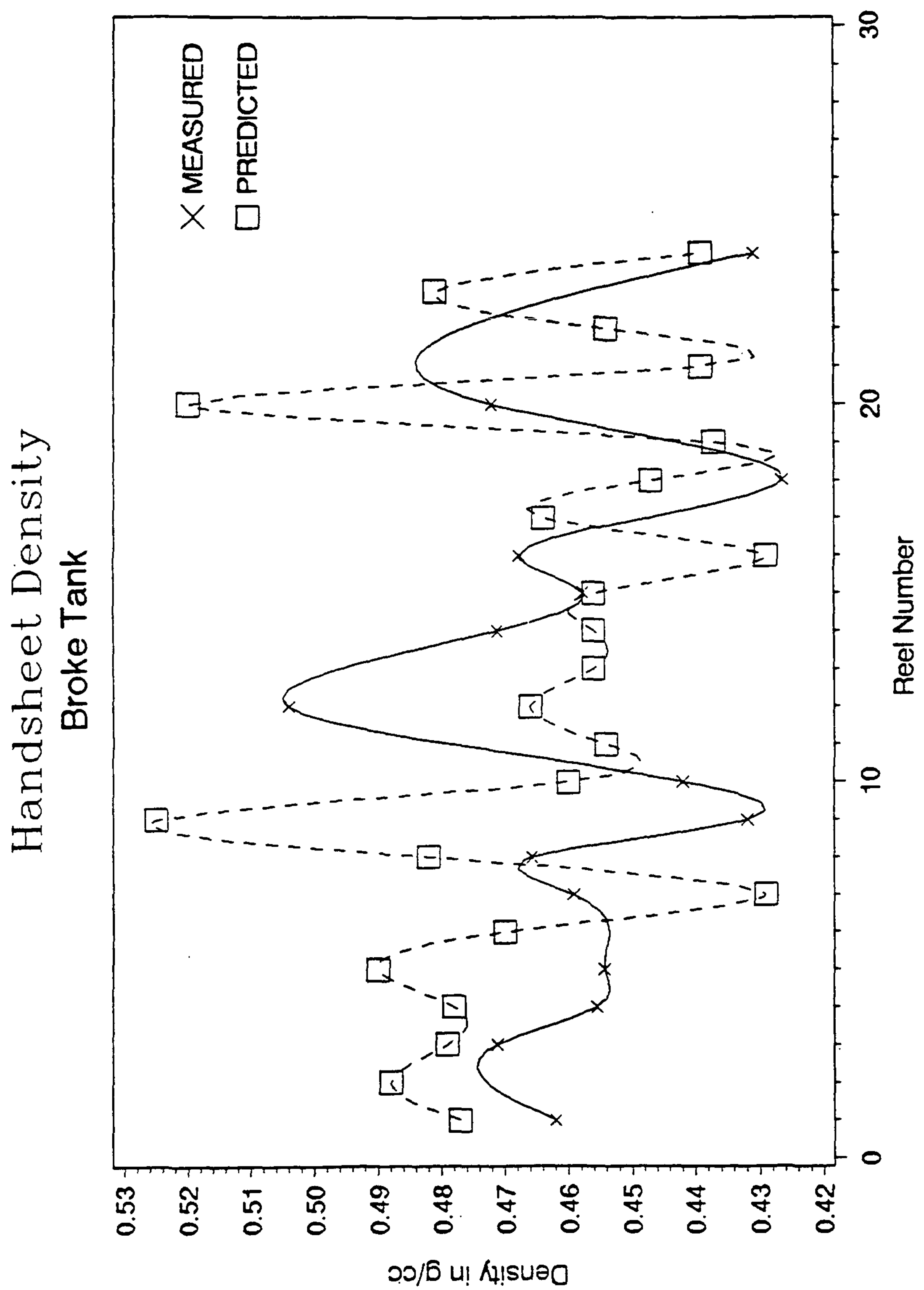

Figure 29

FIGURES

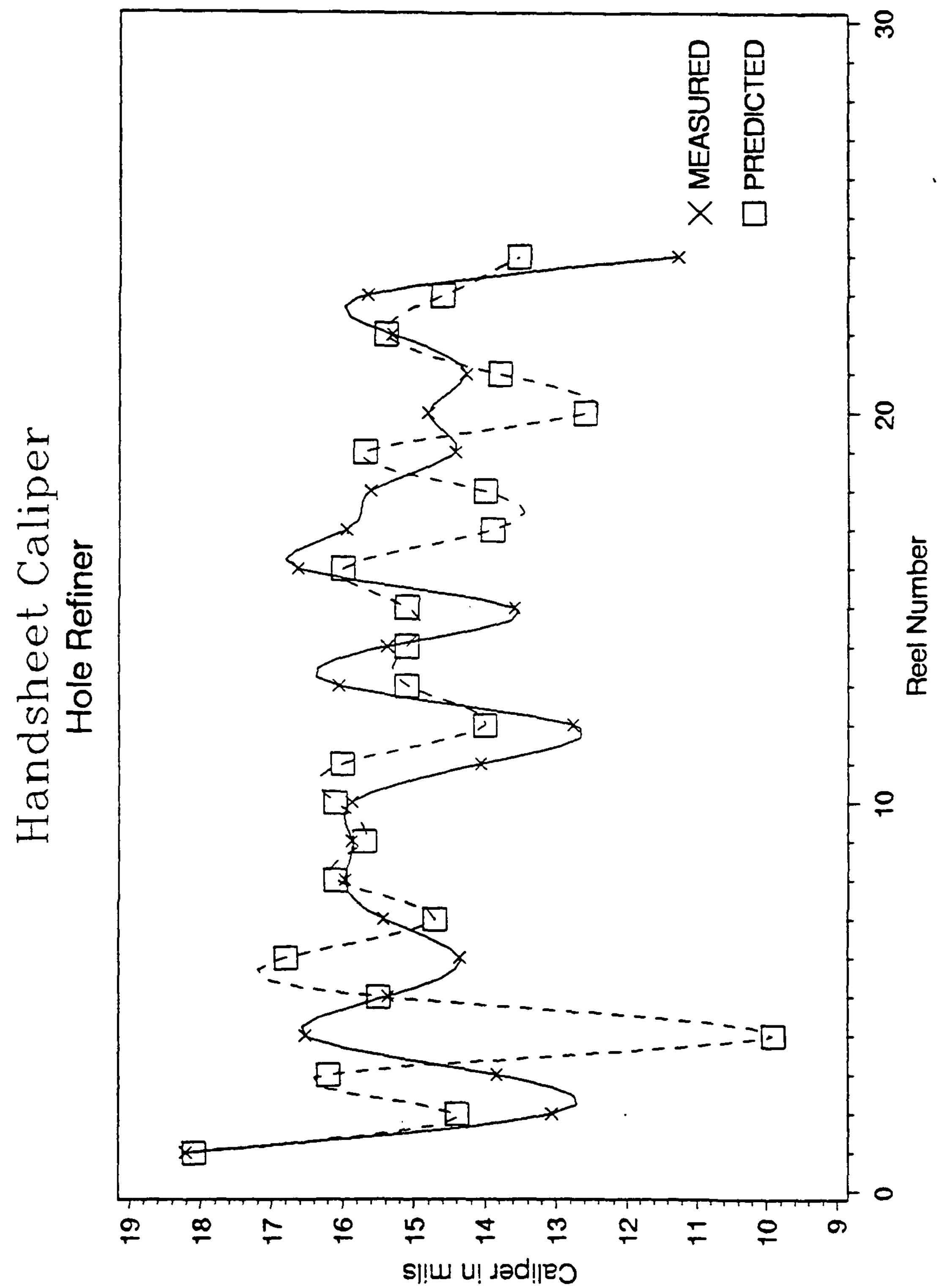

Figure 30

FIGURES

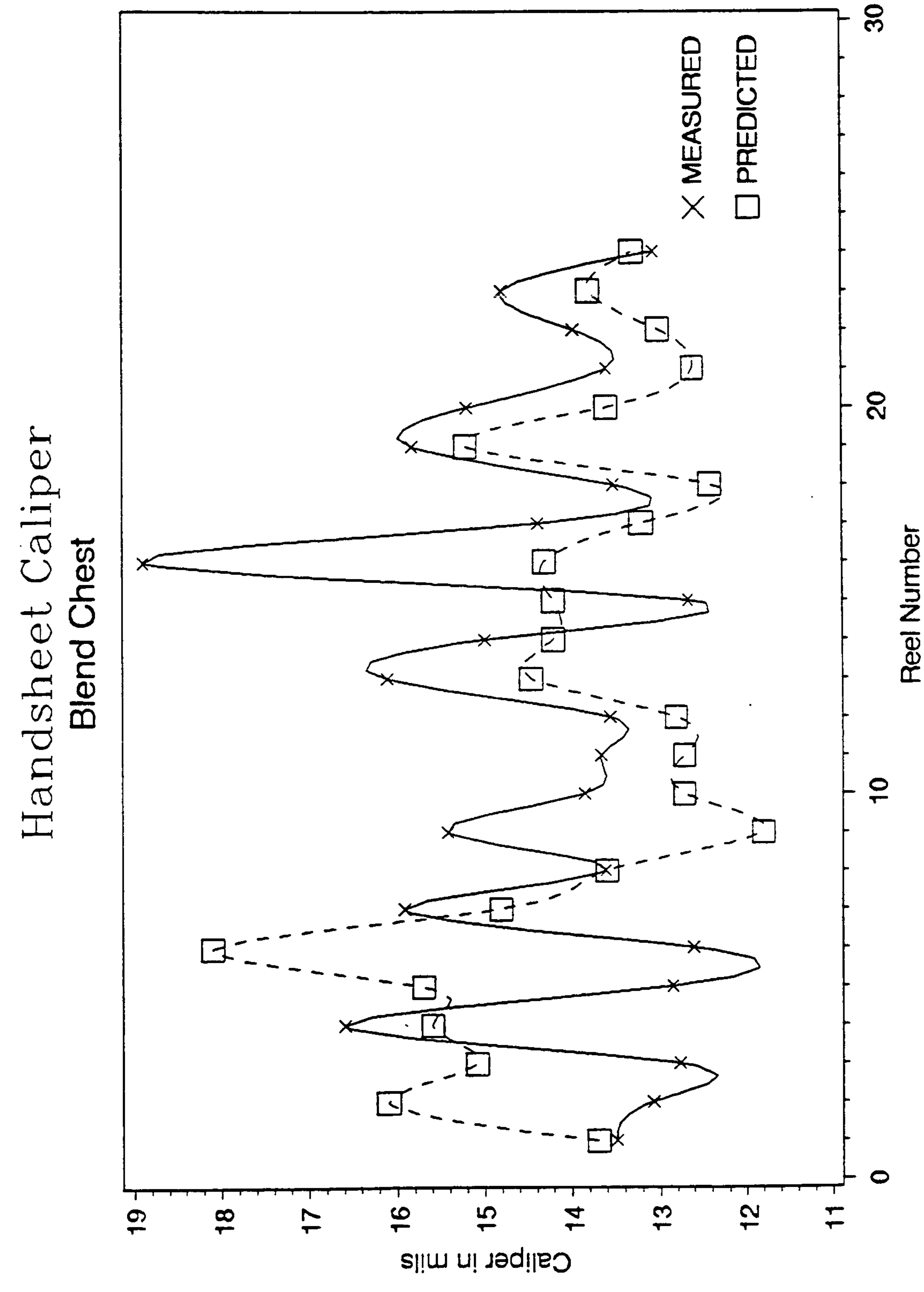

Figure 31

FIGURES

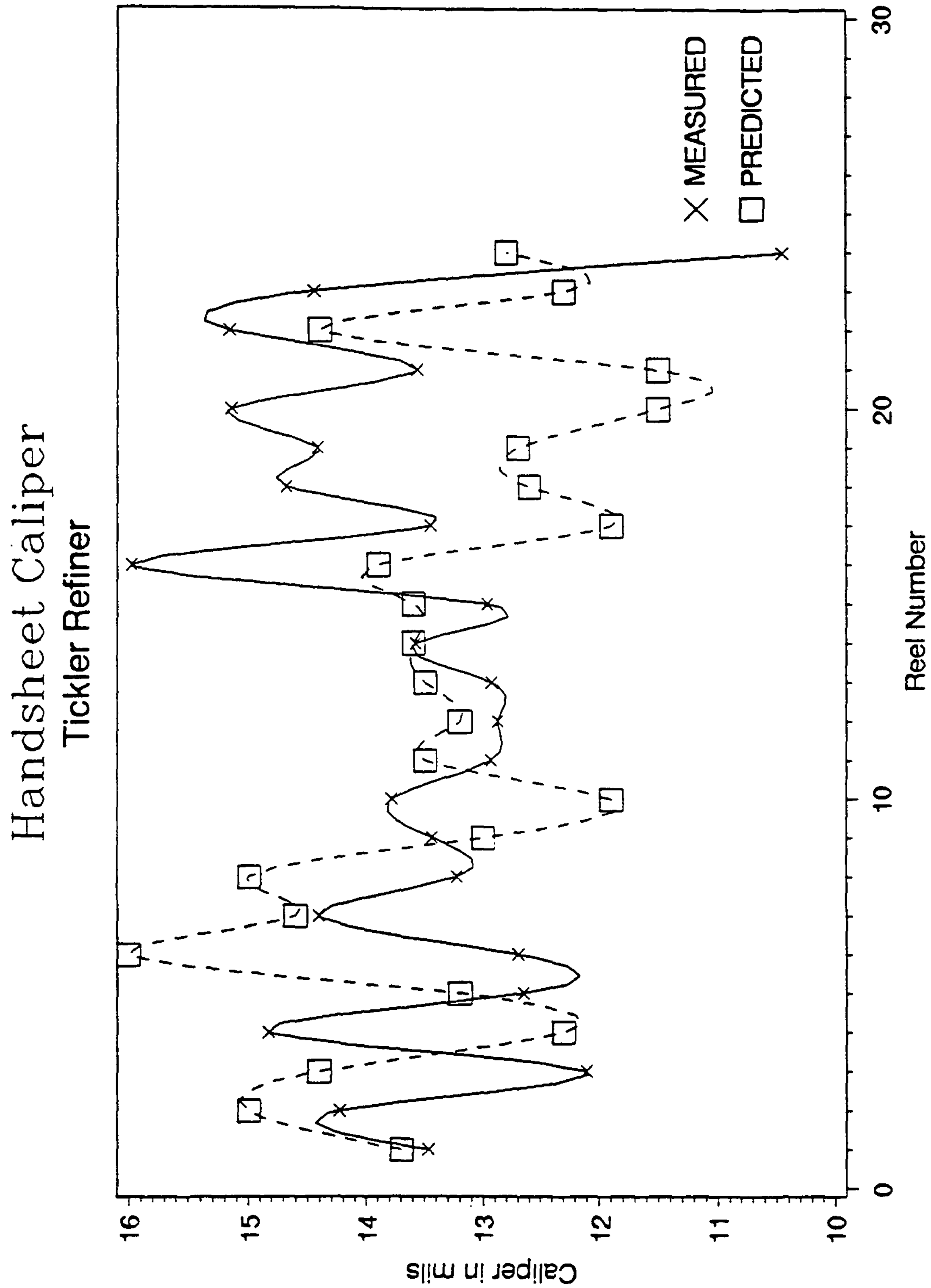

Figure 32

FIGURES

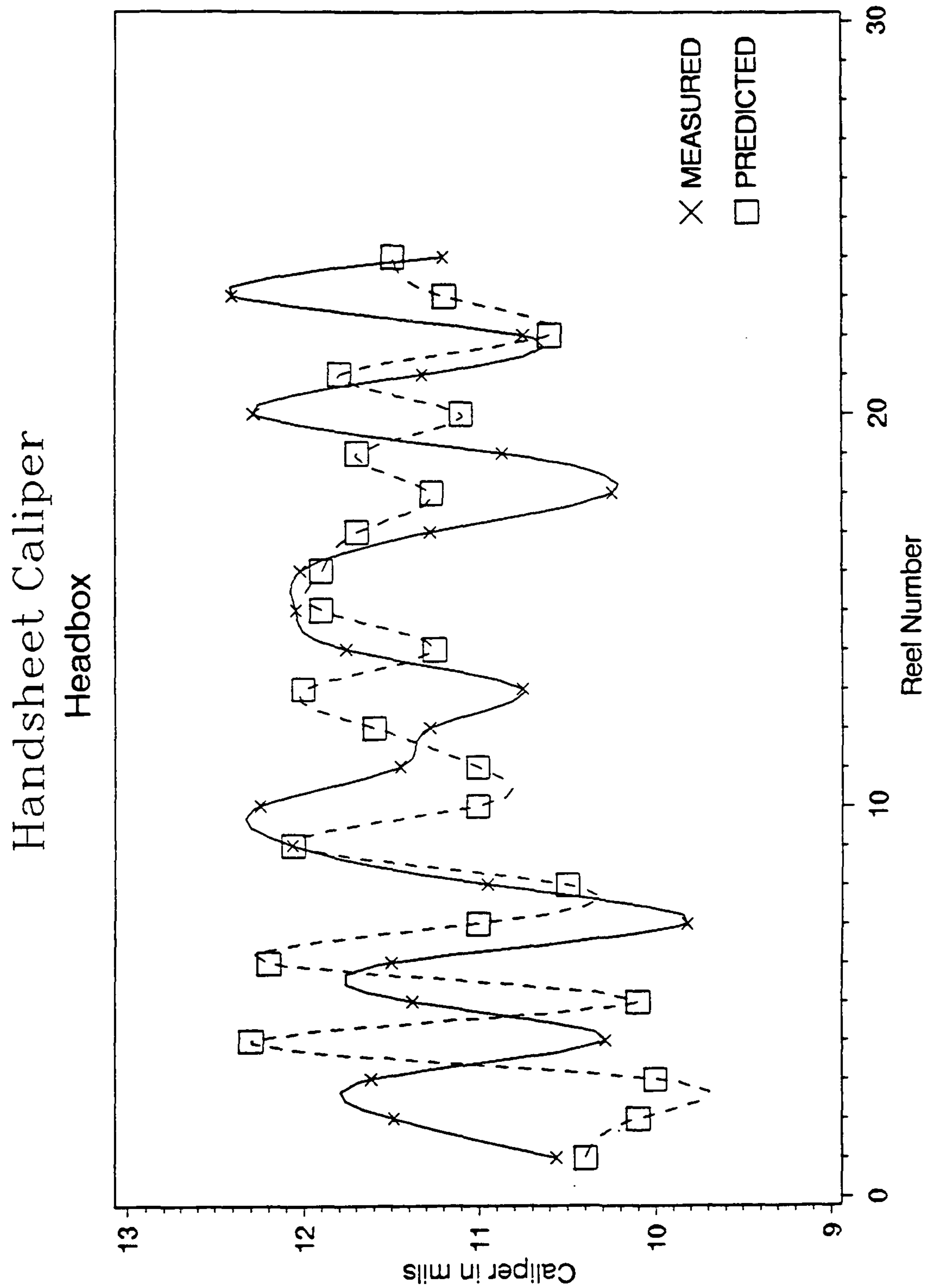

Figure 33

FIGURES

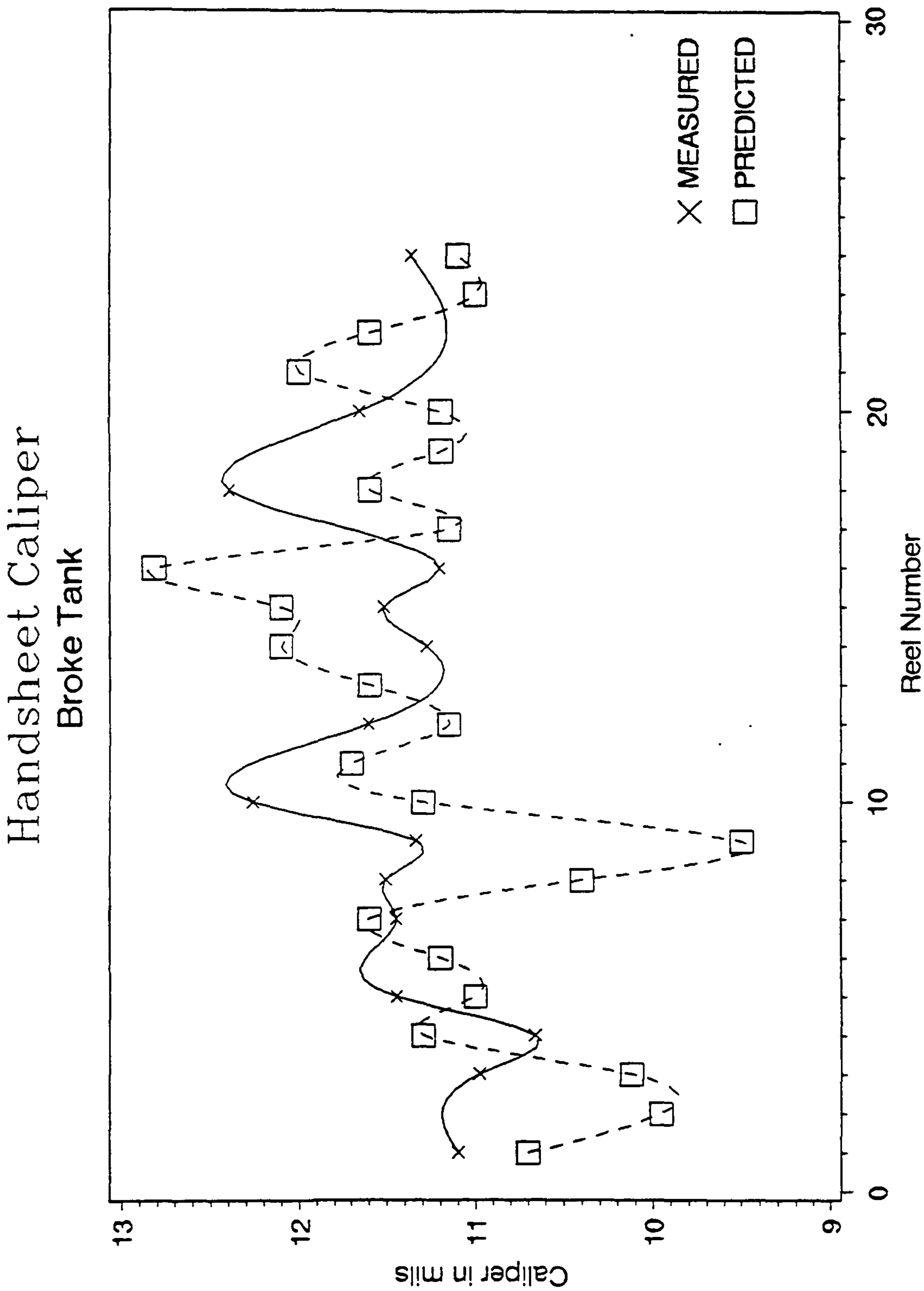

Figure 34

FIGURES

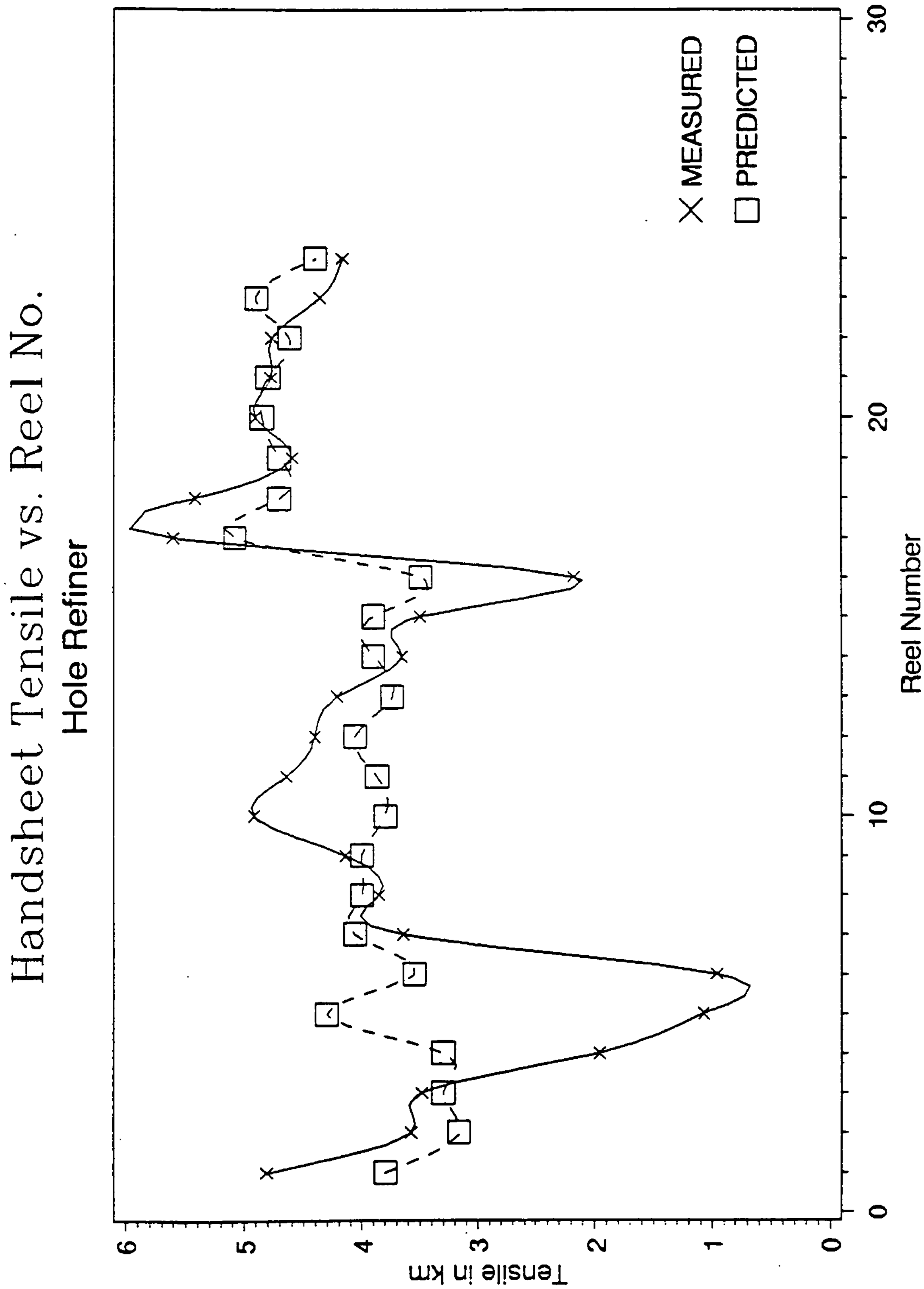

Figure 35

FIGURES

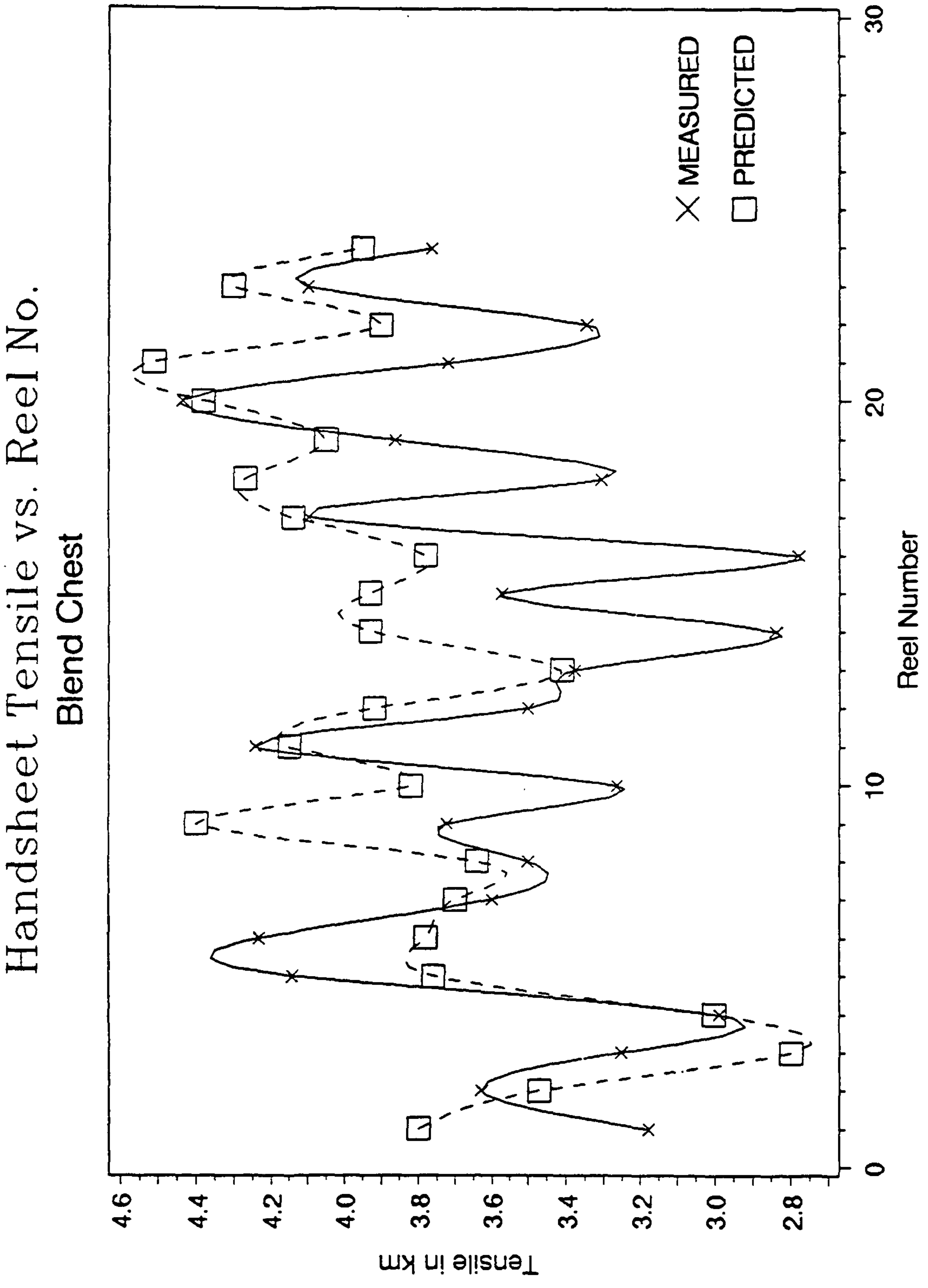

Figure 36

FIGURES

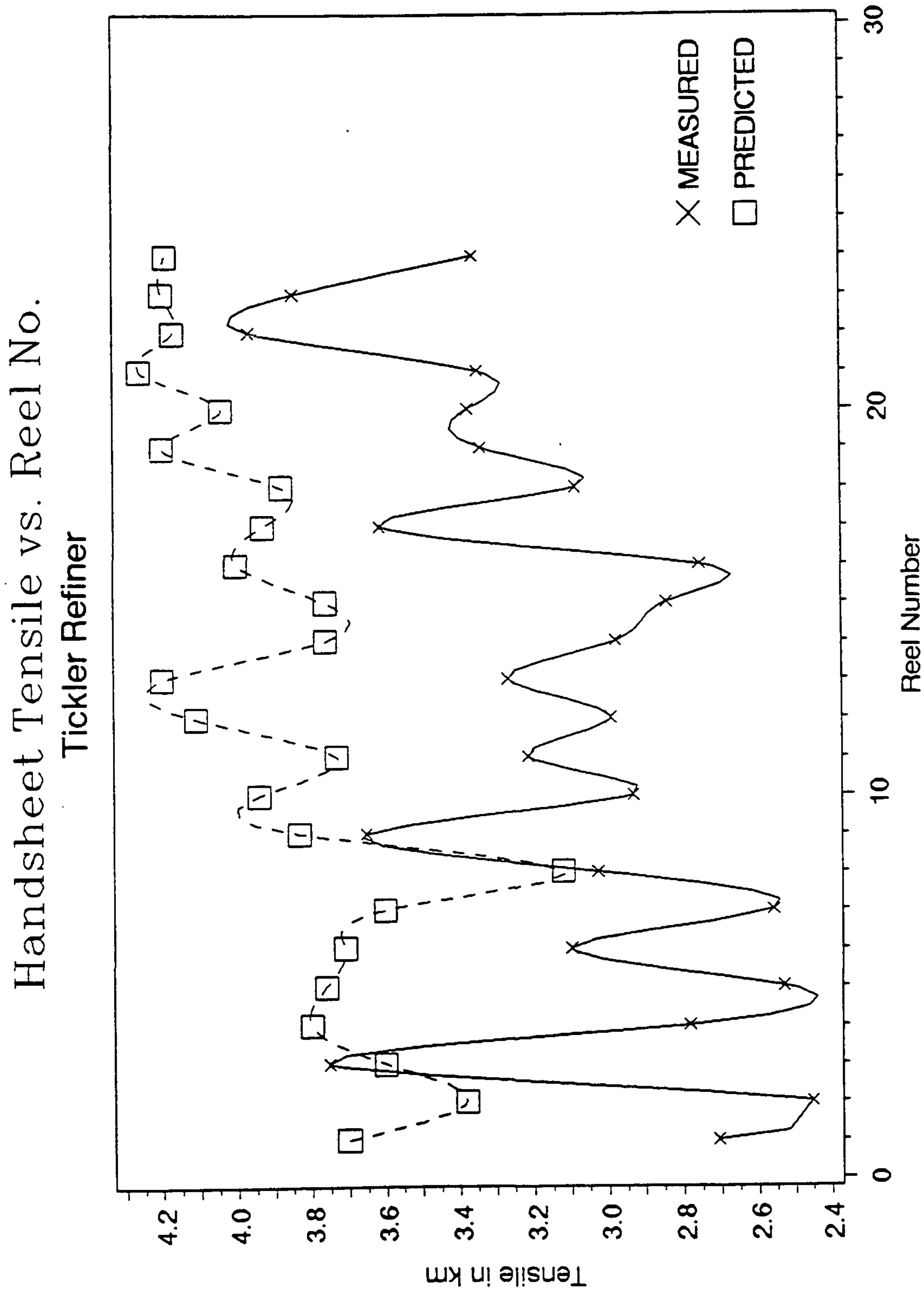

Figure 37

FIGURES

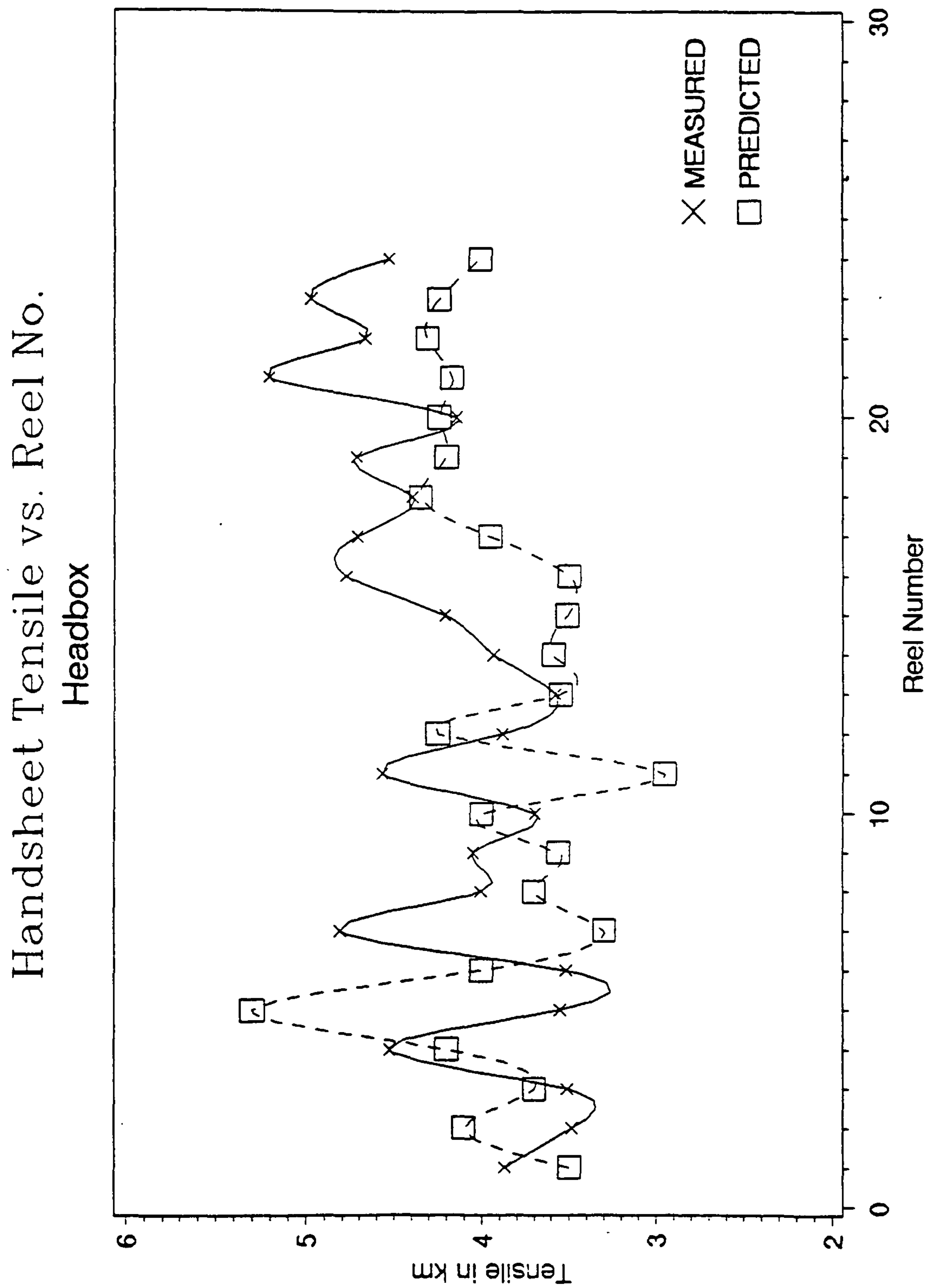

Figure 38

FIGURES

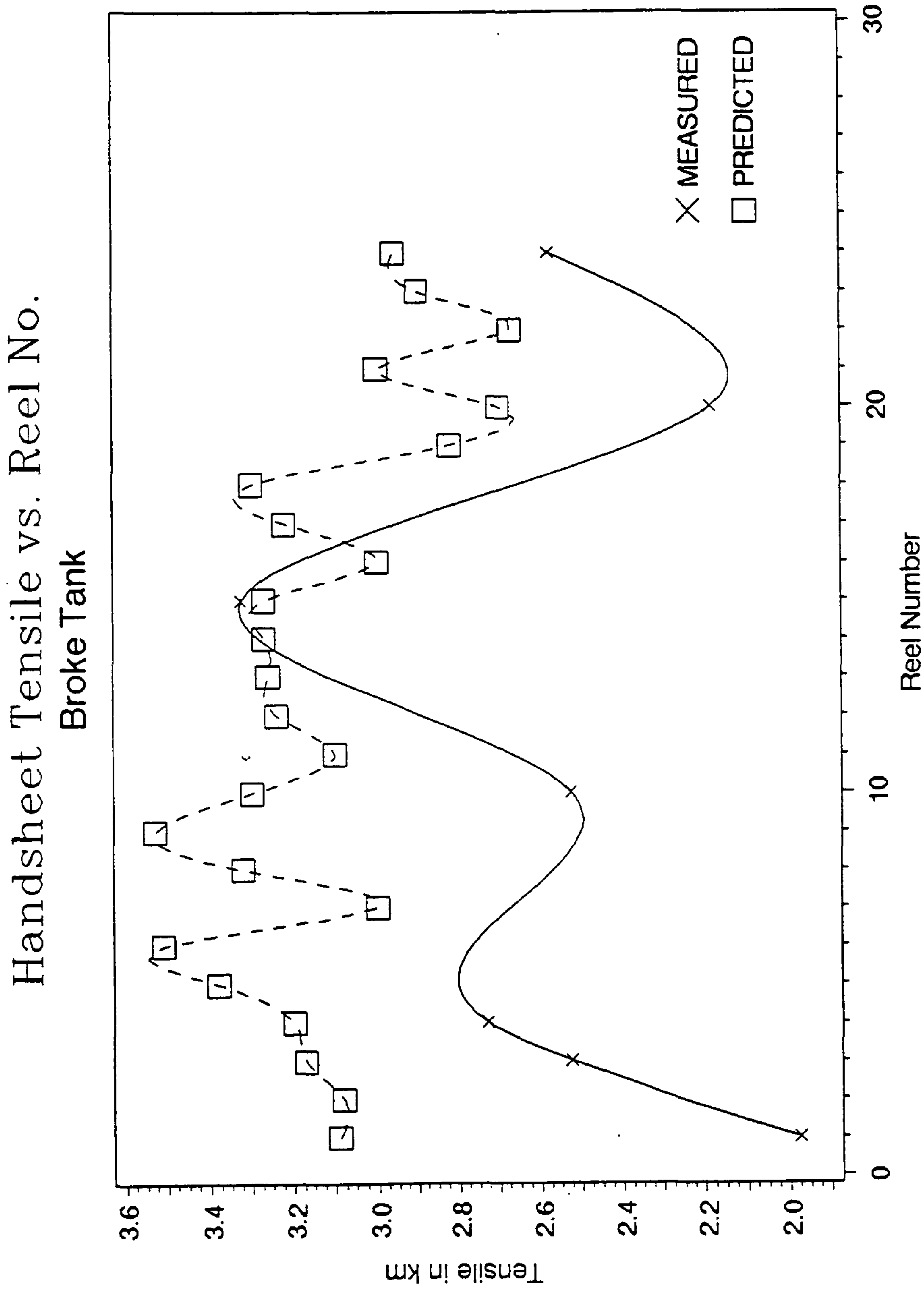

Figure 39

FIGURES

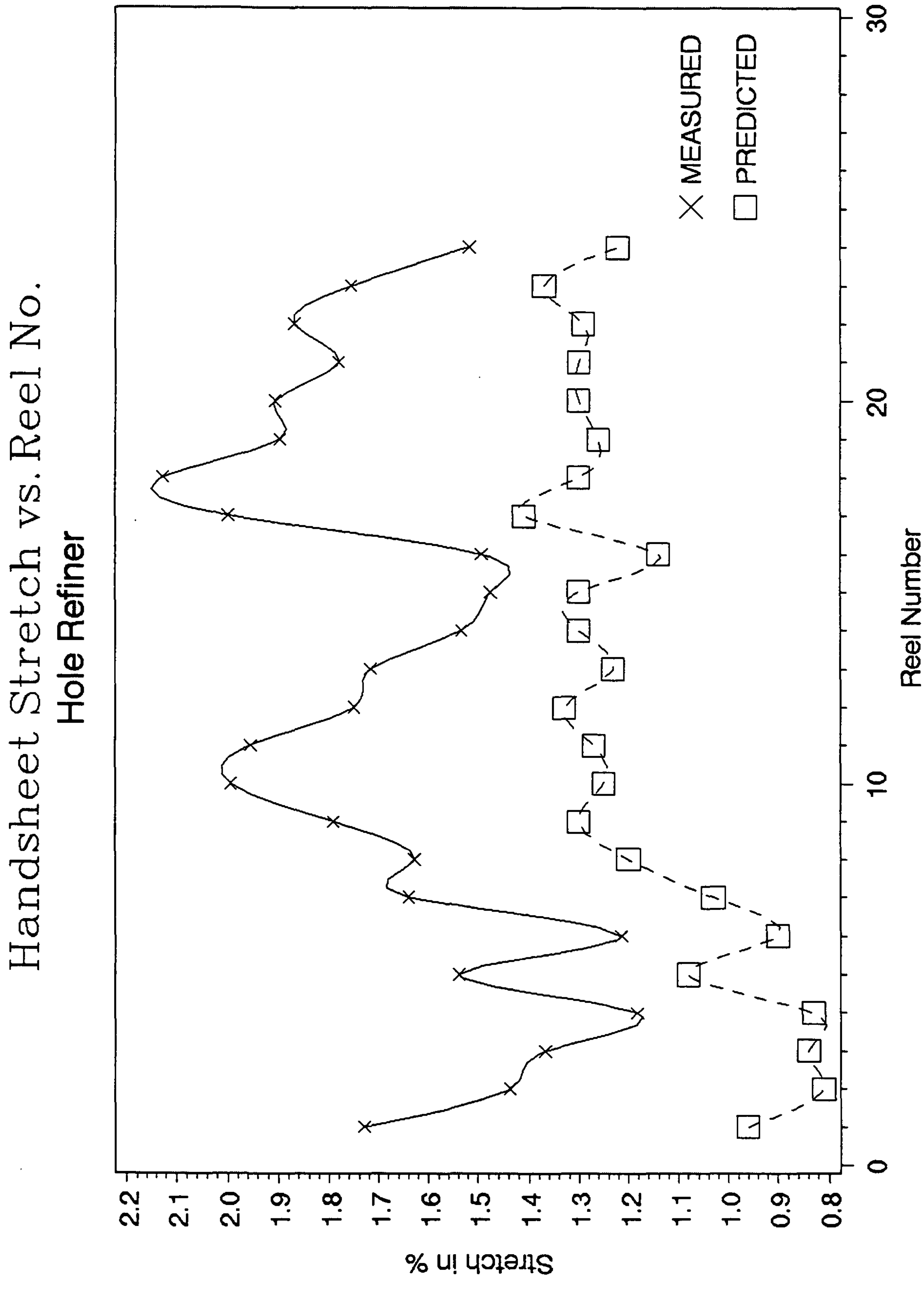

Figure 40

FIGURES

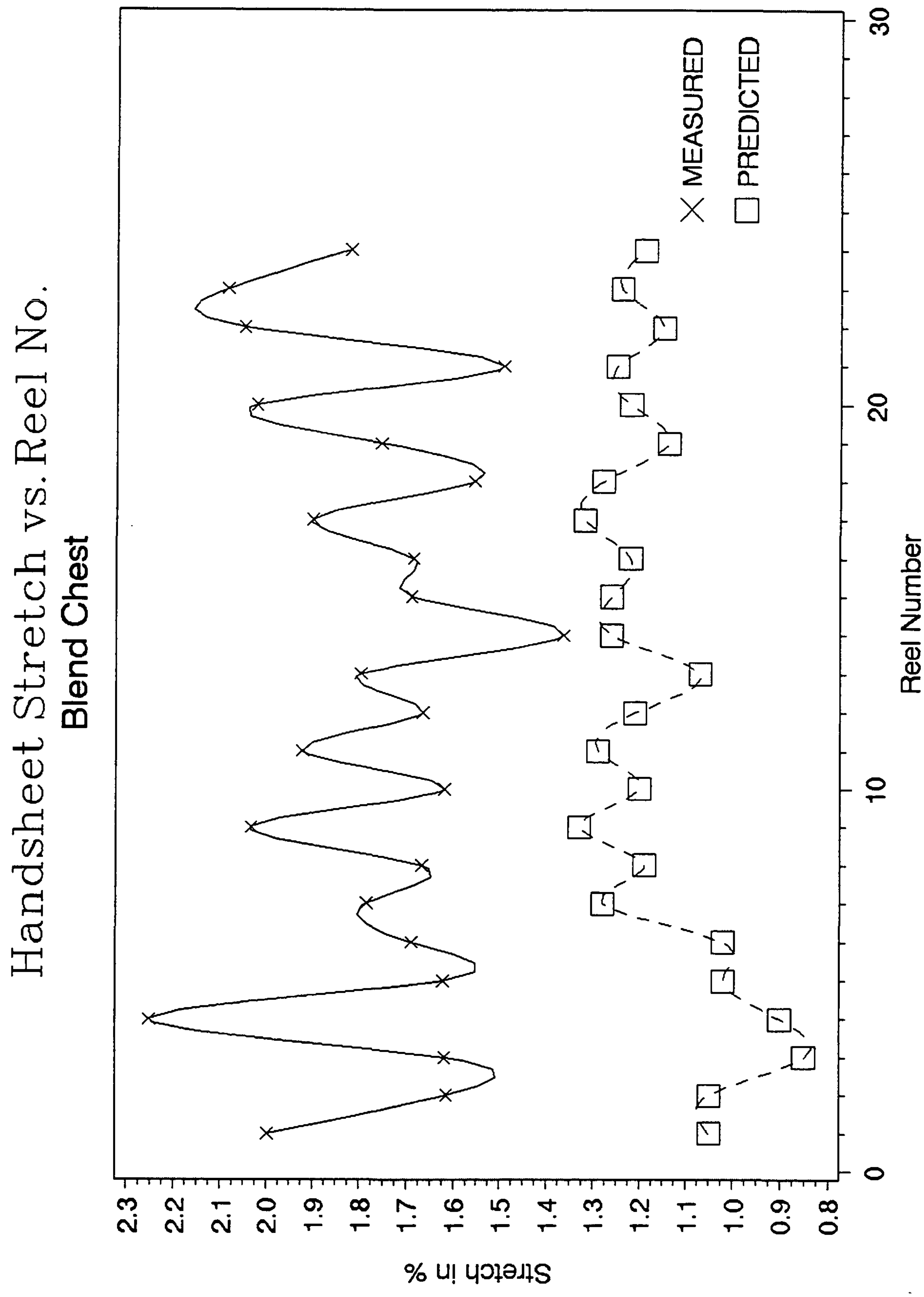

Figure 41

FIGURES

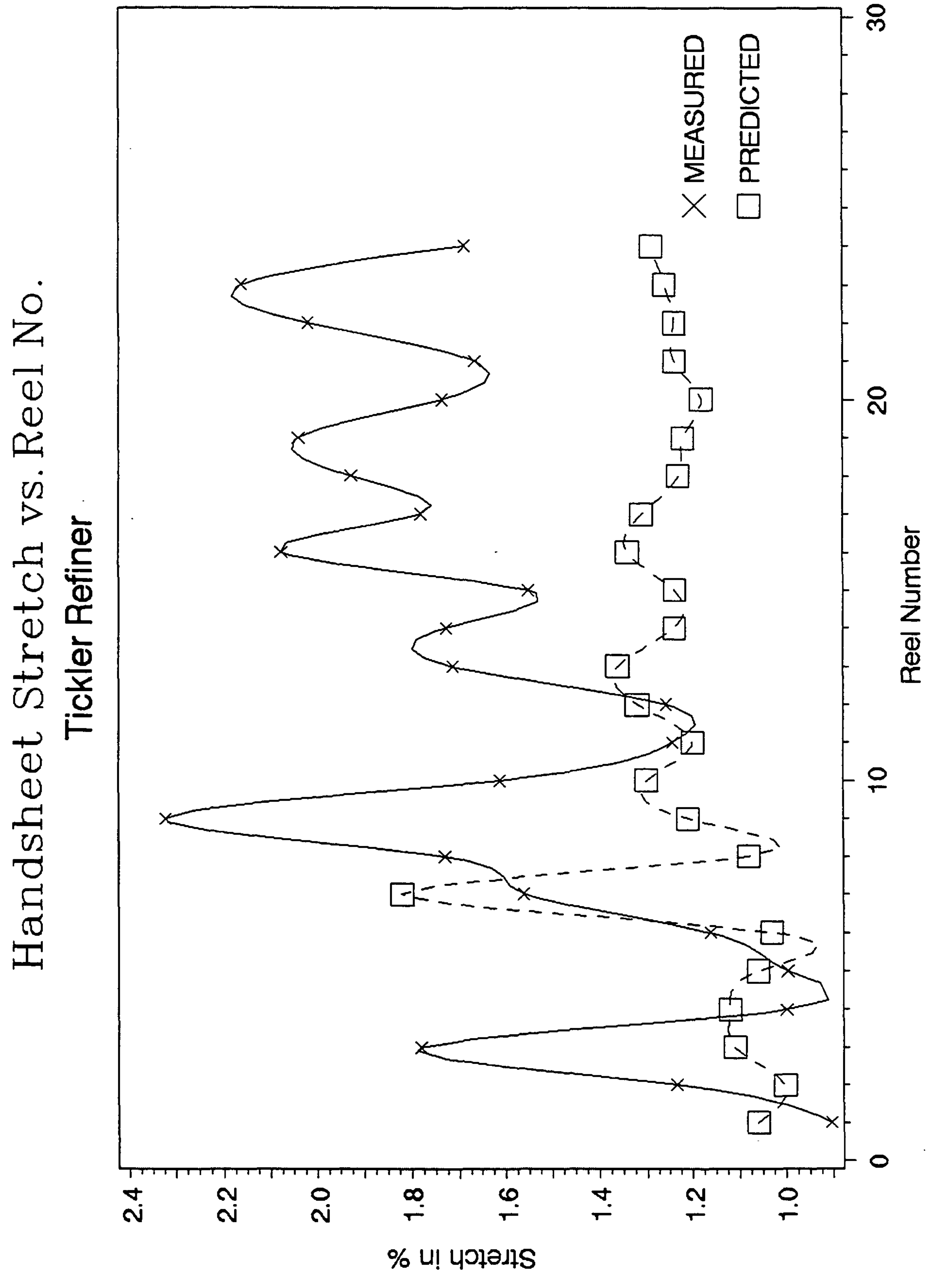

Figure 42

FIGURES

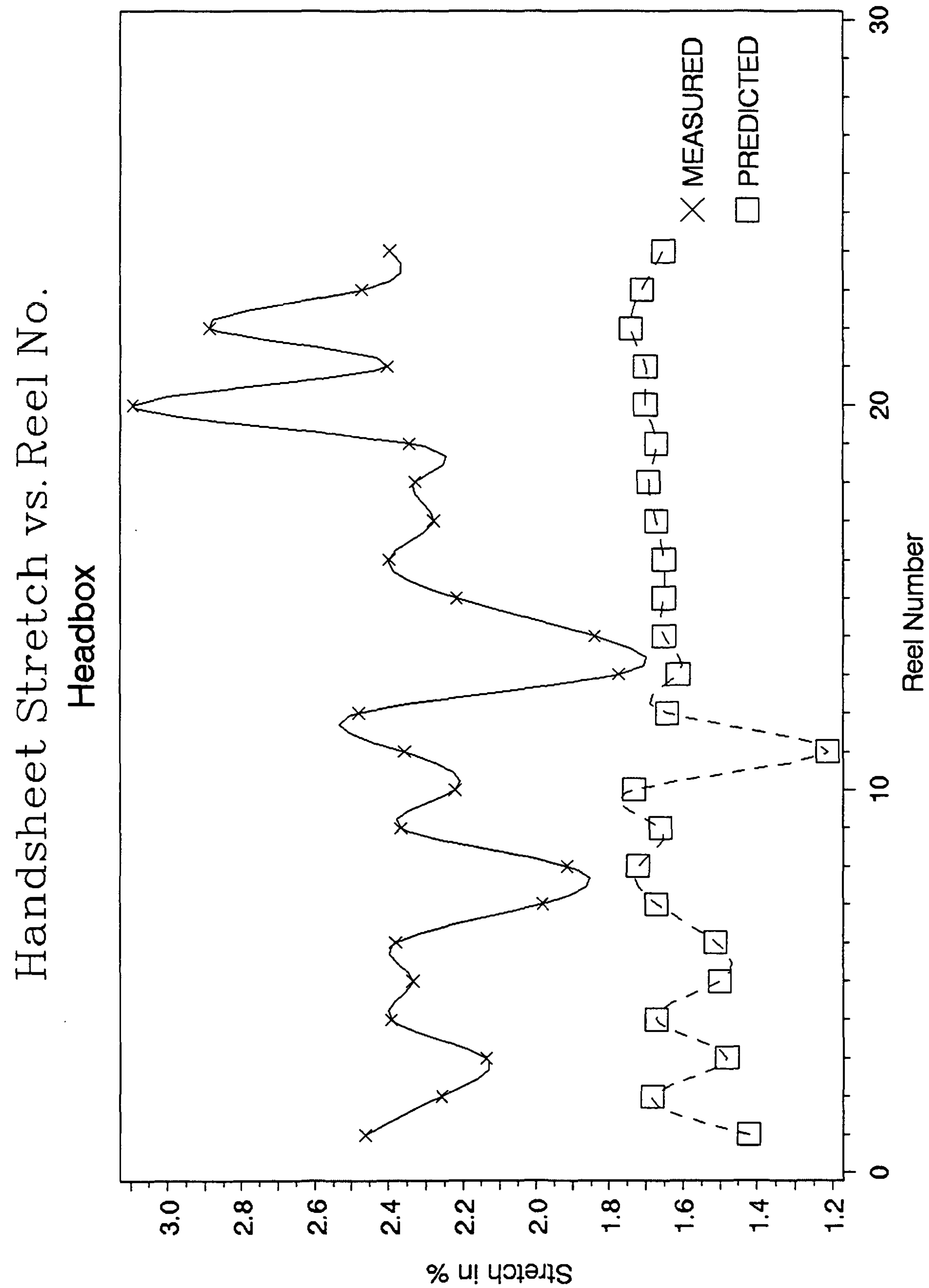

Figure 43

FIGURES

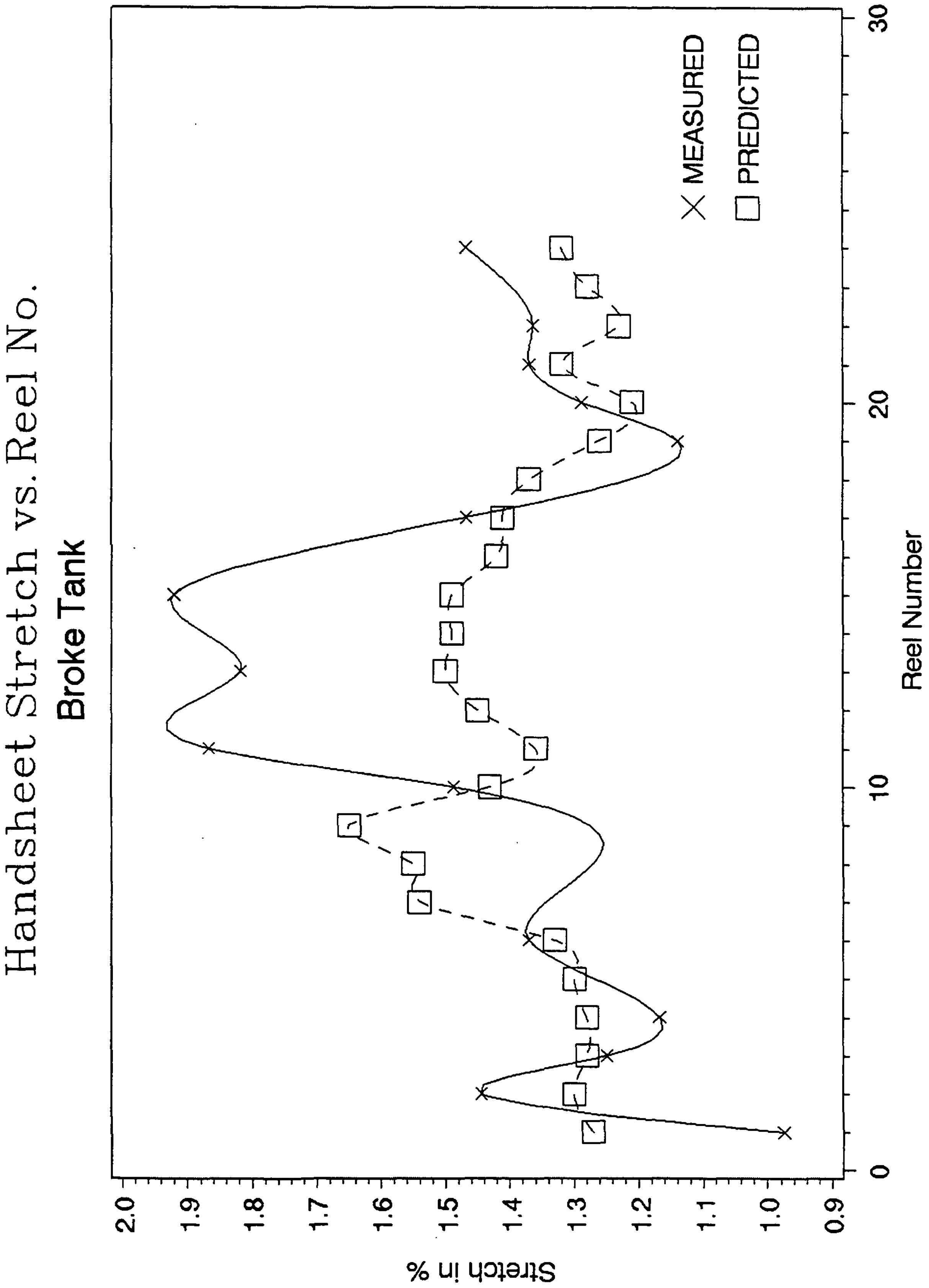

Figure 44

FIGURES

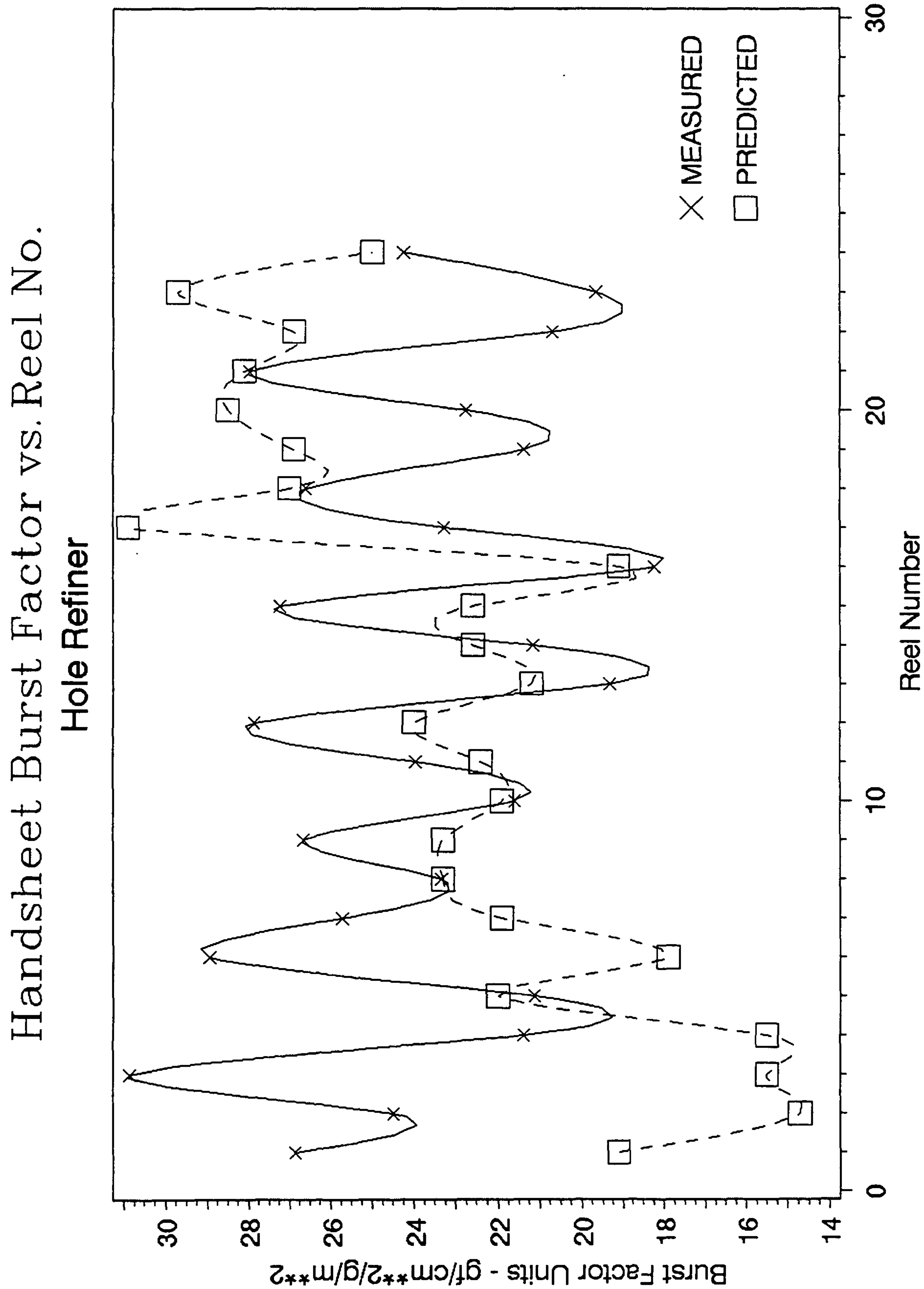

Figure 45

FIGURES

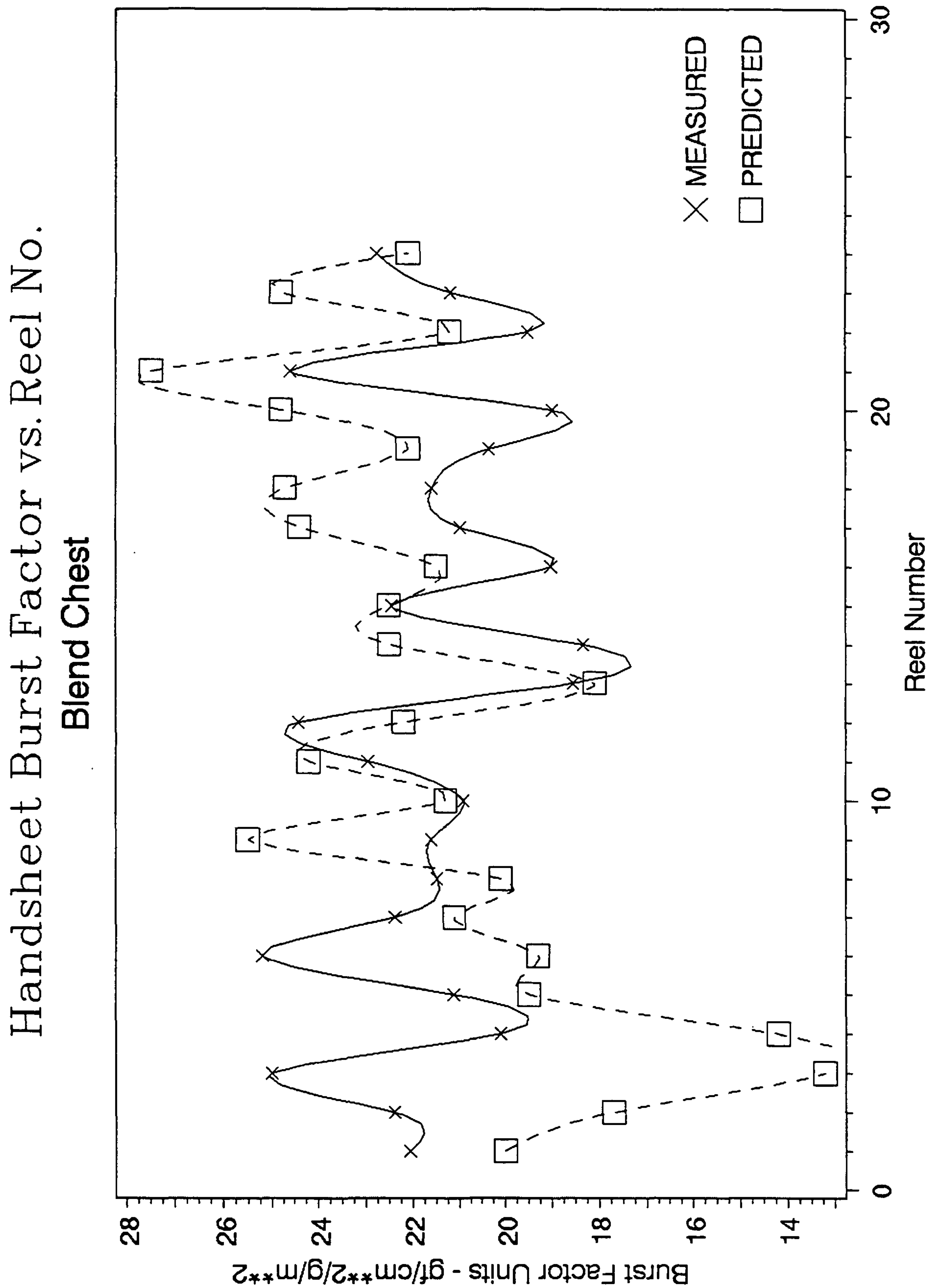

Figure 46

FIGURES

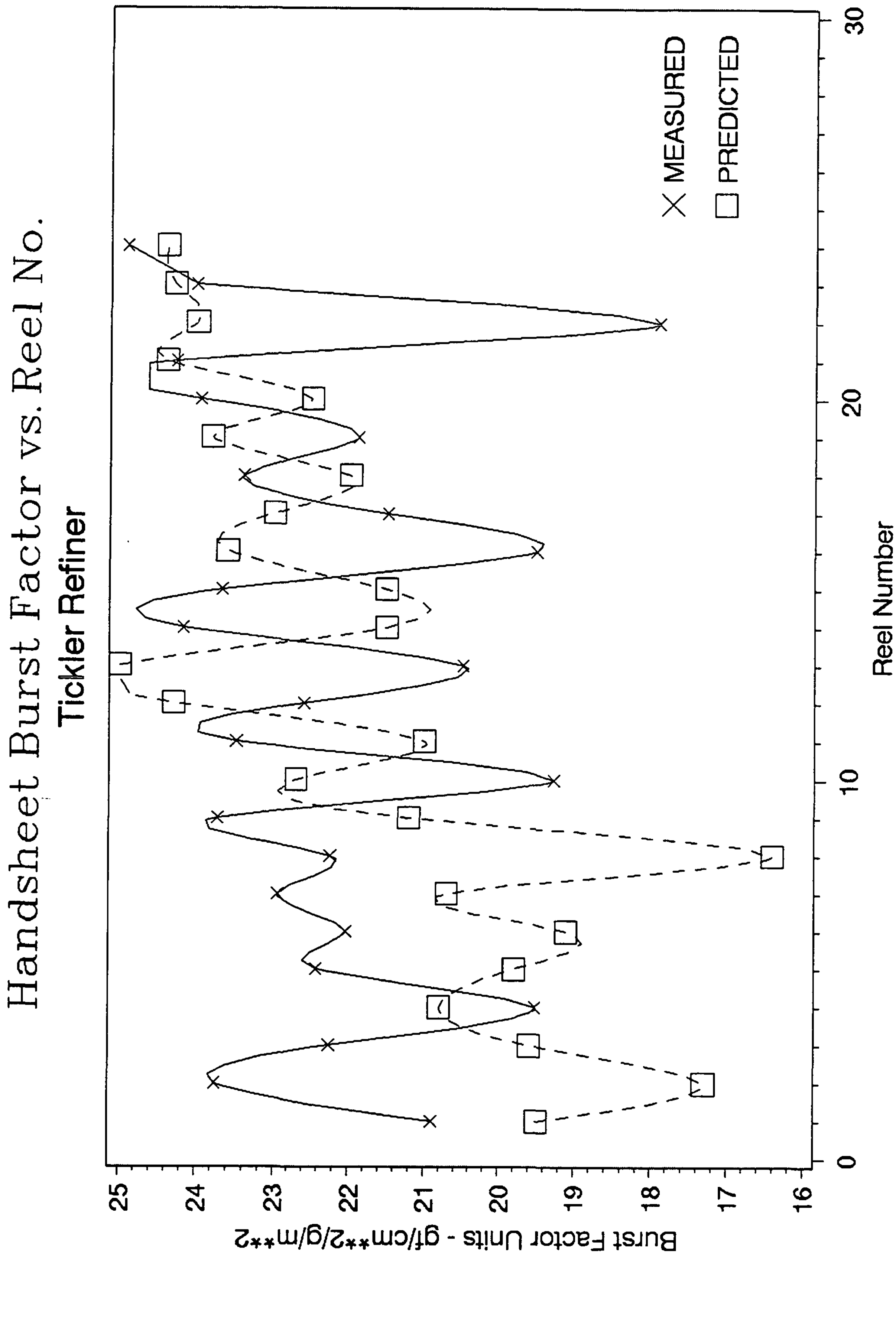

Figure 47

FIGURES

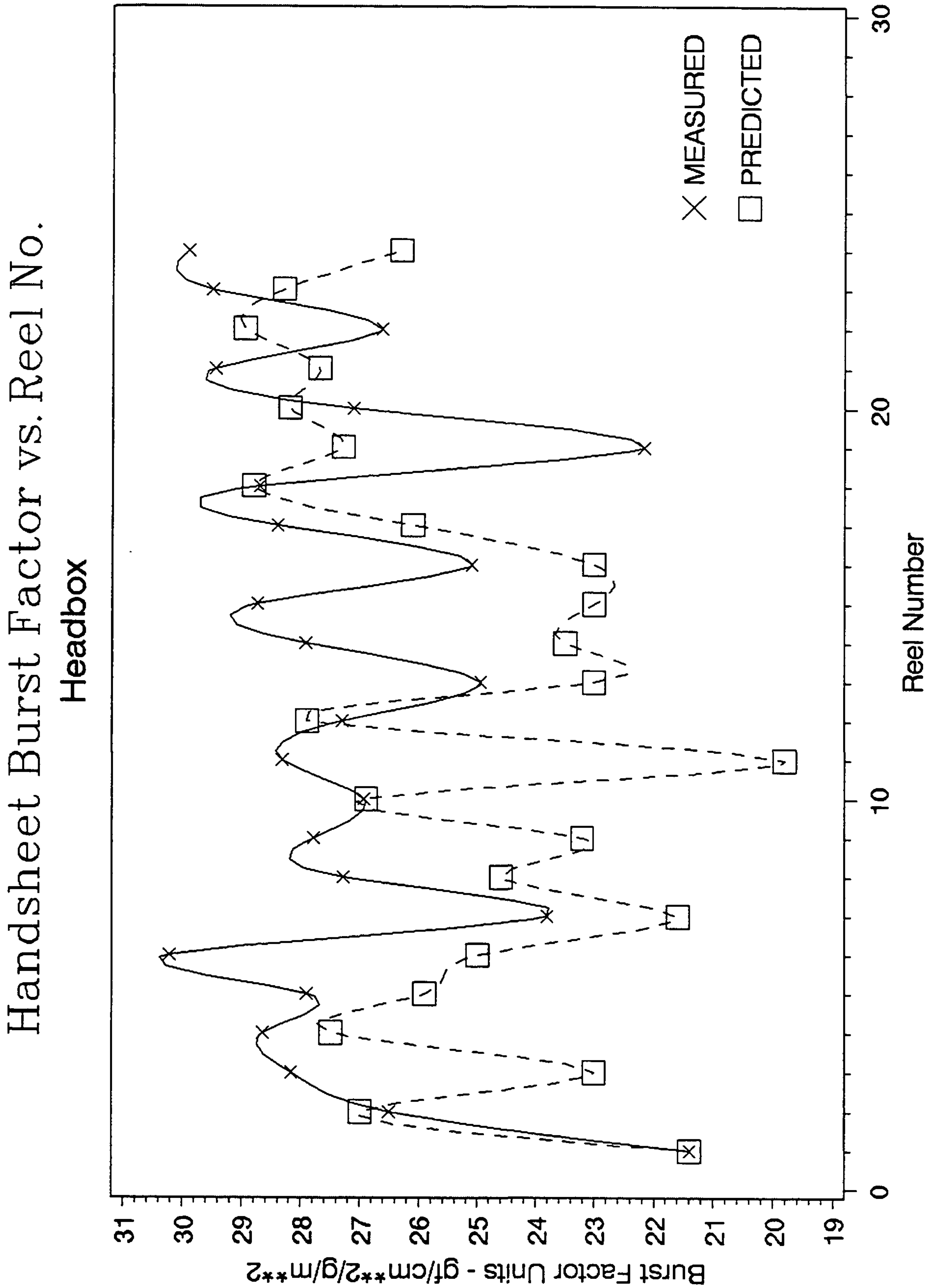

Figure 48

FIGURES

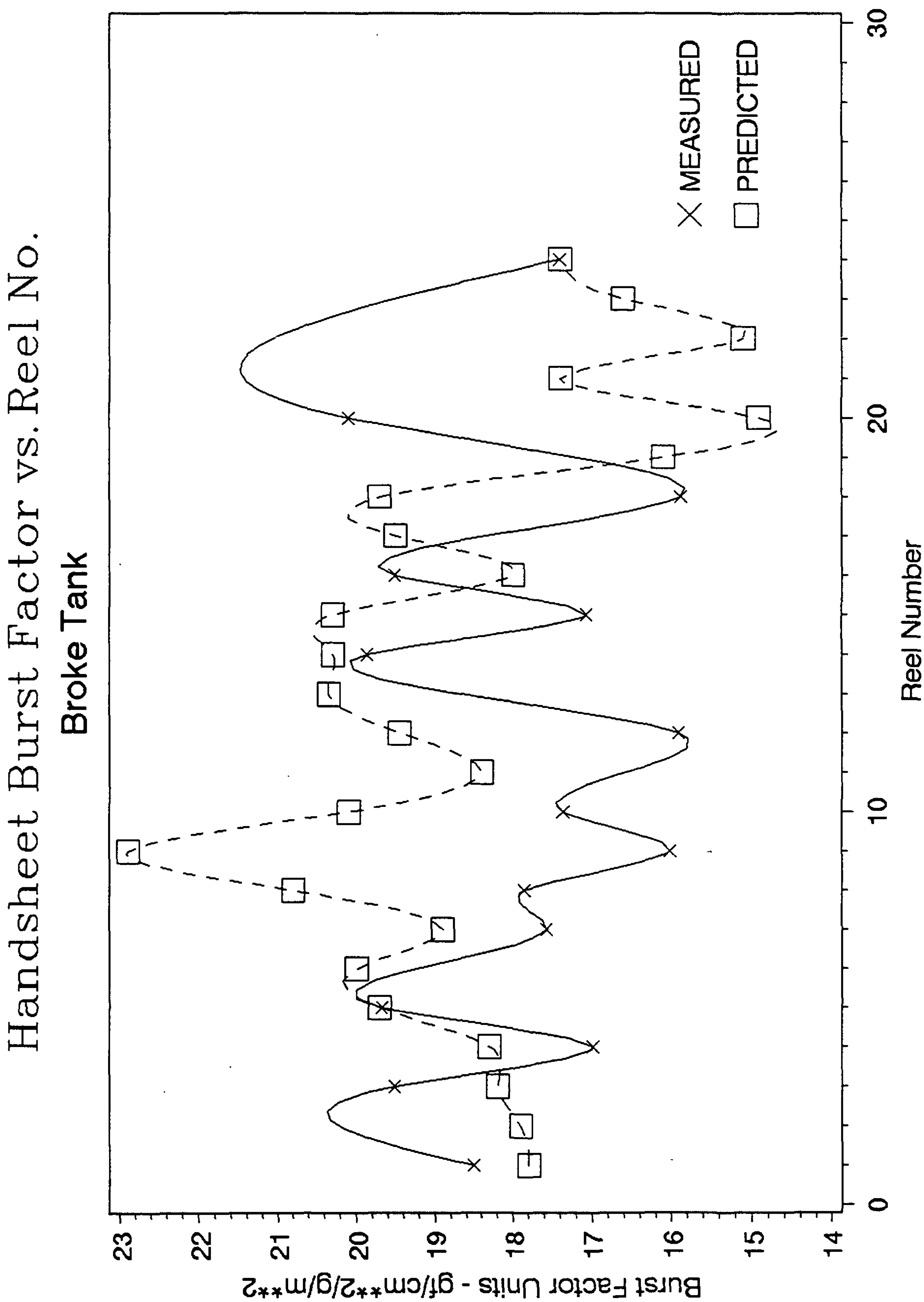

Figure 49

FIGURES

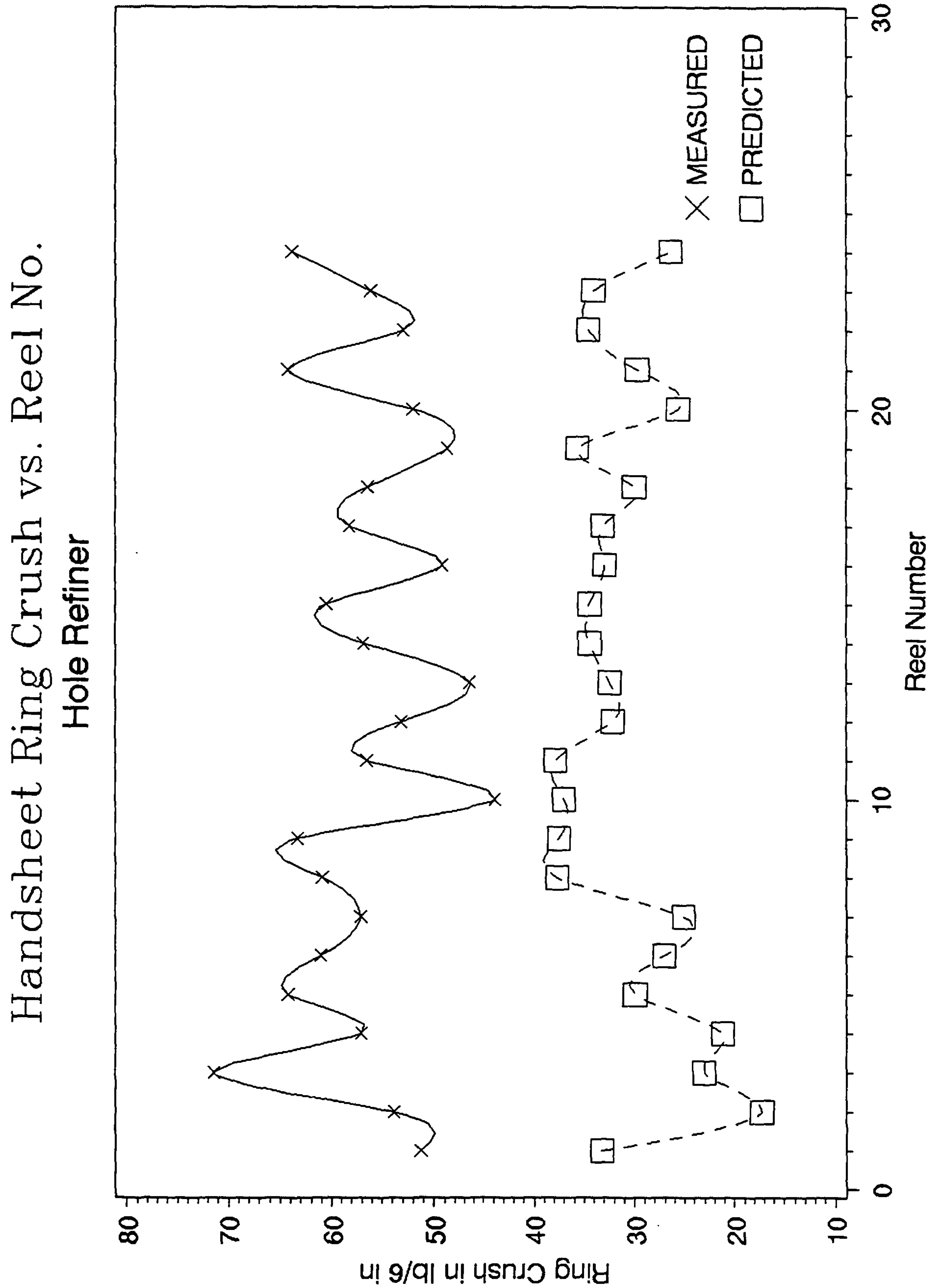

Figure 50

FIGURES

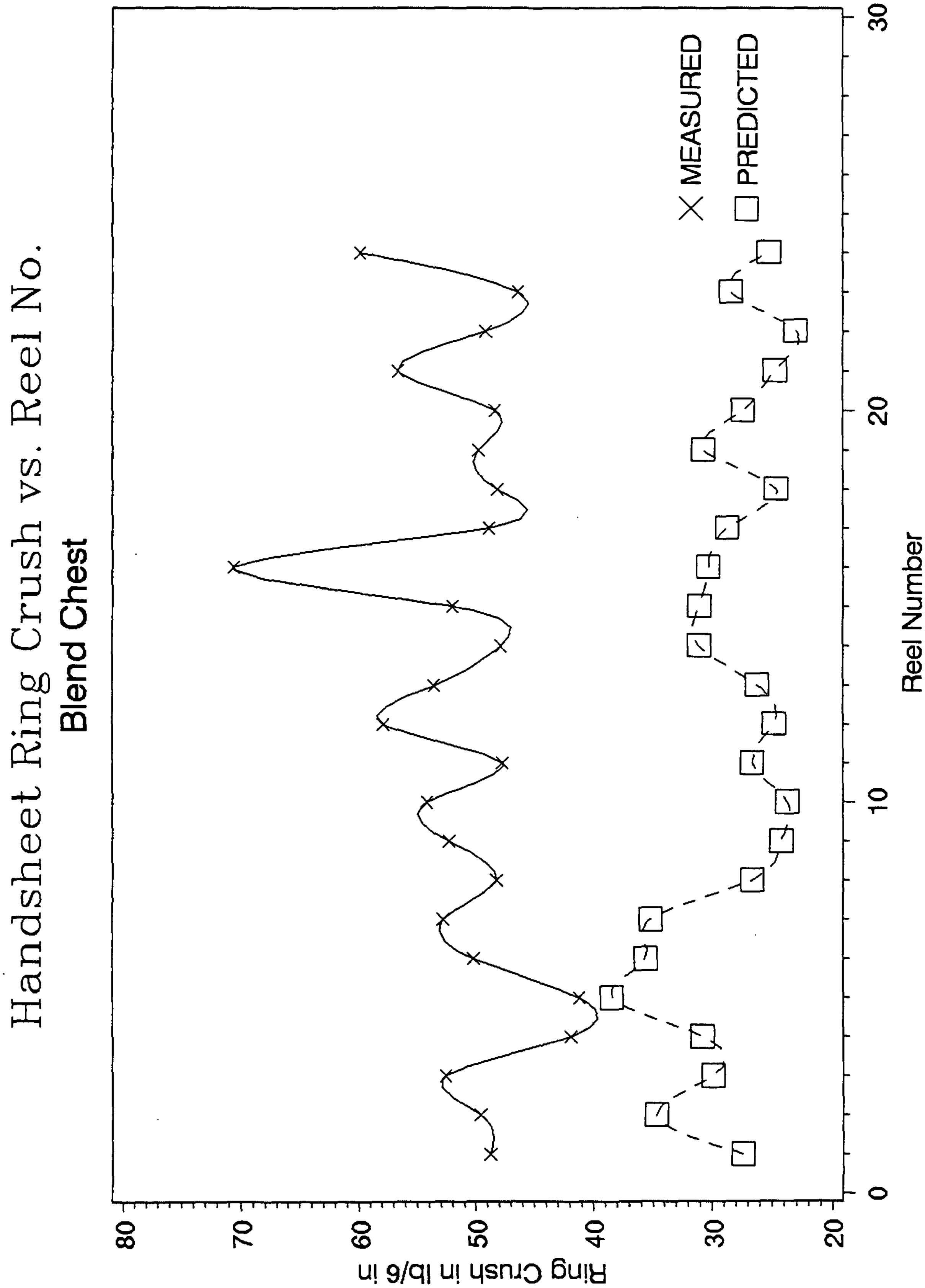

Figure 51

FIGURES

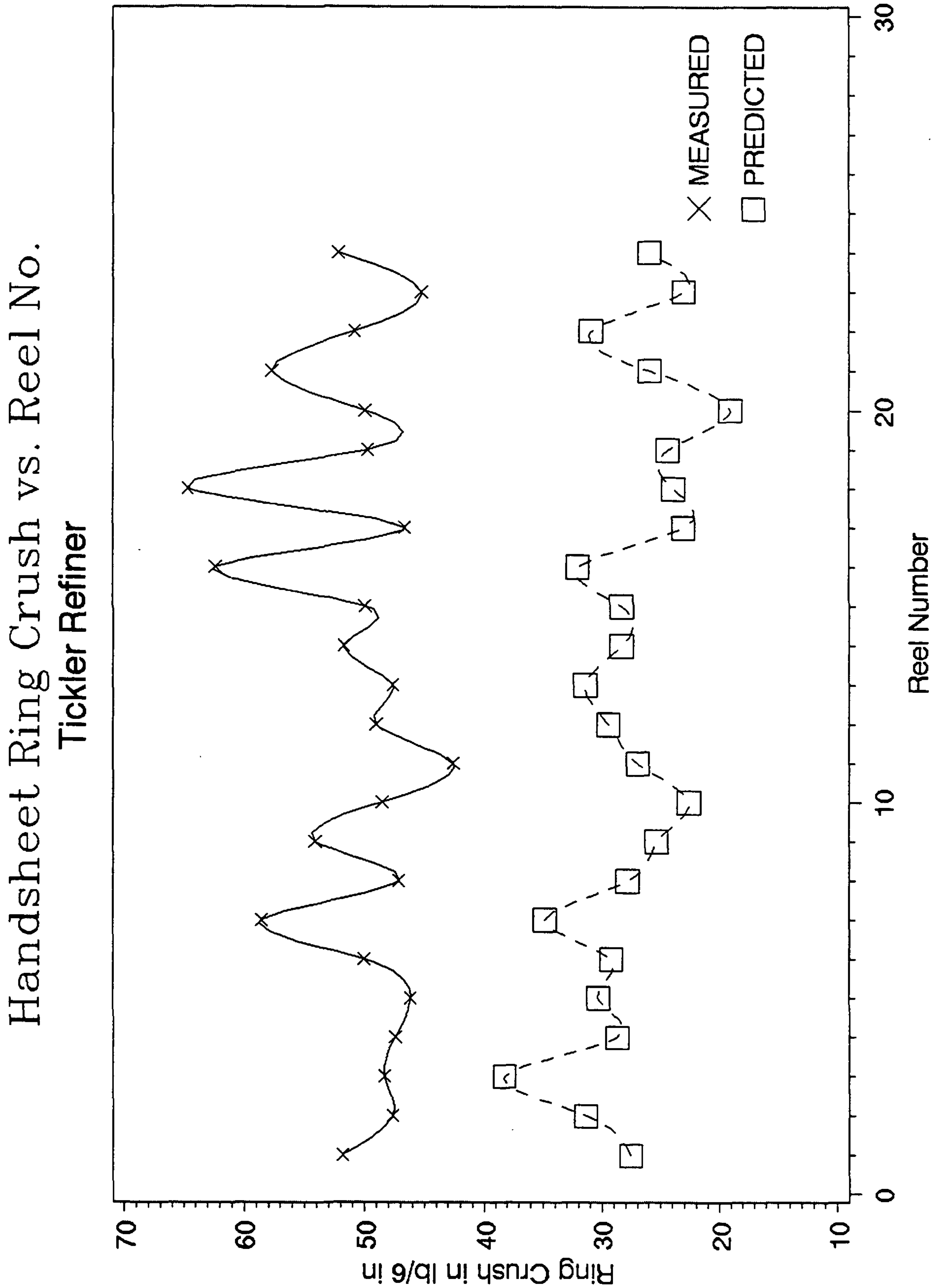

Figure 52

FIGURES

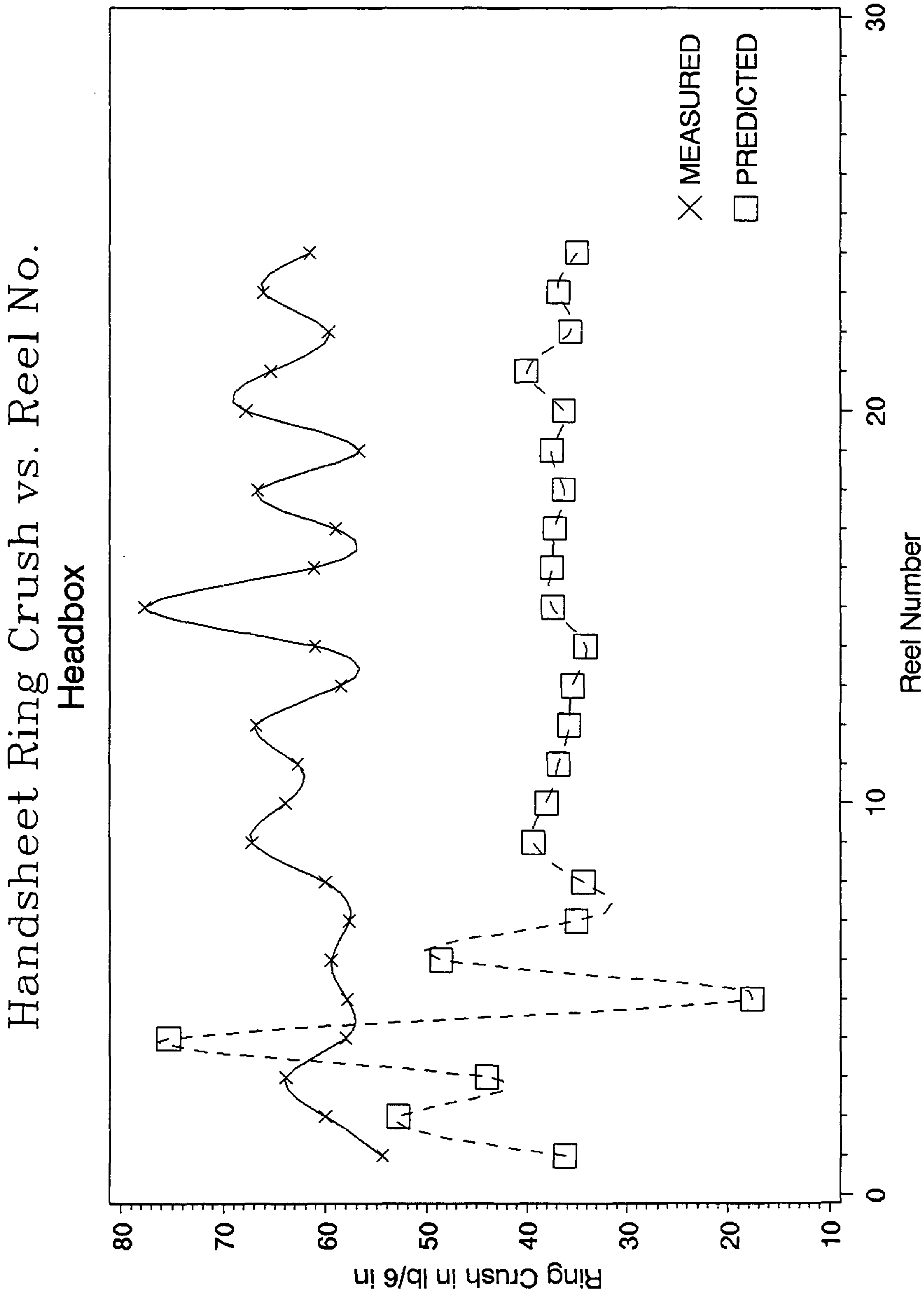

Figure 53

FIGURES

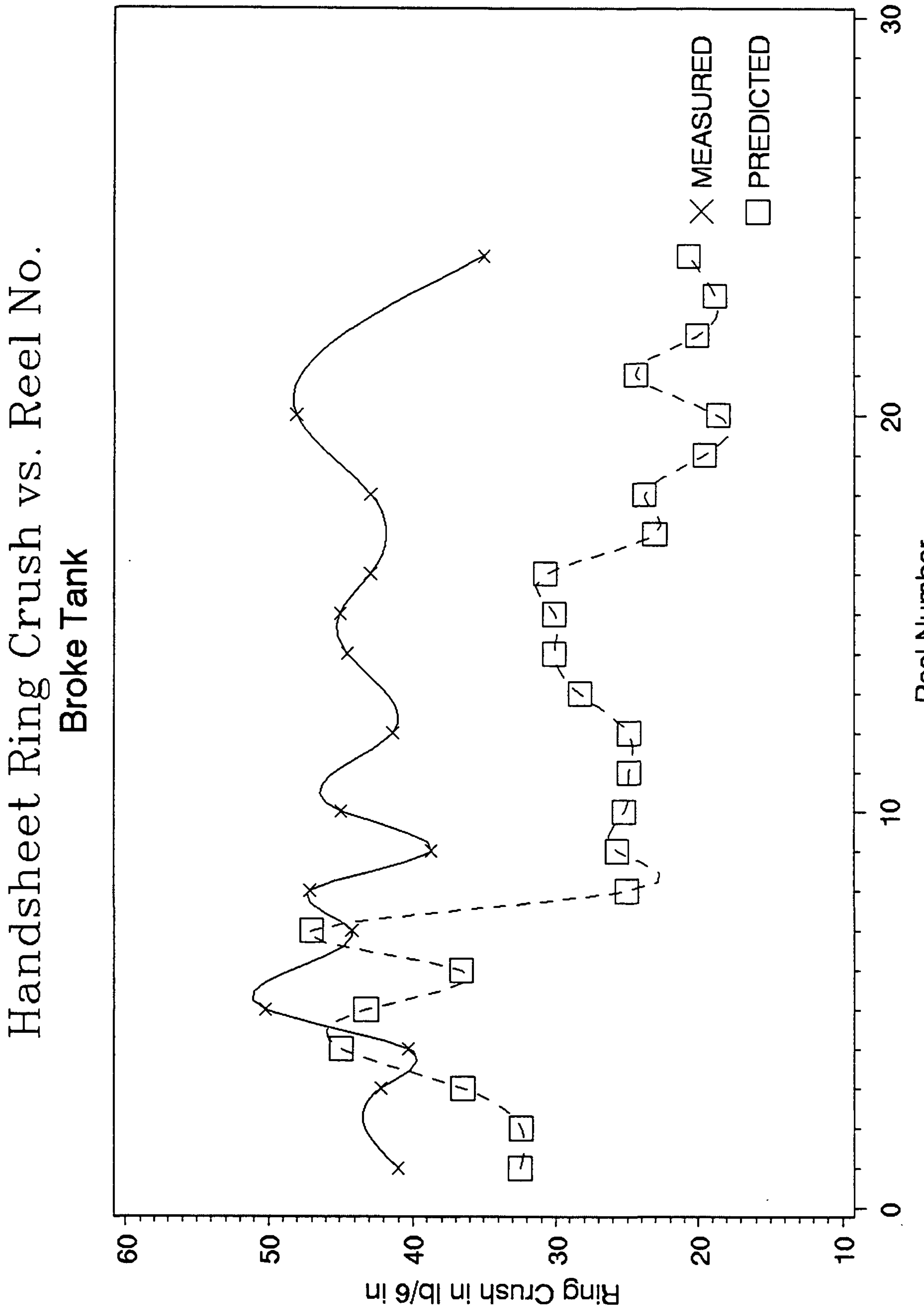

Figure 54

FIGURES

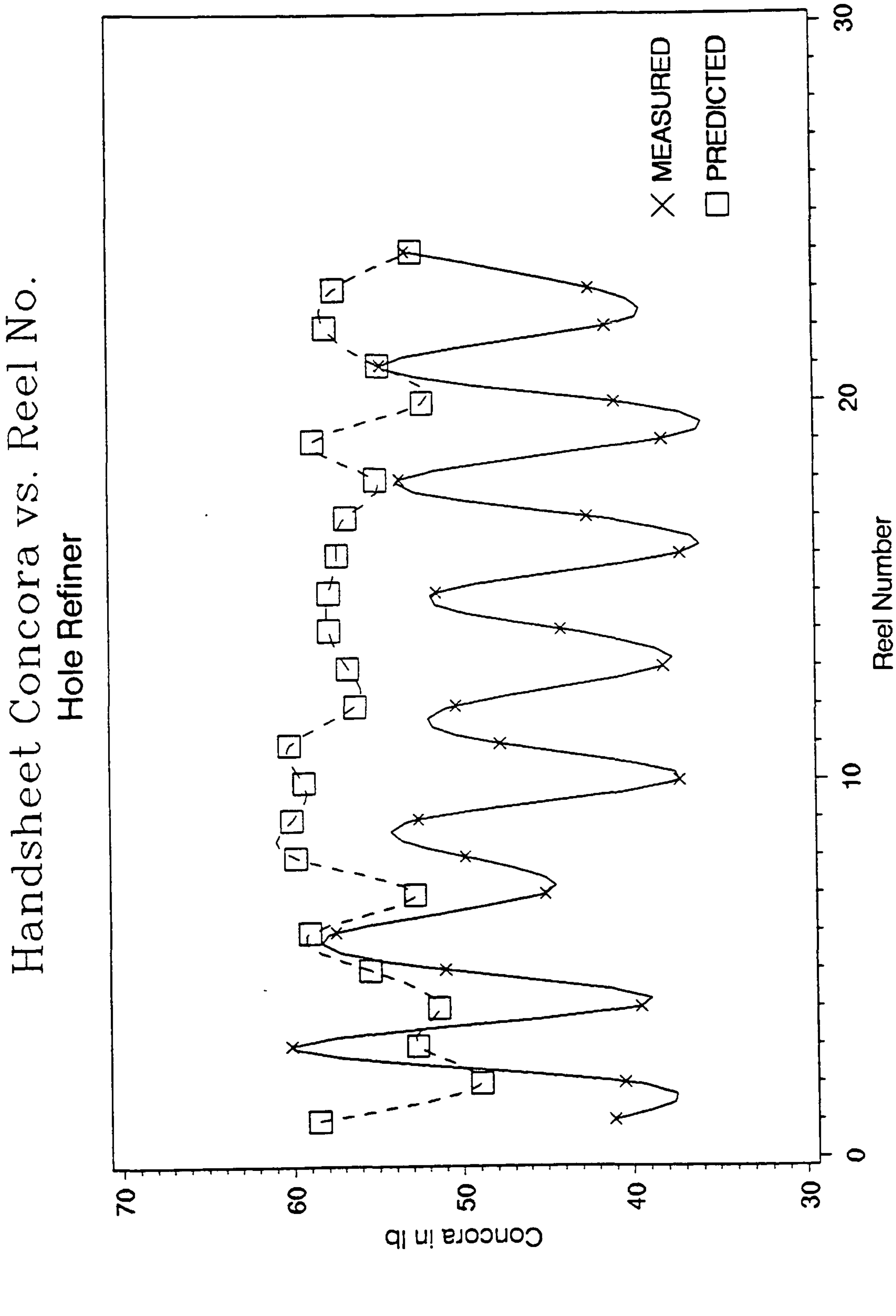

Figure 55

FIGURES

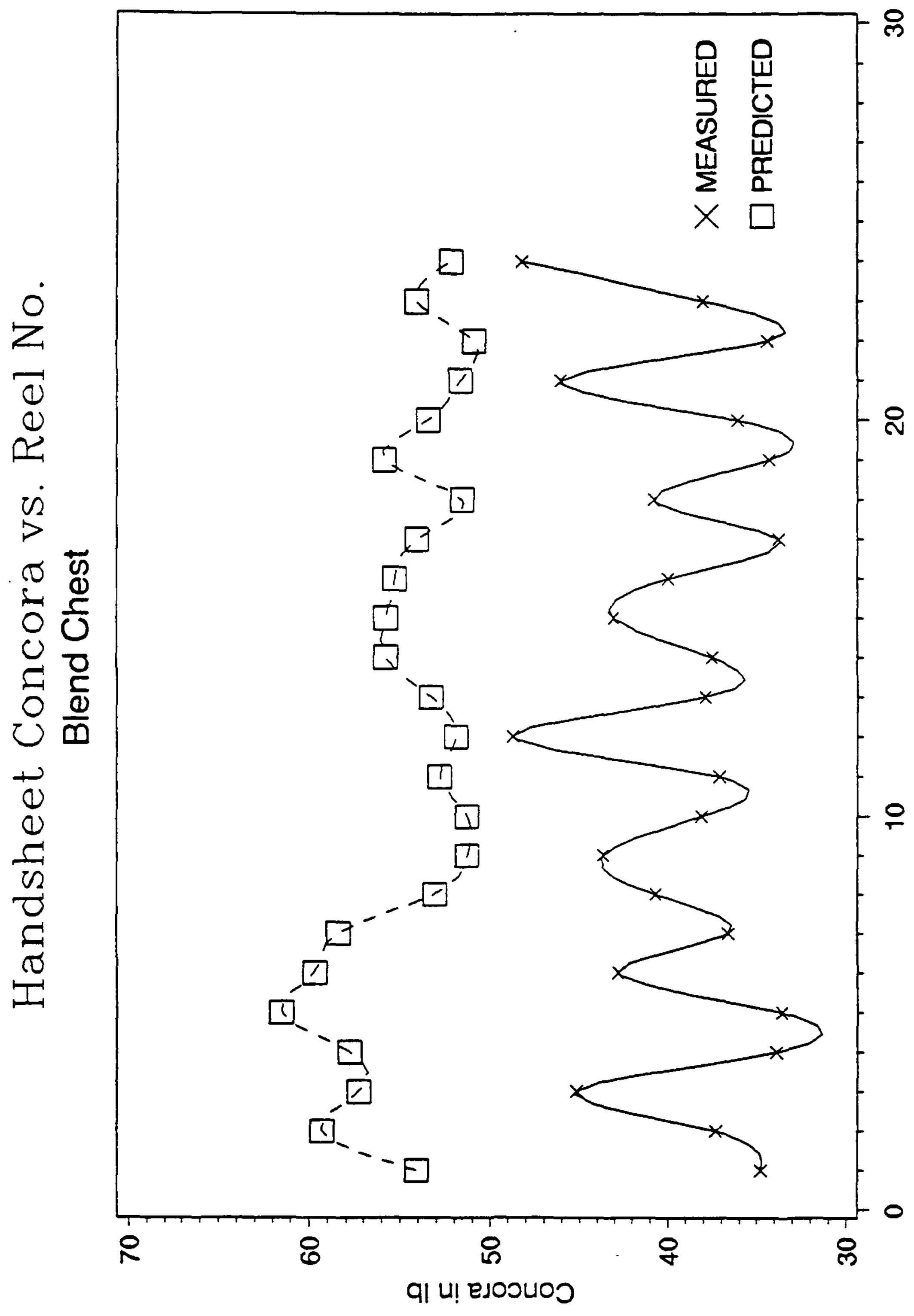

Figure 56

FIGURES

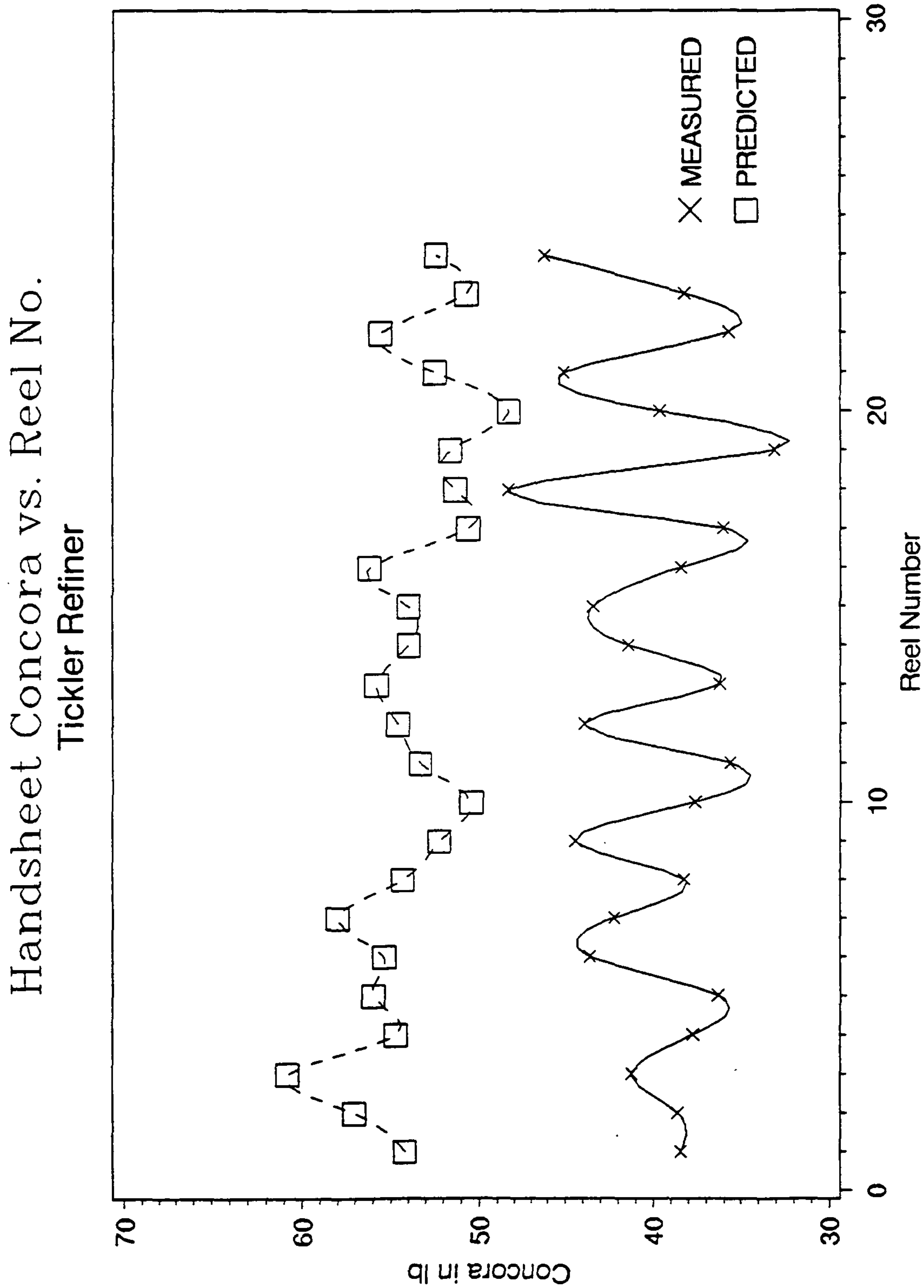

Figure 57

FIGURES

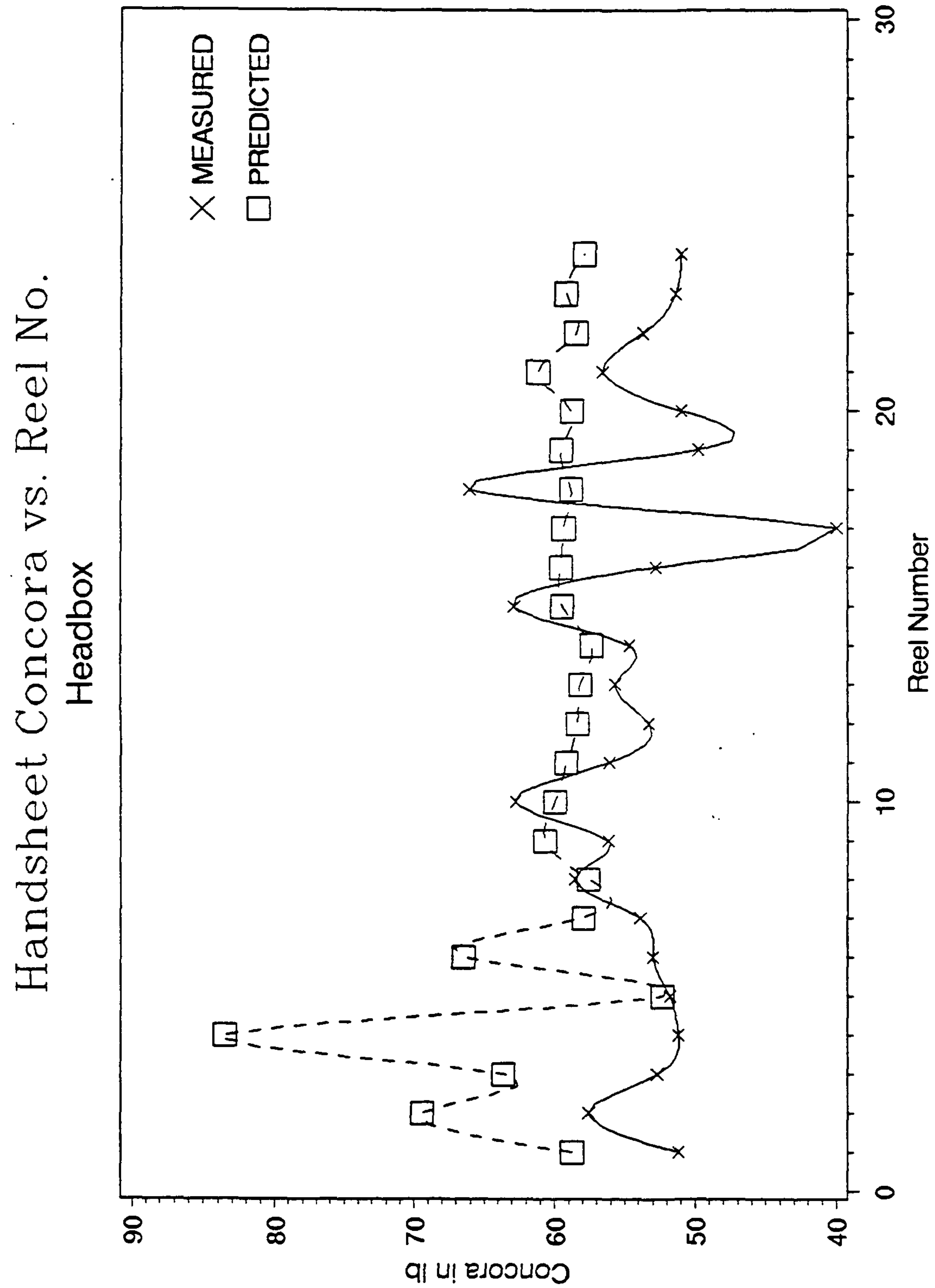

Figure 58

FIGURES

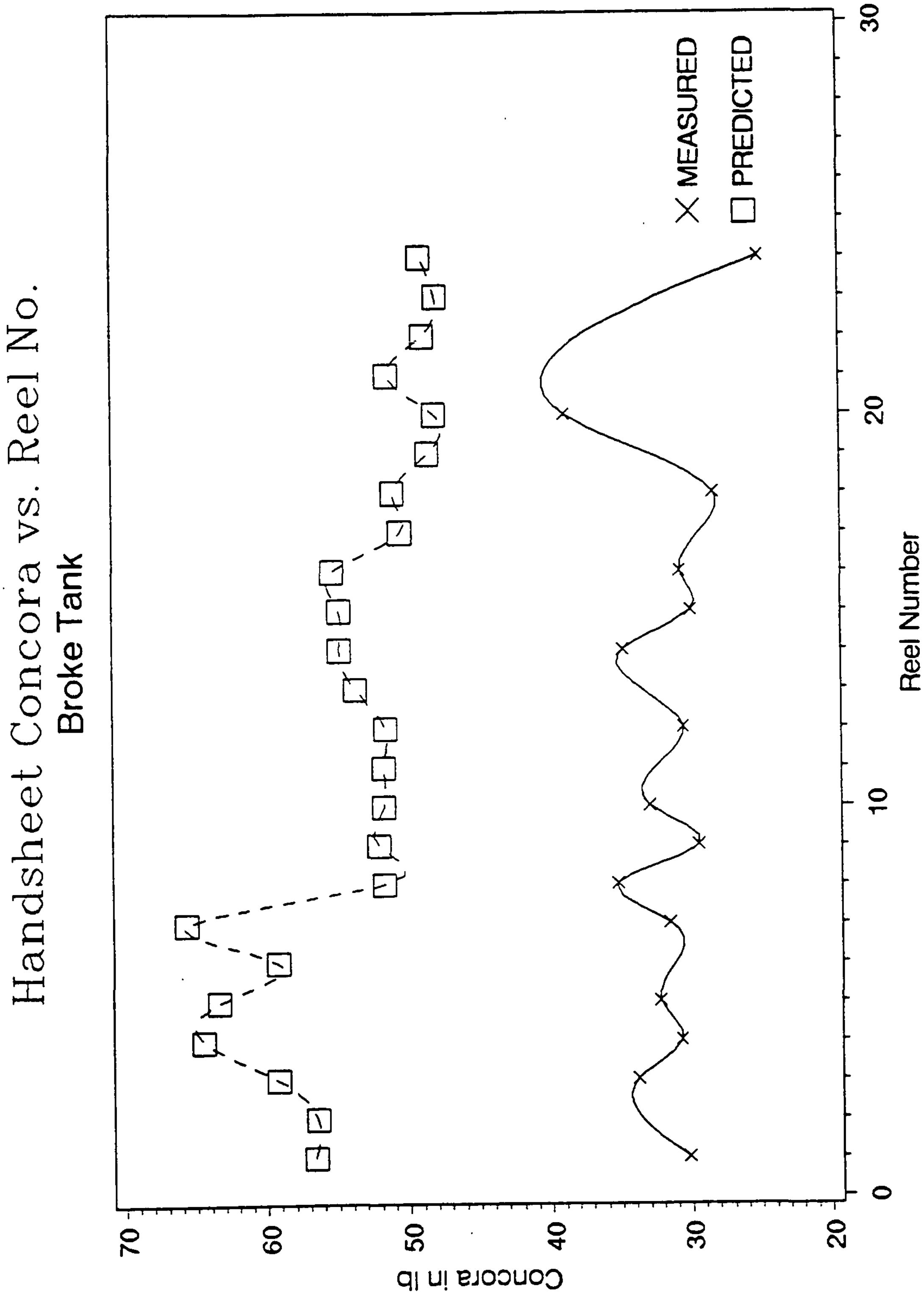

Figure 59

FIGURES

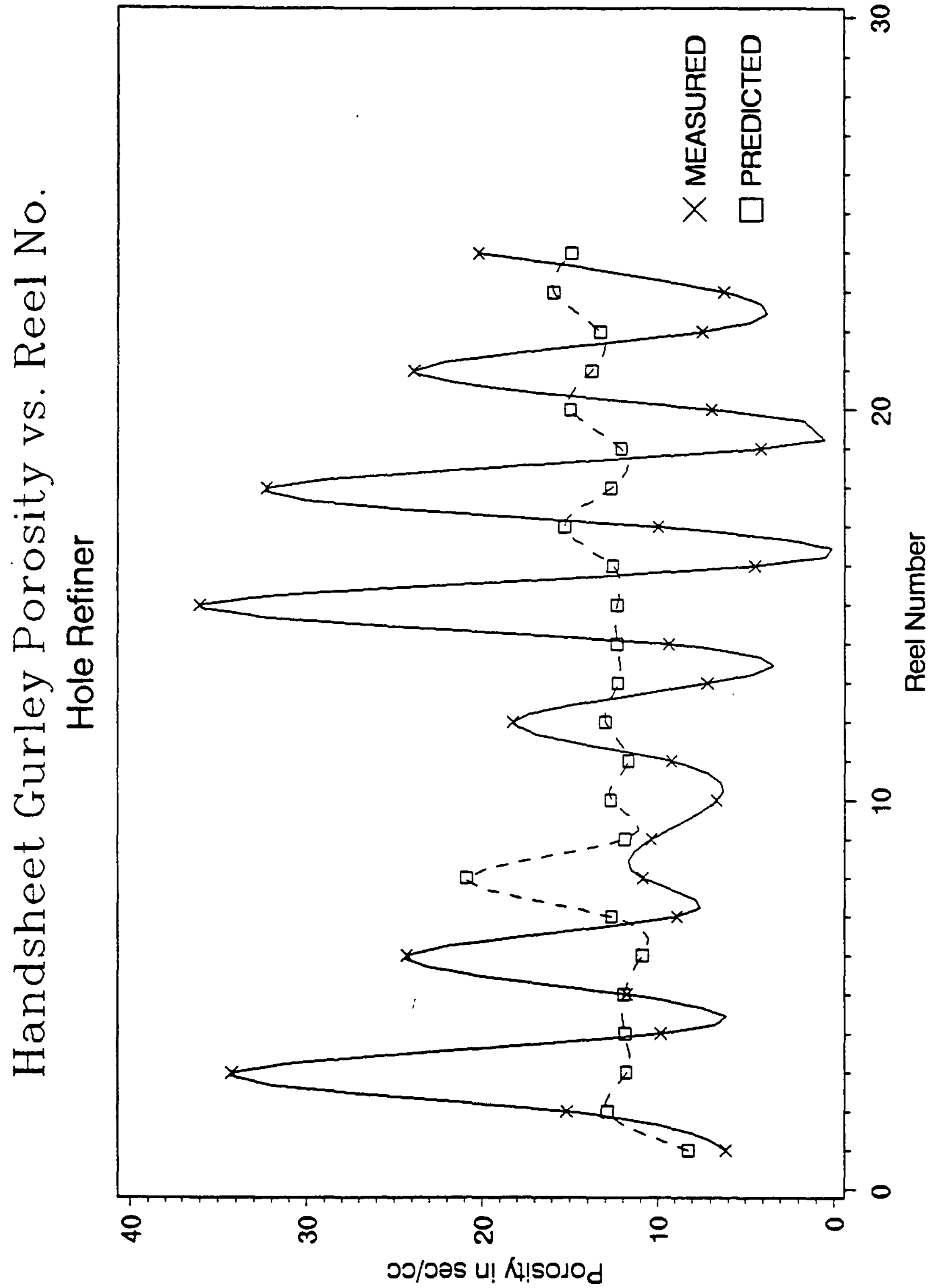

Figure 60

FIGURES

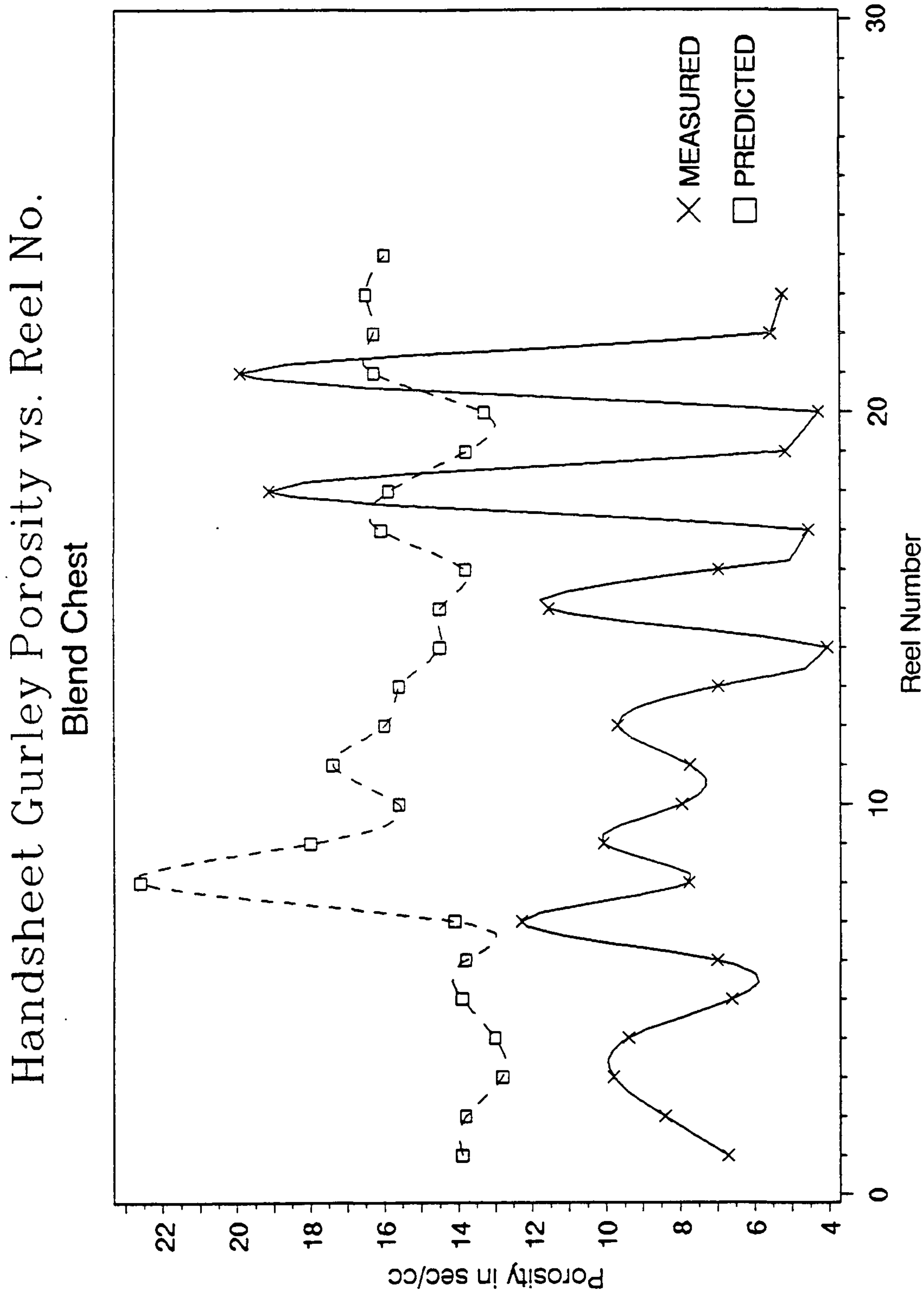

Figure 61

FIGURES

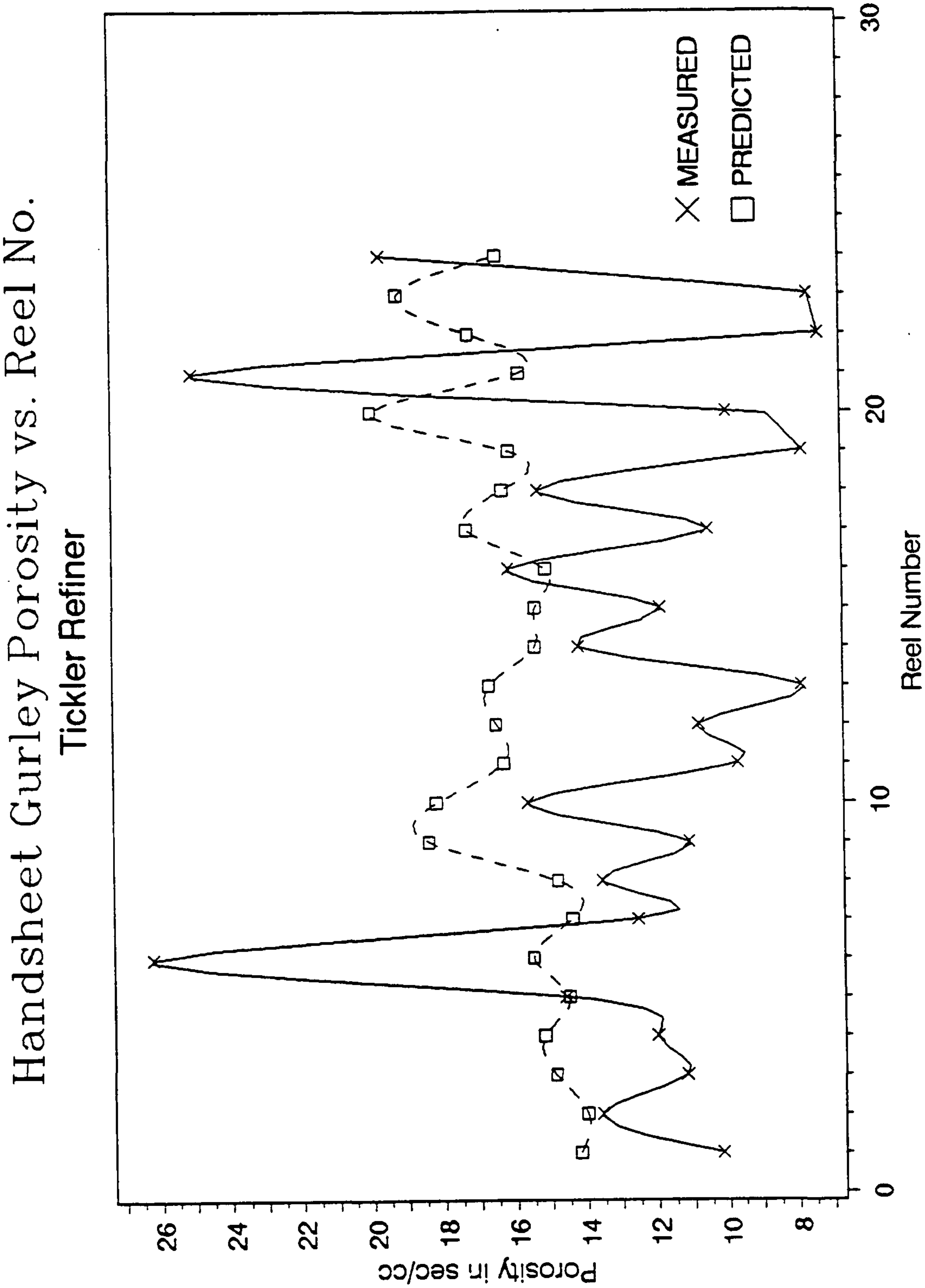

Figure 62

FIGURES

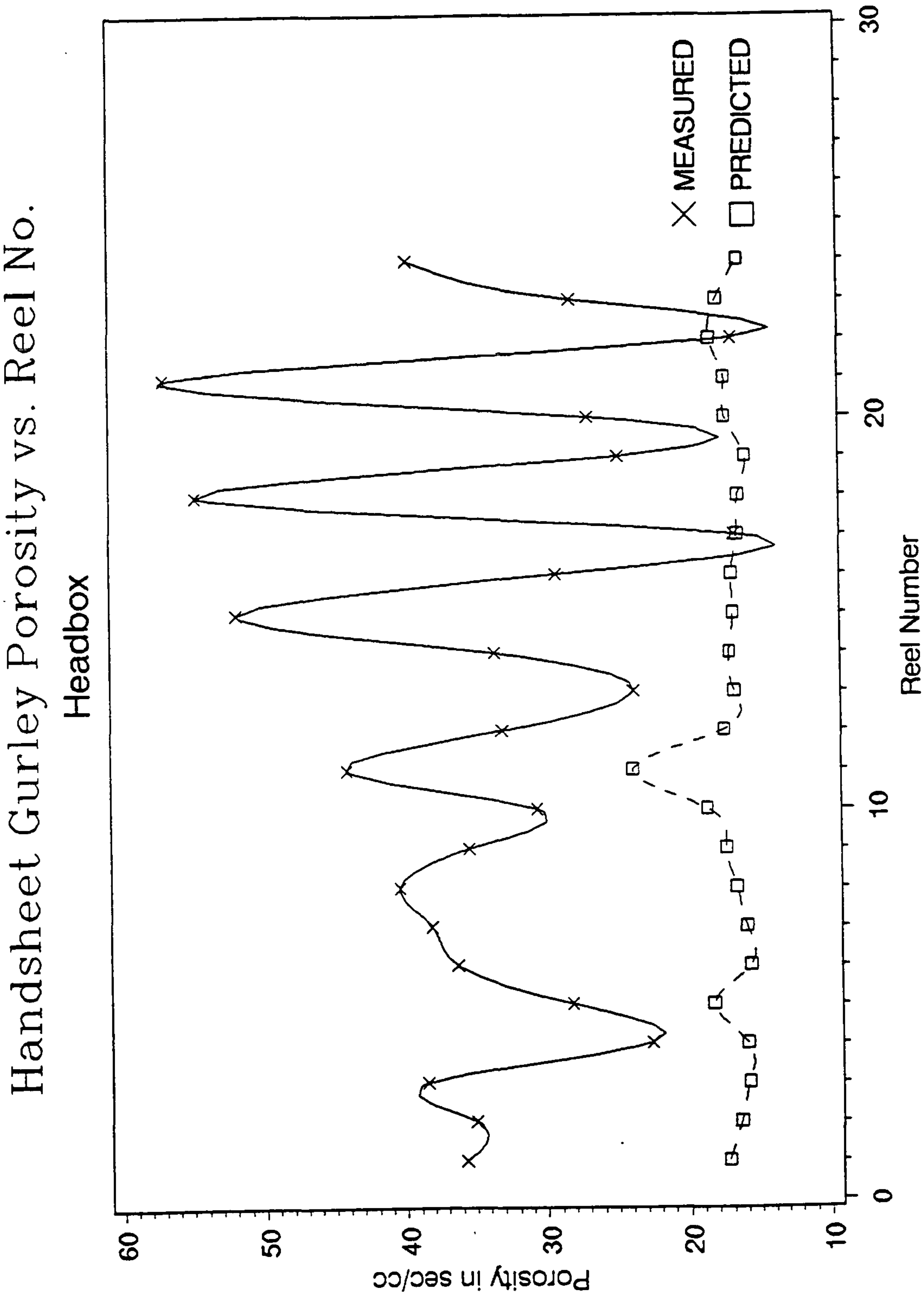

Figure 63

FIGURES

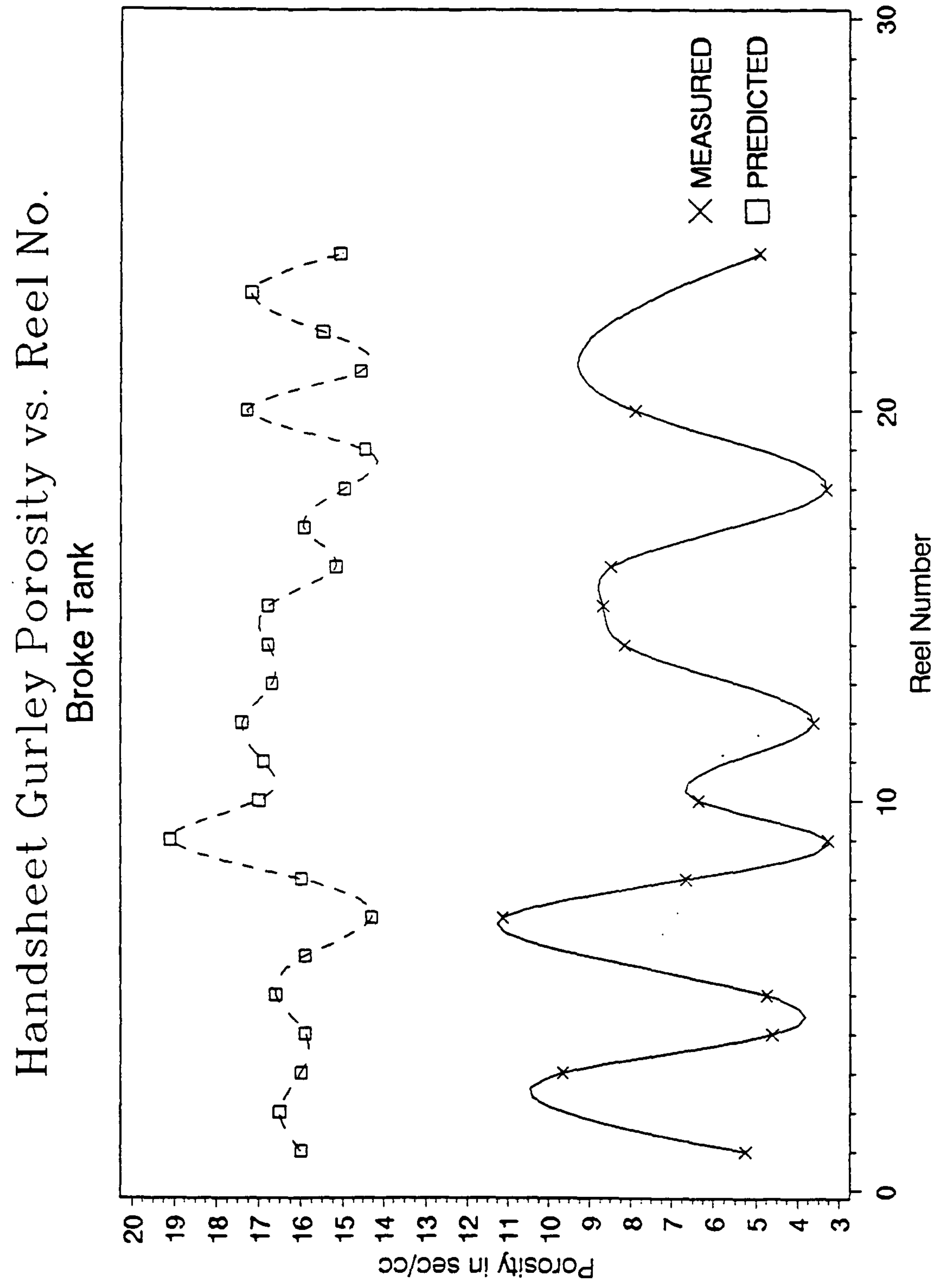

Figure 64

APPENDIX I
PROCESS CONDITIONS

OBS	DATE	DAY	REEL	RLPLT	OCC Flow Ratio	High Density Tank CSF	Measured Primary Refiner CSF	Measured Tickler Refiner CSF
1	4-3-90	1	1	1	0.18359	722	528	482
2	4-3-90	1	1	1	0.18359	722	528	482
3	4-3-90	1	1	1	0.18359	722	528	482
4	4-3-90	1	2	2	0.18764	656	499	427
5	4-3-90	1	2	2	0.18764	656	499	427
6	4-3-90	1	2	2	0.18764	656	499	427
7	4-3-90	1	3	3	0.21970	697	442	489
8	4-3-90	1	3	3	0.21970	697	442	489
9	4-3-90	1	3	3	0.21970	697	442	489
10	4-3-90	1	4	4	0.19376	686	508	459
11	4-3-90	1	4	4	0.19376	686	508	459
12	4-3-90	1	4	4	0.19376	686	508	459
13	4-3-90	1	4	4	0.19376	686	508	459
14	4-3-90	1	4	4	0.19376	686	508	459
15	4-3-90	1	4	4	0.19376	686	508	459
16	4-3-90	1	5	5	0.27540	701	482	474
17	4-3-90	1	5	5	0.27540	701	482	474
18	4-3-90	1	5	5	0.27540	701	482	474
19	4-3-90	1	6	6	0.27540	717	479	469
20	4-3-90	1	6	6	0.27540	717	479	469
21	4-3-90	1	6	6	0.27540	717	479	469
22	4-3-90	1	6	6	0.27540	717	479	469
23	4-3-90	1	6	6	0.27540	717	479	469
24	4-3-90	1	6	6	0.27540	717	479	469
25	4-3-90	1	7	7	0.23404	728	489	503
26	4-3-90	1	7	7	0.23404	728	489	503
27	4-3-90	1	7	7	0.23404	728	489	503
28	4-3-90	1	8	8	0.24661	716	477	489
29	4-3-90	1	8	8	0.24661	716	477	489
30	4-3-90	1	8	8	0.24661	716	477	489
31	4-3-90	1	8	8	0.24661	716	477	489
32	4-3-90	1	8	8	0.24661	716	477	489
33	4-3-90	1	8	8	0.24661	716	477	489
34	4-4-90	2	1	9	0.34741	722	449	466
35	4-4-90	2	1	9	0.34741	722	449	466
36	4-4-90	2	1	9	0.34741	722	449	466
37	4-4-90	2	2	10	0.38025	735	419	432
38	4-4-90	2	2	10	0.38025	735	419	432
39	4-4-90	2	2	10	0.38025	735	419	432
40	4-4-90	2	3	11	0.36939	708	474	476
41	4-4-90	2	3	11	0.36939	708	474	476
42	4-4-90	2	3	11	0.36939	708	474	476
43	4-4-90	2	4	12	0.35671	724	474	448
44	4-4-90	2	4	12	0.35671	724	474	448
45	4-4-90	2	4	12	0.35671	724	474	448
46	4-4-90	2	4	12	0.35671	724	474	448
47	4-4-90	2	4	12	0.35671	724	474	448
48	4-4-90	2	4	12	0.35671	724	474	448
49	4-4-90	2	4	12	0.35671	724	474	448
50	4-4-90	2	4	12	0.35671	724	474	448

APPENDIX I
PROCESS CONDITIONS

OBS	DATE	DAY	REEL	RLPLT	OCC Flow Ratio	High Density Tank CSF	Measured Primary Refiner CSF	Measured Tickler Refiner CSF
51	4-4-90	2	4	12	0.35671	724	474	448
52	4-4-90	2	5	13	0.31845	745	518	468
53	4-4-90	2	5	13	0.31845	745	518	468
54	4-4-90	2	5	13	0.31845	745	518	468
55	4-4-90	2	6	14	0.29913	722	496	452
56	4-4-90	2	6	14	0.29913	722	496	452
57	4-4-90	2	6	14	0.29913	722	496	452
58	4-4-90	2	6	14	0.29913	722	496	452
59	4-4-90	2	6	14	0.29913	722	496	452
60	4-4-90	2	6	14	0.29913	722	496	452
61	4-4-90	2	6	14	0.29913	722	496	452
62	4-4-90	2	6	14	0.29913	722	496	452
63	4-4-90	2	6	14	0.29913	722	496	452
64	4-4-90	2	7	15	0.29913	768	504	464
65	4-4-90	2	7	15	0.29913	768	504	464
66	4-4-90	2	7	15	0.29913	768	504	464
67	4-4-90	2	8	16	0.28306	706	493	480
68	4-4-90	2	8	16	0.28306	706	493	480
69	4-4-90	2	8	16	0.28306	706	493	480
70	4-4-90	2	8	16	0.28306	706	493	480
71	4-4-90	2	8	16	0.28306	706	493	480
72	4-4-90	2	8	16	0.28306	706	493	480
73	4-4-90	2	8	16	0.28306	706	493	480
74	4-4-90	2	8	16	0.28306	706	493	480
75	4-4-90	2	8	16	0.28306	706	493	480
76	4-5-90	3	1	17	0.33333	740	428	419
77	4-5-90	3	1	17	0.33333	740	428	419
78	4-5-90	3	1	17	0.33333	740	428	419
79	4-5-90	3	2	18	0.30798	738	380	387
80	4-5-90	3	2	18	0.30798	738	380	387
81	4-5-90	3	2	18	0.30798	738	380	387
82	4-5-90	3	3	19	0.26036	719	430	444
83	4-5-90	3	3	19	0.26036	719	430	444
84	4-5-90	3	3	19	0.26036	719	430	444
85	4-5-90	3	4	20	0.26426	714	419	368
86	4-5-90	3	4	20	0.26426	714	419	368
87	4-5-90	3	4	20	0.26426	714	419	368
88	4-5-90	3	4	20	0.26426	714	419	368
89	4-5-90	3	4	20	0.26426	714	419	368
90	4-5-90	3	4	20	0.26426	714	419	368
91	4-5-90	3	4	20	0.26426	714	419	368
92	4-5-90	3	4	20	0.26426	714	419	368
93	4-5-90	3	4	20	0.26426	714	419	368
94	4-5-90	3	5	21	0.24638	724	363	422
95	4-5-90	3	5	21	0.24638	724	363	422
96	4-5-90	3	5	21	0.24638	724	363	422
97	4-5-90	3	6	22	0.27157	716	358	424
98	4-5-90	3	6	22	0.27157	716	358	424
99	4-5-90	3	6	22	0.27157	716	358	424
100	4-5-90	3	6	22	0.27157	716	358	424

APPENDIX I
PROCESS CONDITIONS

OBS	DATE	DAY	REEL	RLPLT	OCC Flow Ratio	High Density Tank CSF	Measured Primary Refiner CSF	Measured Tickler Refiner CSF
101	4-5-90	3	6	22	0.27157	716	358	424
102	4-5-90	3	6	22	0.27157	716	358	424
103	4-5-90	3	7	23	0.27937	679	364	395
104	4-5-90	3	7	23	0.27937	679	364	395
105	4-5-90	3	7	23	0.27937	679	364	395
106	4-5-90	3	8	24	0.25329	722	395	389
107	4-5-90	3	8	24	0.25329	722	395	389
108	4-5-90	3	8	24	0.25329	722	395	389
109	4-5-90	3	8	24	0.25329	722	395	389
110	4-5-90	3	8	24	0.25329	722	395	389
111	4-5-90	3	8	24	0.25329	722	395	389
112	4-5-90	3	8	24	0.25329	722	395	389
113	4-5-90	3	8	24	0.25329	722	395	389
114	4-5-90	3	8	24	0.25329	722	395	389

APPENDIX I
PROCESS CONDITIONS

OBS	Measured Stuffbox CSF	Measured Headbox CSF	Semichem. Flow Rate	Primary Refiner Feed Consistency	Primary Refiner Spec. Power
1	460	305	37800	5.9	1.47
2	460	305	37800	5.9	1.47
3	460	305	37800	5.9	1.47
4	460	286	36800	5.6	1.95
5	460	286	36800	5.6	1.95
6	460	286	36800	5.6	1.95
7	442	280	30900	4.7	2.36
8	442	280	30900	4.7	2.36
9	442	280	30900	4.7	2.36
10	442	260	36200	5.3	1.97
11	442	260	36200	5.3	1.97
12	442	260	36200	5.3	1.97
13	442	260	36200	5.3	1.97
14	442	260	36200	5.3	1.97
15	442	260	36200	5.3	1.97
16	450	264	32100	4.7	2.23
17	450	264	32100	4.7	2.23
18	450	264	32100	4.7	2.23
19	450	324	32100	4.7	2.20
20	450	324	32100	4.7	2.20
21	450	324	32100	4.7	2.20
22	450	324	32100	4.7	2.20
23	450	324	32100	4.7	2.20
24	450	324	32100	4.7	2.20
25	476	321	36000	5.1	2.09
26	476	321	36000	5.1	2.09
27	476	321	36000	5.1	2.09
28	476	305	33300	4.7	2.27
29	476	305	33300	4.7	2.27
30	476	305	33300	4.7	2.27
31	476	305	33300	4.7	2.27
32	476	305	33300	4.7	2.27
33	476	305	33300	4.7	2.27
34	453	277	34000	5.6	2.42
35	453	277	34000	5.6	2.42
36	453	277	34000	5.6	2.42
37	453	277	29500	5.3	2.90
38	453	277	29500	5.3	2.90
39	453	277	29500	5.3	2.90
40	453	310	30900	5.2	2.76
41	453	310	30900	5.2	2.76
42	453	310	30900	5.2	2.76
43	434	272	32100	5.4	2.67
44	434	272	32100	5.4	2.67
45	434	272	32100	5.4	2.67
46	434	272	32100	5.4	2.67
47	434	272	32100	5.4	2.67
48	434	272	32100	5.4	2.67
49	434	272	32100	5.4	2.67
50	434	272	32100	5.4	2.67

APPENDIX I
PROCESS CONDITIONS

OBS	Measured Stuffbox CSF	Measured Headbox CSF	Semichem. Flow Rate	Primary Refiner Feed Consistency	Primary Refiner Spec. Power
51	434	272	32100	5.4	2.67
52	434	309	35100	5.9	2.38
53	434	309	35100	5.9	2.38
54	434	309	35100	5.9	2.38
55	434	286	32100	5.4	2.67
56	434	286	32100	5.4	2.67
57	434	286	32100	5.4	2.67
58	434	286	32100	5.4	2.67
59	434	286	32100	5.4	2.67
60	434	286	32100	5.4	2.67
61	434	286	32100	5.4	2.67
62	434	286	32100	5.4	2.67
63	434	286	32100	5.4	2.67
64	463	293	32100	5.4	2.56
65	463	293	32100	5.4	2.56
66	463	293	32100	5.4	2.56
67	463	335	34700	4.9	2.16
68	463	335	34700	4.9	2.16
69	463	335	34700	4.9	2.16
70	463	335	34700	4.9	2.16
71	463	335	34700	4.9	2.16
72	463	335	34700	4.9	2.16
73	463	335	34700	4.9	2.16
74	463	335	34700	4.9	2.16
75	463	335	34700	4.9	2.16
76	406	295	16200	4.0	5.16
77	406	295	16200	4.0	5.16
78	406	295	16200	4.0	5.16
79	406	275	18200	4.0	4.57
80	406	275	18200	4.0	4.57
81	406	275	18200	4.0	4.57
82	416	290	25000	5.2	3.18
83	416	290	25000	5.2	3.18
84	416	290	25000	5.2	3.18
85	416	286	24500	5.1	3.58
86	416	286	24500	5.1	3.58
87	416	286	24500	5.1	3.58
88	416	286	24500	5.1	3.58
89	416	286	24500	5.1	3.58
90	416	286	24500	5.1	3.58
91	416	286	24500	5.1	3.58
92	416	286	24500	5.1	3.58
93	416	286	24500	5.1	3.58
94	457	296	26000	5.4	3.61
95	457	296	26000	5.4	3.61
96	457	296	26000	5.4	3.61
97	457	280	22800	5.3	4.11
98	457	280	22800	5.3	4.11
99	457	280	22800	5.3	4.11
100	457	280	22800	5.3	4.11

APPENDIX I
PROCESS CONDITIONS

OBS	Measured Stuffbox CSF	Measured Headbox CSF	Semichem. Flow Rate	Primary Refiner Feed Consistency	Primary Refiner Spec. Power
101	457	280	22800	5.3	4.11
102	457	280	22800	5.3	4.11
103	390	255	22700	5.6	3.78
104	390	255	22700	5.6	3.78
105	390	255	22700	5.6	3.78
106	387	295	22700	5.6	3.54
107	387	295	22700	5.6	3.54
108	387	295	22700	5.6	3.54
109	387	295	22700	5.6	3.54
110	387	295	22700	5.6	3.54
111	387	295	22700	5.6	3.54
112	387	295	22700	5.6	3.54
113	387	295	22700	5.6	3.54
114	387	295	22700	5.6	3.54

APPENDIX I
PROCESS CONDITIONS

OBS	OCC Mass Flow Rate	OCC Consistency	Tickler Refiner Consistency	Stuffbox Consistency	Headbox Consistency
1	8500	5.6	4.7	4.0	0.84
2	8500	5.6	4.7	4.0	0.84
3	8500	5.6	4.7	4.0	0.84
4	8500	5.6	4.1	4.0	0.86
5	8500	5.6	4.1	4.0	0.86
6	8500	5.6	4.1	4.0	0.86
7	8700	5.7	4.4	3.5	0.82
8	8700	5.7	4.4	3.5	0.82
9	8700	5.7	4.4	3.5	0.82
10	8700	5.7	5.1	3.5	0.80
11	8700	5.7	5.1	3.5	0.80
12	8700	5.7	5.1	3.5	0.80
13	8700	5.7	5.1	3.5	0.80
14	8700	5.7	5.1	3.5	0.80
15	8700	5.7	5.1	3.5	0.80
16	12200	6.0	4.9	4.0	0.92
17	12200	6.0	4.9	4.0	0.92
18	12200	6.0	4.9	4.0	0.92
19	12200	6.0	4.9	4.0	0.86
20	12200	6.0	4.9	4.0	0.86
21	12200	6.0	4.9	4.0	0.86
22	12200	6.0	4.9	4.0	0.86
23	12200	6.0	4.9	4.0	0.86
24	12200	6.0	4.9	4.0	0.86
25	11000	5.4	4.9	3.7	0.86
26	11000	5.4	4.9	3.7	0.86
27	11000	5.4	4.9	3.7	0.86
28	10900	5.4	4.9	3.7	0.84
29	10900	5.4	4.9	3.7	0.84
30	10900	5.4	4.9	3.7	0.84
31	10900	5.4	4.9	3.7	0.84
32	10900	5.4	4.9	3.7	0.84
33	10900	5.4	4.9	3.7	0.84
34	18100	5.5	4.5	3.9	0.84
35	18100	5.5	4.5	3.9	0.84
36	18100	5.5	4.5	3.9	0.84
37	18100	5.5	4.9	3.9	0.84
38	18100	5.5	4.9	3.9	0.84
39	18100	5.5	4.9	3.9	0.84
40	18100	5.5	4.5	3.9	0.82
41	18100	5.5	4.5	3.9	0.82
42	18100	5.5	4.5	3.9	0.82
43	17800	5.4	4.8	3.3	0.84
44	17800	5.4	4.8	3.3	0.84
45	17800	5.4	4.8	3.3	0.84
46	17800	5.4	4.8	3.3	0.84
47	17800	5.4	4.8	3.3	0.84
48	17800	5.4	4.8	3.3	0.84
49	17800	5.4	4.8	3.3	0.84
50	17800	5.4	4.8	3.3	0.84

APPENDIX I
PROCESS CONDITIONS

OBS	OCC Mass Flow Rate	OCC Consistency	Tickler Refiner Consistency	Stuffbox Consistency	Headbox Consistency
51	17800	5.4	4.8	3.3	0.84
52	16400	5.4	4.8	3.3	0.82
53	16400	5.4	4.8	3.3	0.82
54	16400	5.4	4.8	3.3	0.82
55	13700	5.4	4.7	3.3	0.84
56	13700	5.4	4.7	3.3	0.84
57	13700	5.4	4.7	3.3	0.84
58	13700	5.4	4.7	3.3	0.84
59	13700	5.4	4.7	3.3	0.84
60	13700	5.4	4.7	3.3	0.84
61	13700	5.4	4.7	3.3	0.84
62	13700	5.4	4.7	3.3	0.84
63	13700	5.4	4.7	3.3	0.84
64	13700	5.4	5.2	3.3	0.84
65	13700	5.4	5.2	3.3	0.84
66	13700	5.4	5.2	3.3	0.84
67	13700	6.0	4.4	3.9	0.84
68	13700	6.0	4.4	3.9	0.84
69	13700	6.0	4.4	3.9	0.84
70	13700	6.0	4.4	3.9	0.84
71	13700	6.0	4.4	3.9	0.84
72	13700	6.0	4.4	3.9	0.84
73	13700	6.0	4.4	3.9	0.84
74	13700	6.0	4.4	3.9	0.84
75	13700	6.0	4.4	3.9	0.84
76	8100	5.3	5.3	3.7	0.88
77	8100	5.3	5.3	3.7	0.88
78	8100	5.3	5.3	3.7	0.88
79	8100	5.3	4.1	3.7	0.88
80	8100	5.3	4.1	3.7	0.88
81	8100	5.3	4.1	3.7	0.88
82	8800	5.8	5.2	3.7	0.90
83	8800	5.8	5.2	3.7	0.90
84	8800	5.8	5.2	3.7	0.90
85	8800	5.8	4.7	3.7	0.90
86	8800	5.8	4.7	3.7	0.90
87	8800	5.8	4.7	3.7	0.90
88	8800	5.8	4.7	3.7	0.90
89	8800	5.8	4.7	3.7	0.90
90	8800	5.8	4.7	3.7	0.90
91	8800	5.8	4.7	3.7	0.90
92	8800	5.8	4.7	3.7	0.90
93	8800	5.8	4.7	3.7	0.90
94	8500	5.6	4.7	4.1	0.92
95	8500	5.6	4.7	4.1	0.92
96	8500	5.6	4.7	4.1	0.92
97	8500	5.6	5.2	4.1	0.90
98	8500	5.6	5.2	4.1	0.90
99	8500	5.6	5.2	4.1	0.90
100	8500	5.6	5.2	4.1	0.90

APPENDIX I
PROCESS CONDITIONS

OBS	OCC Mass Flow Rate	OCC Consistency	Tickler Refiner Consistency	Stuffbox Consistency	Headbox Consistency
101	8500	5.6	5.2	4.1	0.90
102	8500	5.6	5.2	4.1	0.90
103	8800	5.8	5.1	4.0	0.88
104	8800	5.8	5.1	4.0	0.88
105	8800	5.8	5.1	4.0	0.88
106	7700	5.1	4.8	3.5	0.88
107	7700	5.1	4.8	3.5	0.88
108	7700	5.1	4.8	3.5	0.88
109	7700	5.1	4.8	3.5	0.88
110	7700	5.1	4.8	3.5	0.88
111	7700	5.1	4.8	3.5	0.88
112	7700	5.1	4.8	3.5	0.88
113	7700	5.1	4.8	3.5	0.88
114	7700	5.1	4.8	3.5	0.88

APPENDIX I
PROCESS CONDITIONS

OBS	Wire Speed	Machine Speed	Production Rate tons/hr	Headbox liquid head	Jet to Wire Speed Ratio	Dryer Speed
1	1862	1900	32.1	165	0.96	1900
2	1862	1900	32.1	165	0.96	1900
3	1862	1900	32.1	165	0.96	1900
4	1862	1900	32.1	166	0.96	1900
5	1862	1900	32.1	166	0.96	1900
6	1862	1900	32.1	166	0.96	1900
7	1862	1900	32.1	167	0.96	1900
8	1862	1900	32.1	167	0.96	1900
9	1862	1900	32.1	167	0.96	1900
10	1862	1900	32.1	167	0.96	1900
11	1862	1900	32.1	167	0.96	1900
12	1862	1900	32.1	167	0.96	1900
13	1862	1900	32.1	167	0.96	1900
14	1862	1900	32.1	167	0.96	1900
15	1862	1900	32.1	167	0.96	1900
16	1862	1900	32.1	167	0.96	1900
17	1862	1900	32.1	167	0.96	1900
18	1862	1900	32.1	167	0.96	1900
19	1862	1900	32.1	165	0.96	1900
20	1862	1900	32.1	165	0.96	1900
21	1862	1900	32.1	165	0.96	1900
22	1862	1900	32.1	165	0.96	1900
23	1862	1900	32.1	165	0.96	1900
24	1862	1900	32.1	165	0.96	1900
25	1862	1900	32.1	166	0.96	1900
26	1862	1900	32.1	166	0.96	1900
27	1862	1900	32.1	166	0.96	1900
28	1862	1900	32.1	167	0.96	1900
29	1862	1900	32.1	167	0.96	1900
30	1862	1900	32.1	167	0.96	1900
31	1862	1900	32.1	167	0.96	1900
32	1862	1900	32.1	167	0.96	1900
33	1862	1900	32.1	167	0.96	1900
34	1861	1900	32.1	165	0.96	1900
35	1861	1900	32.1	165	0.96	1900
36	1861	1900	32.1	165	0.96	1900
37	1861	1900	32.1	165	0.96	1900
38	1861	1900	32.1	165	0.96	1900
39	1861	1900	32.1	165	0.96	1900
40	1861	1900	32.1	166	0.96	1900
41	1861	1900	32.1	166	0.96	1900
42	1861	1900	32.1	166	0.96	1900
43	1861	1900	32.1	166	0.96	1900
44	1861	1900	32.1	166	0.96	1900
45	1861	1900	32.1	166	0.96	1900
46	1861	1900	32.1	166	0.96	1900
47	1861	1900	32.1	166	0.96	1900
48	1861	1900	32.1	166	0.96	1900
49	1861	1900	32.1	166	0.96	1900
50	1861	1900	32.1	166	0.96	1900

APPENDIX I
PROCESS CONDITIONS

OBS	Wire Speed	Machine Speed	Production Rate tons/hr	Headbox liquid head	Jet to Wire Speed Ratio	Dryer Speed
51	1861	1900	32.1	166	0.96	1900
52	1861	1900	32.1	166	0.96	1900
53	1861	1900	32.1	166	0.96	1900
54	1861	1900	32.1	166	0.96	1900
55	1861	1900	32.1	166	0.96	1900
56	1861	1900	32.1	166	0.96	1900
57	1861	1900	32.1	166	0.96	1900
58	1861	1900	32.1	166	0.96	1900
59	1861	1900	32.1	166	0.96	1900
60	1861	1900	32.1	166	0.96	1900
61	1861	1900	32.1	166	0.96	1900
62	1861	1900	32.1	166	0.96	1900
63	1861	1900	32.1	166	0.96	1900
64	1861	1900	32.1	166	0.96	1900
65	1861	1900	32.1	166	0.96	1900
66	1861	1900	32.1	166	0.96	1900
67	1861	1900	32.1	165	0.96	1900
68	1861	1900	32.1	165	0.96	1900
69	1861	1900	32.1	165	0.96	1900
70	1861	1900	32.1	165	0.96	1900
71	1861	1900	32.1	165	0.96	1900
72	1861	1900	32.1	165	0.96	1900
73	1861	1900	32.1	165	0.96	1900
74	1861	1900	32.1	165	0.96	1900
75	1861	1900	32.1	165	0.96	1900
76	1372	1400	23.7	89	0.95	1400
77	1372	1400	23.7	89	0.95	1400
78	1372	1400	23.7	89	0.95	1400
79	1372	1400	23.7	89	0.95	1400
80	1372	1400	23.7	89	0.95	1400
81	1372	1400	23.7	89	0.95	1400
82	1372	1400	23.7	89	0.96	1400
83	1372	1400	23.7	89	0.96	1400
84	1372	1400	23.7	89	0.96	1400
85	1372	1400	23.7	89	0.96	1400
86	1372	1400	23.7	89	0.96	1400
87	1372	1400	23.7	89	0.96	1400
88	1372	1400	23.7	89	0.96	1400
89	1372	1400	23.7	89	0.96	1400
90	1372	1400	23.7	89	0.96	1400
91	1372	1400	23.7	89	0.96	1400
92	1372	1400	23.7	89	0.96	1400
93	1372	1400	23.7	89	0.96	1400
94	1372	1400	23.7	89	0.96	1400
95	1372	1400	23.7	89	0.96	1400
96	1372	1400	23.7	89	0.96	1400
97	1372	1400	23.7	89	0.96	1400
98	1372	1400	23.7	89	0.96	1400
99	1372	1400	23.7	89	0.96	1400
100	1372	1400	23.7	89	0.96	1400

APPENDIX I
PROCESS CONDITIONS

OBS	Wire Speed	Machine Speed	Production Rate tons/hr	Headbox liquid head	Jet to Wire Speed Ratio	Dryer Speed
101	1372	1400	23.7	89	0.96	1400
102	1372	1400	23.7	89	0.96	1400
103	1372	1400	23.7	89	0.96	1400
104	1372	1400	23.7	89	0.96	1400
105	1372	1400	23.7	89	0.96	1400
106	1372	1400	23.7	88	0.95	1400
107	1372	1400	23.7	88	0.95	1400
108	1372	1400	23.7	88	0.95	1400
109	1372	1400	23.7	88	0.95	1400
110	1372	1400	23.7	88	0.95	1400
111	1372	1400	23.7	88	0.95	1400
112	1372	1400	23.7	88	0.95	1400
113	1372	1400	23.7	88	0.95	1400
114	1372	1400	23.7	88	0.95	1400

APPENDIX I
PROCESS CONDITIONS

OBS	Lump Breaker Load pli	1st Nip Load pli	2nd Nip Load pli	3rd Nip Load pli	Calender Stack Loading
1	145	380	550	600	ON
2	145	380	550	600	ON
3	145	380	550	600	ON
4	145	380	550	600	ON
5	145	380	550	600	ON
6	145	380	550	600	ON
7	145	380	550	600	ON
8	145	380	550	600	ON
9	145	380	550	600	ON
10	145	380	550	600	ON
11	145	380	550	600	ON
12	145	380	550	600	ON
13	145	380	550	600	ON
14	145	380	550	600	ON
15	145	380	550	600	ON
16	145	380	550	600	ON
17	145	380	550	600	ON
18	145	380	550	600	ON
19	145	380	550	600	ON
20	145	380	550	600	ON
21	145	380	550	600	ON
22	145	380	550	600	ON
23	145	380	550	600	ON
24	145	380	550	600	ON
25	145	380	550	600	OFF
26	145	380	550	600	OFF
27	145	380	550	600	OFF
28	145	380	550	600	OFF
29	145	380	550	600	OFF
30	145	380	550	600	OFF
31	145	380	550	600	OFF
32	145	380	550	600	OFF
33	145	380	550	600	OFF
34	140	380	540	650	ON
35	140	380	540	650	ON
36	140	380	540	650	ON
37	140	380	540	650	ON
38	140	380	540	650	ON
39	140	380	540	650	ON
40	140	380	540	650	ON
41	140	380	540	650	ON
42	140	380	540	650	ON
43	140	380	540	650	ON
44	140	380	540	650	ON
45	140	380	540	650	ON
46	140	380	540	650	ON
47	140	380	540	650	ON
48	140	380	540	650	ON
49	140	380	540	650	ON
50	140	380	540	650	ON

APPENDIX I
PROCESS CONDITIONS

OBS	Lump Breaker Load pli	1st Nip Load pli	2nd Nip Load pli	3rd Nip Load pli	Calender Stack Loading
51	140	380	540	650	ON
52	140	380	540	650	ON
53	140	380	540	650	ON
54	140	380	540	650	ON
55	140	380	540	650	ON
56	140	380	540	650	ON
57	140	380	540	650	ON
58	140	380	540	650	ON
59	140	380	540	650	ON
60	140	380	540	650	ON
61	140	380	540	650	ON
62	140	380	540	650	ON
63	140	380	540	650	ON
64	140	380	540	650	ON
65	140	380	540	650	ON
66	140	380	540	650	ON
67	140	380	540	650	ON
68	140	380	540	650	ON
69	140	380	540	650	ON
70	140	380	540	650	ON
71	140	380	540	650	ON
72	140	380	540	650	ON
73	140	380	540	650	ON
74	140	380	540	650	ON
75	140	380	540	650	ON
76	145	380	540	480	ON
77	145	380	540	480	ON
78	145	380	540	480	ON
79	145	380	540	480	ON
80	145	380	540	480	ON
81	145	380	540	480	ON
82	145	380	540	480	ON
83	145	380	540	480	ON
84	145	380	540	480	ON
85	145	380	540	480	ON
86	145	380	540	480	ON
87	145	380	540	480	ON
88	145	380	540	480	ON
89	145	380	540	480	ON
90	145	380	540	480	ON
91	145	380	540	480	ON
92	145	380	540	480	ON
93	145	380	540	480	ON
94	145	380	540	480	ON
95	145	380	540	480	ON
96	145	380	540	480	ON
97	145	380	540	480	ON
98	145	380	540	480	ON
99	145	380	540	480	ON
100	145	380	540	480	ON

APPENDIX I
PROCESS CONDITIONS

OBS	Lump Breaker Load pli	1st Nip Load pli	2nd Nip Load pli	3rd Nip Load pli	Calender Stack Loading
101	145	380	540	480	ON
102	145	380	540	480	ON
103	145	380	540	480	ON
104	145	380	540	480	ON
105	145	380	540	480	ON
106	145	380	540	480	ON
107	145	380	540	480	ON
108	145	380	540	480	ON
109	145	380	540	480	ON
110	145	380	540	480	ON
111	145	380	540	480	ON
112	145	380	540	480	ON
113	145	380	540	480	ON
114	145	380	540	480	ON

APPENDIX II
MEASURED AND PREDICTED MACHINE PAPER PROPERTIES

OBS	DATE	REEL	ROLL	SET	RLPLT	Measured Basis Weight	Predicted Basis Weight	Measured Caliper
1	4-3-90	1	1	1	1	26.08	26.0	7.680
2	4-3-90	1	2	1	1	25.44	26.0	7.608
3	4-3-90	1	3	1	1	25.84	26.0	7.644
4	4-3-90	2	1	1	2	26.08	26.5	7.790
5	4-3-90	2	2	1	2	25.84	26.5	7.522
6	4-3-90	2	3	1	2	26.00	26.5	7.572
7	4-3-90	3	1	1	3	25.92	28.0	7.588
8	4-3-90	3	2	1	3	25.80	28.0	7.416
9	4-3-90	3	3	1	3	25.84	28.0	7.552
10	4-3-90	4	1	1	4	25.64	25.8	8.244
11	4-3-90	4	2	1	4	25.80	25.8	8.314
12	4-3-90	4	3	1	4	25.28	25.8	8.286
13	4-3-90	4	1	2	4	25.60	25.8	8.372
14	4-3-90	4	2	2	4	25.12	25.8	8.396
15	4-3-90	4	3	2	4	25.36	25.8	8.386
16	4-3-90	5	1	1	5	25.88	25.3	7.752
17	4-3-90	5	2	1	5	25.72	25.3	7.550
18	4-3-90	5	3	1	5	25.92	25.3	7.696
19	4-3-90	6	1	1	6	25.80	24.9	8.436
20	4-3-90	6	2	1	6	25.64	24.9	8.346
21	4-3-90	6	3	1	6	25.80	24.9	8.436
22	4-3-90	6	1	2	6	26.00	24.9	8.276
23	4-3-90	6	2	2	6	25.52	24.9	8.228
24	4-3-90	6	3	2	6	25.80	24.9	8.334
25	4-3-90	7	1	1	7	26.48	26.3	10.016
26	4-3-90	7	2	1	7	26.00	26.3	9.640
27	4-3-90	7	3	1	7	26.16	26.3	9.754
28	4-3-90	8	1	1	8	26.00	24.1	9.537
29	4-3-90	8	2	1	8	25.32	24.1	9.450
30	4-3-90	8	3	1	8	25.90	24.1	9.515
31	4-3-90	8	1	2	8	26.24	24.1	9.804
32	4-3-90	8	3	3	8	25.84	24.1	9.592
33	4-3-90	8	3	2	8	26.00	24.1	9.542
34	4-4-90	1	1	1	9	26.12	26.0	8.712
35	4-4-90	1	2	1	9	25.60	26.0	8.310
36	4-4-90	1	3	1	9	25.88	26.0	8.484
37	4-4-90	2	1	1	10	26.36	26.5	8.816
38	4-4-90	2	2	1	10	25.96	26.5	8.348
39	4-4-90	2	3	1	10	26.04	26.5	8.388
40	4-4-90	3	1	1	11	26.00	27.2	8.478
41	4-4-90	3	2	1	11	25.76	27.2	8.306
42	4-4-90	3	3	1	11	25.60	27.2	8.502
43	4-4-90	4	1	1	12	25.60	26.3	8.512
44	4-4-90	4	2	1	12	25.36	26.3	8.266
45	4-4-90	4	3	1	12	25.36	26.3	8.460
46	4-4-90	4	1	2	12	25.64	26.3	8.776
47	4-4-90	4	2	2	12	25.20	26.3	8.428
48	4-4-90	4	3	2	12	25.32	26.3	8.476
49	4-4-90	4	1	3	12	25.32	26.3	8.474
50	4-4-90	4	2	3	12	24.88	26.3	8.290

APPENDIX II
MEASURED AND PREDICTED MACHINE PAPER PROPERTIES

OBS	DATE	REEL	ROLL	SET	RLPLT	Measured Basis Weight	Predicted Basis Weight	Measured Caliper
51	4-4-90	4	3	3	12	25.16	26.3	8.334
52	4-4-90	5	1	1	13	25.28	26.7	8.736
53	4-4-90	5	2	1	13	25.08	26.7	8.464
54	4-4-90	5	3	1	13	25.40	26.7	8.550
55	4-4-90	6	1	1	14	25.60	24.8	8.712
56	4-4-90	6	2	1	14	25.16	24.8	8.426
57	4-4-90	6	3	1	14	25.44	24.8	8.520
58	4-4-90	6	1	2	14	25.64	24.8	8.622
59	4-4-90	6	2	2	14	25.32	24.8	8.578
60	4-4-90	6	3	2	14	25.52	24.8	8.550
61	4-4-90	6	1	3	14	25.40	24.8	8.278
62	4-4-90	6	2	3	14	25.08	24.8	8.320
63	4-4-90	6	3	3	14	25.28	24.8	8.326
64	4-4-90	7	1	1	15	25.40	24.8	8.342
65	4-4-90	7	2	1	15	25.04	24.8	8.158
66	4-4-90	7	3	1	15	25.48	24.8	8.232
67	4-4-90	8	1	1	16	25.52	26.2	8.276
68	4-4-90	8	2	1	16	25.20	26.2	8.112
69	4-4-90	8	3	1	16	25.32	26.2	8.178
70	4-4-90	8	1	2	16	25.20	26.2	8.332
71	4-4-90	8	2	2	16	24.84	26.2	8.076
72	4-4-90	8	3	2	16	25.12	26.2	8.196
73	4-4-90	8	1	3	16	25.36	26.2	8.562
74	4-4-90	8	2	3	16	25.00	26.2	8.428
75	4-4-90	8	3	3	16	25.16	26.2	8.450
76	4-5-90	1	1	1	17	25.00	25.1	8.260
77	4-5-90	1	2	1	17	24.88	25.1	8.010
78	4-5-90	1	3	1	17	25.12	25.1	8.176
79	4-5-90	2	1	1	18	24.96	25.5	8.324
80	4-5-90	2	2	1	18	24.92	25.5	8.040
81	4-5-90	2	3	1	18	25.32	25.5	7.996
82	4-5-90	3	1	1	19	24.92	24.9	8.340
83	4-5-90	3	2	1	19	25.00	24.9	8.008
84	4-5-90	3	3	1	19	25.24	24.9	8.190
85	4-5-90	4	1	1	20	25.28	24.9	8.296
86	4-5-90	4	2	1	20	24.72	24.9	7.960
87	4-5-90	4	3	1	20	25.20	24.9	8.104
88	4-5-90	4	1	2	20	25.12	24.9	8.214
89	4-5-90	4	2	2	20	24.92	24.9	7.958
90	4-5-90	4	3	2	20	25.08	24.9	8.060
91	4-5-90	4	1	3	20	25.16	24.9	8.266
92	4-5-90	4	2	3	20	24.96	24.9	8.062
93	4-5-90	4	3	3	20	25.28	24.9	8.130
94	4-5-90	5	1	1	21	25.36	25.4	8.230
95	4-5-90	5	2	1	21	24.88	25.4	7.986
96	4-5-90	5	3	1	21	25.20	25.4	8.110
97	4-5-90	6	1	1	22	25.20	25.1	8.262
98	4-5-90	6	2	1	22	24.80	25.1	7.948
99	4-5-90	6	3	1	22	24.96	25.1	8.044

APPENDIX II
MEASURED AND PREDICTED MACHINE PAPER PROPERTIES

OBS	DATE	REEL	ROLL	SET	RLPLT	Measured Basis Weight	Predicted Basis Weight	Measured Caliper
100	4-5-90	6	1	3	22	25.56	25.1	8.256
101	4-5-90	6	2	3	22	25.04	25.1	8.048
102	4-5-90	6	3	3	22	25.12	25.1	8.012
103	4-5-90	7	1	1	23	25.32	25.1	8.232
104	4-5-90	7	2	1	23	25.00	25.1	7.992
105	4-5-90	7	3	1	23	25.04	25.1	8.080
106	4-5-90	8	1	1	24	25.80	25.6	8.312
107	4-5-90	8	2	1	24	24.96	25.6	7.998
108	4-5-90	8	3	1	24	25.04	25.6	7.988
109	4-5-90	8	1	2	24	25.32	25.6	8.230
110	4-5-90	8	2	2	24	24.96	25.6	8.004
111	4-5-90	8	3	2	24	25.04	25.6	8.090
112	4-5-90	8	1	3	24	25.28	25.6	8.168
113	4-5-90	8	2	3	24	24.88	25.6	7.976
114	4-5-90	8	3	3	24	24.92	25.6	7.978

APPENDIX II
MEASURED AND PREDICTED MACHINE PAPER PROPERTIES

OBS	Predicted Caliper	Measured Density	Predicted Density	Measured MD Tensile	Predicted MD Tensile	Measured CD Tensile
1	8.04	0.65302	0.622	5.74648	5.69	2.63129
2	8.04	0.64302	0.622	5.79917	5.69	2.60273
3	8.04	0.65006	0.622	5.72709	5.69	2.47410
4	8.30	0.64380	0.613	5.62572	5.53	2.55289
5	8.30	0.66060	0.613	5.86809	5.53	2.67428
6	8.30	0.66030	0.613	6.00376	5.53	2.51136
7	8.65	0.65688	0.623	5.81103	5.85	2.60647
8	8.65	0.66900	0.623	5.89775	5.85	2.73740
9	8.65	0.65798	0.623	5.89343	5.85	2.56740
10	8.00	0.59808	0.627	5.89004	5.90	2.61096
11	8.00	0.59675	0.627	5.55024	5.90	2.67190
12	8.00	0.58669	0.627	6.04843	5.90	2.51459
13	8.00	0.58802	0.627	5.97940	5.90	2.58060
14	8.00	0.57534	0.627	5.90435	5.90	2.79010
15	8.00	0.58153	0.627	5.98421	5.90	2.55714
16	7.80	0.64199	0.623	5.52276	6.09	2.51721
17	7.80	0.65509	0.623	5.84398	6.09	2.66613
18	7.80	0.64766	0.623	5.89457	6.09	2.44629
19	7.70	0.58812	0.625	5.64636	6.20	2.53295
20	7.70	0.59077	0.625	5.61768	6.20	2.65119
21	7.70	0.58812	0.625	5.76603	6.20	2.39188
22	7.70	0.60413	0.625	5.68622	6.20	2.53964
23	7.70	0.59644	0.625	5.75490	6.20	2.61521
24	7.70	0.59531	0.625	5.81126	6.20	2.43314
25	9.49	0.50840	0.530	5.65470	5.25	2.51639
26	9.49	0.51865	0.530	5.94355	5.25	2.61688
27	9.49	0.51574	0.530	6.00801	5.25	2.45363
28	8.80	0.52427	0.530	5.63796	5.22	2.52022
29	8.80	0.51524	0.530	5.83532	5.22	2.64439
30	8.80	0.52344	0.530	5.79348	5.22	2.41484
31	8.80	0.51468	0.530	5.60299	5.22	2.56743
32	8.80	0.51804	0.530	5.79278	5.22	2.65969
33	8.80	0.52398	0.530	6.05497	5.22	2.48069
34	8.40	0.57655	0.600	5.99103	6.10	2.44982
35	8.40	0.59240	0.600	5.90996	6.10	2.58118
36	8.40	0.58660	0.600	5.74283	6.10	2.30985
37	8.44	0.57498	0.605	5.69987	6.30	2.42835
38	8.44	0.59800	0.605	5.74205	6.30	2.47112
39	8.44	0.59698	0.605	5.60472	6.30	2.32952
40	8.20	0.58974	0.640	5.96662	6.30	2.49082
41	8.20	0.59639	0.640	6.00702	6.30	2.66455
42	8.20	0.57903	0.640	6.11843	6.30	2.40213
43	8.00	0.57835	0.635	6.40121	6.37	2.62319
44	8.00	0.58997	0.635	6.59998	6.37	2.77408
45	8.00	0.57645	0.635	6.36010	6.37	2.56435
46	8.00	0.56182	0.635	5.91629	6.37	2.68929
47	8.00	0.57498	0.635	6.36550	6.37	2.74190
48	8.00	0.57445	0.635	6.50191	6.37	2.53965
49	8.00	0.57459	0.635	6.28116	6.37	2.65306
50	8.00	0.57713	0.635	6.58131	6.37	2.68440

APPENDIX II
MEASURED AND PREDICTED MACHINE PAPER PROPERTIES

OBS	Predicted Caliper	Measured Density	Predicted Density	Measured MD Tensile	Predicted MD Tensile	Measured CD Tensile
51	8.00	0.58055	0.635	6.74506	6.37	2.51044
52	8.13	0.55647	0.633	6.25752	6.26	2.67824
53	8.13	0.56981	0.633	6.43534	6.26	2.83247
54	8.13	0.57128	0.633	6.39430	6.26	2.57039
55	7.63	0.56507	0.625	6.32934	6.10	2.64648
56	7.63	0.57421	0.625	6.36268	6.10	2.68476
57	7.63	0.57419	0.625	6.28345	6.10	2.59295
58	7.63	0.57186	0.625	6.02343	6.10	2.65847
59	7.63	0.56762	0.625	6.30991	6.10	2.78872
60	7.63	0.57398	0.625	6.54111	6.10	2.53437
61	7.63	0.59005	0.625	6.17324	6.10	2.66112
62	7.63	0.57967	0.625	6.50170	6.10	2.78157
63	7.63	0.58388	0.625	6.40873	6.10	2.57247
64	7.63	0.58552	0.625	6.37241	6.10	2.71628
65	7.63	0.59024	0.625	6.41567	6.10	2.84196
66	7.63	0.59521	0.625	6.28062	6.10	2.50949
67	8.03	0.59298	0.628	6.39577	6.04	2.76815
68	8.03	0.59738	0.628	6.60298	6.04	2.85992
69	8.03	0.59538	0.628	6.53196	6.04	2.69192
70	8.03	0.58161	0.628	6.48845	6.04	2.68878
71	8.03	0.59147	0.628	6.67924	6.04	2.82685
72	8.03	0.58938	0.628	6.43048	6.04	2.70986
73	8.03	0.56958	0.628	6.35837	6.04	2.71090
74	8.03	0.57042	0.628	6.43413	6.04	2.81447
75	8.03	0.57258	0.628	6.49208	6.04	2.59913
76	7.80	0.58202	0.618	5.94879	6.30	2.45496
77	7.80	0.59731	0.618	6.00835	6.30	2.52017
78	7.80	0.59082	0.618	5.74446	6.30	2.18388
79	8.00	0.57662	0.612	5.94557	6.21	2.24946
80	8.00	0.59603	0.612	6.02748	6.21	2.54357
81	8.00	0.60893	0.612	5.69590	6.21	2.26183
82	7.92	0.57459	0.612	5.99386	6.00	2.49513
83	7.92	0.60034	0.612	5.91616	6.00	2.59016
84	7.92	0.59263	0.612	5.70120	6.00	2.31364
85	7.87	0.58599	0.608	5.74775	5.93	2.37524
86	7.87	0.59719	0.608	5.91732	5.93	2.50718
87	7.87	0.59797	0.608	5.36303	5.93	2.27740
88	7.87	0.58809	0.608	5.77810	5.93	2.43041
89	7.87	0.60218	0.608	5.68854	5.93	2.56618
90	7.87	0.59837	0.608	5.63373	5.93	2.30754
91	7.87	0.58532	0.608	5.77225	5.93	2.39776
92	7.87	0.59536	0.608	5.97459	5.93	2.56851
93	7.87	0.59795	0.608	5.62577	5.93	2.31157
94	8.02	0.59256	0.610	5.86448	5.87	2.38217
95	8.02	0.59910	0.610	5.88368	5.87	2.56207
96	8.02	0.59753	0.610	5.59572	5.87	2.25112
97	7.94	0.58654	0.610	5.68180	5.92	2.40673
98	7.94	0.60003	0.610	5.88672	5.92	2.59482
99	7.94	0.59669	0.610	5.55207	5.92	2.30252
100	7.94	0.59535	0.610	5.60478	5.92	2.43180

APPENDIX II
MEASURED AND PREDICTED MACHINE PAPER PROPERTIES

OBS	Predicted Caliper	Measured Density	Predicted Density	Measured MD Tensile	Predicted MD Tensile	Measured CD Tensile
101	7.94	0.59831	0.610	5.73578	5.92	2.58675
102	7.94	0.60292	0.610	5.71126	5.92	2.30707
103	7.84	0.59148	0.616	5.57050	6.01	2.36831
104	7.84	0.60154	0.616	5.92625	6.01	2.54348
105	7.84	0.59594	0.616	5.53360	6.01	2.27763
106	8.06	0.59689	0.610	5.52004	5.90	2.33828
107	8.06	0.60013	0.610	5.84430	5.90	2.53305
108	8.06	0.60280	0.610	5.07489	5.90	2.21321
109	8.06	0.59162	0.610	5.60966	5.90	2.34924
110	8.06	0.59968	0.610	5.79286	5.90	2.54917
111	8.06	0.59520	0.610	5.22887	5.90	2.25338
112	8.06	0.59517	0.610	5.76063	5.90	2.38638
113	8.06	0.59985	0.610	5.69739	5.90	2.58074
114	8.06	0.60067	0.610	5.71012	5.90	2.27069

APPENDIX II
MEASURED AND PREDICTED MACHINE PAPER PROPERTIES

OBS	Predicted CD Tensile	Measured Burst Factor	Predicted Burst Factor	Measured MD Stretch	Predicted MD Stretch	Measured CD Stretch
1	2.38	27.8350	29.0	1.617	1.80	2.911
2	2.38	28.0267	29.0	1.559	1.80	2.137
3	2.38	27.9823	29.0	1.461	1.80	2.865
4	2.32	27.2838	28.1	1.577	1.80	2.914
5	2.32	29.2062	28.1	1.657	1.80	2.346
6	2.32	29.0264	28.1	1.630	1.80	2.885
7	2.45	29.3933	29.9	1.679	1.82	2.920
8	2.45	27.9142	29.9	1.615	1.82	2.342
9	2.45	29.5956	29.9	1.530	1.82	2.934
10	2.56	28.7051	27.9	1.581	1.83	2.782
11	2.56	29.1957	27.9	1.476	1.83	2.243
12	2.56	30.3080	27.9	1.764	1.83	2.512
13	2.56	29.4800	27.9	1.615	1.83	2.824
14	2.56	29.9288	27.9	1.554	1.83	2.388
15	2.56	29.1921	27.9	1.523	1.83	2.761
16	2.55	29.9942	30.9	1.544	1.82	2.854
17	2.55	29.3983	30.9	1.677	1.82	2.266
18	2.55	28.4505	30.9	1.616	1.82	2.603
19	2.58	27.8028	31.3	1.466	1.82	2.804
20	2.58	29.8264	31.3	1.530	1.82	2.324
21	2.58	28.3043	31.3	1.550	1.82	2.594
22	2.58	28.0313	31.3	1.627	1.82	2.758
23	2.58	29.6851	31.3	1.632	1.82	2.220
24	2.58	28.0814	31.3	1.600	1.82	2.595
25	2.20	28.7174	25.3	1.532	1.63	2.836
26	2.20	29.7452	25.3	1.721	1.63	2.491
27	2.20	28.2445	25.3	1.679	1.63	2.918
28	2.19	28.2894	25.0	1.562	1.60	2.830
29	2.19	30.3737	25.0	1.493	1.60	2.390
30	2.19	29.6935	25.0	1.587	1.60	3.214
31	2.19	26.5149	25.0	1.501	1.60	2.885
32	2.19	29.5956	25.0	1.637	1.60	2.390
33	2.19	27.8101	25.0	1.710	1.60	2.930
34	2.56	27.4622	30.7	1.617	1.76	2.887
35	2.56	27.1216	30.7	1.463	1.76	2.482
36	2.56	28.7167	30.7	1.485	1.76	2.672
37	2.60	28.3028	32.0	1.595	1.78	2.840
38	2.60	27.0777	32.0	1.538	1.78	2.399
39	2.60	28.4298	32.0	1.464	1.78	2.866
40	2.60	33.4495	32.0	1.580	1.67	2.828
41	2.60	28.2924	32.0	1.591	1.67	2.509
42	2.60	29.9854	32.0	1.556	1.67	2.714
43	2.67	31.5015	32.8	1.770	1.84	2.847
44	2.67	31.1194	32.8	1.745	1.84	2.571
45	2.67	30.7793	32.8	1.636	1.84	2.819
46	2.67	29.3779	32.8	1.653	1.84	2.715
47	2.67	30.9177	32.8	1.752	1.84	2.296
48	2.67	30.4305	32.8	1.723	1.84	2.473
49	2.67	29.1815	32.8	1.532	1.84	2.841
50	2.67	30.5642	32.8	1.563	1.84	2.110

APPENDIX II
MEASURED AND PREDICTED MACHINE PAPER PROPERTIES

OBS	Predicted CD Tensile	Measured Burst Factor	Predicted Burst Factor	Measured MD Stretch	Predicted MD Stretch	Measured CD Stretch
51	2.67	29.8241	32.8	1.701	1.84	2.469
52	2.62	30.9904	32.2	1.602	1.84	2.853
53	2.62	30.4351	32.2	1.690	1.84	2.499
54	2.62	30.7874	32.2	1.648	1.84	2.790
55	2.55	30.4346	31.1	1.648	1.81	3.032
56	2.55	31.0811	31.1	1.673	1.81	2.139
57	2.55	30.2304	31.1	1.558	1.81	2.800
58	2.55	32.1812	31.1	1.510	1.81	2.859
59	2.55	30.5440	31.1	1.604	1.81	2.399
60	2.55	29.3471	31.1	1.676	1.81	2.680
61	2.55	31.1270	31.1	1.510	1.81	2.675
62	2.55	31.0083	31.1	1.597	1.81	2.483
63	2.55	31.2179	31.1	1.526	1.81	2.446
64	2.55	30.2781	31.1	1.633	1.81	2.861
65	2.55	30.3689	31.1	1.672	1.81	2.356
66	2.55	28.2648	31.1	1.601	1.81	2.420
67	2.50	32.2198	30.9	1.699	1.82	3.023
68	2.50	30.4613	30.9	1.789	1.82	2.562
69	2.50	31.1118	30.9	1.799	1.82	3.060
70	2.50	30.1190	30.9	1.639	1.82	2.663
71	2.50	30.7292	30.9	1.741	1.82	2.344
72	2.50	33.2479	30.9	1.598	1.82	2.860
73	2.50	29.7590	30.9	1.630	1.82	2.765
74	2.50	28.9800	30.9	1.668	1.82	2.258
75	2.50	30.6240	30.9	1.643	1.82	2.540
76	2.60	28.3475	32.0	1.718	1.80	3.003
77	2.60	29.5820	32.0	1.794	1.80	2.527
78	2.60	28.2693	32.0	1.715	1.80	2.573
79	2.61	27.0107	31.4	1.740	1.80	2.855
80	2.61	28.4962	31.4	1.810	1.80	2.557
81	2.61	27.5351	31.4	1.749	1.80	2.879
82	2.51	27.4002	30.3	1.717	1.80	3.029
83	2.51	29.2100	30.3	1.747	1.80	2.513
84	2.51	28.1919	30.3	1.745	1.80	2.790
85	2.49	26.7825	29.9	1.715	1.78	2.716
86	2.49	28.4360	29.9	1.733	1.78	2.308
87	2.49	27.7232	29.9	1.615	1.78	2.892
88	2.49	26.2664	29.9	1.683	1.78	2.760
89	2.49	29.4768	29.9	1.684	1.78	2.400
90	2.49	26.3656	29.9	1.751	1.78	2.823
91	2.49	27.5388	29.9	1.541	1.78	2.555
92	2.49	29.1992	29.9	1.774	1.78	2.450
93	2.49	29.3414	29.9	1.622	1.78	2.852
94	2.46	26.1312	29.7	1.711	1.79	2.652
95	2.46	27.7331	29.7	1.719	1.79	2.468
96	2.46	25.6126	29.7	1.674	1.79	2.759
97	2.48	27.7803	29.9	1.621	1.79	2.723
98	2.48	29.5615	29.9	1.746	1.79	2.459
99	2.48	27.1259	29.90	1.607	1.79	2.658
100	2.48	28.1763	29.90	1.667	1.79	2.739

APPENDIX II
MEASURED AND PREDICTED MACHINE PAPER PROPERTIES

OBS	Predicted CD Tensile	Measured Burst Factor	Predicted Burst Factor	Measured MD Stretch	Predicted MD Stretch	Measured CD Stretch
101	2.48	28.7041	29.90	1.705	1.79	2.431
102	2.48	28.0976	29.90	1.780	1.79	2.622
103	2.52	28.1028	30.60	1.631	1.80	2.701
104	2.52	28.3475	30.60	1.769	1.80	2.453
105	2.52	27.7281	30.60	1.693	1.80	2.758
106	2.47	25.6298	29.95	1.592	1.79	3.028
107	2.47	30.3511	29.95	1.694	1.79	2.484
108	2.47	26.4077	29.95	1.440	1.79	2.637
109	2.47	27.9325	29.95	1.569	1.79	2.596
110	2.47	28.7385	29.95	1.682	1.79	2.314
111	2.47	26.1781	29.95	1.550	1.79	2.612
112	2.47	27.4649	29.95	1.692	1.79	2.527
113	2.47	27.6176	29.95	1.647	1.79	2.386
114	2.47	27.6886	29.95	1.781	1.79	2.459

APPENDIX II
MEASURED AND PREDICTED MACHINE PAPER PROPERTIES

OBS	Measured Moisture	Measured Gurley Porosity	Predicted Gurley Porosity	Measured MD Stiffness	Predicted MD Stiffness	Measured CD Stiffness
1	6.840	15.00	20.8	4.25868	4.69	1.92915
2	6.780	12.56	20.8	4.38979	4.69	1.98512
3	6.690	13.70	20.8	4.49597	4.69	1.81209
4	6.700	19.96	20.7	4.24062	4.60	1.77987
5	7.075	18.48	20.7	4.46855	4.60	1.99878
6	6.790	20.66	20.7	4.62134	4.60	1.81854
7	6.991	19.20	20.6	4.28629	4.70	1.82725
8	7.160	16.88	20.6	4.56084	4.70	2.08786
9	7.012	20.12	20.6	4.60207	4.70	1.84317
10	7.073	20.32	20.6	4.19762	4.72	1.79816
11	6.899	16.52	20.6	4.04696	4.72	1.93678
12	6.736	19.16	20.6	4.03330	4.72	1.78248
13	6.553	18.08	20.6	4.18543	4.72	1.76011
14	6.441	18.24	20.6	4.15403	4.72	1.90896
15	6.438	18.16	20.6	4.25628	4.72	1.75473
16	6.554	16.69	21.0	4.26228	4.68	1.74737
17	6.617	15.81	21.0	4.46233	4.68	2.38360
18	6.674	16.15	21.0	4.53363	4.68	1.75832
19	6.691	17.60	21.1	4.11418	4.70	1.73869
20	6.642	13.69	21.1	3.94182	4.70	1.88210
21	6.587	14.68	21.1	3.94168	4.70	1.67501
22	6.586	14.79	21.1	3.96941	4.70	1.76491
23	6.680	13.17	21.1	4.05124	4.70	1.81901
24	6.454	15.83	21.1	4.11068	4.70	1.67919
25	6.746	14.72	17.8	3.41290	3.89	1.37073
26	6.867	11.75	17.8	3.43598	3.89	1.52859
27	6.789	13.21	17.8	3.50945	3.89	1.37199
28	6.720	14.25	17.4	3.43256	3.80	1.45887
29	6.823	12.02	17.4	3.58781	3.80	1.56940
30	6.673	13.53	17.4	3.56902	3.80	1.30140
31	6.747	14.29	17.4	3.54427	3.80	1.50441
32	6.951	10.98	17.4	3.52477	3.80	1.63053
33	6.924	14.22	17.4	3.61949	3.80	1.44523
34	6.906	23.06	20.9	3.98696	4.40	1.56887
35	6.996	19.10	20.9	4.35413	4.40	1.75851
36	6.900	22.10	20.9	4.18067	4.40	1.50844
37	6.945	19.41	22.1	3.90830	4.50	1.57119
38	7.072	17.46	22.1	4.18361	4.50	1.74480
39	7.018	20.41	22.1	4.11583	4.50	1.58732
40	7.081	23.00	23.9	4.13390	4.30	1.49427
41	7.055	20.68	23.9	4.22196	4.30	1.67012
42	6.974	21.40	23.9	4.22061	4.30	1.58843
43	7.070	21.94	23.4	4.49661	4.80	1.84859
44	7.131	23.10	23.4	4.66276	4.80	2.10351
45	6.944	25.68	23.4	4.52931	4.80	1.79806
46	6.559	24.72	23.4	4.19871	4.80	1.97383
47	6.584	22.87	23.4	4.48681	4.80	1.87992
48	6.439	24.17	23.4	4.58527	4.80	1.74364
49	6.688	22.21	23.4	4.35733	4.80	1.76700
50	6.825	19.72	23.4	4.52951	4.80	1.88907

APPENDIX II
MEASURED AND PREDICTED MACHINE PAPER PROPERTIES

OBS	Measured Moisture	Measured Gurley Porosity	Predicted Gurley Porosity	Measured MD Stiffness	Predicted MD Stiffness	Measured CD Stiffness
51	6.761	24.27	23.4	4.50478	4.80	1.79261
52	6.867	20.33	22.8	4.39533	4.80	1.80353
53	6.910	18.59	22.8	4.49335	4.80	2.04201
54	6.918	20.23	22.8	4.51512	4.80	1.77579
55	6.864	19.71	22.1	4.44787	4.68	1.77883
56	6.871	16.86	22.1	4.44591	4.68	2.00449
57	6.836	19.24	22.1	4.52623	4.68	1.80344
58	6.758	20.56	22.1	4.48136	4.68	1.93274
59	6.771	17.55	22.1	4.56887	4.68	2.05451
60	6.749	18.94	22.1	4.68604	4.68	1.89279
61	6.664	19.21	22.1	4.78456	4.68	2.02045
62	6.733	16.98	22.1	4.78051	4.68	2.08356
63	6.801	19.19	22.1	4.81268	4.68	1.98414
64	6.532	17.41	22.1	4.60096	4.68	1.91618
65	6.590	16.18	22.1	4.66548	4.68	2.09743
66	6.489	16.62	22.1	4.63841	4.68	1.85133
67	6.729	22.50	22.0	4.64078	4.72	1.97920
68	6.771	18.09	22.0	4.72018	4.72	2.17186
69	6.749	20.90	22.0	4.70978	4.72	1.93099
70	6.547	21.85	22.0	4.67994	4.72	2.05053
71	6.634	18.37	22.0	4.82222	4.72	2.15603
72	6.589	20.44	22.0	4.85591	4.72	2.05020
73	6.592	19.48	22.0	4.67391	4.72	2.04453
74	8.103	16.63	22.0	4.63809	4.72	2.18894
75	6.677	19.43	22.0	4.76958	4.72	2.00644
76	6.840	22.16	20.7	4.37941	4.60	1.78800
77	6.966	24.90	20.7	4.45761	4.60	1.96343
78	6.955	23.99	20.7	4.32635	4.60	1.66756
79	6.772	21.17	20.1	4.38691	4.60	1.79501
80	6.986	23.31	20.1	4.50331	4.60	1.99839
81	6.909	23.13	20.1	4.45725	4.60	1.70935
82	6.922	19.14	20.2	4.38274	4.58	1.80314
83	7.018	21.17	20.2	4.47579	4.58	2.08008
84	6.950	20.62	20.2	4.31871	4.58	1.74708
85	6.993	23.99	20.1	4.29303	4.55	1.78852
86	7.103	24.45	20.1	4.46955	4.55	2.02112
87	7.093	25.06	20.1	4.13697	4.55	1.71343
88	6.964	22.47	20.1	4.40402	4.55	1.91963
89	7.091	22.81	20.1	4.45674	4.55	2.10511
90	7.053	22.38	20.1	4.34010	4.55	1.84241
91	6.822	20.80	20.1	4.53517	4.55	1.90064
92	7.041	21.28	20.1	4.52341	4.55	2.06168
93	6.967	20.27	20.1	4.41138	4.55	1.81593
94	6.993	24.31	20.3	4.33118	4.56	1.77230
95	7.117	26.44	20.3	4.46351	4.56	2.01122
96	7.047	27.12	20.3	4.26866	4.56	1.69539
97	6.842	26.42	20.4	4.34897	4.55	1.82881
98	6.911	28.78	20.4	4.42582	4.55	2.03110
99	6.871	28.54	20.4	4.32397	4.55	1.73381
100	6.945	26.54	20.4	4.38425	4.55	1.95698

APPENDIX II
MEASURED AND PREDICTED MACHINE PAPER PROPERTIES

OBS	Measured Moisture	Measured Gurley Porosity	Predicted Gurley Porosity	Measured MD Stiffness	Predicted MD Stiffness	Measured CD Stiffness
101	6.986	29.02	20.4	4.47306	4.55	2.12500
102	7.106	28.61	20.4	4.42866	4.55	2.16595
103	6.901	28.80	21.7	4.29378	4.62	1.83052
104	6.983	28.32	21.7	4.47207	4.62	2.01652
105	6.909	27.91	21.7	4.25000	4.62	1.74460
106	7.260	23.05	20.3	4.31627	4.56	1.82435
107	6.862	24.17	20.3	4.45851	4.56	2.02181
108	6.879	22.10	20.3	4.24787	4.56	1.72128
109	6.739	25.54	20.3	4.38984	4.56	1.91276
110	6.831	24.87	20.3	4.53163	4.56	2.13413
111	6.808	24.55	20.3	4.18423	4.56	1.84667
112	6.744	27.16	20.3	4.44148	4.56	1.92644
113	6.867	27.51	20.3	4.49298	4.56	2.16038
114	6.810	26.99	20.3	4.35974	4.56	1.90669

APPENDIX II
MEASURED AND PREDICTED MACHINE PAPER PROPERTIES

OBS	Predicted CD Stiffness	Measured MD STFI	Predicted MD STFI	Measured CD STFI	Predicted CD STFI	Measured MD Ring Crush
1	2.17	20.987	18.8	14.245	12.596	49.08
2	2.17	20.970	18.8	14.418	12.596	48.38
3	2.17	22.470	18.8	14.217	12.596	48.22
4	2.10	21.589	18.9	14.539	12.663	50.94
5	2.10	22.322	18.9	14.589	12.663	51.30
6	2.10	22.066	18.9	14.830	12.663	54.07
7	2.19	22.590	19.7	14.710	13.199	48.86
8	2.19	23.120	19.7	15.140	13.199	49.27
9	2.19	22.438	19.7	14.940	13.199	49.50
10	2.21	23.170	18.5	14.894	12.395	53.87
11	2.21	22.247	18.5	.	12.395	54.09
12	2.21	23.050	18.5	12.752	12.395	52.71
13	2.21	22.326	18.5	15.664	12.395	53.21
14	2.21	23.060	18.5	15.170	12.395	54.40
15	2.21	23.744	18.5	16.770	12.395	53.12
16	2.17	21.278	18.4	14.591	12.328	51.47
17	2.17	21.357	18.4	14.628	12.328	50.72
18	2.17	23.080	18.4	14.451	12.328	50.83
19	2.17	23.720	18.3	14.730	12.261	53.81
20	2.17	22.200	18.3	15.082	12.261	54.65
21	2.17	22.645	18.3	14.502	12.261	53.83
22	2.17	22.529	18.3	14.946	12.261	54.56
23	2.17	22.767	18.3	14.632	12.261	54.04
24	2.17	22.611	18.3	14.752	12.261	54.44
25	1.81	23.396	18.0	15.094	12.060	54.47
26	1.81	22.723	18.0	14.318	12.060	55.95
27	1.81	19.649	18.0	14.690	12.060	54.39
28	1.78	21.616	17.0	14.218	11.390	54.72
29	1.78	21.663	17.0	14.723	11.390	56.06
30	1.78	21.434	17.0	14.492	11.390	50.15
31	1.78	23.072	17.0	14.969	11.390	59.12
32	1.78	23.760	17.0	14.690	11.390	57.64
33	1.78	19.550	17.0	14.460	11.390	55.01
34	2.06	22.138	18.4	14.129	12.328	54.78
35	2.06	22.040	18.4	14.459	12.328	55.57
36	2.06	19.749	18.4	13.660	12.328	52.26
37	2.10	22.345	18.8	14.295	12.596	54.97
38	2.10	22.101	18.8	13.745	12.596	54.16
39	2.10	22.641	18.8	13.937	12.596	54.43
40	2.10	23.610	18.0	14.088	12.060	53.22
41	2.10	22.767	18.0	14.638	12.060	54.37
42	2.10	23.026	18.0	14.197	12.060	55.17
43	2.22	23.764	19.1	14.864	12.797	56.34
44	2.22	24.463	19.1	14.907	12.797	55.96
45	2.22	23.322	19.1	14.890	12.797	55.95
46	2.22	22.326	19.1	15.090	12.797	59.08
47	2.22	23.348	19.1	14.663	12.797	57.98
48	2.22	24.566	19.1	14.581	12.797	57.42
49	2.22	23.071	19.1	14.382	12.797	58.03
50	2.22	24.103	19.1	14.514	12.797	56.77

APPENDIX II
MEASURED AND PREDICTED MACHINE PAPER PROPERTIES

OBS	Predicted CD Stiffness	Measured MD STFI	Predicted MD STFI	Measured CD STFI	Predicted CD STFI	Measured MD Ring Crush
51	2.22	23.041	19.1	14.383	12.797	58.47
52	2.20	22.939	19.2	14.388	12.864	55.46
53	2.20	23.047	19.2	14.682	12.864	56.20
54	2.20	23.299	19.2	14.353	12.864	55.61
55	2.17	23.481	18.2	14.765	12.194	53.50
56	2.17	22.815	18.2	13.978	12.194	54.91
57	2.17	22.744	18.2	11.997	12.194	54.56
58	2.17	22.917	18.2	14.437	12.194	57.68
59	2.17	21.935	18.2	14.237	12.194	59.15
60	2.17	22.320	18.2	14.067	12.194	59.02
61	2.17	23.372	18.2	14.999	12.194	58.59
62	2.17	23.009	18.2	14.638	12.194	58.43
63	2.17	24.287	18.2	14.855	12.194	58.54
64	2.17	22.165	18.2	14.500	12.194	52.20
65	2.17	21.966	18.2	14.459	12.194	58.06
66	2.17	22.686	18.2	14.360	12.194	57.50
67	2.19	23.989	18.9	15.206	12.663	56.27
68	2.19	24.216	18.9	15.346	12.663	57.93
69	2.19	22.930	18.9	14.920	12.663	57.13
70	2.19	24.135	18.9	15.504	12.663	58.94
71	2.19	23.958	18.9	14.399	12.663	58.79
72	2.19	24.882	18.9	14.857	12.663	58.83
73	2.19	23.465	18.9	14.950	12.663	56.46
74	2.19	23.059	18.9	14.977	12.663	58.62
75	2.19	25.228	18.9	15.361	12.663	56.92
76	2.14	22.872	18.3	14.907	12.261	51.41
77	2.14	23.654	18.3	15.300	12.261	52.08
78	2.14	23.614	18.3	14.241	12.261	50.69
79	2.13	23.107	18.4	14.166	12.355	51.92
80	2.13	23.472	18.4	14.400	12.355	52.81
81	2.13	23.670	18.4	13.989	12.355	46.33
82	2.13	23.184	18.3	14.365	12.261	51.32
83	2.13	23.012	18.3	14.504	12.261	53.58
84	2.13	22.252	18.3	14.337	12.261	53.05
85	2.10	23.125	18.1	14.936	12.127	50.75
86	2.10	22.606	18.1	14.980	12.127	50.73
87	2.10	22.362	18.1	13.917	12.127	48.33
88	2.10	23.013	18.1	14.247	12.127	52.44
89	2.10	23.321	18.1	15.018	12.127	52.50
90	2.10	22.653	18.1	14.294	12.127	48.73
91	2.10	23.529	18.1	14.288	12.127	52.96
92	2.10	22.321	18.1	14.756	12.127	52.67
93	2.10	22.553	18.1	14.190	12.127	50.66
94	2.12	22.095	18.4	14.588	12.308	51.55
95	2.12	23.345	18.4	14.694	12.308	49.78
96	2.12	22.716	18.4	14.082	12.308	48.53
97	2.11	23.273	18.2	14.232	12.214	50.55
98	2.11	22.538	18.2	14.940	12.214	50.96
99	2.11	22.487	18.2	14.162	12.214	50.74
100	2.11	22.991	18.2	13.210	12.214	52.30

APPENDIX II
MEASURED AND PREDICTED MACHINE PAPER PROPERTIES

OBS	Predicted CD Stiffness	Measured MD STFI	Predicted MD STFI	Measured CD STFI	Predicted CD STFI	Measured MD Ring Crush
101	2.11	21.988	18.2	15.004	12.214	54.63
102	2.11	22.736	18.2	13.915	12.214	50.16
103	2.14	22.207	18.3	14.025	12.261	50.04
104	2.14	23.336	18.3	14.190	12.261	51.10
105	2.14	22.731	18.3	13.472	12.261	50.00
106	2.11	21.892	18.4	13.733	12.328	50.40
107	2.11	22.317	18.4	14.628	12.328	51.60
108	2.11	21.216	18.4	12.614	12.328	47.07
109	2.11	22.487	18.4	14.411	12.328	53.19
110	2.11	22.200	18.4	14.873	12.328	51.50
111	2.11	22.317	18.4	13.798	12.328	49.42
112	2.11	21.958	18.4	13.841	12.328	52.44
113	2.11	21.578	18.4	14.314	12.328	52.39
114	2.11	21.732	18.4	13.946	12.328	48.58

APPENDIX II
MEASURED AND PREDICTED MACHINE PAPER PROPERTIES

OBS	Measured CD Ring Crush	Predicted CD Ring Crush	Measured Concora	Predicted Concora	TEAMD	TEACD
1	35.29	23.4	53.5	59.1	5.292	5.133
2	37.25	23.4	49.4	59.1	5.760	3.567
3	33.15	23.4	52.1	59.1	4.755	4.765
4	33.20	24.0	55.2	59.6	5.064	4.918
5	34.96	24.0	55.9	59.6	5.532	4.137
6	33.08	24.0	58.0	59.6	5.685	4.855
7	29.28	27.8	54.2	62.3	5.614	5.026
8	26.63	27.8	55.5	62.3	5.402	4.140
9	29.09	27.8	57.7	62.3	5.096	5.066
10	22.79	24.2	55.4	58.7	5.280	4.806
11	27.31	24.2	53.1	58.7	4.623	3.914
12	25.73	24.2	56.9	58.7	6.020	4.190
13	26.06	24.2	.	58.7	5.506	4.884
14	33.42	24.2	52.5	58.7	5.106	4.227
15	26.17	24.2	53.3	58.7	5.108	4.669
16	25.81	22.0	52.7	58.0	4.886	4.731
17	26.87	22.0	50.6	58.0	5.593	4.840
18	24.99	22.0	54.9	58.0	5.467	4.248
19	32.20	21.4	49.6	57.5	4.745	4.743
20	35.21	21.4	47.8	57.5	4.804	4.028
21	32.33	21.4	54.0	57.5	5.027	4.177
22	29.66	21.4	50.3	57.5	5.304	4.719
23	26.70	21.4	51.2	57.5	5.325	3.711
24	33.23	21.4	53.5	57.5	5.422	4.185
25	23.28	20.1	52.8	56.4	5.101	4.823
26	28.75	20.1	48.8	56.4	5.868	4.262
27	26.59	20.1	53.6	56.4	5.807	4.818
28	26.83	16.1	48.2	53.1	5.012	4.738
29	25.50	16.1	48.3	53.1	4.802	4.069
30	19.48	16.1	48.3	53.1	5.221	5.252
31	26.86	16.1	53.3	53.1	5.011	5.097
32	29.50	16.1	47.7	53.1	5.437	4.129
33	30.35	16.1	54.7	53.1	5.977	4.895
34	27.16	21.9	50.9	57.9	5.544	4.785
35	26.32	21.9	49.4	57.9	4.838	4.135
36	25.71	21.9	54.4	57.9	4.874	4.105
37	26.65	23.5	49.8	59.2	5.269	4.702
38	26.83	23.5	49.0	59.2	5.030	3.868
39	25.49	23.5	48.4	59.2	4.653	4.565
40	27.44	23.5	53.4	60.1	5.396	4.126
41	28.26	23.5	53.3	60.1	5.383	4.416
42	25.32	23.5	54.3	60.1	5.332	4.323
43	30.50	24.5	63.9	60.0	6.313	4.789
44	30.81	24.5	52.3	60.0	6.324	4.466
45	31.15	24.5	60.1	60.0	5.712	4.570
46	39.08	24.5	55.9	60.0	5.490	4.767
47	40.93	24.5	52.8	60.0	6.133	3.998
48	37.28	24.5	53.8	60.0	6.189	4.030
49	33.60	24.5	54.4	60.0	5.351	4.940
50	36.93	24.5	52.6	60.0	5.681	3.512

APPENDIX II
MEASURED AND PREDICTED MACHINE PAPER PROPERTIES

OBS	Measured CD Ring Crush	Predicted CD Ring Crush	Measured Concora	Predicted Concora	TEAMD	TEACD
51	33.70	24.5	56.0	60.0	6.469	4.076
52	31.20	25.1	53.6	60.5	5.525	4.832
53	33.16	25.1	51.2	60.5	5.918	4.359
54	32.49	25.1	54.0	60.5	5.781	4.516
55	30.54	21.0	53.6	57.1	5.816	5.158
56	38.80	21.0	51.6	57.1	5.801	3.524
57	33.83	21.0	54.2	57.1	5.402	4.595
58	38.83	21.0	51.4	57.1	5.059	4.902
59	38.85	21.0	51.6	57.1	5.595	4.169
60	37.55	21.0	52.9	57.1	6.117	4.365
61	33.61	21.0	53.4	57.1	5.233	4.562
62	36.58	21.0	49.7	57.1	5.636	4.292
63	35.66	21.0	52.1	57.1	5.358	3.962
64	31.14	21.0	53.2	57.1	5.723	4.941
65	29.40	21.0	51.0	57.1	5.853	4.131
66	28.41	21.0	55.0	57.1	5.546	3.798
67	28.42	23.8	56.6	59.4	6.059	6.505
68	26.43	23.8	55.5	59.4	6.529	4.596
69	26.33	23.8	58.3	59.4	6.564	5.280
70	40.70	23.8	55.4	59.4	5.839	4.536
71	42.60	23.8	52.0	59.4	6.349	4.059
72	41.30	23.8	56.2	59.4	5.658	4.920
73	42.56	23.8	54.3	59.4	5.822	4.795
74	43.23	23.8	51.7	59.4	5.886	3.935
75	38.83	23.8	55.3	59.4	5.894	4.191
76	37.53	21.5	54.8	57.5	5.642	4.709
77	38.84	21.5	54.5	57.5	5.954	3.991
78	33.16	21.5	55.2	57.5	5.500	3.578
79	27.55	22.0	50.2	57.9	5.754	4.327
80	26.30	22.0	52.2	57.9	6.052	4.084
81	26.13	22.0	53.3	57.9	5.624	4.187
82	27.96	21.4	52.3	57.4	5.685	4.815
83	28.29	21.4	54.5	57.4	5.742	4.088
85	35.78	20.5	52.5	56.7	5.551	4.129
86	38.74	20.5	53.9	56.7	5.622	3.583
87	34.90	20.5	56.2	56.7	4.906	4.242
88	38.21	20.5	53.4	56.7	5.425	4.305
89	38.68	20.5	52.6	56.7	5.286	3.866
90	33.77	20.5	50.8	56.7	5.521	4.183
91	38.34	20.5	53.9	56.7	4.917	3.893
92	40.31	20.5	53.1	56.7	5.901	3.950
93	35.65	20.5	51.6	56.7	5.087	4.261
94	34.89	25.4	57.3	57.7	5.656	3.941
95	33.97	25.4	58.9	57.7	5.572	3.970
96	29.69	25.4	55.6	57.7	5.229	3.977
97	35.00	21.7	55.6	57.2	5.179	4.176
98	36.18	21.7	57.9	57.2	5.686	3.958
99	31.84	21.7	56.7	57.2	4.931	3.840
100	40.71	21.7	54.8	57.2	5.322	4.361

APPENDIX II
MEASURED AND PREDICTED MACHINE PAPER PROPERTIES

OBS	Measured CD Ring Crush	Predicted CD Ring Crush	Measured Concora	Predicted Concora	TEAMD	TEACD
101	42.40	21.7	59.6	57.2	5.487	3.981
102	35.97	21.7	55.6	57.2	5.721	3.886
103	36.20	21.4	53.3	57.5	5.152	4.114
104	36.98	21.4	56.3	57.5	5.829	3.930
105	32.19	21.4	57.6	57.5	5.250	4.034
106	35.56	21.9	54.3	57.8	5.027	4.706
107	37.86	21.9	53.3	57.8	5.502	3.955
108	33.77	21.9	53.3	57.8	4.312	3.693
109	36.69	21.9	53.9	57.8	4.901	3.924
110	38.89	21.9	55.2	57.8	5.403	3.704
111	34.54	21.9	53.7	57.8	4.680	3.736
112	36.01	21.9	56.8	57.8	5.501	3.867
113	39.57	21.9	55.7	57.8	5.185	3.873
114	35.10	21.9	56.8	57.8	5.697	3.529

APPENDIX III
MEASURED AND PREDICTED HANDSHEET PROPERTIES
LOCATION BLEND CHEST

OBS	DATE	DAY	REEL	RLPLT	Basis Weight lb/1000 sq ft	Measured Caliper mils	Predicted Caliper mils	Measured Density g/cc
1	4-3-90	1	1	1	27.0440	13.4882	13.70	0.3858
2	4-3-90	1	2	2	27.4798	13.0787	16.10	0.4043
3	4-3-90	1	3	3	28.2982	12.7677	15.08	0.4265
4	4-3-90	1	4	4	29.3192	16.5866	15.60	0.3401
5	4-3-90	1	5	5	25.2210	12.8465	15.70	0.3778
6	4-3-90	1	6	6	27.0972	12.5984	18.10	0.4139
7	4-3-90	1	7	7	28.4026	15.9173	14.80	0.3434
8	4-3-90	1	8	8	27.9975	13.6063	13.60	0.3959
9	4-4-90	2	1	9	28.5990	15.4094	11.80	0.3571
10	4-4-90	2	2	10	28.4783	13.8465	12.70	0.3958
11	4-4-90	2	3	11	26.1151	13.6575	12.70	0.3881
12	4-4-90	2	4	12	28.6726	13.5591	12.80	0.4069
13	4-4-90	2	5	13	29.7550	16.1063	14.45	0.3555
14	4-4-90	2	6	14	28.9734	14.9882	14.20	0.3720
15	4-4-90	2	7	15	27.4716	12.6575	14.20	0.4176
16	4-4-90	2	8	16	33.9943	18.8898	14.30	0.3463
17	4-5-90	3	1	17	26.9458	14.3740	13.20	0.3607
18	4-5-90	3	2	18	27.6230	13.5197	12.40	0.3932
19	4-5-90	3	3	19	28.8916	15.8268	15.20	0.3513
20	4-5-90	3	4	20	26.7965	15.1890	13.60	0.3395
21	4-5-90	3	5	21	27.4716	13.5984	12.60	0.3887
22	4-5-90	3	6	22	27.1034	13.9685	13.00	0.3734
23	4-5-90	3	7	23	26.1908	14.7874	13.80	0.3408
24	4-5-90	3	8	24	28.2225	13.0591	13.30	0.4159

APPENDIX III
MEASURED AND PREDICTED HANDSHEET PROPERTIES
LOCATION BLEND CHEST

OBS	Predicted Density g/cc	Measured Tensile km	Predicted Tensile km	Measured Burst Factor	Predicted Burst Factor	Measured Stretch %	Predicted Stretch %
1	0.378	4.118	3.80	22.0589	20.0	1.997	1.05
2	0.350	4.775	3.47	22.3892	17.7	1.615	1.05
3	0.348	4.408	2.80	24.9927	13.2	1.619	0.85
4	0.352	4.195	3.00	20.1020	14.2	2.253	0.90
5	0.365	5.003	3.76	21.1170	19.5	1.622	1.02
6	0.360	5.493	3.78	25.1986	19.3	1.689	1.02
7	0.374	4.897	3.70	22.3703	21.1	1.786	1.28
8	0.384	4.694	3.64	21.4874	20.1	1.668	1.19
9	0.442	5.101	4.40	21.6135	25.5	2.034	1.33
10	0.378	4.451	3.82	20.8975	21.3	1.620	1.20
11	0.425	5.305	4.15	22.9536	24.2	1.924	1.29
12	0.391	4.808	3.92	24.4157	22.2	1.666	1.21
13	0.386	4.811	3.41	18.5515	18.1	1.798	1.07
14	0.361	3.938	3.93	18.3425	22.5	1.364	1.26
15	0.361	4.701	3.93	22.4481	22.5	1.690	1.26
16	0.353	4.527	3.78	19.0289	21.5	1.686	1.22
17	0.413	5.287	4.14	20.9657	24.4	1.903	1.32
18	0.420	4.372	4.27	21.5966	24.7	1.557	1.28
19	0.363	5.343	4.05	20.3498	22.1	1.756	1.14
20	0.405	5.691	4.38	18.9904	24.8	2.023	1.22
21	0.421	4.894	4.51	24.5935	27.5	1.495	1.25
22	0.406	4.342	3.90	19.5179	21.2	2.050	1.15
23	0.382	5.143	4.30	21.1858	24.8	2.087	1.24
24	0.407	5.089	3.95	22.7677	22.1	1.821	1.19

APPENDIX III
MEASURED AND PREDICTED HANDSHEET PROPERTIES
LOCATION BLEND CHEST

OBS	Measured Moisture %	Measured Gurley Porosity	Predicted Gurley Porosity sec/cc	Predicted STFI lb/in	Measured Ring Crush lb/6 in	Predicted Ring Crush lb/6 in	Measured Concora lb
1	4.16	6.70	13.9	17.3	48.8	27.4	34.8
2	5.39	8.40	13.8	18.9	49.6	34.7	37.3
3	6.47	9.79	12.8	18.3	52.6	29.9	45.2
4	7.25	9.38	13.0	18.4	41.9	30.8	33.9
5	6.34	6.60	13.9	19.5	41.2	38.4	33.6
6	6.32	6.99	13.8	19.0	50.2	35.6	42.8
7	6.19	12.29	14.1	18.6	52.8	35.2	36.6
8	6.47	7.76	22.6	17.0	48.3	26.6	40.7
9	6.28	10.06	18.0	16.5	52.3	24.2	43.7
10	6.15	7.95	15.6	16.5	54.2	23.7	38.1
11	6.44	7.74	17.4	16.9	47.8	26.6	37.1
12	6.25	9.68	16.0	16.7	57.9	24.8	48.7
13	6.13	6.97	15.6	17.1	53.6	26.2	37.9
14	6.51	4.05	14.5	17.8	47.9	31.1	37.5
15	6.25	11.54	14.5	17.8	52.0	31.1	43.1
16	6.36	6.96	13.8	17.7	70.6	30.3	40.0
17	6.32	4.55	16.1	17.3	48.9	28.7	33.8
18	6.55	19.13	15.9	16.6	48.2	24.6	40.8
19	6.13	5.18	13.8	17.8	49.8	30.7	34.3
20	6.46	4.27	13.3	17.2	48.4	27.4	36.1
21	6.25	19.91	16.3	16.6	56.6	24.7	46.1
22	6.41	5.56	16.3	16.4	49.2	23.0	34.4
23	6.45	5.24	16.5	17.3	46.4	28.4	38.0
24	6.11	.	16.0	16.8	59.9	25.2	48.2

APPENDIX III
MEASURED AND PREDICTED HANDSHEET PROPERTIES
LOCATION BLEND CHEST

OBS	Predicted Concora lb	ENERGY	SLOPE	Measured CSF ml	Predicted CSF ml
1	54.1	59.65	542.1	542	497
2	59.3	53.34	663.1	.	473
3	57.3	51.20	623.9	561	.
4	57.8	63.91	475.5	567	495
5	61.5	58.03	699.5	565	481
6	59.7	66.40	754.9	572	478
7	58.4	61.55	668.4	562	487
8	53.1	54.30	637.1	548	485
9	51.3	73.35	635.1	495	449
10	51.3	49.91	610.3	650	449
11	52.8	73.36	700.2	554	447
12	51.9	57.44	678.0	600	447
13	53.3	63.58	638.6	554	453
14	55.8	43.28	625.8	555	459
15	55.8	58.09	644.2	545	459
16	55.3	54.82	616.7	565	468
17	54.1	74.01	716.3	494	469
18	51.6	48.68	617.6	508	469
19	55.9	66.26	683.2	525	483
21	51.7	54.66	722.3	595	475
22	50.9	66.81	564.8	473	455
23	54.1	79.83	638.0	480	425
24	52.2	67.24	652.1	517	468

APPENDIX III
MEASURED AND PREDICTED HANDSHEET PROPERTIES
LOCATION BROKE TANK

OBS	DATE	DAY	REEL	RLPLT	Basis Weight lb/1000 sq ft	Measured Caliper mils	Predicted Caliper mils	Measured Density g/cc
25	4-3-90	1	1	1	26.6471	11.0984	10.70	0.4620
26	4-3-90	1	2	2	.	.	9.95	.
27	4-3-90	1	3	3	26.8722	10.9764	10.12	0.4711
28	4-3-90	1	4	4	25.2210	10.6575	11.30	0.4554
29	4-3-90	1	5	5	27.0215	11.4488	11.00	0.4542
30	4-3-90	1	6	6	.	.	11.20	.
31	4-3-90	1	7	7	27.3223	11.4488	11.60	0.4592
32	4-3-90	1	8	8	27.8481	11.5079	10.40	0.4657
33	4-4-90	2	1	9	25.4461	11.3386	9.50	0.4318
34	4-4-90	2	2	10	28.1468	12.2598	11.30	0.4418
35	4-4-90	2	3	11	.	.	11.70	.
36	4-4-90	2	4	12	30.3995	11.6063	11.15	0.5040
37	4-4-90	2	5	13	.	.	11.60	.
38	4-4-90	2	6	14	27.6230	11.2795	12.10	0.4712
39	4-4-90	2	7	15	27.3980	11.5197	12.10	0.4577
40	4-4-90	2	8	16	27.2466	11.2087	12.82	0.4678
41	4-5-90	3	1	17	.	.	11.15	.
42	4-5-90	3	2	18	27.4716	12.3976	11.60	0.4264
43	4-5-90	3	3	19	.	.	11.20	.
44	4-5-90	3	4	20	28.5990	11.6575	11.20	0.4721
45	4-5-90	3	5	21	.	.	12.00	.
46	4-5-90	3	6	22	.	.	11.60	.
47	4-5-90	3	7	23	.	.	11.00	.
48	4-5-90	3	8	24	25.4461	11.3661	11.10	0.4308

APPENDIX III
MEASURED AND PREDICTED HANDSHEET PROPERTIES
LOCATION BROKE TANK

OBS	Predicted Density g/cc	Measured Tensile km	Predicted Tensile km	Measured Burst Factor	Predicted Burst Factor	Measured Stretch %	Predicted Stretch %
25	0.477	2.522	3.09	18.5034	17.8	0.975	1.27
26	0.488	3.082	3.08	.	17.9	1.444	1.30
27	0.479	3.249	3.17	19.5146	18.2	1.249	1.28
28	0.478	3.297	3.20	16.9848	18.3	1.168	1.28
29	0.490	.	3.38	19.6834	19.7	.	1.30
30	0.470	3.453	3.51	.	20.0	1.370	1.33
31	0.429	.	3.00	17.5727	18.9	.	1.54
32	0.482	.	3.32	17.8500	20.8	.	1.55
33	0.525	.	3.53	16.0155	22.9	.	1.65
34	0.460	3.405	3.30	17.3643	20.1	1.487	1.43
35	0.454	3.855	3.10	.	18.4	1.866	1.36
36	0.466	.	3.24	15.9121	19.5	.	1.45
37	0.456	3.952	3.26	.	20.4	1.817	1.50
38	0.456	.	3.27	19.8688	20.3	.	1.49
39	0.456	4.363	3.27	17.0676	20.3	1.921	1.49
40	0.429	.	3.00	19.5208	18.0	.	1.42
41	0.464	3.238	3.22	.	19.5	1.467	1.41
42	0.447	.	3.30	15.8811	19.7	.	1.37
43	0.437	2.775	2.82	.	16.1	1.140	1.26
44	0.520	2.993	2.70	20.0956	14.9	1.288	1.21
45	0.439	3.751	3.00	.	17.4	1.369	1.32
46	0.454	3.150	2.67	.	15.1	1.364	1.23
47	0.481	.	2.90	.	16.6	.	1.28
48	0.439	3.143	2.96	17.3995	17.4	1.468	1.32

APPENDIX III
MEASURED AND PREDICTED HANDSHEET PROPERTIES
LOCATION BROKE TANK

OBS	Measured Moisture %	Measured Gurley Porosity	Predicted Gurley Porosity sec/cc	Predicted STFI lb/in	Measured Ring Crush lb/6 in	Predicted Ring Crush lb/6 in	Measured Concora lb
25	6.14	5.25	16.0	18.1	41.0	32.5	30.2
26	.	.	16.5	18.0	.	32.4	.
27	5.46	9.66	16.0	18.8	42.2	36.5	33.8
28	6.19	4.61	15.9	20.4	40.3	44.9	30.7
29	5.54	4.74	16.6	20.1	50.2	43.2	32.2
30	.	.	15.9	18.8	.	36.6	.
31	5.88	11.13	14.3	20.7	44.2	47.0	31.5
32	5.45	6.67	16.0	16.6	47.1	25.0	35.2
33	5.50	3.28	19.1	16.7	38.7	25.7	29.4
34	6.04	6.36	17.0	16.6	44.9	25.2	32.9
35	.	.	16.9	16.6	.	24.9	.
36	5.49	3.64	17.4	16.6	41.4	24.9	30.5
37	.	.	16.7	17.2	.	28.3	.
38	5.60	8.17	16.8	17.5	44.5	30.1	34.8
39	5.59	8.70	16.8	17.5	45.0	30.1	29.9
40	6.01	8.50	15.2	17.7	42.9	30.7	30.7
41	.	.	16.0	16.3	.	23.1	.
42	5.42	3.32	15.0	16.4	42.9	23.8	28.3
43	.	.	14.5	15.7	.	19.6	.
44	5.41	7.91	17.3	15.5	48.1	18.6	38.9
45	.	.	14.6	16.50	.	24.4	.
46	.	.	15.5	15.77	.	20.0	.
47	.	.	17.2	15.50	.	18.8	.
48	5.30	4.91	15.1	15.80	35.0	20.7	25.0

APPENDIX III
MEASURED AND PREDICTED HANDSHEET PROPERTIES
LOCATION BROKE TANK

OBS	Predicted Concora lb	ENERGY	SLOPE	Measured CSF ml	Predicted CSF ml
25	56.6	19.88	565.6	551	548
26	56.5	33.62	501.7	579	540
27	59.2	31.08	559.8	596	551
28	64.5	31.14	606.9	598	548
29	63.4	.	.	.	548
30	59.2	34.96	584.6	614	543
31	65.7	.	.	.	549
32	51.7	.	.	.	501
33	52.1	.	.	.	503
34	51.7	41.17	534.9	593	497
35	51.7	63.70	565.6	608	491
36	51.6	.	.	.	491
37	53.7	53.80	560.9	613	499
38	54.8	.	.	.	499
39	54.8	63.03	605.5	599	499
40	55.3	.	.	.	517
41	50.5	37.65	556.8	578	533
42	51.0	.	.	.	533
43	48.5	25.65	514.1	688	552
44	48.0	30.26	503.5	573	552
45	51.4	37.63	588.0	583	550
46	48.8	33.44	519.5	558	536
47	47.9	.	.	.	536
48	49.0	35.34	498.2	563	534

APPENDIX III
MEASURED AND PREDICTED HANDSHEET PROPERTIES
LOCATION HEADBOX

OBS	DATE	DAY	REEL	RLPLT	Basis Weight lb/1000 sq ft	Measured Caliper mils	Predicted Caliper mils	Measured Density g/cc
49	4-3-90	1	1	1	28.2225	10.5669	10.40	0.5139
50	4-3-90	1	2	2	30.0557	11.4882	10.10	0.4829
51	4-3-90	1	3	3	29.0532	11.6181	10.00	0.4812
52	4-3-90	1	4	4	25.5955	10.2874	12.30	0.4788
53	4-3-90	1	5	5	28.8895	11.3780	10.10	0.4886
54	4-3-90	1	6	6	28.6645	11.5000	12.20	0.4796
55	4-3-90	1	7	7	24.9960	9.8189	11.00	0.4899
56	4-3-90	1	8	8	28.5212	10.9488	10.50	0.5013
57	4-4-90	2	1	9	29.2783	12.0669	12.06	0.4669
58	4-4-90	2	2	10	30.6900	12.2480	11.00	0.4822
59	4-4-90	2	3	11	28.5212	11.4488	11.00	0.4794
60	4-4-90	2	4	12	29.9534	11.2795	11.60	0.5110
61	4-4-90	2	5	13	28.7483	10.7480	12.00	0.5147
62	4-4-90	2	6	14	28.3780	11.7598	11.25	0.4643
63	4-4-90	2	7	15	31.9790	12.0472	11.90	0.5108
64	4-4-90	2	8	16	29.2783	12.0197	11.90	0.4687
65	4-5-90	3	1	17	27.7028	11.2795	11.70	0.4726
66	4-5-90	3	2	18	29.5729	10.2480	11.27	0.5553
67	4-5-90	3	3	19	27.4716	10.8661	11.70	0.4865
68	4-5-90	3	4	20	29.6465	12.2874	11.10	0.4643
69	4-5-90	3	5	21	29.1146	11.3268	11.80	0.4946
70	4-5-90	3	6	22	27.3980	10.7480	10.60	0.4905
71	4-5-90	3	7	23	29.4215	12.4094	11.20	0.4562
72	4-5-90	3	8	24	28.4394	11.2087	11.50	0.4882

APPENDIX III
MEASURED AND PREDICTED HANDSHEET PROPERTIES
LOCATION HEADBOX

OBS	Predicted Density g/cc	Measured Tensile km	Predicted Tensile km	Measured Burst Factor	Predicted Burst Factor	Measured Stretch %	Predicted Stretch %
49	0.516	5.233	3.50	21.3925	21.4	2.461	1.42
50	0.488	5.019	4.10	26.4966	27.0	2.256	1.68
51	0.479	4.890	3.70	28.1679	23.0	2.137	1.48
52	0.480	5.549	4.20	28.6428	27.5	2.391	1.67
53	0.546	4.916	5.30	27.9046	25.9	2.335	1.50
54	0.463	4.830	4.00	30.2149	25.0	2.380	1.51
55	0.480	5.759	3.30	23.8088	21.6	1.980	1.67
56	0.500	5.472	3.70	27.2922	24.6	1.914	1.72
57	0.479	5.676	3.56	27.7894	23.2	2.366	1.66
58	0.509	5.431	4.00	26.9326	26.9	2.221	1.73
59	0.497	6.245	2.95	28.3254	19.8	2.356	1.21
60	0.470	5.570	4.25	27.3070	27.9	2.480	1.64
61	0.456	4.928	3.55	24.9514	23.0	1.772	1.61
62	0.473	5.346	3.59	27.9213	23.5	1.840	1.65
63	0.474	6.448	3.51	28.7374	23.0	2.216	1.65
64	0.475	6.696	3.50	25.0988	23.0	2.398	1.65
65	0.480	6.253	3.95	28.3994	26.1	2.278	1.67
66	0.490	6.227	4.35	28.7034	28.8	2.328	1.69
67	0.480	6.207	4.20	22.1760	27.3	2.344	1.67
68	0.520	5.883	4.24	27.1193	28.2	3.094	1.70
69	0.520	7.264	4.17	29.4515	27.7	2.403	1.70
70	0.536	6.127	4.31	26.6272	29.0	2.887	1.74
71	0.497	7.004	4.24	29.5010	28.3	2.472	1.71
72	0.475	6.174	4.01	29.8980	26.3	2.395	1.65

APPENDIX III
MEASURED AND PREDICTED HANDSHEET PROPERTIES
LOCATION HEADBOX

OBS	Measured Moisture %	Measured Gurley Porosity	Predicted Gurley Porosity sec/cc	Predicted STFI lb/in	Measured Ring Crush lb/6 in	Predicted Ring Crush lb/6 in	Measured Concora lb
49	6.59	35.70	17.3	18.7	54.5	36.2	51.2
50	6.92	35.02	16.5	21.8	60.0	52.9	57.6
51	6.87	38.48	15.9	20.1	63.9	44.0	52.7
52	6.58	22.60	16.0	25.9	58.0	75.3	51.2
53	6.96	28.20	18.3	29.6	57.9	17.6	51.8
54	5.83	36.25	15.7	21.0	59.4	48.5	53.0
55	6.60	38.10	16.0	18.5	57.7	35.0	53.9
56	6.91	40.41	16.7	18.4	60.0	34.3	58.6
57	6.93	35.40	17.4	19.3	67.2	39.3	56.2
58	5.93	30.61	18.7	19.0	63.9	38.0	62.8
59	6.51	44.11	23.9	18.8	62.7	36.8	56.1
60	8.15	33.02	17.5	18.6	66.8	35.7	53.3
61	6.55	23.80	16.8	18.5	58.5	35.4	55.7
62	6.90	33.50	17.1	18.3	61.0	34.1	54.7
63	5.98	51.89	16.8	18.9	77.6	37.4	62.9
64	6.82	29.21	16.9	18.9	61.1	37.5	52.8
65	8.30	16.72	16.5	18.9	59.0	37.2	40.0
66	6.63	54.71	16.4	18.7	66.7	36.3	66.1
67	6.68	24.81	15.9	18.9	56.7	37.5	49.8
68	7.29	26.90	17.3	18.7	67.8	36.3	51.0
69	6.57	56.93	17.3	19.1	65.4	40.0	56.6
70	6.70	16.81	18.3	18.6	59.7	35.6	53.7
71	5.78	28.09	17.8	18.8	66.1	36.8	51.4
72	6.47	39.65	16.3	18.4	61.5	34.9	51.0

APPENDIX III
MEASURED AND PREDICTED HANDSHEET PROPERTIES
LOCATION HEADBOX

OBS	Predicted Concora lb	ENERGY	SLOPE	Measured CSF ml	Predicted CSF ml
49	58.8	8.06	640.6	367	447
50	69.4	6.99	609.5	371	413
51	63.6	6.49	589.4	331	449
52	83.5	102.00	669.1	350	444
53	52.3	7.25	636.1	355	428
54	66.5	89.24	617.6	405	422
55	58.0	6.95	713.1	398	432
56	57.6	6.42	715.5	346	431
57	60.7	100.30	683.7	383	412
58	60.0	89.37	681.8	400	386
59	59.2	109.80	724.0	375	380
60	58.4	102.00	641.7	397	376
61	58.2	70.29	717.9	407	383
62	57.4	73.26	695.5	409	386
63	59.5	102.70	790.7	386	386
64	59.6	117.60	788.1	374	398
65	59.4	103.10	755.7	354	407
66	58.9	106.50	740.7	374	407
67	59.6	106.30	746.6	361	426
68	58.8	136.20	647.7	363	416
69	61.2	129.10	841.9	355	416
70	58.5	11.21	718.0	338	398
71	59.2	127.00	774.3	339	367
72	57.9	109.60	722.6	372	401

APPENDIX III
MEASURED AND PREDICTED HANDSHEET PROPERTIES
LOCATION HOLE REFINER

OBS	DATE	DAY	REEL	RLPLT	Basis Weight lb/1000 sq ft	Measured Caliper mils	Predicted Caliper mils	Measured Density g/cc
73	4-3-90	1	1	1	22.4446	18.2165	18.10	0.2371
74	4-3-90	1	2	2	26.0456	13.0591	14.40	0.3838
75	4-3-90	1	3	3	29.0532	13.8386	16.20	0.4040
76	4-3-90	1	4	4	28.4394	16.5276	9.90	0.3311
77	4-3-90	1	5	5	30.5468	15.3661	15.50	0.3825
78	4-3-90	1	6	6	25.8205	14.3583	16.80	0.3460
79	4-3-90	1	7	7	28.9714	15.4291	14.70	0.3613
80	4-3-90	1	8	8	27.9279	15.9685	16.10	0.3365
81	4-4-90	2	1	9	28.0711	15.8661	15.70	0.3404
82	4-4-90	2	2	10	27.7847	15.8661	16.10	0.3370
83	4-4-90	2	3	11	27.3141	14.0591	16.00	0.3738
84	4-4-90	2	4	12	26.7289	12.7598	14.00	0.4031
85	4-4-90	2	5	13	27.4778	16.0472	15.10	0.3295
86	4-4-90	2	6	14	27.8461	15.3780	15.10	0.3484
87	4-4-90	2	7	15	27.3448	13.5866	15.10	0.3873
88	4-4-90	2	8	16	27.3550	16.6378	16.00	0.3164
89	4-5-90	3	1	17	27.6210	15.9488	13.90	0.3333
90	4-5-90	3	2	18	27.0747	15.6181	14.00	0.3336
91	4-5-90	3	3	19	27.8461	14.4291	15.70	0.3714
92	4-5-90	3	4	20	27.0890	14.8071	12.60	0.3520
93	4-5-90	3	5	21	27.8931	14.2795	13.80	0.3759
94	4-5-90	3	6	22	28.1530	15.3189	15.40	0.3536
95	4-5-90	3	7	23	30.1785	15.6575	14.60	0.3709
96	4-5-90	3	8	24	27.7499	11.2598	13.53	0.3968

APPENDIX III
MEASURED AND PREDICTED HANDSHEET PROPERTIES
LOCATION HOLE REFINER

OBS	Predicted Density g/cc	Measured Tensile km	Predicted Tensile km	Measured Burst Factor	Predicted Burst Factor	Measured Stretch %	Predicted Stretch %
73	0.237	5.169	3.80	26.8675	19.1	1.730	0.96
74	0.334	4.460	3.16	24.4941	14.7	1.437	0.81
75	0.340	4.847	3.30	30.8744	15.5	1.368	0.84
76	0.342	2.666	3.30	21.3810	15.5	1.182	0.83
77	0.343	1.563	4.30	21.1201	22.0	1.538	1.08
78	0.313	1.183	3.55	28.9498	17.9	1.213	0.90
79	0.363	5.059	4.06	25.7170	21.9	1.639	1.03
80	0.343	5.151	4.00	23.3425	23.3	1.628	1.20
81	0.344	5.569	4.00	26.6698	23.3	1.791	1.30
82	0.364	6.538	3.80	21.6003	21.9	1.994	1.25
83	0.334	6.077	3.87	23.9618	22.4	1.955	1.27
84	0.374	5.638	4.06	27.8584	24.0	1.750	1.33
85	0.354	5.543	3.74	19.3304	21.2	1.716	1.23
86	0.354	4.875	3.90	21.1551	22.6	1.533	1.30
87	0.354	4.588	3.90	27.2310	22.6	1.475	1.30
88	0.363	2.854	3.50	18.2085	19.1	1.493	1.14
89	0.401	7.415	5.08	23.2792	30.9	1.999	1.41
90	0.355	7.034	4.70	26.6000	27.0	2.126	1.30
91	0.345	6.136	4.70	21.3720	26.9	1.897	1.26
92	0.408	6.363	4.85	22.7546	28.5	1.906	1.30
93	0.382	6.378	4.80	27.9841	28.1	1.781	1.30
94	0.339	6.426	4.62	20.6948	26.9	1.869	1.29
95	0.368	6.310	4.90	19.6630	29.7	1.756	1.37
96	0.396	5.542	4.40	24.2433	25.0	1.517	1.22

APPENDIX III
MEASURED AND PREDICTED HANDSHEET PROPERTIES
LOCATION HOLE REFINER

OBS	Measured Moisture %	Measured Gurley Porosity	Predicted Gurley Porosity sec/cc	Predicted STFI lb/in	Measured Ring Crush lb/6 in	Predicted Ring Crush lb/6 in	Measured Concora lb
73	5.69	6.11	8.2	18.6	51.2	33.2	41.1
74	6.76	15.20	12.9	15.8	53.8	17.2	40.5
75	6.14	34.22	11.8	16.9	71.4	23.0	60.1
76	6.08	9.83	11.9	16.5	57.0	21.1	39.5
77	6.21	11.77	12.0	17.7	64.2	29.9	51.0
78	6.10	24.31	10.9	18.8	61.0	27.0	57.5
79	6.56	8.86	12.6	16.9	57.1	25.1	45.1
80	6.40	10.87	20.9	19.0	60.9	37.7	49.8
81	6.43	10.35	11.9	19.0	63.3	37.5	52.6
82	6.53	6.62	12.7	18.9	43.8	37.0	37.2
83	5.96	9.18	11.7	19.1	56.5	37.9	47.7
84	6.02	18.21	13.0	18.0	53.1	32.1	50.3
85	4.73	7.15	12.3	18.1	46.4	32.4	38.1
86	6.36	9.32	12.4	18.4	56.8	34.4	44.1
87	5.13	36.03	12.4	18.4	60.5	34.4	51.4
88	5.48	4.46	12.6	18.3	49.2	32.9	37.1
89	6.41	9.97	15.3	18.1	58.2	33.1	42.5
90	7.69	32.30	12.7	17.6	56.4	30.0	53.6
91	5.85	4.10	12.1	18.7	48.7	35.6	38.1
92	6.27	6.88	15.0	16.7	52.0	25.6	40.9
93	6.20	23.90	13.8	17.5	64.2	29.7	54.7
94	6.61	7.38	13.3	18.4	52.9	34.5	41.4
95	7.77	6.20	15.9	18.3	56.1	34.0	42.3
96	6.22	20.18	14.9	17.0	63.8	26.3	53.2

APPENDIX III
MEASURED AND PREDICTED HANDSHEET PROPERTIES
LOCATION HOLE REFINER

OBS	Predicted Concora lb	ENERGY	SLOPE	Measured CSF ml	Predicted CSF ml
73	58.5	65.48	694.2	620	528
74	48.9	54.72	679.0	548	465
75	52.7	56.30	714.7	589	526
76	51.4	35.30	575.1	612	527
77	55.5	26.31	445.0	570	526
78	59.0	18.41	417.5	584	526
79	52.8	55.61	670.9	560	527
80	59.8	57.92	702.2	590	526
81	60.0	71.56	725.8	482	526
82	59.3	94.23	818.9	492	525
83	60.1	84.17	742.1	494	525
84	56.3	72.94	735.3	475	526
85	56.7	66.86	721.1	587	526
86	57.8	51.41	654.4	568	526
87	57.8	62.68	712.7	548	526
88	57.3	42.15	608.2	574	527
89	56.8	104.90	869.2	386	482
90	55.0	104.70	806.4	410	482
91	58.7	83.30	762.5	481	525
92	52.2	83.97	772.1	474	499
93	54.8	77.84	782.9	405	506
94	57.9	81.13	763.2	407	467
95	57.4	77.65	798.7	430	423
96	52.8	64.32	777.6	425	488

APPENDIX III
MEASURED AND PREDICTED HANDSHEET PROPERTIES
LOCATION TICKLER REFINER

OBS	DATE	DAY	REEL	RLPLT	Basis Weight lb/1000 sq ft	Measured Caliper mils	Predicted Caliper mils	Measured Density g/cc
97	4-3-90	1	1	1	27.2466	13.4685	13.70	0.3893
98	4-3-90	1	2	2	27.5473	14.2283	15.00	0.3726
99	4-3-90	1	3	3	26.8722	12.1063	14.40	0.4271
100	4-3-90	1	4	4	27.2466	14.8268	12.30	0.3536
101	4-3-90	1	5	5	27.2466	12.6496	13.20	0.4145
102	4-3-90	1	6	6	27.8481	12.6969	16.00	0.4220
103	4-3-90	1	7	7	30.3238	14.4094	14.60	0.4049
104	4-3-90	1	8	8	27.4716	13.2283	15.00	0.3996
105	4-4-90	2	1	9	27.8481	13.4370	13.00	0.3988
106	4-4-90	2	2	10	26.1949	13.7874	11.90	0.3656
107	4-4-90	2	3	11	26.8722	12.9370	13.50	0.3997
108	4-4-90	2	4	12	27.1729	12.8780	13.20	0.4060
109	4-4-90	2	5	13	26.7208	12.9291	13.50	0.3977
110	4-4-90	2	6	14	28.3719	13.5787	13.60	0.4021
111	4-4-90	2	7	15	27.3980	12.9685	13.60	0.4065
112	4-4-90	2	8	16	33.1759	15.9764	13.90	0.3996
113	4-5-90	3	1	17	27.0215	13.4488	11.90	0.3866
114	4-5-90	3	2	18	31.4511	14.6772	12.60	0.4123
115	4-5-90	3	3	19	28.8240	14.4173	12.70	0.3847
116	4-5-90	3	4	20	27.2466	15.1496	11.50	0.3461
117	4-5-90	3	5	21	28.0732	13.5669	11.50	0.3982
118	4-5-90	3	6	22	30.1744	15.1693	14.40	0.3828
119	4-5-90	3	7	23	27.4716	14.4488	12.30	0.3659
120	4-5-90	3	8	24	27.3980	10.4528	12.80	0.4198

APPENDIX III
MEASURED AND PREDICTED HANDSHEET PROPERTIES
LOCATION TICKLER REFINER

OBS	Predicted Density g/cc	Measured Tensile km	Predicted Tensile km	Measured Burst Factor	Predicted Burst Factor	Measured Stretch %	Predicted Stretch %
97	0.382	3.531	3.70	20.8925	19.5	0.902	1.06
98	0.353	3.235	3.38	23.7432	17.3	1.234	1.00
99	0.404	4.829	3.60	22.2535	19.6	1.780	1.11
100	0.408	3.631	3.80	19.5208	20.8	0.998	1.12
101	0.379	3.304	3.76	22.4225	19.8	0.995	1.06
102	0.400	4.131	3.71	22.0414	19.1	1.162	1.03
103	0.378	3.716	3.60	22.9440	20.7	1.562	1.82
104	0.388	3.981	3.12	22.2388	16.4	1.731	1.08
105	0.446	4.870	3.83	23.7191	21.2	2.322	1.21
106	0.440	3.678	3.94	19.2783	22.7	1.612	1.30
107	0.388	4.135	3.73	23.4839	21.0	1.244	1.20
108	0.390	3.891	4.11	22.5891	24.3	1.258	1.32
109	0.404	4.179	4.20	20.4859	25.0	1.713	1.36
110	0.381	4.045	3.76	24.1679	21.5	1.727	1.24
111	0.381	3.727	3.76	23.6628	21.5	1.553	1.24
112	0.373	4.375	4.00	19.5113	23.6	2.076	1.34
113	0.438	4.677	3.93	21.4921	23.0	1.780	1.31
114	0.425	4.648	3.88	23.4014	22.0	1.927	1.23
115	0.420	4.609	4.20	21.8936	23.8	2.040	1.22
116	0.507	4.403	4.04	23.9525	22.5	1.736	1.18
117	0.404	4.500	4.26	24.2714	24.4	1.666	1.24
118	0.421	5.730	4.17	17.9125	24.0	2.021	1.24
119	0.440	5.060	4.20	24.0179	24.3	2.161	1.26
120	0.412	4.407	4.19	24.9220	24.4	1.688	1.29

APPENDIX III
MEASURED AND PREDICTED HANDSHEET PROPERTIES
LOCATION TICKLER REFINER

OBS	Measured Moisture %	Measured Gurley Porosity	Predicted Gurley Porosity sec/cc	Predicted STFI lb/in	Measured Ring Crush lb/6 in	Predicted Ring Crush lb/6 in	Measured Concora lb
97	6.74	10.19	14.2	17.4	51.8	27.5	38.4
98	6.76	13.57	14.0	18.2	47.6	31.3	38.6
99	6.41	11.18	14.9	19.3	48.3	38.2	41.2
100	6.68	12.00	15.2	17.5	47.4	28.7	37.7
101	6.36	14.60	14.5	17.9	46.1	30.3	36.3
102	6.46	26.22	15.5	17.7	50.0	29.2	43.6
103	6.26	12.53	14.4	14.6	58.5	34.8	42.2
104	6.39	13.54	14.8	17.3	47.1	27.8	38.2
105	6.08	11.09	18.4	16.8	54.1	25.3	44.4
106	6.30	15.62	18.2	16.2	48.5	22.6	37.6
107	6.33	9.68	16.3	17.1	42.6	26.9	35.6
108	6.00	10.80	16.5	17.5	49.0	29.4	43.9
109	6.44	7.88	16.7	17.8	47.6	31.4	36.2
110	6.53	14.17	15.4	17.3	51.7	28.3	41.4
111	6.12	11.85	15.4	17.3	49.9	28.3	43.4
112	6.25	16.14	15.1	17.9	62.3	32.0	38.4
113	6.82	10.52	17.3	16.3	46.6	23.1	36.0
114	5.98	15.30	16.3	16.5	64.6	23.9	48.3
115	6.68	7.80	16.1	16.6	49.7	24.4	33.1
116	6.23	9.94	20.0	15.6	49.9	19.0	39.6
117	5.97	25.04	15.8	16.9	57.7	25.9	45.1
118	6.23	7.29	17.2	17.8	50.8	30.9	35.7
119	6.81	7.60	19.2	16.3	45.2	23.1	38.2
120	5.84	19.70	16.4	16.8	52.2	25.9	46.2

APPENDIX III
MEASURED AND PREDICTED HANDSHEET PROPERTIES
LOCATION TICKLER REFINER

OBS	Predicted Concora lb	ENERGY	SLOPE	Measured CSF ml	Predicted CSF ml
97	54.2	24.69	654.8	540	493
98	57.1	32.53	574.8	498	460
99	60.8	62.04	654.4	538	495
100	54.7	27.21	638.8	495	490
101	56.0	29.44	659.3	555	476
102	55.4	41.22	749.4	549	474
103	58.0	43.10	530.7	564	482
104	54.3	49.84	547.8	593	481
105	52.2	84.10	584.6	523	443
106	50.4	46.54	563.4	577	443
107	53.3	39.29	655.6	572	437
108	54.6	37.33	623.0	564	433
109	55.8	54.07	587.3	555	444
110	54.0	51.38	560.4	554	451
111	54.0	46.26	561.8	566	451
112	56.2	65.16	539.8	540	453
113	50.6	60.73	629.7	549	463
114	51.3	67.40	621.9	462	463
115	51.6	70.12	604.6	492	478
116	48.3	58.12	622.2	519	478
117	52.5	53.24	639.5	565	470
118	55.6	85.66	763.6	470	449
119	50.7	79.13	646.9	478	420
120	52.4	53.88	644.2	529	461

APPENDIX IV
MEASURED AND PREDICTED HANDSHEET PROPERTIES
BLEND CHEST

OBS	DATE	DAY	REEL	RLPLT	Basis Weight lb/1000 sq ft	Measured Caliper mils	Measured Density g/cc
1	4-3-90	1	1	1	13.0596	11.0591	0.2272
2	4-3-90	1	2	2	13.9455	8.8583	0.3026
3	4-3-90	1	3	3	13.5854	8.0591	0.3244
4	4-3-90	1	4	4	13.3154	7.8898	0.3248
5	4-3-90	1	5	5	12.8346	8.6969	0.2840
6	4-3-90	1	6	6	13.4361	8.8661	0.2916
7	4-3-90	1	7	7	13.0903	9.7087	0.2594
8	4-3-90	1	8	8	14.0356	8.4173	0.3209
9	4-4-90	2	1	9	13.2867	9.1693	0.2788
10	4-4-90	2	2	10	13.8412	10.0984	0.2637
11	4-4-90	2	3	11	13.2867	9.2677	0.2759
12	4-4-90	2	4	12	13.5118	8.7283	0.2979
13	4-4-90	2	5	13	13.6468	8.9094	0.2947
14	4-4-90	2	6	14	13.2867	10.1496	0.2519
15	4-4-90	2	7	15	12.7609	7.9173	0.3101
16	4-4-90	2	8	16	16.6483	10.7165	0.2989
17	4-5-90	3	1	17	13.2867	8.9764	0.2848
18	4-5-90	3	2	18	13.4361	8.6890	0.2976
19	4-5-90	3	3	19	14.2606	10.3465	0.2652
20	4-5-90	3	4	20	12.8346	9.8268	0.2513
21	4-5-90	3	5	21	13.2110	8.7874	0.2893
22	4-5-90	3	6	22	12.5809	9.6378	0.2512
23	4-5-90	3	7	23	13.2110	9.3071	0.2781
24	4-5-90	3	8	24	13.1353	8.3386	0.3031

APPENDIX IV
MEASURED AND PREDICTED HANDSHEET PROPERTIES
BLEND CHEST

OBS	Measured Tensile km	Measured Burst Factor	Measured Stretch %	Measured Moisture %	Measured Gurley Porosity
1	2.49067	18.8774	0.856	5.72	2.49
2	3.54508	21.0489	1.447	5.72	3.85
3	3.14421	20.3159	1.393	6.61	2.38
4	3.05746	17.9750	1.290	6.20	2.73
5	3.38509	18.5252	1.323	6.56	2.74
6	4.27617	20.6487	1.492	6.41	3.55
7	4.03985	16.3623	1.493	5.66	2.34
8	2.51830	18.4046	1.217	6.58	3.03
9	4.00684	18.8252	1.822	6.39	3.09
10	3.15248	18.7669	1.538	5.76	2.66
11	4.12940	19.0307	1.665	6.39	3.42
12	3.85512	19.0436	1.690	6.30	3.28
13	3.52630	19.9928	1.584	5.78	2.78
14	3.76014	18.5006	1.622	6.50	2.26
15	3.69749	17.7985	1.524	6.88	4.39
16	3.15014	16.9841	1.598	5.82	3.21
17	3.91885	18.5006	1.520	6.43	2.80
18	3.91257	18.7229	1.601	6.69	4.75
19	3.96012	16.2997	1.807	5.97	2.15
20	4.05853	16.4643	1.508	6.56	1.64
21	3.44666	21.3269	1.554	6.31	4.77
22	3.48655	16.7849	1.385	5.63	1.55
23	3.49881	18.2802	1.420	6.52	2.27
24	2.85619	20.6837	1.151	6.39	6.03

APPENDIX IV
MEASURED AND PREDICTED HANDSHEET PROPERTIES
BLEND CHEST

OBS	Zero-Span Breaking Length km	ENERGY	SLOPE	Measured CSF ml
1	8.6887	9.15	283.1	542
2	9.4189	23.61	318.6	.
3	8.4481	19.64	277.8	561
4	9.1259	18.57	279.2	567
5	9.3280	18.20	292.5	565
6	10.4714	29.03	377.4	572
7	10.1667	26.62	342.5	562
8	8.1198	14.54	268.1	548
9	9.7696	33.12	321.2	495
10	8.8284	21.82	268.0	650
11	9.4063	30.35	326.7	554
12	9.08940	29.07	313.4	600
13	9.27602	24.32	286.1	554
14	9.11763	26.18	295.9	555
15	9.56121	22.29	275.3	545
16	7.94929	26.35	317.5	565
17	9.85338	24.81	310.2	494
18	8.74920	26.96	319.2	508
19	8.96354	33.09	332.4	525
20	9.83415	24.78	323.4	493
21	8.40650	22.70	286.4	595
22	9.76690	20.88	292.5	473
23	8.86547	22.35	298.9	480
24	8.76112	14.27	271.7	517

APPENDIX IV
MEASURED AND PREDICTED HANDSHEET PROPERTIES
BROKE TANK

OBS	DATE	DAY	REEL	RLPLT	Basis Weight lb/1000 sq ft	Measured Caliper mils	Measured Density g/cc
25	4-3-90	1	1	1	13.2867	6.97638	0.3665
26	4-3-90	1	2	2	.	.	.
27	4-3-90	1	3	3	13.4361	6.74803	0.3831
28	4-3-90	1	4	4	12.0100	6.25984	0.3692
29	4-3-90	1	5	5	13.5854	6.75984	0.3867
30	4-3-90	1	6	6	.	.	.
31	4-3-90	1	7	7	12.8346	6.76772	0.3649
32	4-3-90	1	8	8	13.2151	6.95669	0.3655
33	4-4-90	2	1	9	12.0100	6.04724	0.3822
34	4-4-90	2	2	10	13.6611	6.61811	0.3972
35	4-4-90	2	3	11	.	.	.
36	4-4-90	2	4	12	12.8346	6.61811	0.3732
37	4-4-90	2	5	13	.	.	.
38	4-4-90	2	6	14	13.2110	6.38976	0.3978
39	4-4-90	2	7	15	13.2867	7.17717	0.3562
40	4-4-90	2	8	16	13.8862	7.22835	0.3697
41	4-5-90	3	1	17	.	.	.
42	4-5-90	3	2	18	13.0596	7.16929	0.3505
43	4-5-90	3	3	19	.	.	.
44	4-5-90	3	4	20	14.1113	7.02756	0.3864
45	4-5-90	3	5	21	.	.	.
46	4-5-90	3	6	22	.	.	.
47	4-5-90	3	7	23	.	.	.
48	4-5-90	3	8	24	12.8346	6.54331	0.3540

APPENDIX IV
MEASURED AND PREDICTED HANDSHEET PROPERTIES
BROKE TANK

OBS	Measured Tensile km	Measured Burst Factor	Measured Stretch %	Measured Moisture %	Measured Gurley Porosity
25	2.61152	13.9566	1.232	6.27	1.86
26	.	.	1.036	.	.
27	2.11944	14.9890	0.989	5.70	2.67
28	2.96909	16.0387	1.315	6.01	2.34
29	.	16.4220	.	5.95	2.97
30	.	.	1.406	.	.
31	.	14.0003	.	5.92	3.42
32	.	15.4681	.	5.86	3.07
33	.	15.6198	.	5.66	1.94
34	2.88685	15.2577	1.285	5.83	2.53
35	.	.	1.161	.	.
36	.	14.1347	.	5.84	1.96
37	.	.	1.154	.	.
38	.	16.2781	.	6.17	2.41
39	2.76708	13.0262	1.388	5.74	1.45
40	.	14.3893	.	5.97	2.77
41	.	.	0.970	.	.
42	.	13.5609	.	5.75	1.78
43	.	.	1.085	.	.
44	1.85381	18.2855	0.806	5.82	2.51
45	.	.	0.876	.	.
46	.	.	0.965	.	.
47	.	.	.	.	.
48	1.51117	12.4995	0.770	5.39	1.61

APPENDIX IV
MEASURED AND PREDICTED HANDSHEET PROPERTIES
BROKE TANK

OBS	Zero-Span Breaking Length km	ENERGY	SLOPE	Measured CSF ml
25	7.2271	14.16	244.9	551
26	.	11.32	273.7	579
27	7.5980	10.63	256.3	596
28	8.7474	15.22	258.8	598
29	.	.	.	.
30	.	19.65	292.2	614
31	.	.	.	.
32	.	.	.	.
33	.	.	.	.
34	10.1042	17.23	286.9	593
35	.	14.60	296.7	608
36	.	.	.	.
37	.	12.52	293.5	613
38	.	.	.	.
39	10.7521	17.58	284.7	599
40	.	.	.	.
41	.	9.90	290.5	578
42	.	.	.	.
43	.	11.07	246.1	688
44	9.2557	7.99	271.5	573
45	.	8.49	262.9	583
46	.	10.97	259.4	558
47	.	.	.	.
48	9.3762	8.51	240.8	563

APPENDIX IV
MEASURED AND PREDICTED HANDSHEET PROPERTIES
HEADBOX

OBS	DATE	DAY	REEL	RLPLT	Basis Weight lb/1000 sq ft	Measured Caliper mils	Measured Density g/cc
49	4-3-90	1	1	1	13.5854	6.88976	0.3794
50	4-3-90	1	2	2	12.8346	7.53937	0.3276
51	4-3-90	1	3	3	13.5036	6.91732	0.3756
52	4-3-90	1	4	4	15.5701	6.84646	0.3859
53	4-3-90	1	5	5	13.1353	6.98819	0.3617
54	4-3-90	1	6	6	13.8105	6.64961	0.2996
55	4-3-90	1	7	7	13.2785	6.59843	0.3872
56	4-3-90	1	8	8	12.6852	6.69685	0.3645
57	4-4-90	2	1	9	13.6673	6.74803	0.3897
58	4-4-90	2	2	10	14.1174	6.86614	0.3956
59	4-4-90	2	3	11	13.8105	7.58661	0.3503
60	4-4-90	2	4	12	13.5036	6.97638	0.3725
61	4-4-90	2	5	13	13.8923	7.17717	0.3725
62	4-4-90	2	6	14	13.2867	6.51969	0.3921
63	4-4-90	2	7	15	13.5036	6.73622	0.3857
64	4-4-90	2	8	16	15.0176	7.41732	0.3896
65	4-5-90	3	1	17	14.0356	7.23622	0.3732
66	4-5-90	3	2	18	13.5036	7.17717	0.3620
67	4-5-90	3	3	19	12.9860	6.32677	0.3950
68	4-5-90	3	4	20	13.1353	6.74803	0.3746
69	4-5-90	3	5	21	13.8105	7.41732	0.3583
70	4-5-90	3	6	22	13.5036	6.85827	0.3789
71	4-5-90	3	7	23	13.1353	7.79921	0.3241
72	4-5-90	3	8	24	13.4422	6.97638	0.3708

APPENDIX IV
MEASURED AND PREDICTED HANDSHEET PROPERTIES
HEADBOX

OBS	Measured Tensile km	Measured Burst Factor	Measured Stretch %	Measured Moisture %	Measured Gurley Porosity
49	3.17494	24.4002	1.562	5.04	5.57
50	3.76411	21.1684	1.611	6.62	4.20
51	3.23129	24.1649	1.815	6.92	10.07
52	3.86575	22.0287	1.879	5.58	8.47
53	3.89726	21.4498	1.825	6.54	4.30
54	3.90476	22.5870	1.707	7.19	9.28
55	4.29546	23.9574	1.731	5.55	9.24
56	4.00428	22.2109	1.980	6.69	4.80
57	4.11829	24.8221	2.234	7.33	8.15
58	3.73706	22.7375	1.891	6.37	9.10
59	4.19955	22.3372	1.831	6.73	6.48
60	3.96413	24.6013	1.619	6.94	7.96
61	4.10117	25.0304	1.838	6.08	9.19
62	3.96284	21.5949	1.652	6.50	5.32
63	4.87013	24.1542	2.158	6.99	6.77
64	4.10388	24.7917	2.045	5.11	11.54
65	4.29732	23.4538	1.747	6.77	6.84
66	4.10173	24.8355	1.744	6.22	6.40
67	4.82471	24.5525	2.089	6.69	14.62
68	4.24216	21.4826	1.901	6.63	4.96
69	4.56085	23.3885	1.994	5.17	6.10
70	3.50959	24.6439	1.380	5.49	16.97
71	4.98919	19.1844	2.299	7.00	2.68
72	4.80384	23.7833	2.248	5.52	14.70

APPENDIX IV
MEASURED AND PREDICTED HANDSHEET PROPERTIES
HEADBOX

OBS	Zero-Span Breaking Length km	ENERGY	SLOPE	Measured CSF ml
49	7.6784	2.09	288.2	367
50	10.0945	2.28	310.6	371
51	7.9999	2.31	274.1	331
52	8.2892	38.66	352.1	350
53	8.9637	2.68	304.2	355
54	9.3005	31.55	331.3	405
55	8.8390	2.82	351.0	398
56	9.5305	35.50	.	346
57	9.4477	43.18	314.5	383
58	9.1290	36.29	324.0	400
59	7.8803	37.66	351.8	375
60	11.9998	30.27	346.6	397
61	9.6064	35.24	255.9	407
62	9.8953	30.68	335.9	409
63	10.1075	48.14	367.1	386
64	9.4263	43.00	353.4	374
65	9.9007	34.63	365.6	354
66	9.7730	32.56	337.1	374
67	9.5527	44.54	365.2	361
68	10.0800	37.47	348.8	363
69	10.4877	43.28	382.0	355
70	9.3561	1.98	317.6	338
71	9.9999	50.74	368.5	339
72	10.1490	49.67	365.8	372

APPENDIX IV
MEASURED AND PREDICTED HANDSHEET PROPERTIES
HOLE REFINER

OBS	DATE	DAY	REEL	RLPLT	Basis Weight lb/1000 sq ft	Measured Caliper mils	Measured Density g/cc
73	4-3-90	1	1	1	13.3604	10.0669	0.2554
74	4-3-90	1	2	2	13.2785	8.5276	0.2996
75	4-3-90	1	3	3	13.8923	9.7480	0.2742
76	4-3-90	1	4	4	13.2785	10.5394	0.2424
77	4-3-90	1	5	5	13.2785	10.0591	0.2540
78	4-3-90	1	6	6	13.6673	9.6772	0.2718
79	4-3-90	1	7	7	13.6673	10.7677	0.2442
80	4-3-90	1	8	8	13.5854	8.8268	0.2962
81	4-4-90	2	1	9	12.8284	8.9488	0.2758
82	4-4-90	2	2	10	13.2785	13.7874	0.1853
83	4-4-90	2	3	11	13.4218	8.4291	0.3017
84	4-4-90	2	4	12	12.8509	9.5787	0.2582
85	4-4-90	2	5	13	13.2785	11.0984	0.2302
86	4-4-90	2	6	14	13.7287	11.0787	0.2385
87	4-4-90	2	7	15	13.2253	8.7874	0.2896
88	4-4-90	2	8	16	13.5036	9.9173	0.2620
89	4-5-90	3	1	17	12.4601	11.5984	0.2067
90	4-5-90	3	2	18	12.9246	8.8780	0.2801
91	4-5-90	3	3	19	13.4422	9.0984	0.2843
92	4-5-90	3	4	20	13.2785	9.5394	0.2678
93	4-5-90	3	5	21	13.6918	8.2480	0.3194
94	4-5-90	3	6	22	13.5854	9.8268	0.2660
95	4-5-90	3	7	23	13.4422	8.8661	0.2917
96	4-5-90	3	8	24	13.8412	9.4567	0.2816

APPENDIX IV
MEASURED AND PREDICTED HANDSHEET PROPERTIES
HOLE REFINER

OBS	Measured Tensile km	Measured Burst Factor	Measured Stretch %	Measured Moisture %	Measured Gurley Porosity
73	3.80504	17.4841	1.400	5.49	2.03
74	3.72473	26.4148	1.505	6.00	5.60
75	3.70894	24.4510	1.578	4.92	17.90
76	3.12097	18.1872	1.332	5.23	3.04
77	3.43700	21.3917	1.493	6.03	4.12
78	3.24148	24.7379	1.315	5.15	10.38
79	2.94513	18.0065	1.152	5.57	2.28
80	2.99361	24.1357	1.075	5.02	5.24
81	3.23211	21.3579	1.045	5.82	3.54
82	3.48102	19.1074	1.173	6.35	1.61
83	3.44077	20.6600	1.196	5.74	3.47
84	4.25969	22.5733	1.587	5.57	6.49
85	3.85051	17.3212	1.391	6.46	2.14
86	3.16463	20.2610	1.254	6.02	3.89
87	4.16593	24.6733	1.533	5.54	15.70
88	3.93630	18.5015	1.656	5.92	1.53
89	4.65970	18.6781	1.454	6.25	2.06
90	4.93808	24.0796	1.596	6.08	9.93
91	3.97136	16.5863	1.604	6.20	1.74
92	4.29389	20.2117	1.538	5.16	2.36
93	4.45857	23.7801	1.580	5.60	11.02
94	4.12620	16.8981	1.643	5.58	1.70
95	4.79452	21.1740	1.906	6.30	2.54
96	4.45269	22.4330	1.888	5.39	9.15

APPENDIX IV
MEASURED AND PREDICTED HANDSHEET PROPERTIES
HOLE REFINER

OBS	Zero-Span Breaking Length km	ENERGY	SLOPE	Measured CSF ml
73	8.6413	23.20	341.1	620
74	10.1949	23.72	342.9	548
75	8.8627	27.22	337.3	589
76	8.6853	18.39	283.0	612
77	9.4354	22.37	292.1	570
78	9.3572	18.17	309.4	584
79	7.1707	15.78	310.3	560
80	8.8352	16.84	317.3	590
81	10.1572	16.66	349.4	482
82	9.9992	21.10	336.1	492
83	8.1224	20.82	345.0	494
84	9.29684	28.41	341.6	475
85	8.39172	21.92	315.9	587
86	7.15214	18.63	285.4	568
87	8.20559	27.46	344.5	548
88	8.71920	28.77	306.9	574
89	9.97076	33.53	391.3	386
90	9.58374	34.17	390.3	410
91	7.95353	27.23	325.6	481
92	8.14942	29.85	348.3	474
93	7.97573	31.23	364.4	405
94	6.73569	30.86	336.4	407
95	8.86027	41.13	357.1	430
96	8.79262	38.04	335.5	425

APPENDIX IV
MEASURED AND PREDICTED HANDSHEET PROPERTIES
TICKLER REFINER

OBS	DATE	DAY	REEL	RLPLT	Basis Weight lb/1000 sq ft	Measured Caliper mils	Measured Density g/cc
97	4-3-90	1	1	1	13.1353	7.89764	0.3200
98	4-3-90	1	2	2	13.5118	8.96850	0.2899
99	4-3-90	1	3	3	13.6611	8.83858	0.2974
100	4-3-90	1	4	4	12.7609	8.63780	0.2843
101	4-3-90	1	5	5	13.8862	9.07874	0.2943
102	4-3-90	1	6	6	13.3604	8.38976	0.3064
103	4-3-90	1	7	7	14.0356	9.37795	0.2879
104	4-3-90	1	8	8	13.2867	7.86614	0.3250
105	4-4-90	2	1	9	13.3604	8.15748	0.3152
106	4-4-90	2	2	10	12.4601	7.62992	0.3142
107	4-4-90	2	3	11	13.2110	9.12992	0.2784
108	4-4-90	2	4	12	13.2110	9.1969	0.2764
109	4-4-90	2	5	13	12.5358	9.2165	0.2617
110	4-4-90	2	6	14	13.8862	8.6693	0.3082
111	4-4-90	2	7	15	14.1113	9.3189	0.2914
112	4-4-90	2	8	16	16.6626	10.0472	0.3191
113	4-5-90	3	1	17	13.7368	8.5787	0.3081
114	4-5-90	3	2	18	14.6371	9.1693	0.3072
115	4-5-90	3	3	19	13.6611	10.5591	0.2490
116	4-5-90	3	4	20	13.5118	9.2165	0.2821
117	4-5-90	3	5	21	13.6611	8.3661	0.3142
118	4-5-90	3	6	22	13.9619	9.3465	0.2874
119	4-5-90	3	7	23	13.2867	8.9488	0.2857
120	4-5-90	3	8	24	13.2110	8.7283	0.2912

APPENDIX IV
MEASURED AND PREDICTED HANDSHEET PROPERTIES
TICKLER REFINER

OBS	Measured Tensile km	Measured Burst Factor	Measured Stretch %	Measured Moisture %	Measured Gurley Porosity
97	3.09460	18.8233	1.151	6.36	3.05
98	2.94503	21.1713	1.224	6.96	3.84
99	3.35908	19.9928	1.199	6.50	4.15
100	1.90110	19.4882	0.617	6.65	3.60
101	1.51400	17.5984	0.742	6.64	2.77
102	2.87996	20.3353	0.876	6.50	6.07
103	2.80835	18.9474	1.442	6.23	4.48
104	3.17562	18.2950	1.276	6.33	2.76
105	3.78473	19.7973	1.423	6.00	5.66
106	3.33601	17.9974	1.285	6.62	3.35
107	2.81612	17.7361	1.057	6.37	3.00
108	3.07371	20.0103	1.384	6.16	3.91
109	3.36750	16.0654	1.161	6.24	2.51
110	3.37079	19.0477	1.530	6.57	4.48
111	2.72523	18.9476	1.170	6.06	6.16
112	2.80161	18.2032	1.614	6.42	3.91
113	3.05636	17.2665	1.710	6.47	3.45
114	2.78423	20.5258	1.275	5.95	7.07
115	3.51954	16.5204	1.693	6.80	1.59
116	3.02383	19.4798	1.453	6.40	2.37
117	3.49509	19.7824	1.469	6.12	6.10
118	3.80111	17.7089	1.749	6.35	2.76
119	3.65172	19.2579	1.782	6.53	2.51
120	3.23332	19.5859	1.354	5.94	5.50

APPENDIX IV
MEASURED AND PREDICTED HANDSHEET PROPERTIES
TICKLER REFINER

OBS	Zero-Span Breaking Length km	ENERGY	SLOPE	Measured CSF ml
97	8.5209	15.19	301.1	540
98	7.4593	16.49	279.9	498
99	9.0172	17.28	320.7	538
100	8.8048	4.97	272.1	495
101	7.7928	5.24	238.3	555
102	10.2668	13.06	352.9	549
103	8.2829	18.88	261.6	564
104	8.5169	16.56	302.4	593
105	10.0538	23.55	345.6	523
106	10.4375	18.25	289.1	577
107	9.7131	13.35	289.4	572
108	9.56328	20.52	285.5	564
109	9.79703	16.11	318.2	555
110	9.65969	22.90	307.7	554
111	8.88303	14.49	279.8	566
112	7.74566	24.14	286.6	540
113	9.20172	24.89	273.5	549
114	8.71609	16.21	284.1	462
115	8.35597	27.03	308.2	492
116	8.11406	21.50	297.4	519
117	8.57789	24.39	330.0	565
118	8.92931	31.55	339.9	470
119	8.08852	29.44	297.3	478
120	8.28006	19.75	296.4	529

APPENDIX V

Dependent Variable: DENS

Source	DF	Sum of Squares	Mean Square	F Value	Pr > F
Model	1	39.62713495	39.62713495	57067.60	0.0001
Error	113	0.07846599	0.00069439		
Uncorrected Total	114	39.70560094			

R-Square	C.V.	Root MSE	DENS Mean
0.998024	4.471125	0.026351	0.58936547

Dependent Variable: DENS

Source	DF	Type I SS	Mean Square	F Value	Pr > F
PDENS	1	39.62713495	39.62713495	57067.60	0.0001

Source	DF	Type III SS	Mean Square	F Value	Pr > F
PDENS	1	39.62713495	39.62713495	57067.60	0.0001

Parameter	Estimate	T for H0: Parameter=0	Pr > |T|	Std Error of Estimate
PDENS	0.9613394119	238.89	0.0001	0.00402422

APPENDIX V

Dependent Variable: CALCR

Source	DF	Sum of Squares	Mean Square	F Value	Pr > F
Model	1	7896.761727	7896.761727	45678.57	0.0001
Error	113	19.535069	0.172877		
Uncorrected Total	114	7916.296796			

R-Square	C.V.	Root MSE	CALCR Mean
0.997532	4.997854	0.415784	8.31926023

Dependent Variable: CALCR

Source	DF	Type I SS	Mean Square	F Value	Pr > F
PCAL	1	7896.761727	7896.761727	45678.57	0.0001

Source	DF	Type III SS	Mean Square	F Value	Pr > F
PCAL	1	7896.761727	7896.761727	45678.57	0.0001

Parameter	Estimate	T for H0: Parameter=0	Pr > |T|	Std Error of Estimate
PCAL	1.031425951	213.73	0.0001	0.00482594

APPENDIX V

Dependent Variable: BWLB

Source	DF	Sum of Squares	Mean Square	F Value	Pr > F
Model	1	73632.11402	73632.11402	99999.99	0.0
Error	113	77.54238	0.68622		
Uncorrected Total	114	73709.65640			

R-Square	C.V.	Root MSE	BWLB Mean
0.998948	3.258171	0.828381	25.4247368

Dependent Variable: BWLB

Source	DF	Type I SS	Mean Square	F Value	Pr > F
PBW	1	73632.11402	73632.11402	99999.99	0.0

Source	DF	Type III SS	Mean Square	F Value	Pr > F
PBW	1	73632.11402	73632.11402	99999.99	0.0

Parameter	Estimate	T for H0: Parameter=0	Pr > |T|	Std Error of Estimate
PBW	0.9926993197	327.57	0.0001	0.00303050

APPENDIX V
GENERAL LINEAR MODELS PROCEDURE

Dependent Variable: MMDCDTEN

Source	DF	Sum of Squares	Mean Square	F Value	Pr > F
Model	1	630.0044613	630.0044613	49881.93	0.0001
Error	113	1.4271801	0.0126299		
Uncorrected Total	114	631.4316414			

R-Square	C.V.	Root MSE	MMDCDTEN Mean
0.997740	4.780812	0.112383	2.35070680

Dependent Variable: MMDCDTEN

Source	DF	Type I SS	Mean Square	F Value	Pr > F
PDCDTEN	1	630.0044613	630.0044613	49881.93	0.0001

Source	DF	Type III SS	Mean Square	F Value	Pr > F
PDCDTEN	1	630.0044613	630.0044613	49881.93	0.0001

Parameter	Estimate	T for H0: Parameter=0	Pr > |T|	Std Error of Estimate
PDCDTEN	0.9842062183	223.34	0.0001	0.00440671

APPENDIX V
GENERAL LINEAR MODELS PROCEDURE

Dependent Variable: MMDCDMOD

Source	DF	Sum of Squares	Mean Square	F Value	Pr > F
Model	1	633.2535578	633.2535578	22126.96	0.0001
Error	113	3.2339575	0.0286191		
Uncorrected Total	114	636.4875153			

R-Square	C.V.	Root MSE	MMDCDMOD Mean
0.994919	7.176000	0.169172	2.35746620

Dependent Variable: MMDCDMOD

Source	DF	Type I SS	Mean Square	F Value	Pr > F
PDCDMOD	1	633.2535578	633.2535578	22126.96	0.0001

Source	DF	Type III SS	Mean Square	F Value	Pr > F
PDCDMOD	1	633.2535578	633.2535578	22126.96	0.0001

Parameter	Estimate	T for H0: Parameter=0	Pr > |T|	Std Error of Estimate
PDCDMOD	1.094436635	148.75	0.0001	0.00735749

APPENDIX V

Dependent Variable: STFICD

Source	DF	Sum of Squares	Mean Square	F Value	Pr > F
Model	1	23733.44673	23733.44673	53574.36	0.0001
Error	112	49.61601	0.44300		
Uncorrected Total	113	23783.06274			

R-Square	C.V.	Root MSE	STFICD Mean
0.997914	4.591597	0.665583	14.4956637

Dependent Variable: STFICD

Source	DF	Type I SS	Mean Square	F Value	Pr > F
PSTFICD	1	23733.44673	23733.44673	53574.36	0.0001

Source	DF	Type III SS	Mean Square	F Value	Pr > F
PSTFICD	1	23733.44673	23733.44673	53574.36	0.0001

Parameter	Estimate	T for H0: Parameter=0	Pr > |T|	Std Error of Estimate
PSTFICD	1.173360946	231.46	0.0001	0.00506936

APPENDIX V

Dependent Variable: STFIMD

Source	DF	Sum of Squares	Mean Square	F Value	Pr > F
Model	1	58879.51200	58879.51200	62278.85	0.0001
Error	113	106.83217	0.94542		
Uncorrected Total	114	58986.34417			

R-Square	C.V.	Root MSE	STFIMD Mean
0.998189	4.278209	0.972326	22.7274035

Dependent Variable: STFIMD

Source	DF	Type I SS	Mean Square	F Value	Pr > F
PSTFIMD	1	58879.51200	58879.51200	62278.85	0.0001

Source	DF	Type III SS	Mean Square	F Value	Pr > F
PSTFIMD	1	58879.51200	58879.51200	62278.85	0.0001

Parameter	Estimate	T for H0: Parameter=0	Pr > |T|	Std Error of Estimate
PSTFIMD	1.232768113	249.56	0.0001	0.00493982

APPENDIX V

Dependent Variable: EYGPA

Source	DF	Sum of Squares	Mean Square	F Value	Pr > F
Model	1	390.7002211	390.7002211	15481.64	0.0001
Error	113	2.8517078	0.0252364		
Uncorrected Total	114	393.5519289			

R-Square	C.V.	Root MSE	EYGPA Mean
0.992754	8.597286	0.158860	1.84778696

Dependent Variable: EYGPA

Source	DF	Type I SS	Mean Square	F Value	Pr > F
PEY	1	390.7002211	390.7002211	15481.64	0.0001

Source	DF	Type III SS	Mean Square	F Value	Pr > F
PEY	1	390.7002211	390.7002211	15481.64	0.0001

Parameter	Estimate	T for H0: Parameter=0	Pr > |T|	Std Error of Estimate
PEY	0.8712876060	124.43	0.0001	0.00700250

APPENDIX V

Dependent Variable: EXGPA

Source	DF	Sum of Squares	Mean Square	F Value	Pr > F
Model	1	2147.176631	2147.176631	54200.98	0.0001
Error	113	4.476505	0.039615		
Uncorrected Total	114	2151.653136			

R-Square	C.V.	Root MSE	EXGPA Mean
0.997920	4.593345	0.199035	4.33312536

Dependent Variable: EXGPA

Source	DF	Type I SS	Mean Square	F Value	Pr > F
PEX	1	2147.176631	2147.176631	54200.98	0.0001

Source	DF	Type III SS	Mean Square	F Value	Pr > F
PEX	1	2147.176631	2147.176631	54200.98	0.0001

Parameter	Estimate	T for H0: Parameter=0	Pr > |T|	Std Error of Estimate
PEX	0.9482783790	232.81	0.0001	0.00407317

APPENDIX V

Dependent Variable: CONCORA

Source	DF	Sum of Squares	Mean Square	F Value	Pr > F
Model	1	325027.1675	325027.1675	44206.90	0.0001
Error	112	823.4698	7.3524		
Uncorrected Total	113	325850.6373			

R-Square	C.V.	Root MSE	CONCORA Mean
0.997473	5.056286	2.711532	53.6269646

Dependent Variable: CONCORA

Source	DF	Type I SS	Mean Square	F Value	Pr > F
PCONC	1	325027.1675	325027.1675	44206.90	0.0001

Source	DF	Type III SS	Mean Square	F Value	Pr > F
PCONC	1	325027.1675	325027.1675	44206.90	0.0001

Parameter	Estimate	T for H0: Parameter=0	Pr > |T|	Std Error of Estimate
PCONC	0.9243005785	210.25	0.0001	0.00439611

APPENDIX V

Dependent Variable: TMDKIL

Source	DF	Sum of Squares	Mean Square	F Value	Pr > F
Model	1	4041.613272	4041.613272	31831.68	0.0001
Error	113	14.347414	0.126968		
Uncorrected Total	114	4055.960686			

R-Square	C.V.	Root MSE	TMDKIL Mean
0.996463	5.983355	0.356326	5.95528863

Dependent Variable: TMDKIL

Source	DF	Type I SS	Mean Square	F Value	Pr > F
PBLMD	1	4041.613272	4041.613272	31831.68	0.0001

Source	DF	Type III SS	Mean Square	F Value	Pr > F
PBLMD	1	4041.613272	4041.613272	31831.68	0.0001

Parameter	Estimate	T for H0: Parameter=0	Pr > |T|	Std Error of Estimate
PBLMD	0.9940178419	178.41	0.0001	0.00557140

APPENDIX V

Dependent Variable: TCDKIL

Source	DF	Sum of Squares	Mean Square	F Value	Pr > F
Model	1	732.6095009	732.6095009	20601.07	0.0001
Error	113	4.0184740	0.0355617		
Uncorrected Total	114	736.6279748			

R-Square	C.V.	Root MSE	TCDKIL Mean
0.994545	7.432508	0.188578	2.53720745

Dependent Variable: TCDKIL

Source	DF	Type I SS	Mean Square	F Value	Pr > F
PBLCD	1	732.6095009	732.6095009	20601.07	0.0001

Source	DF	Type III SS	Mean Square	F Value	Pr > F
PBLCD	1	732.6095009	732.6095009	20601.07	0.0001

Parameter	Estimate	T for H0: Parameter=0	Pr > |T|	Std Error of Estimate
PBLCD	1.010897105	143.53	0.0001	0.00704307

APPENDIX V
HANDSHEET DATA
GENERAL LINEAR MODELS PROCEDURE

Dependent Variable: TENKIL

Source	DF	Sum of Squares	Mean Square	F Value	Pr > F
Model	1	1379.489660	1379.489660	2391.82	0.0001
Error	102	58.828792	0.576753		
Uncorrected Total	103	1438.318452			

R-Square	C.V.	Root MSE	TENKIL Mean
0.959099	20.87845	0.759442	3.63744614

Dependent Variable: TENKIL

Source	DF	Type I SS	Mean Square	F Value	Pr > F
PBLMD	1	1379.489660	1379.489660	2391.82	0.0001

Source	DF	Type III SS	Mean Square	F Value	Pr > F
PBLMD	1	1379.489660	1379.489660	2391.82	0.0001

Parameter	Estimate	T for H0: Parameter=0	Pr > |T|	Std Error of Estimate
PBLMD	0.9356837178	48.91	0.0001	0.01913219

Sum of Residuals	0.55188879
Sum of Squared Residuals	58.82879223
Sum of Squared Residuals - Error SS	0.00000000
Press Statistic	59.97918624
First Order Autocorrelation	0.47132810
Durbin-Watson D	1.04955808

APPENDIX V
HANDSHEET DATA
GENERAL LINEAR MODELS PROCEDURE

Dependent Variable: CONC

Source	DF	Sum of Squares	Mean Square	F Value	Pr > F
Model	1	207574.7418	207574.7418	2973.56	0.0001
Error	110	7678.7482	69.8068		
Uncorrected Total	111	215253.4900			

R-Square	C.V.	Root MSE	CONC Mean
0.964327	19.36179	8.355047	43.1522523

Dependent Variable: CONC

Source	DF	Type I SS	Mean Square	F Value	Pr > F
PCONC	1	207574.7418	207574.7418	2973.56	0.0001

Source	DF	Type III SS	Mean Square	F Value	Pr > F
PCONC	1	207574.7418	207574.7418	2973.56	0.0001

Parameter	Estimate	T for H0: Parameter=0	Pr > |T|	Std Error of Estimate
PCONC	0.7663134662	54.53	0.0001	0.01405297

Sum of Residuals	6.76292219
Sum of Squared Residuals	7678.74824362
Sum of Squared Residuals - Error SS	0.00000000
Press Statistic	7828.54199540
First Order Autocorrelation	0.35875732
Durbin-Watson D	1.27195407

APPENDIX V
HANDSHEET DATA
GENERAL LINEAR MODELS PROCEDURE

Dependent Variable: RING

Source	DF	Sum of Squares	Mean Square	F Value	Pr > F
Model	1	305915.3421	305915.3421	1684.77	0.0001
Error	110	19973.4679	181.5770		
Uncorrected Total	111	325888.8100			

R-Square	C.V.	Root MSE	RING Mean
0.938711	25.14551	13.47505	53.5882883

Dependent Variable: RING

Source	DF	Type I SS	Mean Square	F Value	Pr > F
PRCCD	1	305915.3421	305915.3421	1684.77	0.0001

Source	DF	Type III SS	Mean Square	F Value	Pr > F
PRCCD	1	305915.3421	305915.3421	1684.77	0.0001

Parameter	Estimate	T for H0: Parameter=0	Pr > |T|	Std Error of Estimate
PRCCD	1.620873265	41.05	0.0001	0.03948924

Sum of Residuals	290.38253052
Sum of Squared Residuals	19973.46785692
Sum of Squared Residuals - Error SS	0.00000000
Press Statistic	20699.62445399
First Order Autocorrelation	0.27040685
Durbin-Watson D	1.45299353

APPENDIX V
HANDSHEET DATA
GENERAL LINEAR MODELS PROCEDURE

Dependent Variable: BF

Source	DF	Sum of Squares	Mean Square	F Value	Pr > F
Model	1	58166.58117	58166.58117	3377.57	0.0001
Error	110	1894.35731	17.22143		
Uncorrected Total	111	60060.93848			

R-Square	C.V.	Root MSE	BF Mean
0.968459	18.06273	4.149871	22.9747739

Dependent Variable: BF

Source	DF	Type I SS	Mean Square	F Value	Pr > F
PBF	1	58166.58117	58166.58117	3377.57	0.0001

Source	DF	Type III SS	Mean Square	F Value	Pr > F
PBF	1	58166.58117	58166.58117	3377.57	0.0001

Parameter	Estimate	T for H0: Parameter=0	Pr > |T|	Std Error of Estimate
PBF	1.010681439	58.12	0.0001	0.01739050

Sum of Residuals	42.09283898
Sum of Squared Residuals	1894.35731447
Sum of Squared Residuals - Error SS	0.00000000
Press Statistic	1925.14267806
First Order Autocorrelation	0.43662669
Durbin-Watson D	1.12491302

APPENDIX V
HANDSHEET DATA
GENERAL LINEAR MODELS PROCEDURE

Dependent Variable: GURLEY

Source	DF	Sum of Squares	Mean Square	F Value	Pr > F
Model	1	29038.37525	29038.37525	200.31	0.0001
Error	109	15801.73495	144.97005		
Uncorrected Total	110	44840.11020			

R-Square	C.V.	Root MSE	GURLEY Mean
0.647598	75.16166	12.04035	16.0192727

Dependent Variable: GURLEY

Source	DF	Type I SS	Mean Square	F Value	Pr > F
PPOROS	1	29038.37525	29038.37525	200.31	0.0001

Source	DF	Type III SS	Mean Square	F Value	Pr > F
PPOROS	1	29038.37525	29038.37525	200.31	0.0001

Parameter	Estimate	T for H0: Parameter=0	Pr > |T|	Std Error of Estimate
PPOROS	1.033530534	14.15	0.0001	0.07302579

Sum of Residuals	-5.35157137
Sum of Squared Residuals	15801.73495140
Sum of Squared Residuals - Error SS	-0.00000000
Press Statistic	16124.03840429
First Order Autocorrelation	0.45080806
Durbin-Watson D	1.09418614

APPENDIX V
HANDSHEET DATA
GENERAL LINEAR MODELS PROCEDURE

Dependent Variable: DENS

Source	DF	Sum of Squares	Mean Square	F Value	Pr > F
Model	1	18.97638561	18.97638561	13608.31	0.0001
Error	110	0.15339173	0.00139447		
Uncorrected Total	111	19.12977734			

	R-Square	C.V.	Root MSE	DENS Mean
	0.991982	9.080856	0.037343	0.41122342

Dependent Variable: DENS

Source	DF	Type I SS	Mean Square	F Value	Pr > F
PDENS	1	18.97638561	18.97638561	13608.31	0.0001

Source	DF	Type III SS	Mean Square	F Value	Pr > F
PDENS	1	18.97638561	18.97638561	13608.31	0.0001

Parameter	Estimate	T for H0: Parameter=0	Pr > |T|	Std Error of Estimate
PDENS	0.9823405210	116.65	0.0001	0.00842093

Sum of Residuals	0.20960388
Sum of Squared Residuals	0.15339173
Sum of Squared Residuals - Error SS	0.00000000
Press Statistic	0.15639569
First Order Autocorrelation	0.15198814
Durbin-Watson D	1.69317604

APPENDIX V

Dependent Variable: STRMD

Source	DF	Sum of Squares	Mean Square	F Value	Pr > F
Model	1	305.4091733	305.4091733	32404.44	0.0001
Error	113	1.0650157	0.0094249		
Uncorrected Total	114	306.4741890			

R-Square	C.V.	Root MSE	STRMD Mean
0.996525	5.929689	0.097082	1.63721930

Dependent Variable: STRMD

Source	DF	Type I SS	Mean Square	F Value	Pr > F
PSTR	1	305.4091733	305.4091733	32404.44	0.0001

Source	DF	Type III SS	Mean Square	F Value	Pr > F
PSTR	1	305.4091733	305.4091733	32404.44	0.0001

Parameter	Estimate	T for H0: Parameter=0	Pr > |T|	Std Error of Estimate
PSTR	0.9152364378	180.01	0.0001	0.00508430

APPENDIX V

Dependent Variable: GPORO

Source	DF	Sum of Squares	Mean Square	F Value	Pr > F
Model	1	47940.33867	47940.33867	2690.86	0.0001
Error	113	2013.20874	17.81601		
Uncorrected Total	114	49953.54741			

R-Square	C.V.	Root MSE	GPORO Mean
0.959698	20.60869	4.220901	20.4811667

Dependent Variable: GPORO

Source	DF	Type I SS	Mean Square	F Value	Pr > F
PPOROS	1	47940.33867	47940.33867	2690.86	0.0001

Source	DF	Type III SS	Mean Square	F Value	Pr > F
PPOROS	1	47940.33867	47940.33867	2690.86	0.0001

Parameter	Estimate	T for H0: Parameter=0	Pr > |T|	Std Error of Estimate
PPOROS	0.9737352427	51.87	0.0001	0.01877135